Bulletin of the Geological Society of Denmark

VOLUME 62 | DECEMBER 2014 | COPENHAGEN

DGF

Bulletin of the Geological Society of Denmark

is published by the Geological Society of Denmark (DGF, Dansk Geologisk Forening), founded in 1893

Chief editor

Lotte Melchior Larsen, Geological Survey of Denmark and Greenland (GEUS), Øster Voldgade 10, DK-1350 Copenhagen K, Denmark.
Tel: +45 91333889; Fax: +45 38142250;
E-mail: lml@geus.dk

Scientific editors

Lars B. Clemmensen, Department of Geosciences and Natural Resource Management, University of Copenhagen, Øster Voldgade 10, DK-1350 Copenhagen K, Denmark.
Tel: +45 35322449; E-mail: larsc@ign.ku.dk;
(clastic sedimentology, sedimentary basins and palaeoclimatology).

Ole Graversen, Department of Geosciences and Natural Resource Management, University of Copenhagen, Øster Voldgade 10, DK-1350 Copenhagen K, Denmark. Tel: +45 35322537;
E-mail: oleg@ign.ku.dk;
(structural geology and tectonics).

Michael Houmark-Nielsen, Natural History Museum of Denmark, University of Copenhagen, Øster Voldgade 5–7, DK-1350 Copenhagen K, Denmark.
Tel: +45 35324344; E-mail: michaelhn@snm.ku.dk;
(Quaternary geology).

Jesper Milàn, Geomuseum Faxe, Østsjællands Museum, Østervej 2, DK-4640 Faxe, Denmark.
Tel: +45 23319488; E-mail: jesperm@oesm.dk;
(palaeontology).

Lars Nielsen, Department of Geosciences and Natural Resource Management, University of Copenhagen, Øster Voldgade 10, DK-1350 Copenhagen K, Denmark.
Tel: +45 35322454; E-mail: ln@ign.ku.dk;
(geophysics).

Jan Audun Rasmussen, Natural History Museum of Denmark, Øster Voldgade 5–7, DK-1350 Copenhagen K, Denmark.
Tel: +45 35322386; E-mail: janr@snm.ku.dk;
(palaeontology).

Erik Thomsen, Department of Geoscience, University of Aarhus, Høegh-Guldbergs Gade 2, DK-8000 Aarhus C, Denmark. Tel: +45 87156443;
E-mail: erik.thomsen@geo.au.dk;
(palaeontology and stratigraphy).

Henrik Tirsgaard, Mærsk Olie og Gas AS, Esplanaden 50, DK-1263 Copenhagen K, Denmark. Tel: +45 61209140;
E-mail: Henrik.tirsgaard@maerskoil.com;
(carbonate sedimentology, petroleum geology and sedimentary basins).

J. Richard Wilson, Department of Geoscience, University of Aarhus, Høegh-Guldbergs Gade 2, DK-8000 Aarhus C, Denmark. Tel: +45 25321169;
E-mail: jrw@geo.au.dk;
(igneous petrology and geochemistry).

The *Bulletin* publishes contributions of international interest in all fields of geological sciences, with a natural emphasis on results of new work on material from Denmark, the Faroes and Greenland. Contributions based on foreign material may also be submitted to the Bulletin if the subject is relevant for the geology of the area of primary interest. The rate of publishing is one volume per year. All articles are published as pdf-files immediately after acceptance and technical production.

Scientific editing and reviewing are done on an unpaid collegial basis; technical production expenses are covered by the membership fees.

The bulletin is freely accessible on the web page of the Geological Society of Denmark:
http://2dgf.dk/publikationer/bulletin/index.html

Instructions to authors:

See inside the back cover and also http://2dgf.dk/publikationer/bulletin/vejledning.html

---

Cover: The sea cliff at Trelde Næs in eastern Jutland just east of the town Fredericia. The cliff exposes Early to Middle Eocene expanding clays from the Lillebælt Clay Formation and the Søvind Marl Formation. The clay is unstable and forms landslides. Wave-washed fossil remains such as shark teeth from the clay can be found on the shore. See this volume pp. 39–88: Carlsen, A.W. & Cuny, G.: A study of the sharks and rays from the Lillebælt Clay (Early–Middle Eocene) of Denmark, and their palaeoecology. Photo: Gilles Cuny.

Rinkite–nacareniobsite-(Ce) solid solution series and hainite from the Ilímaussaq alkaline complex: occurrence and compositional variation[*]

JØRN G. RØNSBO, HENNING SØRENSEN[†], ENCARNACIÓN RODA-ROBLES, FRANÇOIS FONTAN[†]
& PIERRE MONCHOUX

Rønsbo, J.G., Sørensen, H., Roda-Robles, E., Fontan, F. & Monchoux, P., 2014. Rinkite–nacareniobsite-(Ce) solid solution series and hainite from the Ilímaussaq alkaline complex: occurrence and compositional variation. ©2014 by Bulletin of the Geological Society of Denmark, Vol. 62, pp. 1–15. ISSN 2245-7070. (www.2dgf.dk/publikationer/bulletin).

Received 1 August 2013
Accepted in revised form
20 February 2014
Published online
14 March 2014

In the Ilímaussaq alkaline complex, minerals from the rinkite–nacareniobsite-(Ce) solid solution series have been found in pulaskite pegmatite, sodalite foyaite, naujaite and naujaite pegmatite from the roof sequence, and in marginal pegmatite, kakortokite and lujavrite from the floor sequence. The electron microprobe analyses embrace almost the full extension of the solid solution series and confirm its continuity. The solid solution series shows similar compositional variations in the roof and floor sequences: Rinkite members of the series are found in the less evolved rocks in the two sequences, whereas nacareniobsite-Ce members occur in the most evolved rocks and pegmatites in the two sequences. The REE (+Y) content varies from 0.83 atoms per formula unit (apfu) in rinkite from pulaskite pegmatite to 1.31 apfu in nacareniobsite-(Ce) from naujaite pegmatite. The main substitution mechanisms in the solid solution series investigated in this work are $2Ca^{2+} = Na^{+} + REE^{3+}$ and $Ti^{4+} + Ca^{2+} = Nb^{5+} + Na^{+}$. The increased contents of Nb^{5+} and REE^{3+} are only to a minor degree compensated through the $F^{1-} = O^{2-}$ substitution. The chondrite normalised REE patterns of the minerals develop in a similar way in the two sequences, showing relative La-enrichment and Y-depletion from the less to the most evolved rocks.

Hainite has not previously been found in the Ilímaussaq complex. It was here identified in a pulaskite pegmatite sample by a combination of X-ray diffraction giving the unit cell dimensions a = 9.5923(7) Å, b = 7.3505(5) Å, c = 5.7023(4) Å, α = 89.958(2)°, β = 100.260(1)°, γ = 101.100(2)°, and X-ray powder pattern and electron microprobe data giving the empirical formula $(Ca_{1.62}Zr_{0.16}Y_{0.22})(Na_{0.87}Ca_{1.11})(Ca_{1.65}REE_{0.35})Na(Ti_{0.81}Nb_{0.09}Fe_{0.08}Zr_{0.02})(Si_2O_7)_2O_{0.99}F_{2.96}$. Based on published and the present data it is documented that minerals from the hainite-götzenite solid solution series show a compositional variation between the ideal end members $(Y,REE,Zr)Na_2Ca_4Ti(Si_2O_7)_2OF_3$ and $NaCa_6Ti(Si_2O_7)_2OF_3$.

Keywords: Ilímaussaq, rinkite, nacareniobsite-(Ce), hainite, götzenite.

Jørn G. Rønsbo [jornronsbo@gmail.com], Henning Sørensen, Department of Geosciences and Natural Resource Management, University of Copenhagen, Øster Voldgade 10, DK-1350 Copenhagen K, Denmark. Encarnacion Roda-Robles,[encar.roda@ehu.es] Departamento de Mineralogia y Petrologia, Universidad del Pais Vasco/EHU Apdo. 644, E-48080, Bilbao, Spain, François Fontan, Pierre Monchoux, Université de Toulouse, UPS (FSI-OMP), CNRS, IRD-GET, 14 Avenue Edouard Belin, F-31400 Toulouse, France.

Na-bearing disilicates enriched in Ti, Nb, Zr and/or REE (including Y) are typical minerals in agpaitic nepheline syenites both as rock forming minerals and in pegmatites. In the Ilímaussaq alkaline complex, vuonnomite, lomonosovite, murmanite, hiortdahlite, rosenbuschite, epistolite, rinkite and nacareniobsite-(Ce) are present (Petersen 2001). The complex is the type locality for the latter three minerals.

Rinkite and nacareniobsite-(Ce) belong to the rinkite group of minerals together with mosandrite, whereas the other mineral pair of interest in this work, hainite and götzenite, belong to the rosenbuschite

---

[*] Contribution to the Mineralogy of Ilímaussaq no. 145
[†] Deceased

group together with rosenbuschite, seidozerite, kochite and grenmarite. Based on the structural topology, Sokolova (2006) defined four groups of titanium disilicates where the rinkite and rosenbuschite groups belong to the same group (Group I). In this paper we will refer to the traditionally used classification, and when referring to structural sites we use the following general formula for both mineral groups: $M(1)_2M(2)_2M(3)_2M(4)M(5)(Si_2O_7)_2F_2X_2$.

The present study is a paragenetic and mineral chemical investigation of rinkite, nacareniobsite-(Ce) and hainite. The aim of the study is to document the compositional variations in the rinkite–nacareniobsite-(Ce) solid solution series, which has never been investigated, neither in the Ilímaussaq alkaline complex nor elsewhere. During the study a rosenbuschite-group mineral was discovered with the chemical composition of hainite which has not previously been identified in the Ilímaussaq complex.

Geological setting

The Ilímaussaq alkaline complex belongs to the late Precambrian Gardar province of South Greenland (e.g. Upton 2013). The most differentiated and undersaturated rocks in the province are found in this complex, which is characterised by extreme enrichment in incompatible elements including Nb, Zr, REE and F. The basic description of the complex was given by Ussing (1912). Discussions of the petrology and geochemistry of the complex are presented by Larsen & Sørensen (1987), Sørensen & Larsen (1987), Bailey *et al.* (2001), Marks & Markl (2001) and Sørensen (2006). Geological and geochemical evidence indicates that the complex was emplaced in several pulses leading to the formation of an incomplete augite syenite shell, followed by acid peralkaline sheets in the top of the intrusion and finally, a volumetrically dominant sequence of layered perakaline nepheline syenites.

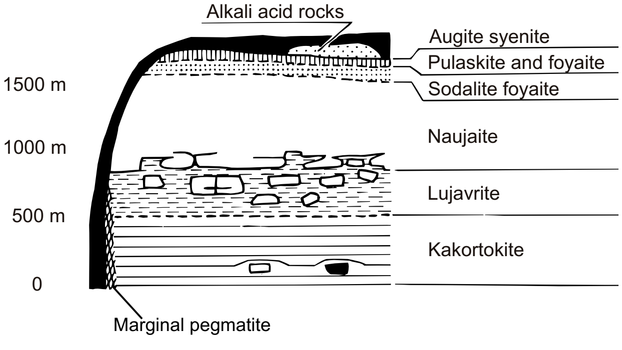

Fig. 1. Diagrammatic E–W section of the southern part of the Ilímaussaq alkaline complex (modified after Andersen *et al.* 1981).

According to one model, the main pulse of peralkaline silica-undersaturated magma led to the formation of the main layered sequence of cumulitic nepheline syenites consisting of a roof sequence, a floor sequence, and an intermediate horizon between the roof and the floor zones. Sørensen (2006) suggested that the floor sequence and the intermediate horizon were formed by a separate magma pulse. In all models, the roof sequence (pulaskite, foyaite, sodalite foyaite and naujaite) crystallized successively downwards from a single magma which became progressively more differentiated. Following Sørensen (2006), a later magma pulse intruded the consolidated roof sequence and formed the floor cumulates (kakortokite) and the intermediate horizon (lujavrite), and it is suggested that the marginal pegmatite represents the early stage of evolution of this melt (Fig. 1). The floor cumulates consist of a layered sequence of kakortokites made of tripartite units, with each unit composed of a lower black layer rich in arfvedsonite which grades upward into a red facies rich in eudialyte which again grades upward into a white facies rich in alkali feldspar. The kakortokites grade upwards into the intermediate horizon which is made up of various types of lujavritic rocks. Moreover, lujavrites also intrude and engulf the overlying roof sequence and locally penetrate into volcanic rocks in the roof, as is the case in the Kvanefjeld area in the northern part of the complex (Sørensen *et al.* 2011). In this work, for the sake of clarity of presentation, we treat the marginal pegmatite, kakortokite and lujavrite together as the 'floor sequence'.

Mineralogy of rinkite, nacareniobsite-(Ce), hainite and götzenite

Rinkite and nacareniobsite-(Ce)

Rinkite, $Na_2Ca_4REETi(Si_2O_7)_2OF_3$, was first described by Lorenzen (1884) based on material collected by K.J.V. Steenstrup in the years 1874, 1876 and 1877 in the Kangerluarsuk area of the Ilímaussaq complex. The type material is kept in the Natural History Museum of Denmark, University of Copenhagen, unfortunately without any information about the exact locality. The crystal structure of rinkite was established by Galli and Alberti (1971).

Some authors, including Fleischer (1958, 1987) and Sokolova & Cámara (2008), argued that rinkite is identical to mosandrite, originally described from nepheline syenite pegmatites in Langesund Fjord, Norway, by Erdmann (1841) and reinvestigated by Brøgger (1890). Johnstrupite (Brøgger 1890) from Langesund, Norway, and rinkolite and lovchorrite (Bohnstedt 1926) from Khibina, Russia, have also been described as minerals related to rinkite or used as synonyms. Fleischer (1958, 1987) suggested the use of mosandrite in favour of rinkite, rinkolite, lovchorrite and johnstrupite, whereas Slepnev (1957) considered mosandrite to represent an intensively Na- and Ca-leached product of minerals such as rinkite, johnstrupite and rinkolite. Petersen *et al.* (1989) confirmed the existence of a Na- and Ca-leaching process in the niobian rinkite analogue nacareniobsite-(Ce) and further documented that mosandrite crystals from the type locality consist of a Na-Ca-poor fine-grained intergrowth of two minerals. The johnstrupite sample from Barkevik, Langesund (Brøgger 1890) is identical to rinkite (Bellezza *et al.* 2009a).

Recent crystal chemical investigation of mosandrite crystals from the type locality in Langesund, Norway, by Sokolova & Cámara (2008) and Bellezza *et al.* (2009b) led to different results and conclusions. Sokolova & Cámara (2008) concluded that the crystal structure of the museum specimen labelled as mosandrite is chemically and topologically identical to rinkite from the Ilímaussaq alkaline complex. However, they later corrected their statement (Cámara *et al.* 2011) and concluded that the investigated crystal was not mosandrite but rinkite, in agreement with Bellezza *et al.* (2009b) who concluded that mosandrite, $\mathrm{Ti(\square,Ca,Na)_3(Ca,REE)_4(Si_2O_7)_2[H_2O,OH,F]_4{\sim}1H_2O}$, is a unique mineral species of the rinkite group and differs from rinkite in chemical composition, with low Ca, Na and F contents and a high amount of H_2O.

Cámara *et al.* (2011) studied the crystal structure of four mineral samples from different localities: Kangerluarsuk, Ilímaussaq, Greenland; Mont Saint-Hilaire, Canada; and two in the Khibina Massif, Russia. They concluded that the four investigated specimens are rinkite and defined rinkite as a valid mineral species with the ideal formula $\mathrm{Na_2Ca_4REETi(Si_2O_7)_2OF_3}$. They further suggested a formal redefinition of mosandrite as a valid mineral species. The latest IMA (International Mineralogical Association) official List of Mineral Names (October 2013) includes both mosandrite and rinkite as redefined valid species.

Nacareniobsite-(Ce), $\mathrm{Na_3Ca_3REENb(Si_2O_7)_2OF_3}$, was described by Petersen *et al.* (1989) from lujavrite in the Kvanefjeld area of the Ilímaussaq complex and suggested to be a Nb-rich rinkite analogue related by the substitution $\mathrm{Nb^{5+} + Na^{+} = Ti^{4+} + Ca^{2+}}$. The crystal structure determination by Sokolova & Hawthorne (2008) confirmed this conclusion.

Table 1. X-ray powder patterns of hainite and götzenite

1		2		3	
d-obs	I	d-obs	I	d-obs	I
		5.57	5	5.640	10
				5.220	10
4.295	10	4.29	5	4.370	10
3.961	50	3.90	10	3.970	20
3.557	10	3.59	5	3.610	10
3.340	10				
3.259	10	3.27	10	3.290	20
3.073	90	3.07	80	3.090	90
2.961	100	2.97	100	2.980	100
2.824	30	2.81	10	2.850	10
2.628	50	2.61	20	2.640	30
2.493	50	2.49	10	2.500	50
2.309	10	2.30	5	2.310	10
2.244	20	2.24	5	2.250	20
2.200	30	2.19	5	2.210	20
				2.120	10
2.043	20	2.04	5	2.060	10
1.984	20			1.991	10
1.896	70	1.90	30	1.913	80
1.865	30			1.871	20
1.822	50	1.83	10	1.833	70
1.787	10	1.79	5	1.797	20

1. Hainite, Johan & Cech 1989. 2 Hainite, Ilímaussaq alkaline complex sample 104029 , Debye Scherrer camera (360 mm) Toulouse, this paper. 3. Götzenite, Sharygin *et al.* 1996.

Hainite and götzenite

In a pegmatite in the uppermost part of the pulaskite in the Ilímaussaq complex, Semenov (1969) found a mineral which is low in REE and high in Ca compared to rinkite, and named it Ca-rinkolite. The sample described by Semenov, and specimens collected by the authors, are included in the present study. Our X-ray diffraction data (Table 1) show that the mineral belongs to the rosenbuschite group of Na, Ti and Zr disilicates and is a member of the götzenite–hainite solid solution series.

Götzenite was first described by Sahama & Hytönen (1957) from nephelinite, Mt. Shareru, Zaire, and the chemical data given by Sahama & Hytönen (1957) are REE- and Zr-free but the high Al content indicates a considerable amount of mineral impurities. The crystal structure was determined by Canillo *et al.* (1972). A götzenite sample from Pian di Celli (Sharygin *et al.* 1996) is low in Zr and REE and approaches the ideal composition $\mathrm{NaCa_6Ti(Si_2O_7)_2OF_3}$. Zirconium- and/or REE-bearing götzenite is reported by Sharygin *et al.* (1996), Christiansen *et al.* (2003) and Bellezza *et al.* (2004). The crystal structural data show that Zr can substitute for Ca in the M(1) site (Christiansen *et al.* 2003, Bellezza *et al.* 2004) and for Ti in the M(5) site (Christiansen *et al.* 2003), and the REE substitute for Ca in the M(1) and M(3) sites (Atencio *et al.* 1999, Christiansen *et al.* 2003).

Hainite was first described by Blumrich (1893) in phonolites from Hradiste, Bohemia. A reinvestigation of the type material by Johan and Cech (1989) included microprobe analyses and X-ray powder diffraction data, and they concluded that hainite is isostructural with götzenite but is different in having the (Ca+Na)/(Ti+Zr+Nb) ratio equal to 4, whereas this ratio is 7 in götzenite and 3 in rosenbuschite. Hainite is also described from the Pocos de Caldas alkaline complex, Minas Gerais, by Rastsvetaeva *et al.* (1995) and Atencio *et al.* (1999). According to Rastsvetaeva *et al.* (1995), Ca and Na in hainite are ordered in two independent M(2) sites, leading to space group P1, whereas they are randomly distributed in götzenite, space group $P\bar{1}$ (Canillo *et al.* 1972). Christiansen *et al.* (2003) did not observe any ordering in the M(2) site in hainite from Langesund and reported space group $P\bar{1}$. The same result was obtained by Giester *et al.* (2005) by a crystal structural investigation of hainite from Hradiste. Christiansen *et al.* (2003) observed a small excess Na over Ca in the M(2) site for the sample from Langesund and concluded that "the overall Na/Ca value of this specimen corresponds to that of hainite (Johan & Cech 1989) and we therefore consider the sample as hainite". Based on the crystal structural determination of hainite published by Rastsvetaeva *et al.* (1995), Atencio *et al.* (1999) suggested the simplified formula for hainite to be $Na_2Ca_5Ti(Si_2O_7)_2(OH)_2F_2$.

Electron microprobe analysis and formula calculation

The major part of the electron microprobe analyses presented in this paper were performed on a JEOL 733 Superprobe at the Department of Geosciences and Natural Resource Management, University of Copenhagen. Analytical conditions were 15 nA beam current, 5 microns beam size, and 15 kV acceleration potential except for F which was analysed at 10 kV in order to reduce possible F migration under the electron beam. This was based on analyses of the rinkite type material for F at 8 kV giving 7.7±0.3 wt.% F, at 10 kV giving 7.8±0.3 wt.% F, at 12 kV giving 7.8±0.3 wt.% F, and at 15 kV giving 7.2±0.2 wt.% F. The following X-ray lines and standards were used: FKα: apatite, NaKα: albite, SiKα and CaKα: wollastonite, FeKα: haematite, TiKα: TiO_2, ZrLα: baddeleyite, NbLα: columbite, LaLα: synthetic glass containing 15 wt% La_2O_3, CeLα: CeO_2, PrLβ: $Pr_3Ga_5O_{12}$, NdLα: $Nd_3Ga_5O_{12}$, SmLα: $SmFeO_3$, YLα: $Y_3Al_5O_{15}$. The accuracy of the REE analyses are discussed in Rønsbo (1989).

Of the analyses used here, those from sample 104024, 104034 and 104038 were performed on a Camebax SX50 at Laboratoire de Minéralogie, Université Poul Sabatier, Toulouse. These results have been calibrated towards internal standards to give results comparable to the data obtained in Copenhagen.

The empirical formulae were calculated on the basis of 4 Si in accordance to the structural refinements of the rinkite and rosenbuschite group minerals which show the tetrahedral position to be fully occupied by silicon (Christiansen *et al.* 2003; Belezza *et al.* 2004; Sokolova & Cámara 2008; Sokolova & Hawthorne 2008; Bellezza *et al.* 2009b).

All sample numbers are GGU numbers. The accepted analyses are given in a supplementary data file at the web site http://2dgf.dk/publikationer/bulletin/190bull62.html.

Occurrence, zonation and compositional variation of hainite and rinkite–nacareniobsite-(Ce) in the Ilímaussaq complex

Pulaskite pegmatite

The pegmatite forms a lenticular body in a small occurrence of quartz syenite and pulaskite overlying foyaite on the plateau around Point 535 m between the fiords Kangerluarsuk and Tunulliarfik (Steenfelt 1981). The contact relations are obscured by scree, but pulaskite and its pegmatites are most probably intrusive into the quartz syenite.

The pegmatite is composed of large plates of perthitic alkali feldspar with minor clinopyroxene and amphibole. Hainite occurs as prismatic brown grains that may attain a length of more than 5 cm. Semenov (1969) described the mineral from this locality, referred it to the rinkite group and named it Ca-rinkolite. The name was, however, never approved by the IMA. New X-ray powder diffraction data (Table 1) and the unit cell dimensions a = 9.5923(7) Å, b = 7.3505(5) Å, c=5.7023(4) Å, α = 89.958(2)°, β = 100.260(1)°, γ = 101.100(2)° (numbers in parentheses are 1σ for the last digit), established by the single crystal method, show that the mineral belongs to the rosenbuschite group and is either götzenite or hainite.

The mineral was analysed by electron microprobe in three different samples (104029, 104373 and an unnumbered sample donated by E. Semenov). The mean values for the different samples do not differ significantly, and the analysis in Table 2 (no. 1) is the mean of all 56 analyses. This composition is that of hainite rather than götzenite. The formula calculation gave a total number of cations of 11.96 compared to the ideal

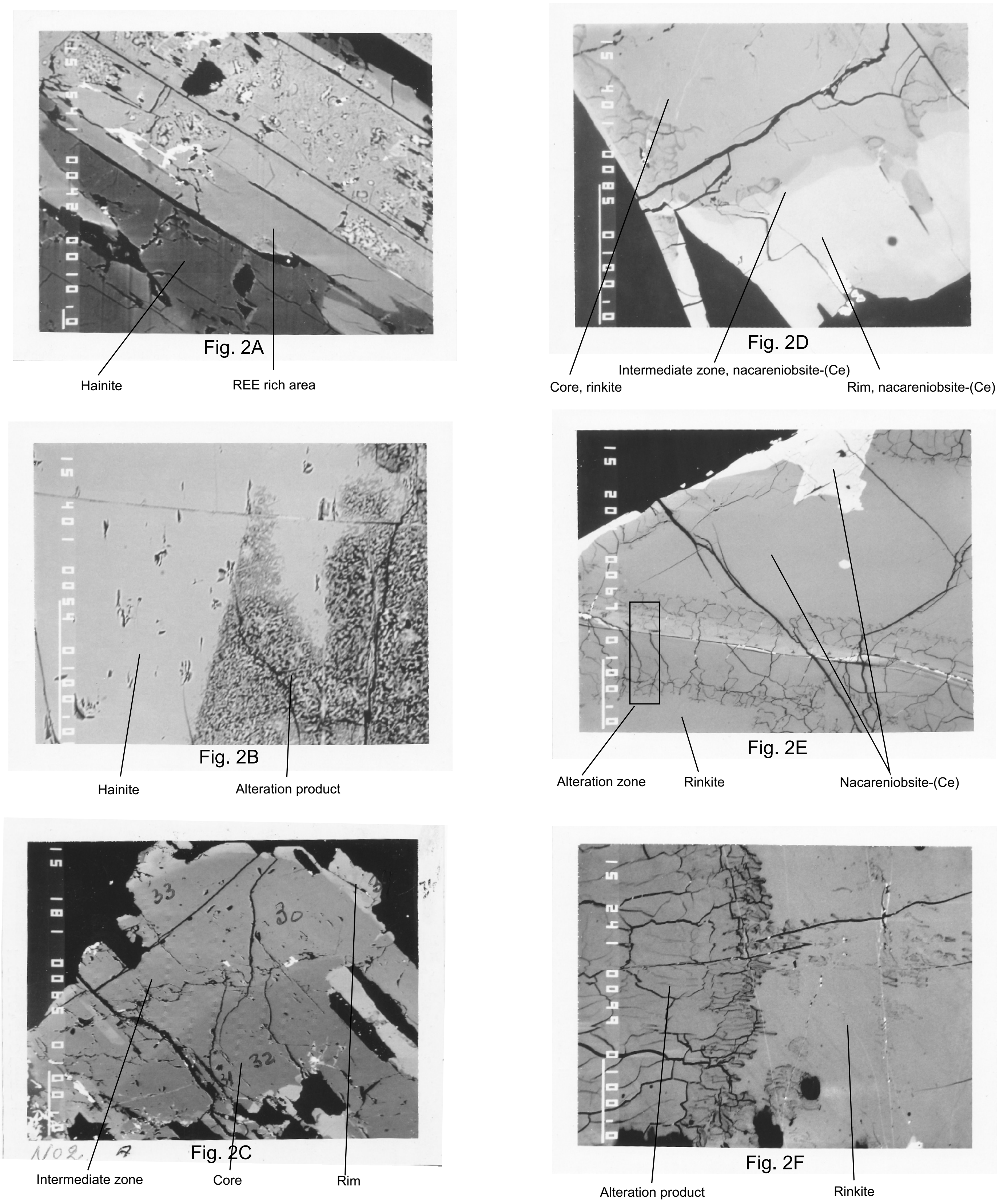

Fig. 2. Backscattered electron images of hainite, rinkite and nacareniobsite-(Ce). **A**, pulaskite pegmatite sample 104029; hainite crystal with REE-enriched area. **B**, Pulaskite pegmatite sample 104373; partly altered hainite. **C**. Sodalite foyaite sample 104375; zoned rinkite. **D**, Naujaite pegmatite sample 104013; zoned rinkite–nacareniobsite-(Ce) crystal. **E**, Naujaite pegmatite sample 104013; zoned rinkite–nacareniobsite-(Ce) crystal with alteration zone. **F**, Naujaite pegmatite sample 104013; partly altered rinkite.

Table 2.
Microprobe analyses of hainite, rinkite and nacareniobsite-(Ce) in pulaskite pegmatite, sodalite foyaite, naujaite and naujaite pegmatite

No.	1	2	3	4	5	6	7	8	9
Rock	Pul.pegmatite	Pul.pegmatite	Pul.pegmatite	Sodal. foyaite	Sodal. foyaite	Sodal. foyaite	Naujaite	Nau.pegmatite	Nau.pegmatite
Sample	Average	104029	104373	104375	104375	104375	104001	104013	104013
Mineral	Hainite	Rinkite	Alteration product	Rinkite	Rinkite	Rinkite	Rinkite	Rinkite	Nacareniobsite-(Ce)
Zone				Core	Mantle	Rim		Core	Core
N	56	3	2	2	2	4	6	5	6
Oxides wt%									
SiO_2	30.65 (.02)	30.02 (.07)	26.80 (.08)	29.67 (.08)	29.57 (.08)	29.09 (.06)	29.64 (.05)	29.00 (.05)	29.38 (.05)
TiO_2	8.23 (.01)	8.91 (.05)	12.74 (.08)	6.17 (.06)	6.28 (.06)	5.28 (.04)	5.64 (.04)	5.43 (.04)	4.32 (.03)
ZrO_2	2.87 (.03)	0.82 (.11)	2.28 (.32)	2.21 (.30)	0.04 (.01)	0.57 (.07)	0.53 (.06)	0.38 (.04)	0.11 (.02)
Nb_2O_5	1.43 (.02)	1.70 (.12)	4.06 (17)	3.28 (.16)	4.62 (.17)	6.28 (.14)	6.55 (.13)	7.12 (.13)	9.35 (.13)
FeO	0.70 (.01)	n.d.	0.66 (.05)	0.20 (.03)	0.08 (.02)	n.d.	n.d	0.05 (.01)	0.03 (.00)
CaO	31.34 (.02)	28.64 (.10)	19.85 (.10)	26.54 (.09)	24.90 (.11)	22.06 (.07)	23.14 (.06)	23.04 (.06)	22.44 (.06)
Na_2O	7.44 (.02)	7.58 (.07)	3.46 (.09)	7.69 (.07)	8.26 (.08)	9.03 (.06)	9.25 (.06)	9.36 (.06)	9.60 (.05)
La_2O_3	0.95 (.01)	1.65 (.05)	2.23 (.07)	2.33 (.07)	2.87 (.08)	3.08 (.05)	2.92 (.04)	3.89 (.05)	4.67 (.08)
Ce_2O_3	3.14 (.02)	5.36 (.07)	5.88 (.11)	6.65 (.09)	8.22 (.10)	9.36 (.07)	9.12 (.06)	9.86 (.07)	10.02 (.07)
Pr_2O_3	0.45 (.02)	0.86 (.11)	0.65 (.11)	0.81 (.13)	1.04 (.14)	1.24 (.10)	1.07 (.09)	1.00 (.09)	1.01 (.08)
Nd_2O_3	2.06 (.03)	3.60 (.13)	3.41 (.16)	4.02 (.17)	4.56 (.18)	5.12 (.13)	5.04 (.10)	3.85 (.11)	3.42 (.09)
Sm_2O_3	0.34 (.01)	0.66 (.07)	0.70 (.08)	0.74 (.09)	0.69 (.09)	0.92 (.07)	0.81 (.05)	0.52 (.05)	0.44 (.04)
Y_2O_3	3.17 (.01)	3.48 (.05)	5.27 (.06)	2.08 (.07)	1.72 (.07)	1.41 (.05)	2.07 (.04)	1.93 (.05)	1.29 (.04)
F	7.17 (.08)	7.01 (.30)	5.07 (.32)	8.03 (.43)	7.61 (.40)	7.90 (.30)	7.10 (.24)	6.69 (.25)	6.88 (.20)
Total	99.94	100.29	93.06	100.42	100.46	101.34	102.88	102.12	102.96
-O for F	-3.02	-2.95	-2.13	-3.38	-3.20	-3.33	-2.99	-2.82	-2.90
	96.92	97.34	90.93	97.04	97.26	98.01	99.89	99.30	100.06
Cations based on 4 Si									
Si	4.00	4.00	4.00	4.00	4.00	4.00	4.00	4.00	4.00
Ti	0.81	0.89	1.43	0.63	0.64	0.55	0.57	0.56	0.44
Zr	0.18	0.05	0.17	0.15	0.00	0.04	0.03	0.03	0.01
Nb	0.08	0.10	0.27	0.20	0.28	0.39	0.40	0.44	0.58
Fe	0.08	0.00	0.08	0.02	0.01	0.00	0.00	0.01	0.00
Ca	4.38	4.09	3.17	3.83	3.61	3.25	3.35	3.40	3.27
Na	1.88	1.95	1.00	2.01	2.16	2.40	2.42	2.50	2.53
La	0.05	0.08	0.12	0.12	0.14	0.16	0.15	0.20	0.23
Ce	0.15	0.26	0.32	0.33	0.41	0.47	0.45	0.50	0.50
Pr	0.02	0.04	0.04	0.04	0.05	0.06	0.05	0.05	0.05
Nd	0.10	0.17	0.18	0.19	0.22	0.25	0.24	0.19	0.17
Sm	0.01	0.03	0.04	0.03	0.03	0.04	0.04	0.02	0.02
Y	0.22	0.25	0.42	0.15	0.12	0.10	0.15	0.14	0.09
F	2.96	2.95	2.39	3.42	3.26	3.44	3.03	2,92	2.96
Cations	11.96	11.91	11.24	11.70	11.67	11.71	11.85	12.04	11.89
Charges	32.81	32.88	34.61	32.41	32.27	32.45	32.76	33.18	32.95

N: number of analyses. n.d.: not detected. Numbers in parentheses are standard deviations calculated on the basis of the total counting time and count rates on peak and background and given in weight percent.

Table 3.

Microprobe analyses of rinkite and nacareniobsite-(Ce) in naujaite pegmatite, marginal pegmatite, kakortokite and lujavrite

No.	1	2	3	4	5	6	7	8
Rock	Nau.pegmatite	Nau.pegmatite	Nau.pegmatite	Marg. pegmatite	Kakortokite -6	Kakortokite +7	Lujavrite	Lujavrite
Sample	104013	104013	104013	104358	104024	104016	104010	104010
Mineral	Alteration	Nacareniobsite-(Ce)	Nacareniobsite-(Ce)	Rinkite	Rinkite	Rinkite	Nacareniobsite-(Ce)	Nacareniobsite-(Ce)
Zone		Intermediate	Rim					
N	2	2	6	3	3	13	4	3
Oxides wt%								
SiO_2	28.40 (.08)	28.57 (.08)	27.98 (.04)	29.07 (.07)	28.66 (.07)	29.55 (.03)	28.30 (.06)	28.50 (.07)
TiO_2	6.01 (.06)	4.03 (.05)	1.32 (.02)	6.87 (.05)	7.12 (.05)	5.86 (.02)	3.29 (.03)	1.50 (.03)
ZrO_2	0.37 (.06)	0.38 (.07)	0.12 (.01)	1.63 (.23)	0.78 (.11)	0.57 (.04)	0.12 (.02)	0.43 (.06)
Nb_2O_5	8.92 (.23)	10.22 (.24)	14.31 (.16)	3.04 (.12)	4.23 (.14)	6.11 (.07)	10.66 (.18)	13.77 (.23)
FeO	n.d.	n.d.	n.d.	n.d.	0.06 (.01)	0.03 (.00)	n.d.	n.d.
CaO	18.80 (.09)	20.96 (.10)	18.30 (.06)	20.43 (.08)	23.03 (.08)	22.62 (.04)	19.72 (.07)	19.06 (.08)
Na_2O	2.97 (.09)	10.08 (.10)	11.18 (.06)	8.15 (.07)	7.90 (.07)	8.76 (.03)	9.95 (.07)	10.93 (.09)
La_2O_3	5.48 (.10)	4.80 (.09)	3.47 (.05)	2.93 (.06)	3.51 (.04)	3.53 (.03)	4.83 (.08)	4.34 (.07)
Ce_2O_3	11.40 (.12)	10.79 (.11)	11.47 (.07)	8.82 (.09)	10.10 (.10)	10.02 (.04)	11.25 (.08)	11.44 (.10)
Pr_2O_3	1.07 (.14)	1.16 (.14)	1.35 (.08)	1.22 (.12)	1.00 (.12)	1.14 (.05)	1.14 (.10)	1.19 (.12)
Nd_2O_3	3.71 (.17)	4.04 (.17)	5.45 (.10)	4.99 (.15)	4.99 (.15)	4.89 (.07)	4.04 (.12)	4.91 (.15)
Sm_2O_3	0.54 (.08)	0.55 (.08)	0.60 (.04)	0.83 (.06)	0.78 (.05)	0.77 (.04)	0.64 (.05)	0.55 (.07)
Y_2O_3	1.63 (.07)	1.07 (0.6)	0.49 (.03)	3.08 (.05)	1.69 (.06)	1.42 (.03)	0.95 (.06)	0.67 (.06)
F	4.46 (.24)	6.76 (.38)	6.29 (.19)	8.13 (.35)	6.74 (.30)	7.23 (.14)	6.21 (.23)	6.66 (.30)
Total	93.76	103.41	102.33	99.19	100.59	102.50	101.10	103.95
-O for F	-1.88	-2.85	-2.65	-3.42	-2.84	-3.04	-2.61	-2.80
	91.88	100.56	99.68	95.77	97.75	99.46	98.49	101.15
Cations based on 4 Si								
Si	4.00	4.00	4.00	4.00	4.00	4.00	4.00	4.00
Ti	0.64	0.42	0.14	0.71	0.75	0.60	0.35	0.16
Zr	0.03	0.03	0.01	0.11	0.05	0.04	0.01	0.03
Nb	0.57	0.65	0.92	0.19	0.27	0.37	0.68	0.87
Fe	n.d.	n.d.	n.d.	n.d.	0.01	0.00	n.d.	n.d.
Ca	2.84	3.14	2.80	3.01	3.44	3.28	2.99	2.87
Na	0.81	2.73	3.09	2.17	2.13	2.30	2.72	2.97
La	0.28	0.25	0.18	0.15	0.18	0.18	0.25	0.22
Ce	0.59	0.55	0.60	0.44	0.52	0.50	0.58	0.59
Pr	0.06	0.06	0.07	0.06	0.05	0.06	0.06	0.06
Nd	0.19	0.20	0.28	0.25	0.25	0.24	0.20	0.25
Sm	0.03	0.03	0.03	0.04	0.04	0.04	0.03	0.03
Y	0.12	0.08	0.04	0.22	0.13	0.10	0.07	0.05
F	1.98	2.99	2.84	3.54	2.97	3.10	2.78	2.96
Cations	10.16	12.14	12.16	11.35	11.82	11.71	11.94	12.10
Charges	31.83	33.57	33.49	31.90	33.09	32.63	33.11	33.42

N: number of analyses. n.d.: not detected. Numbers in parentheses are standard deviations calculated on the basis of the total counting time and count rates on peak and background and given in weight percent.

value 12.00. The calculated F content is 2.96 apfu and the number of positive charges is 32.81.

The rosenbuschite group minerals are generally Zr-bearing. The mean value for Zr in the hainite from Ilímaussaq is 2.9 wt.% ZrO_2, which is low compared to hainite and götzenite from other localities (Cundari & Ferguson 1991; Sharygin *et al.* 1996; Johan & Cech 1989; Christiansen *et al.* 2003). The Ti+Nb content is 0.90 apfu (atoms per formula unit) and the apparent deficit, 0.10 apfu, is compensated by 0.08 Fe apfu and 0.02 Zr apfu. Most of the Zr, 0.16 apfu, is assigned to the M(1) site.

The Ilímaussaq hainite is rich in REE, 0.55 apfu, compared to götzenite and hainite from most localities (Sahama & Hytönen 1957; Cundari & Ferguson 1991; Sharygin *et al.* 1996; Christiansen *et al.* 2003; Johan & Cech 1989; Atencio *et al.* 1999), and only hainite from Langesund (Christiansen *et al.* 2003) has a comparable REE content, 0.44 apfu. It is notable that Y is the dominant REE in the hainite from Ilímaussaq. The crystal chemical formula for the average hainite from the pulaskite pegmatite is: $(Ca_{1.62}Zr_{0.16}Y_{0.22})(Na_{0.87}Ca_{1.11})(Ca_{1.65}REE_{0.35})Na(Ti_{0.81}Nb_{0.09}Fe_{0.08}Zr_{0.02})(Si_2O_7)_2O_{0.99}F_{2.96}$.

Backscattered electron images and microprobe analyses of sample 104029 revealed mineral grains enriched in REE compared to hainite (Fig. 2A). The interface towards hainite is sharp, without any sign of resorption, and parallel to one of the traces of the cleavages observed in hainite. These grains have a composition like rinkite (Table 2 no. 2). Compared to hainite, the contents of Ti, Nb and REE are higher and the Zr and Fe contents are lower, while the Y/(La+Ce) ratio is 0.74 compared to 1.10 in hainite. The REE patterns for hainite and two rinkite grains are given in Fig. 3A.

In thin section it is seen that hainite is altered to a brown and black material which in a backscattered electron image appears to be a fine-grained intergrowth of more than one phase (Fig. 2B). The mean composition is given in Table 2 no. 3.

Sodalite foyaite

The sodalite foyaite is characterised by a foyaitic texture formed by platy crystals of alkali feldspar up to 3 cm long, with interstitial nepheline, sodalite, Na-clinopyroxene, Na-amphibole and aenigmatite. Rinkite is an accessory mineral occurring as prismatic grains varying in size from micron scale to a few millimetres long. The crystals are often in parallel intergrowth with clinopyroxene and appear to have formed interstitially at a late stage in the crystallisation of the sodalite foyaite. Aggregates of prismatic rinkite are also embedded in analcime.

Two samples from the uppermost part of the sodalite foyaite (104374 and 104375) and a lower sample from just above the underlying naujaite (154346) have been analysed. All rinkite crystals are zoned with the lowest Nb content in the central part of the crystal. The highest Nb content, 7.4 wt.% Nb_2O_5, 0.46 Nb apfu, is found in the sample close to the naujaite. A backscattered electron image of rinkite in sample 104375 is shown in Fig. 2C. In the core of this crystal, Ti+Nb add up to 0.83 apfu (Table 2 no. 4), whereas they add up to 0.92 apfu in the mantle of the crystal (Table 2 no. 5) and 0.94 apfu in the narrow rim (Table 2 no. 6). The Zr content is normally less than 0.7 wt% ZrO_2, but the core of the zoned crystal has 2.2 wt% ZrO_2. Such a Zr enrichment in rinkite is only observed in this sample. The analysed rinkite crystals in samples 104374 and 154346 have Ti+Nb contents between 0.94 and 1.01 apfu.

Cerium is the dominant REE in the rinkite. In the Zr-enriched core the total REE content is 0.86 apfu (Table 2 no. 4). In other parts of this crystal the REE contents vary between 0.97 and 1.08 apfu (Table 2 nos 5 and 6).

The REE patterns for different parts of zoned rinkite crystals in sample 104375 and 154346 are shown in Figs 3B and 3C. The shapes of the REE patterns for the core, mantle and rim of the zoned crystal in sample 104375 are rather similar in the LREE region, whereas a slight Y decrease takes place from the core to the rim (Fig. 3B). For rinkite in sample 154346 the REE pattern for the core is similar to those in Fig. 3B whereas the REE pattern for the rim shows a distinct LREE enrichment (Fig. 3C).

Naujaite

Naujaite was examined in samples from three localities in the complex. All are typical naujaite with more or less densely packed euhedral crystals of sodalite up to about 0.5 cm across. Sodalite can make up more than 50 vol.% of some rocks. Microcline perthite forms laths up to several centimetres long which poikilitically enclose numerous sodalite crystals. Aegirine is the predominant mafic mineral and occurs as large poikilitic grains. Arfvedsonite occurs as parallel intergrowths in aegirine but may also form poikilitic grains. When rinkite is present it forms prismatic crystals from few millimetres up to more than 1 cm long. Rinkite grows in parallel alignment with aegirine and arfvedsonite in analcime–natrolite aggregates.

Rinkite crystals from the investigated naujaite samples (104001, 104034 and 104038) are slightly zoned, with 5.4–6.0 wt% TiO_2 and 6.0–7.6 wt% Nb_2O_5. The Zr variation is 0.3–1.2 wt% ZrO_2. One analysis (sample 104001) is listed in Table 2 no. 7. The REE patterns for two slightly different parts of this crystal are shown in Fig. 3D.

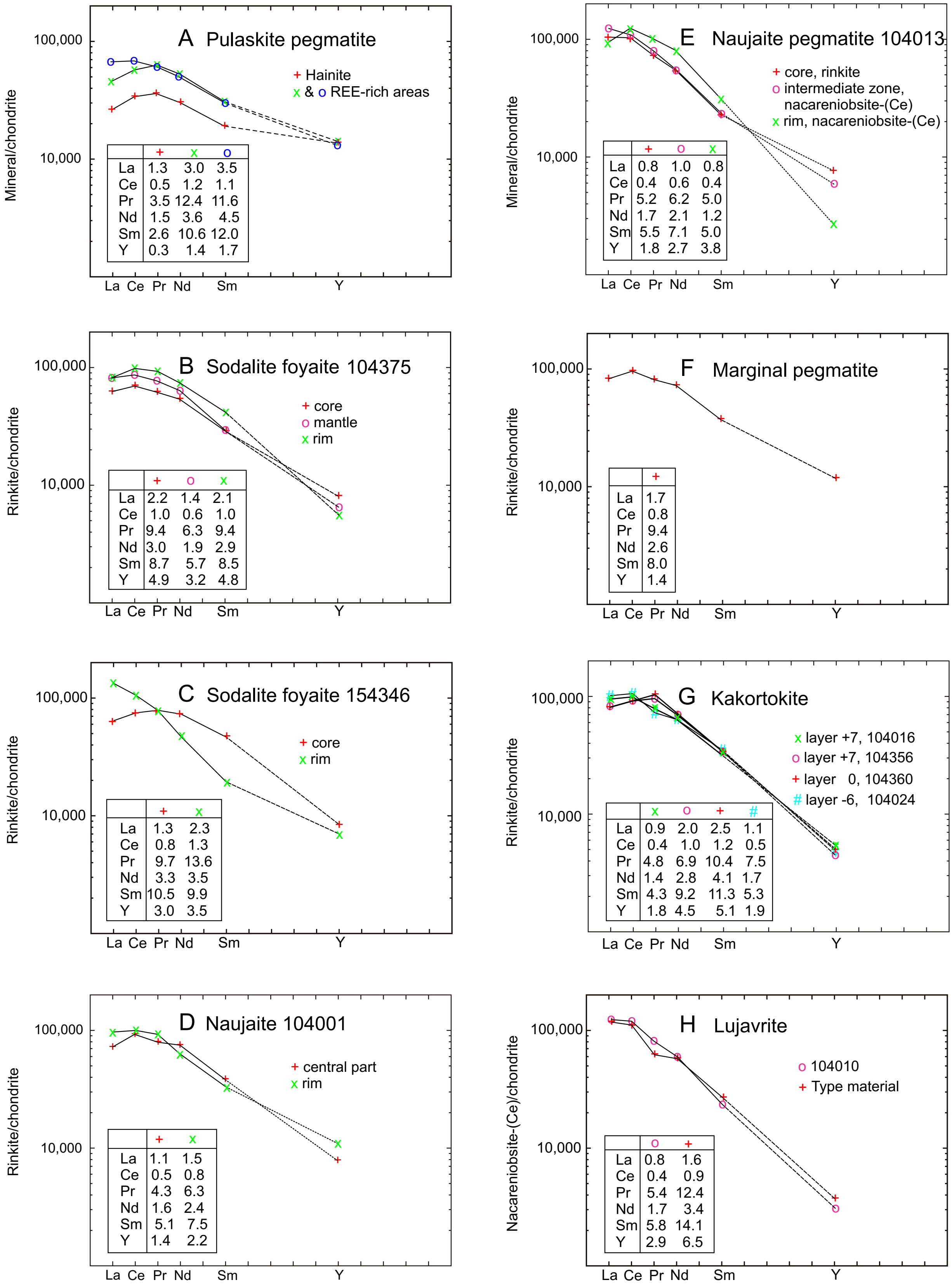

A

	+	x	o
La	1.3	3.0	3.5
Ce	0.5	1.2	1.1
Pr	3.5	12.4	11.6
Nd	1.5	3.6	4.5
Sm	2.6	10.6	12.0
Y	0.3	1.4	1.7

B

	+	o	x
La	2.2	1.4	2.1
Ce	1.0	0.6	1.0
Pr	9.4	6.3	9.4
Nd	3.0	1.9	2.9
Sm	8.7	5.7	8.5
Y	4.9	3.2	4.8

C

	+	x
La	1.3	2.3
Ce	0.8	1.3
Pr	9.7	13.6
Nd	3.3	3.5
Sm	10.5	9.9
Y	3.0	3.5

D

	+	x
La	1.1	1.5
Ce	0.5	0.8
Pr	4.3	6.3
Nd	1.6	2.4
Sm	5.1	7.5
Y	1.4	2.2

E

	+	o	x
La	0.8	1.0	0.8
Ce	0.4	0.6	0.4
Pr	5.2	6.2	5.0
Nd	1.7	2.1	1.2
Sm	5.5	7.1	5.0
Y	1.8	2.7	3.8

F

	+
La	1.7
Ce	0.8
Pr	9.4
Nd	2.6
Sm	8.0
Y	1.4

G

	x	o	+	#
La	0.9	2.0	2.5	1.1
Ce	0.4	1.0	1.2	0.5
Pr	4.8	6.9	10.4	7.5
Nd	1.4	2.8	4.1	1.7
Sm	4.3	9.2	11.3	5.3
Y	1.8	4.5	5.1	1.9

H

	o	+
La	0.8	1.6
Ce	0.4	0.9
Pr	5.4	12.4
Nd	1.7	3.4
Sm	5.8	14.1
Y	2.9	6.5

Fig. 3. Chondrite-normalised REE patterns for hainite, rinkite and nacareniobsite-(Ce) in different Ilímaussaq rocks. Chondrite normalisation factors from Boynton (1983). The standard deviations, listed in each diagram, are calculated on the basis of the total counting time and count rates on peak and background and given in per cent.

Naujaite pegmatite

The pegmatitic facies of naujaite (sample 104013) is generally rich in sodalite. Prismatic aegirine may grow between the sodalite crystals to form a poikilitic texture, and aegerine crystals often enclose arfvedsonite in parallel growth. Zoned rinkite–nacareniobsite-(Ce) grains occur in some pegmatites as prismatic crystals that may attain lengths of several centimetres and in places poikilitically enclose sodalite. Rinkite–nacareniobsite-(Ce) grains are often altered into a brownish material. Backscattered electron images show that the crystals are zoned, and often three zones with different Ti and Nb contents can be identified (Fig. 2D). Interlobal borders between the different zones indicate partial resorption prior to the formation of the next zone (Figs 2D and 2E).

The central and dominating parts of the crystals have 5.4–4.3 wt% TiO_2 and 7.1–9.4 wt% Nb_2O_5 and represent intermediate members of the rinkite–nacareniobsite-(Ce) solid solution series (Table 2 nos 8 and 9). The outer parts of the cores are often altered (Figs 2D–F) and show a marked Na and Ca leaching (Table 3 no. 1). The intermediate zones are less developed; when present they have 3.5–4.0 wt% TiO_2 and 9.8–10.9 wt% Nb_2O_5 (Table 3 no. 2). In the rim zones the Ti content is reduced to approximately 1.3 wt% TiO_2 whereas the Nb content is more than 14.0 wt% Nb_2O_5 (Table 3 no. 3).

The REE patterns for different zones in rinkite–nacareniobsite-(Ce) crystals in a naujaite pegmatite are shown in Fig. 3E. The three REE patterns represent mean values for rims, intermediate zones and cores. The rim zones have lower La and Y compared to the cores, whereas the intermediate zones show a slight La enrichment compared to the cores.

Marginal pegmatite

The marginal pegmatite occurs along the contact between the kakortokite and the country rock. The zone is characterised by its heterogeneity and consist of a matrix of massive kakortokite-like rocks cut by an anastomosing network of pegmatite veins. The thickness decreases upwards from about 100 m to 25 m (Bohse & Andersen 1981). At the south coast of Kangerluarsuk the pegmatite passes gradually laterally into the kakortokite. The matrix in the marginal pegmatite is supposed to be the border facies for the lower part of the complex, the kakortokites and lujavrites (Bohse & Andersen 1981; Sørensen 2006).

The pegmatite veins consist of crystals of eudialyte, sodalite, nepheline, perthitic alkali feldspar, albite and aegirine in a matrix of analcime, natrolite and tugtupite. Scattered grains of aenigmatite are partly overgrown with ussingite. Rinkite occurs as prismatic grains in natrolite and grows along the large crystals of aegirine. Rinkite prisms also form sheath-like aggregates. The examined sample (104358) is from the uppermost part of Laksetværelv close to the contact against the augite syenite.

The investigated crystals show only minor compositional variation, with 6.8–7.0 wt% TiO_2. The Zr and Y contents are slightly elevated, 1.6 wt% ZrO_2 and 3.1 wt% Y_2O_3, compared to most other rinkites. The analyses are characterized by low totals with a mean value of 95.77, indicating minor alteration although it was not observed during the analytical work. The Ti+Nb sum is 0.90 apfu whereas the Ti+Nb+Zr sum is 1.01 apfu (Table 3 no. 4). The REE pattern is given in Fig. 3F.

Kakortokite

The major part of the kakortokite is layered. A total of 29 unit are exposed and numbered from –11 to +17 (Bohse & Andersen 1981). Rinkite is a rare component and occurs as small prismatic grains up to 5 mm long, interstitial to laths of microcline. Rinkite may also grow along or across grains of aegirine and be associated with eudialyte. Sørensen & Larsen (1987) pointed out that the amount of rinkite appears to increase upwards in each unit.

The investigated rinkite material includes samples from unit –6 (104024), unit 0 (104360), and unit +7 (104016 and 104356). The TiO_2 content varies between 7.1 and 5.4 wt% TiO_2 (Table 3 nos 5 and 6), and the data suggest Nb enrichment in the rinkite upwards in the layered succession, from about 4 to about 6 wt% Nb_2O_5. The REE patterns for rinkite from units – 6, 0 and +7 are given in Fig. 3G. There is no significant stratigraphic evolution in REE.

Lujavrite and late veins

Two nacareniobsite-(Ce) bearing samples were examined. One of them (104010) is from the northern branch of Lilleelv at the head of Kangerluarsuk. It is a dyke of black arfvedsonite lujavrite intersecting naujaite pegmatite. The extremely fine-grained rock is faintly layered. It contains thin prismatic or ruler-shaped grains, up to 5 cm long, of nacareniobsite-(Ce). In thin section the rock is seen to be composed of stout prismatic grains of arfvedsonite which make up about 50 vol.%, albite laths, eudialyte, nepheline and rounded grains of sodalite and analcime. The prismatic grains of nacareniobsite-(Ce) are zoned and enclose needles of arfvedsonite and aegirine. The investigation also includes the type material from Kvanefjeld (Petersen *et al.* 1989). At this locality nacareniobsite-(Ce) occurs in dissolution cavities in black arfvedsonite lujavrite. The mineral is clearly of late- and post-magmatic origin, in accordance with its presence in late ussingite veins.

In the zoned nacareniobsite-(Ce) grains in sample 104010 the Nb content varies between 10.7 and 13.8 wt% Nb_2O_5. Selected analyses are listed in Table 3 nos 7 and 8. The REE patterns for nacareniobsite-(Ce) from the two different localities are very similar (Fig. 3H).

Discussion

The rinkite–nacareniobsite-(Ce) solid solution series

Structural data (Galli & Alberti 1971; Sokolova & Hawthorne 2008; Cámara *et al.* 2011) confirm that rinkite and nacareniobsite-(Ce) are isostructural and have the ideal formulae $Na_2Ca_4REETi(Si_2O_7)_2OF_3$ and $Na_3Ca_3REENb(Si_2O_7)_2OF_3$, as suggested by Petersen *et al.* (1989). The structural determinations assign the REE to two different sites, M(1) and M(3), which also contain Ca. However, the rinkite data from different localities presented by Cámara *et al.* (2011) show some divergence from the ideal composition. In rinkite from Mont Saint-Hilaire the REE content is only 0.75 apfu. In our samples we have observed comparably low REE contents in the material found intergrown with hainite (Table 2 no. 2) and in the cores of zoned grains in the sodalite foyaite (Table 2 no. 4). We assume that these crystals are rinkite.

The structural data assign Ti and Nb to the M(5) site together with minor amounts of Zr and Ta (Galli & Alberti 1971; Sokolova & Hawthorne 2008; Cámara *et al.* 2011). The formula calculations of our microprobe analyses normally have Ti+Nb close to the ideal value of 1.0, and when the sum is 0.90 apfu or lower the deficit is compensated by increased Zr as seen in the rinkite from the sodalite foyaite (Table 2 no. 4) and the marginal pegmatite (Table 3 no. 4).

The Nb versus Ti+Zr diagram in Fig. 4 shows a strong negative correlation (slope: -1.04, r: -0.989), confirming the $Ti^{4+} = Nb^{5+}$ substitution in the M(5) site of the rinkite–nacareniobsite-(Ce) series. The diagram further shows that the rinkite–nacareniobsite-(Ce) compositions in the Ilímaussaq complex span almost the full extension of the solid solution series and confirm its continuity. Moreover, the roof sequence and the floor sequence show similar compositional evolution, with the most Ti-rich compositions in the less evolved rocks (pulaskite pegmatite and marginal pegmatite) and the most Nb-rich compositions in the most evolved rocks (naujaite pegmatite and lujavrite).

The REE contents show a considerable variation, from 0.83 apfu in rinkite in pulaskite pegmatite to 1.31 apfu in nacareniobsite-(Ce) from naujaite pegmatite. The relation between REE and Nb in the solid solution series is shown in Fig. 5. In rinkite from the roof sequence there is a 1:1 correlation (slope: 1.0, r: 0.94) between REE and Nb content, whereas rinkite from the marginal pegmatite and kakortokite unit –6 differ significant from this trend with a REE content of about 1.15 apfu. In the nacareniobsite-(Ce) part of the solid solution series the correlation between REE and Nb is less pronounced and different (slope: 0.43, r: 0.68). If the rinkite analyses from the less

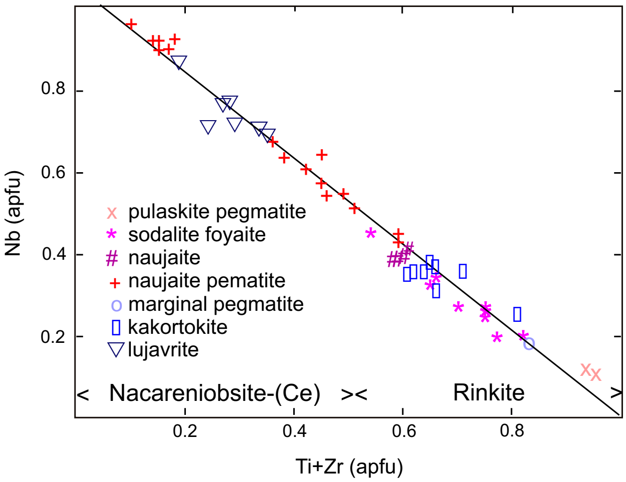

Fig. 4. Ti+Zr versus Nb in the rinkite–nacareniobsite-(Ce) solid solution series in Ilímaussaq. The solid line represents the regression line; slope: -1.04, r: -0.99.

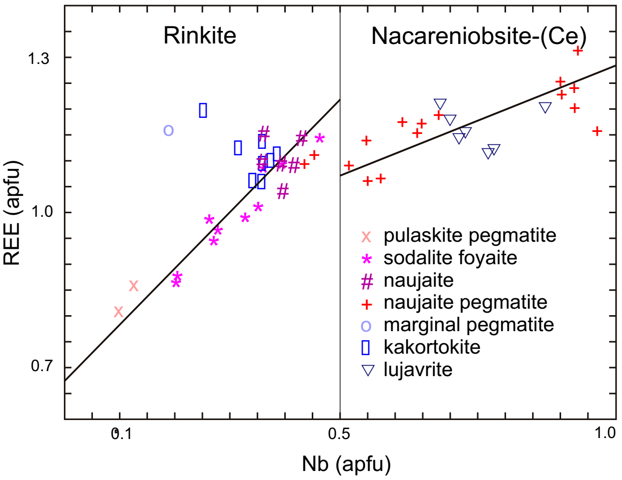

Fig. 5. Nb versus REE in the rinkite–nacareniobsite-(Ce) solid solution series in Ilímaussaq. The solid lines represent regression lines. Rinkite analyses in pulaskite pegmatite, sodalite foyaite and naujaite; slope: 1.0, r: 0.94. Nacareniobsite-(Ce) analyses in naujaite and lujavrite; slope: 0.58, r: 0.68.

evolved roof rocks, pulaskite and sodalite foyaite, are excluded from the comparison, it may be argued that the REE contents in the rinkite-nacareniobsite-(Ce) solid solution are almost independent of the Nb content (Fig. 5).

Petersen *et al.* (1989) suggested that the increase in Nb from rinkite to nacareniobsite-(Ce) is stoichiometrically balanced by the coupled substitution Ti^{4+} + Ca^{2+} = Nb^{5+} + Na^{+}. However the concurrent increase in the REE content in rinkite from the roof sequence should also be charge compensated. For REE as well as Nb this could be achieved by the above-mentioned substitution and the coupled substitution $2Ca^{2+}$ = Na^{+} + REE^{3+}, but also through a F^{1-} = O^{2-} substitution in the X site.

The idealized F content in the rinkite–nacareniobsite-(Ce) series is 3.0 apfu according to the proposed formulae in the literature. However, we found higher F contents than this. In rinkite with Nb<0.33 apfu the F content is 3.23 ± 0.22 apfu, whereas the F content is 2.84 ± 0.26 apfu in nacareniobsite-(Ce) with Nb>0.75 apfu. Our data therefore indicate some F^{1-} = O^{2-} substitution in the X site; however, the Na versus REE+Nb plot in Fig. 6 (slope: 0.936, r: 0.976) shows that the Nb and REE enrichment in both minerals is primarily compensated by the Ca^{2+} = Na^{+} substitution. This compensation model was also suggested by Cámara *et al.* (2011).

Hainite and götzenite

Besides the major cations in hainite and götzenite: Na, Ca, Ti and Si, the two minerals contain Zr and REE in various amounts. A reinvestigation of the hainite type material by Johan & Cech (1989) documented the presence of 6.5 wt% ZrO_2 and minor amounts of REE. Christiansen *et al.* (2003) reported 1.4 wt% ZrO_2 and 6.1 wt% REE_2O_3 in götzenite from Langesund and 4.0 wt% ZrO_2 and 9.9 wt% REE_2O_3 in hainite from Werner Bjerge, East Greenland. Lower concentrations of Zr and REE are reported in götzenite from Pian di Celle Volcano by Sharygin *et al.* (1996) and Bellezza *et al.* (2004), and in hainite from Pocos de Caldas by Atencio *et al.* (1999). The crystal structural data for the two minerals show that Zr, Y and other REE are concentrated in the M(1) site, whereas only a minor amount of REE is located in the M(3) site.

Sharygin *et al.* (1996) suggested that the substitution Ca^{2+} + $2F^{1-}$ = Zr^{4+} + $2O^{2-}$ played a major role in götzenite from Pian di Celli. However, the REE and Zr substitutions for Ca in the M(1) and M(3) sites and Nb for Ti in the M(5) site in götzenite and hainite could in principle also be stoichiometrically balanced by substitutions such as $2Ca^{2+}$ = REE^{3+} + Na^{+}, $3Ca^{2+}$ = Zr^{4+} + $2Na^{+}$ and Ca^{2+} + Ti^{4+} = Na^{+} + Nb^{5+} as observed for the rinkite–nacareniobsite-(Ce) series.

The published microprobe analyses of götzenite and hainite show that most samples contain Zr, Y and REE; however one of the götzenite analysis from Pian di Celli (Sharygin *et al.*; 1996) approach the ideal end member $NaCa_6Ti(Si_2O_7)_2OF_3$, whereas no hainite analysis is near to the Zr, Y and REE free ideal end member, $Na_2Ca_5Ti(Si_2O_7)_2(OH)_2F_2$, suggested by Atencio *et al.* (1999).

For comparison with our data we have calculated the cation contents of 20 published hainite and götzenite analyses on the basis of 4 Si atoms. The calculated mean number of cations for the published analyses is 12.0 ± 0.1 for hainite and 11.8 ± 0.2 for götzenite, the ideal being 12.0. The mean number of positive charges is calculated to be 32.9 ± 0.2 for hainite and 32.8 ± 0.2 for götzenite. However, some examples such as hainite from Hradiste (Johan & Cech 1989) have a low cation content (11.7) and a low number of positive charges. The calculated Ca and Na contents in the published hainite and götzenite analyses are plotted in Fig. 7. This shows that there is a good negative correlation between the two elements (slope: -0.58 r: -0.98), indicating that only approximately half of the Ca atoms are replaced by Na. The published data do not indicate the existence of the hainite end member suggested by Atencio *et al.* (1999), but a compositional variation between 'end members' having $NaCa_6$ and Na_2Ca_4 in the M(1)–M(4) sites, which suggests that one Ca cation should be replaced by REE, Y and/or Zr.

The charge balancing mechanism for the Y, REE and Zr substitution in the M(1) –M(4) sites and Nb for Ti in M(5) can be further evaluated by comparing the calculated Na apfu content and the excess of positive charges (EPC) introduced by the above-mentioned substitu-

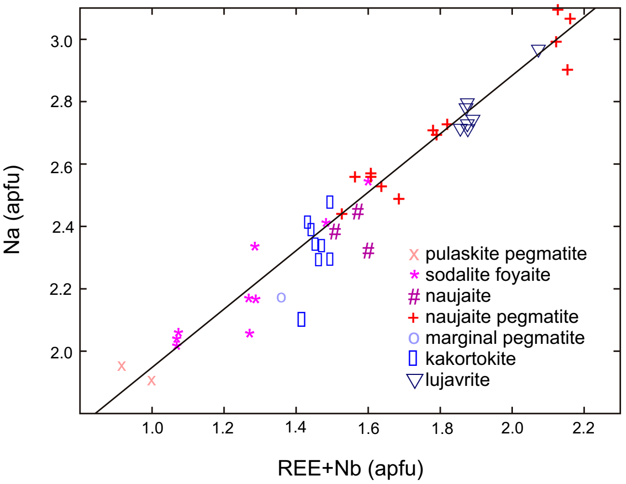

Fig. 6. Na versus REE+Nb in the rinkite–nacareniobsite-(Ce) solid solution series in Ilímaussaq. The solid line represents the regression line; slope: 0.936, r: 0.98.

tion, using the equation EPC = REE + Y + 2*Zr(M(1)) + Nb –2*Fe^{2+}(M(5)). The plot (Fig. 8) shows that there is a high positive correlation (slope: 0.91, r: 0.98) between Na and EPC, indicating that the increase in Na from 1.0 to 1.9 apfu is primarily related to the introduction of REE, Y, Zr and Nb by the charge compensating substitutions $2Ca^{2+} = REE^{3+} + Na^{+}$, $3Ca^{2+} = Zr^{4+} + 2Na^{+}$ and $Ca^{2+} + Ti^{4+} = Na^{+} + Nb^{5+}$, whereas the substitution $Ca^{2+} + 2F^{1-} = Zr^{4+} + 2O^{2-}$ can only play a minor role. The previously published analyses and our data thus indicate that the investigated götzenite–hainite samples show a compositional variation between the following ideal end members: $NaCa_6Ti(Si_2O_7)_2OF_3$ and $(Y,REE,Zr)Na_2Ca_4\,Ti(Si_2O_7)_2OF_3$. The content of F in the X-position in hainite and götzenite has been discussed by Sokolova (2006) who concluded that the chemical formulae for hainite and götzenite should be based on OF_3, in contradiction to the formula given by Rastsvetaeva *et al.* (1995), Atencio *et al.* (1999) and Christiansen *et al.* (2003).

REE evolution in investigated minerals related to the evolution of the Ilímaussaq complex

In hainite and the rinkite–nacareniobsite-(Ce) series the REE are located in the M(1) and M(3) sites. In rinkite–nacareniobsite-(Ce) the average bond lengths for the two sites deviate by less than 1% (Sokolova & Hawthorne 2008; Cámara *et al.* 2011), whereas the differences between the two sites can be more than 4% in hainite–götzenite (Christiansen *et al.* 2003), favouring the Zr, Y and HREE substitution for Ca in the M(1) site in hainite–götzenite. These crystal structural differences can explain the relatively high Y content in the Ilímaussaq hainite but also mean that a comparison of the REE patterns for hainite with the patterns for rinkite–nacareniobsite-(Ce) is not meaningful.

The chondrite normalised REE patterns for rinkite–nacareniobsite-(Ce) from the roof sequence in Fig. 3A–E and the floor sequence in Fig. 3F–H show identical changes with evolution of the magmas. During the evolution of both sequences there is a slight relative increase in La and Ce and a relative decrease in Y from rinkite in pulaskite pegmatite and marginal pegmatite to nacareniobsite-(Ce) in naujaite pegmatite and lujavrite. A comparable evolution was observed for REE in apatite from the roof sequence (Rønsbo 2008). Relatively similar REE patterns are observed in rinkite from the less evolved rocks: pulaskite pegmatite, sodalite foyaite and marginal pegmatite; also the more evolved naujaite and kakortokite have similar REE patterns, and so have nacareniobsite-(Ce) in the most evolved rocks naujaite pegmatite and lujavrite. These data support the conclusion that the REE content in the roof and floor sequences evolved in a similar way (Rønsbo 2008).

Conclusions

Rinkite is a minor mineral in the Ilímaussaq complex. In the roof sequence it occurs in all investigated rock types (pulaskite pegmatite, sodalite foyaite, naujaite and naujaite pegmatite); in the floor sequence it occurs in marginal pegmatite and kakortokite but not in lujavrite. In pulaskite pegmatite it is intergrown with hainite. Nacareniobsite-(Ce) occurs in the most evolved rocks in both the roof and floor sequences, respectively in naujaite pegmatite and lujavrite, as

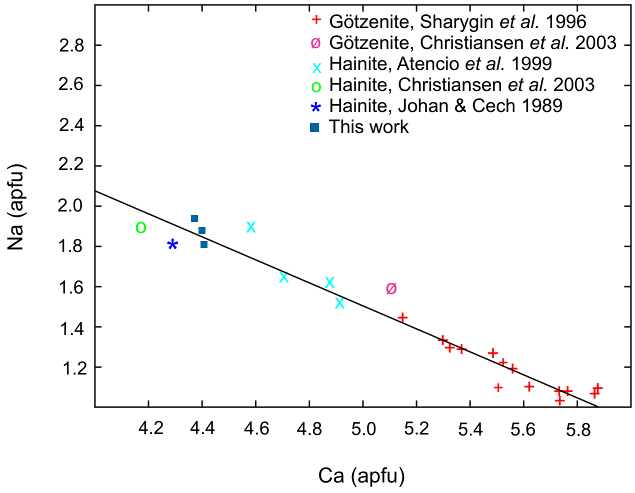

Fig. 7. Na versus Ca in hainite and götzenite in published and present analyses. The solid line represents the regression line; slope: -0.58, r: -0.98.

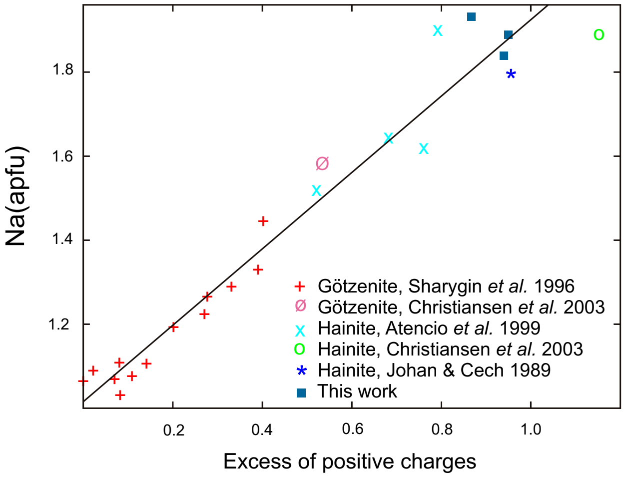

Fig. 8. Na versus Excess of positive charges (EPS) in hainite and götzenite in published and present analyses. The solid line represents the regression line; slope: 0.91, r: 0.98.

overgrowths on rinkite in naujaite pegmatite and as individual crystals in both rock types. The two minerals are members of a solid solution series, and in both the roof sequence and the floor sequence the compositional variation spans from rinkite in the less evolved rocks to nacareniobsite-(Ce) in the most evolved rocks.

Rinkite crystals in sodalite foyaite and naujaite pegmatite have developed a pronounced zonation, and three generations can be observed. Particularly crystals from the naujaite pegmatite represent intermediate members of the rinkite–nacareniobsite solid solution series.

Rinkite in the roof sequence shows an increase in REE contents from 0.83 apfu in Nb-poor rinkite in pulaskite pegmatite to 1.15 apfu in Nb-rich rinkite from sodalite foyaite and naujaite. In the floor sequence, rinkite in marginal pegmatite and kakortokite has REE contents around 1.15 apfu without a specific trend. In the nacareniobsite-(Ce) part of the solid solution series there is also an increase in the REE content with increasing Nb content, but less pronounced.

The chondrite normalised REE patterns for rinkite–nacareniobsite-(Ce) from the roof and floor sequences show identical changes with evolution. In both sequences there is a slight relative increase in La and Ce, and a relative decrease in Y, from rinkite in pulaskite pegmatite and marginal pegmatite to nacareniobsite-(Ce) in naujaite pegmatite and lujavrite. Further, rinkite in the less evolved rocks (pulaskite pegmatite, sodalite foyaite and marginal pegmatite) show mutually similar REE patterns; rinkite in the more evolved rocks (naujaite and kakortokite) show mutually similar REE patterns; and nacareniobsite-Ce in the most evolved rocks (naujaite pegmatite and lujavrite) also show mutually similar REE patterns.

The REE and Nb in the rinkite–nacareniobsite-(Ce) series are primarily stoichiometrically balanced by the coupled substitutions $2Ca^{2+} = Na^{+} + REE^{3+}$ and $Ti^{4+} + Ca^{2+} = Nb^{5+} + Na^{+}$.

The presence of hainite in a pulaskite pegmatite is established by X-ray powder diffraction data and single crystal information coupled with microprobe analysis. The mineral has a high REE content compared to published hainite and götzenite analyses and has Y as the dominant REE. The empirical formula is $(Ca_{1.62}Zr_{0.16}Y_{0.22})(Na_{0.87}Ca_{1.11})(Ca_{1.65}REE_{0.35})Na(Ti_{0.81}Nb_{0.09}Fe_{0.08}Zr_{0.02})(Si_2O_7)_2O_{0.99}F_{2.96}$, calculated on the basis of the microprobe analyses.

Based on previously published analyses it is suggested that the götzenite–hainite solid solution series shows compositional variation between the ideal end members $NaCa_6Ti(Si_2O_7)_2OF_3$ and $(Y,REE,Zr)Na_2Ca_4Ti(Si_2O_7)_2OF_3$.

Acknowledgements

We thank Eugene I. Semenov for the hainite sample and Henrik Friis and Helene Almind for the single crystal investigation. We further thank John C. Bailey, Lotte M. Larsen and the reviewers Tonci Balic-Zunic and Adrian Finch for valuable criticism. The field work in the Ilímaussaq alkaline complex was partly supported by INTAS project no. 93–1474.

References

Andersen, S., Bohse, H. & Steenfelt, A. 1981: A geological section through the southern part of the Ilímaussaq intrusion. Rapport Grønlands Geologiske Undersøgelse 103, 39–42.

Atencio, D., Coutinho, J.M.V., Ulbricht, M.N.C., Vlach, S.R.F., Rastsvetaeva, R.K. & Pushcharovskii, D.Y. 1999: Hainite from Pocos de Caldas, Minas Gerais, Brazil. Canadian Mineralogist 37, 91–98.

Bailey, J.C., Gwozdz, R., Rose-Hansen, J. & Sørensen, H. 2001: Geochemical overview of the Ilímaussaq alkaline complex, South Greenland. Geology of Greenland Survey Bulletin 190, 35–53.

Bellezza, M., Merlino, S. & Perchiazzi, N. 2004: Chemical and structural study of the Zr-, Ti-disilicates in the venanzite from Pian di Celle, Umbria, Italy. European Journal of Mineralogy 16, 957–969.

Bellezza, M., Merlino, S., Perchiazzi, N. & Raade, G. 2009a: "Johnstrupite" : A chemical and structural study. Atti della Societá Toscana di Scienza Naturali, Serie A 114, 1–3.

Bellezza, M., Merlino, S. & Perchiazzi, N. 2009b: Mosandrite: structural and crystal-chemical relationships with rinkite. Canadian Mineralogist 47, 897– 908.

Blumrich, J. 1893: Die Phonolite des Friedländer Bezirkes in Nordböhmen. Tschermaks Mineralogische und Petrographische Mitteilungen 13, 465–495.

Bohnsted, E.M. 1926: Two new minerals of the mosandrite group from Khibina Tundra. Bulletin of the Academy of Sciences of USSR 20, 1181 (in Russian).

Bohse, H. & Andersen, S. 1981: Review of the stratigraphic divisions of the kakortokite and lujavrite in southern Ilímaussaq. Rapport Grønlands Geologiske Undersøgelse 103, 53–62.

Boynton, W.V. 1983: Cosmochemistry of rare earth elements: meteoritic studies. In: Henderson, P. (ed): Rare Earth Element Geochemistry, 63–114. Amsterdam: Elsevier.

Brøgger, W.C. 1890: Die Mineralien der Syenitpegmatitgänge der südnorwegischen Augit- Nephelinsyenite. Zeitschrift für Kristallographie 16, 586–597.

Cámara, F., Sokolova, E. & Hawthorne, F.C. 2011: From structural topology to chemical composition. XII. Titanium silicates: the crystal chemistry of rinkite $Na_2Ca_4REETi(Si_2O_7)_2OF_3$. Mineralogical Magazine 75, 2755–2774.

Canillo, E., Mazzi, F. & Rossi, G. 1972: Crystal structure of götzenite. Soviet Physics and Crystallography 16, 1026–1030.

Christiansen, C.C., Johnsen, O. & Makovicky, E. 2003: Crystal chemistry of the rosenbuschite group. Canadian Mineralogist 41, 1203–1224.

Cundari, A. & Ferguson, A.K. 1991: Petrogenetic relationships between melilitite and lamproite. Contributions to Mineralogy and Petrology 107, 343–357.

Erdmann, A 1841: Mosandrite. In: J.J. Berzelius. Jahresbericht über die Fortschritte der physischen Wissenschaften 21, 178–179.

Fleischer, M. 1958: Rinkite, johnstrupite, rinkolite, lovchorrite and calcium rinkite (all = mosandrite). American Mineralogist 43, 795–796.

Fleischer, M. 1987: Glossary of Mineral Species, 5th edition. Mineralogical Record Corporation. Tucson, Arizona, 227 pp.

Galli, E. & Alberti, A. 1971: The crystal structure of rinkite. Acta Crystallographica B27, 1277–1284.

Giester, G., Pertlik, F. & Ulrych, J. 2005: Die kristallstruktur des minerals hainite. Mitteilungen der Österreichischen Mineralogischen Geselschaft 151, p. 45.

Johan, Z. & Cech, F. 1989: Nouvelles données sur la haïnite, $Na_2Ca_4[(Ti, Zr, Mn, Fe\ Nb, Ta)_{1,5}\square_{0,5}](Si_2O_7)_2F_4$ et ses relations cristallochimiques avec götzenite, $Na_2Ca_5Ti(Si_2O_7)_2F_4$. Comptes Rendus de l'Académie des Sciences, Paris, 308, Série. II, 1237–1242.

Larsen, L.M. & Sørensen, H. 1987: The Ilímaussaq intrusion – progressive crystallisation and formation of layering in an agpaitic magma. In: Fitton, J.G. & Upton, B.G.J. (eds), Alkaline Igneous Rocks. Special Publication, Geological Society, London 30, 473–488.

Lorenzen, J. 1884: Untersuchungen einiger Mineralien aus Kangerdluarsuk in Grönland. Zeitschrift für Kristallographie 9, 243–254.

Marks, M. & Markl, G. 2001: Fractionation and assimilation processes in the alkaline augite syenite unit of the Ilímaussaq intrusion, South Greenland, as deduced from phase equilibria. Journal of Petrology 46, 1947–1969.

Petersen, O.V. 2001: List of all minerals in the Ilímaussaq alkaline complex, South Greenland. In Sørensen, H. (ed.): The Ilímaussaq alkaline complex, South Greenland: status of mineralogical research with new results. Geology of Greenland Survey Bulletin 190, 25–33.

Petersen, O.V., Rønsbo, J.G. & Leonardsen, E.S. 1989: Nacareniobsite-(Ce), a new mineral species from the Ilímaussaq alkaline complex, South Greenland, and its relation to mosandrite and the rinkite series. Neues Jahrbuch für Mineralogie Monatshefte 2, 84–96.

Rastsvetaeva, R.K., Pushcharovskii, D.Y. & Atenzio, D. 1995: Crystal structure of giannetite. Crystallography Reports 40, 574–578.

Rønsbo, J.G. 1989: Coupled substitution involving REEs and Na and Si in apatites in alkaline rocks from the Ilímaussaq intrusion, South Greenland, and the petrological implications. American Mineralogist 74, 896-901.

Rønsbo, J.G. 2008: Apatite in the Ilímaussaq alkaline complex: occurrence, zonation and compositional variation. Lithos 106, 71–82.

Sahama, T.G. & Hytönen, K. 1957: Götzenite and combeite, two new silicates from Belgian Congo. Mineralogical Magazine 31, 503–510.

Semenov, E.I. 1969: The mineralogy of the Ilímaussaq alkaline massif. Izvestiya Akademii Nauk SSSR, 412 pp. (in Russian).

Sharygin, V.V., Stoppa, F. & Kolesov, B.A. 1996: Zr-Ti disilicates from the Pian di Celle volcano, Umbria, Italy. European Journal of Mineralogy 8, 1199–1212.

Slepnev, Y.S. 1957: On minerals of the rinkite group. Izvestiya Akademii Nauk SSSR, Seriya geologicheskaya 3, 63–75. (in Russian).

Sokolova, E. 2006: From structure topology to chemical composition. I. Structural hierarchy and stereochemistry in titanium disilicate minerals. Canadian Mineralogist 44, 1273–1330.

Sokolova E. & Cámara F. 2008: From structural topology to chemical composition. VIII. Titanium silicates: the crystal chemistry of mosandrite from the type locality of Låven (Skådön), Langesundsfjorden, Larvik, Vestfold, Norway. Mineralogical Magazine 72, 887–897.

Sokolova, E. & Hawthorne, F.C. 2008: From structural topology to chemical composition. V. Titanium silicates: crystal chemistry of nacareniobsite-Ce. Canadian Mineralogist 46, 1323–1342.

Sørensen, H. 2006: The Ilímaussaq alkaline complex, South Greenland – an overview of 200 years of research and an outlook. Meddelelser om Grønland, Geoscience 45, 70 pp.

Sørensen H. & Larsen, L.M. 1987: Layering in the Ilímaussaq alkaline intrusion. In: Parsons, I. (ed.) Origins of Igneous Layering. NATO Advanced Science Institute Series C, Mathematical and Physical Sciences 196, 1–28. Dordrecht: D. Reidel Publishing Company.

Sørensen, H, Bailey, J.C. & Rose-Hansen, J. 2011: The emplacement and crystallization of the U-Th-REE-rich agpaitic and hyperagpaitic lujavrites at Kvanefjeld, Ilímaussaq alkaline complex, South Greenland.

Steenfelt, A. 1981: Field relations in the roof zone of the Ilímaussaq intrusion with special reference to the position of the alkali acid rocks. Rapport Grønlands Geologiske Undersøgelse 103, 43–52.

Upton, B.G.J. 2013: Tectono-magmatic evolution of the younger Gardar southern rift, South Greenland. Geological Survey of Denmark and Greenland, Bulletin 29, 124 pp.

Ussing, N.V. 1912: Geology of the country around Julianehaab, Greenland. Meddelelser om Grønland 38, 426 pp.

A new eusuchian (Crocodylia) tooth from the Early or Middle Paleocene, with a description of the Early–Middle Paleocene boundary succession at Gemmas Allé, Copenhagen, Denmark

DANIELA SCHWARZ-WINGS, JESPER MILÀN & PALLE GRAVESEN

Schwarz-Wings, D., Milàn, J. & Gravesen, P., 2014. A new eusuchian (Crocodylia) tooth from the Early or Middle Paleocene, with a description of the Early–Middle Paleocene boundary succession at Gemmas Allé, Copenhagen, Denmark. © 2014 by Bulletin of the Geological Society of Denmark, Vol. 62, pp. 17–26. ISSN 2245-7070. (www.2dgf.dk/publikationer/bulletin).

A recently found crocodylian tooth crown from the basal conglomerate of the Middle Paleocene (Selandian) Lellinge Greensand Formation, differs morphologically from other finds of crocodylian teeth from the Paleocene of southern Scandinavia. The tooth is conical and blunt with a narrow rounded apex, and slightly curved along the axis of its length. The morphology of the tooth suggests it belongs to either the longirostrine eusuchian *Aigialosuchus*, which is known from the Campanian of southern Sweden, or to a member of the Alligatoridae which are the most common crocodylians in northern Europe in the Late Cretaceous. Gavialoid crocodylians, in particular *Thoracosaurus* which is known from the Danian limestome of the Limhamn quarry in southern Sweden and from the Faxe quarry in eastern Denmark, can be excluded because of their deviating tooth morphology. Regardless of its assignment, the tooth is interesting in a stratigraphic context as it demonstrates the existence of at least two crocodylian taxa in Scandinavia during the Early and Middle Paleocene.

Received 11 April 2014
Accepted in revised form
5 August 2014

Keywords: Crocodylian diversity, Eusuchia, Middle Paleocene, Danian/Selandian boundary, Echinoderm conglomerate, Lellinge Greensand Formation.

Daniela Schwarz-Wings [d.schwarz-wings@mfn-berlin.de], Museum für Naturkunde, Leibniz Institute for Research on Evolution and Biodiversity, Invalidenstrasse 43, DE 10115 Berlin, Germany. Jesper Milàn [jesperm@oesm.dk], Geomuseum Faxe/Østsjællands Museum, Østervej 2, DK-4640 Faxe, Denmark; also Department of Geosciences and Natural Resource Management, University of Copenhagen, Øster Voldgade 10, DK-1350 Copenhagen K, Denmark. Palle Gravesen [palgeolbot@gmail.com], Det Sorte Geomuseum, Skolegade 2B, DK-4874 Gedser, Denmark; also Natural History Museum of Denmark, University of Copenhagen, Øster Voldgade 5–7, DK-1350 Copenhagen K, Denmark.

Corresponding author: Jesper Milàn

The Scandinavian fossil record of Cretaceous and Paleocene Crocodyliformes is extremely scarce, with only a few scattered finds. The Early Cretaceous (Berriasian) of Bornholm and southern Sweden has yielded teeth and skeletal fragments of the non-eusuchian crocodiles *Theriosuchus*, *Bernissartia* and cf. *Goniopholis* (Rees 2000, 2002; Schwarz-Wings *et al.* 2009).

An undesribed jaw fragment preserved in flint of a longirostrine crocodylian with some affinities to *Thoracosaurus* is known from the Maastrichtian chalk of Møns Klint, Denmark (Gravesen & Jakobsen 2012), and fragmentary material of the poorly known eusuchian crocodyliform *Aigialosuchus* is described from the Campanian of southern Sweden (Persson 1959). The eusuchian *Thoracosaurus* is well known from a number of skeletal remains from the Danian of Limhamn quarry in southern Sweden, including a complete skull as well as postcranial material (Lundgren 1890; Troedsson 1923, 1924). Skeletal remains of *Thoracosaurus* sp. comprising a basioccipital, a cervical vertebra, a humerus and a number of isolated teeth, are known from the middle Danian limestone of Faxe quarry, Denmark (Bendix-Almgreen,1972; Bonde *et al.* 2008). From the same quarry, a bite trace *Nihilichnus* in a turtle carapace bears indirect evidence of the presence of a crocodylian (Milàn *et al.* 2011). Finally, an imprint of a 'reptilian' tooth resembling the long slender thoracosaurine teeth is mentioned from the

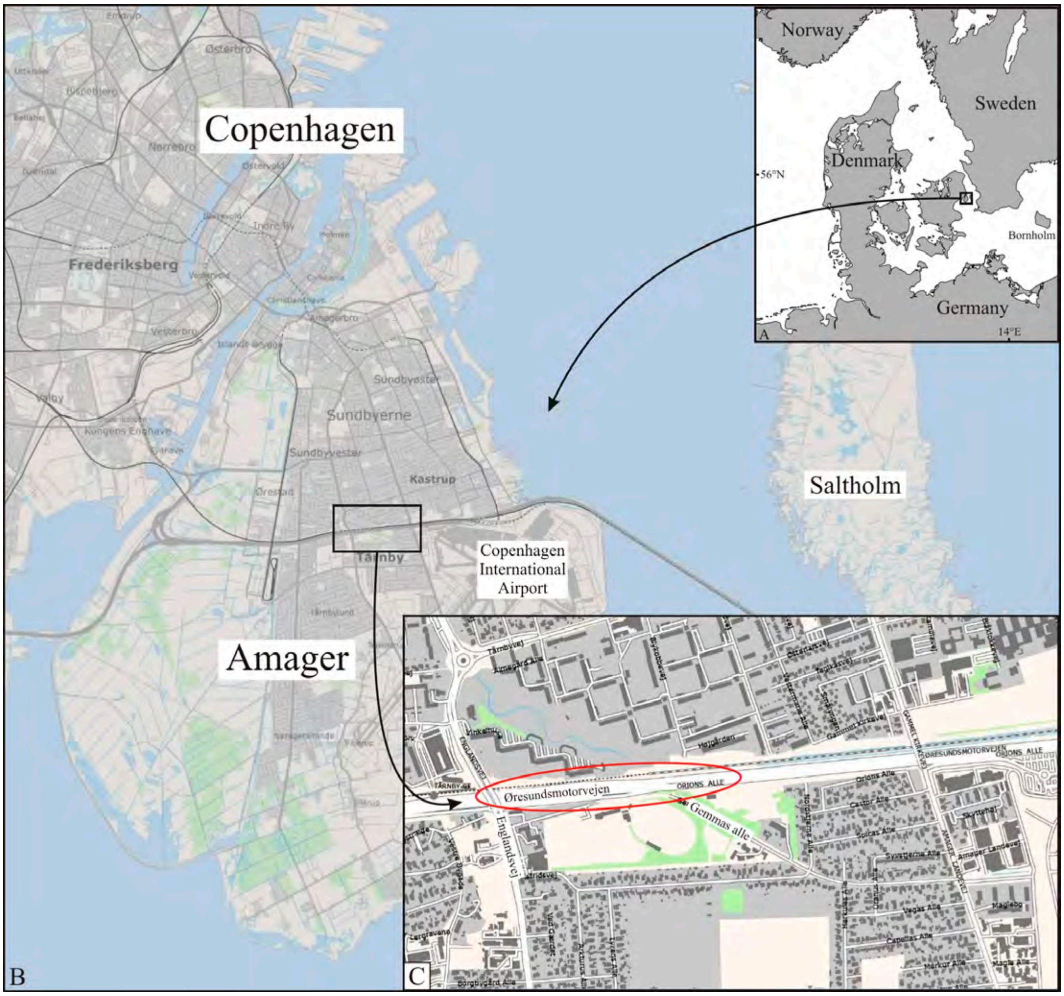

Fig. 1. Location map. **A–B**: The site is located on the island of Amager, part of Copenhagen. **C**: The excavation site (55°37′46″N, 12°36′34″Ø) was open during construction of Øresundsmotorvejen (E20) to Sweden.

lower Selandian *Crania* limestone of Copenhagen (Rosenkrantz 1920a).

In this paper, we describe a newly found crocodylian tooth of a type of eusuchian crocodile hitherto unknown from the Early and Middle Paleocene of Denmark and discuss its implications for the northern European, Paleocene crocodylian diversity. Furthermore, we present the hitherto most detailed description of the now lost locality at Gemmas Allé, Copenhagen, where it was found.

Geological setting

The tooth was discovered in material collected in 1994 from a large road cut at Gemmas Allé on the island of Amager (Fig. 1), when large-scale excavations prior to the coming tunnel and bridge connection between Denmark and Sweden opened a large exposure of the strata at the Danian/Selandian boundary, which in the Danish area is developed as an erosional unconformity (Stouge *et al*. 2000; Clemmensen & Thomsen 2005) marking the boundary between the Lower and Middle Paleocene (Schmitz *et al*. 2011).

The tooth was found in material from the basal conglomerate of the Selandian (Middle Paleocene) Lellinge Greensand Formation (Stouge *et al.* 2000; Clemmensen & Thomsen 2005; Schmitz *et al*. 2011) (Fig. 2A). This characteristic conglomerate occurs at both sides of Øresund, the sound that separates Denmark from Sweden, and contains abundant reworked Danian fossils (Fig. 2D.). In Sweden it occurs in the locality of Klagshamn. In Denmark it could previously been seen in a number of classical, now inaccessible localities in the Copenhagen area, viz., Copenhagen South Harbour, Vestre Gasværk, Sundkrogen and Svanemøllebugten (e.g. Rørdam 1897, 1899; Rosenkrantz 1920a, 1920b, 1924, 1925, 1930, 1938, 1942; Harder 1922; Gry 1935; Milthers 1935; Berthelsen 1962, 1995; Stenestad 1976; Gravesen 1994; Knudsen 1994; Schnetler 2001; Heilmann-Clausen & Surlyk 2006). It may occasionally be exposed during larger construction works. The site at Gemmas Allé was accessible for most of the year 1994 due to the kind understanding of the construction company Per Aarsleff A/S. The section extended for several hundred metres from the road Englandsvej eastwards along Gemmas Allé almost to the buildings of Copenhagen International Airport (Fig. 1B). The site has also been described in literature as the Tårnby Torv locality (e.g. Gravesen 1994). Based on 10 individual sections accurately measured by PG in 1994, a composite log has been made (Fig. 2A).

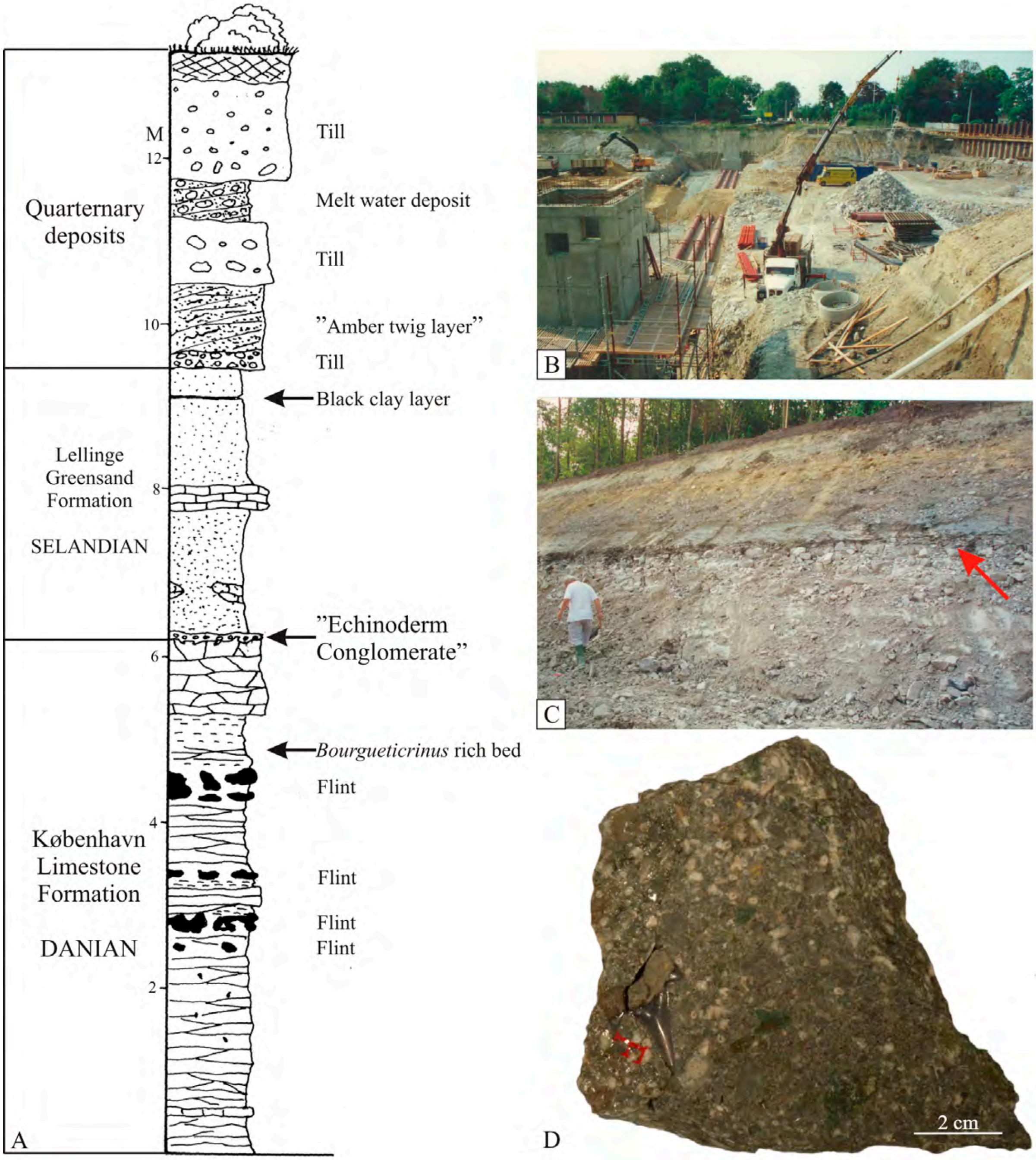

Fig. 2. **A**: Composite log of the section at the Gemmas Allé site, modified after Gravesen (1994). **B**: The western part of the excavation near Englandsvej. **C**: The boundary between the Danian København Limestone Formation and the Selandian Lellinge Greensand Formation. The basal conglomerate of the Lellinge Greensand Formation is indicated by arrow. **D**: Sample of the conglomerate from the Gemmas Allé site. Note the prominent shark tooth beside the red mark. All photos by Sten Lennart Jakobsen.

Upper Danian limestone

The section excavated in 1994 exposed well over 6 m of light grey, fine-grained Danian limestone described as calcarenite, in Danish 'Kalksandskalk', belonging to the top of the København Limestone Formation (København Kalk Formationen of Stenestad 1976). The limestone is partly indurated forming a hard, coherent limestone of the type previously known in Danish and German literature as 'Saltholmskalk', and partly developed as more greyish and softer, marly limestone. The limestone includes a few coherent bands of greyish to black flint as well as scattered, irregular flints nodules. The hard limestone contains only scattered invertebrate macrofossils, most commonly *Echinocorys obliqa*, *Carneithyris lens*, *Crania (Danocrania) tuberculata*, *Lima testis*, *Septifer hauniensis*, several oysters (*Exogyra canaliculata*, *"Pycnodonte" vesicularis*), nautiloids (*Cimomia* sp., *Eutrephoceras bellerophon*), *Volutolithes nodifer*, (?) *Scaphella* sp., *Ditrupula schlotheimi*, *Xanthilithes* sp. and trace fossils in the form of burrows of the decapod *Callianassa*.

The softer beds contain a diverse late Danian macro- and mesofauna, which besides many bryozoans comprise species such as *Echinocorys obliqua*, *Cyclaster suecicus*, *Tylocidaris vexillifera* (all index fossils for the later Danian), *Phymosoma* sp., *Stereocidaris*/*Cidaris* spp., ossicles of asteroids (*Recurvaster* sp., *Pycinaster rosenkrantzi*) and stalk ossicles of the crinoid *Bourgueticrinus* cf. *danicus*. The latter characterises a particularly fossiliferous layer near the top of the Danian, just below the indurated limestone beds forming the very top of the Danian at this site. In addition to the species mentioned above the fossiliferous layer also contains *Amussium* sp., *Chlamys palaeocaenica*, *Stegoconcha* sp., *Temnocidaris danica*, ?*Palaeodiadema* sp., *Democrinus* sp., *Nielsenicrinus obsoletus, Isselicrinus paucicirrhus*, comatulids, *Ditrupula schlotheimi*, *Spirorbis hisingeri*, *Crania (Danocrania) tuberculata*, *Argyrotheca scabricula*, "*Scalpellum steenstrupi*" and several species of shark's teeth.

The Danian/Selandian boundary

At Gemmas Allé, the base of the Selandian Lellinge Greensand Formation is developed as a conglomerate. The conglomerate is a greenish, glauconitic and speckled deposit with reworked clasts of light-grey, upper Danian limestone nodules set in a darker, glauconitic matrix and with plentiful reworked late Danian fossils such as *Crania (Danocrania) tuberculata*, *Isocrania posselti*, *Carneithyris lens*, *Echinocorys obliqua*, *Plicatula ravni*, *Graphularia* stems, ossicles of asteroids and crinoids including *Bourgueticrinus,* and frequent often large and dark shark's teeth such as impressive specimens of *Cretalamna appendiculata*, as well as dark coloured vertebrate bone fragments. In its matrix are also seen numerous, shiny, brownish and rounded pellets, possibly fecal pellets from gastropods (Fig. 2D).

In the course of time, the conglomerate has carried widely different names. Apparently the first detailed description was published by the German geologist W. Deecke (1899), based on a glacial erratic boulder from the Rügen area. Rather misleadingly, he named the rock an "Echinodermenbreckzie". Grönwall (1904) changed the name to the more appropriate "Ekinodermkonglomerat" in his study of glacial erratics of the southern Funen area in Denmark. Due to its content of numerous reworked specimens of the brachiopod *Crania* (*Danocrania*) *tuberculata*, it has also been named the "Upper Crania Limestone" e.g. in Rosenkrantz (1920a), or "Forsteningskonglomerat", i.e. fossiliferous conglomerate (Rosenkrantz 1930). Gry (1935) used the widely different name of "Paleocene shelly conglomerate". The rock is widely distributed and well-known as a glacial erratic (German: "Geschiebe") under the name of "Echinodermenkonglomerat" (see e.g. Hucke-Voigt 1967; Gravesen 1993; Schulz 2003; Rohde 2008; Rudolph *et al*. 2010). By dissolution of the rock in acid it is known to yield abundant shark´s teeth such as the impressive fauna described from glacial erratics by Reinecke & Engelhard (1997). Today the unit is generally referred to as the basal conglomerate of the Lellinge Greensand Formation (Clemmensen & Thomsen 2005).

Lower Selandian deposits

The basal conglomerate is followed by a 2–3 m thick sequence of greensand belonging to the lower Selandian Lellinge Greensand Formation, which contains a diverse fauna (e.g. Franke 1927; Ravn 1939; Schnetler 2001; Schwarzhans 2003; Christiansen 2007).

At the Gemmas Allé site, macrofossils were not particularly well-preserved but included typical Lellinge Greensand Formation macrofossils such as *Nucula densistria*, *Dentalium rugiferum*, *Lima testis* and the solitary coral *Trochocyathus calcitrapa.* The greensand beds were partly rather loose and partly forming indurated beds. Distinct cross bedding in the greensand was observed in a part of the exposure at the corner of Gemmas Allé in 1992, between 210 and 225 cm above the base of the Selandian (Claus Heilmann-Clausen, personal communication 2014).

In one of the measured sections the greensand also included a few centimetres of a black clay or marl, similar to the typical 'sorte ler' (black clay) which has previously been found and described from the lower Selandian deposits of the Copenhagen area, e.g. at the classical site of Vestre Gasværk (Rosenkrantz 1930; Milthers 1935). At Gemmas Allé, the macrofossils in the black clay layer are crushed due to Pleistocene glacial deformation because this incompetent layer acted as a kind of lubricant during dislocation of the Selandian and Pleistocene strata in the top part of the sequence. Similar glacial deformation was also evident at the Vestre Gasværk locality. Though mostly crushed, the early Selandian species in the black clay at Gemmas Allé were readily identifiable and showed a very diverse early Selandian invertebrate fauna (table 3 in Schnetler 2001).

Quaternary deposits

The Pleistocene strata comprise three different Late Weichselian tills and at least two horizons of meltwater deposits, the lower one (above the lowermost Weichselian till) being developed as a typical 'amber-and-twigs-layer' (Danish 'rav-pindelag'). These are meltwater sands or gravels with abundant Baltic amber plus various plant remains, probably of both Late Tertiary (Neogene) and Pleistocene age. Amber-and-twigs-layers have been found in several localities in the Greater Copenhagen area as for example Valby Bakke, Vestre Gasværk, Frihavnen and Ordrup as well as the recent excavation at Nørreport Station in Central Copenhagen (see e.g. Milthers 1935; Berthelsen 1995; Ørestadsselskabet I/S 2001).

Description of the tooth

The tooth was found in a bulk sample collected in 1994 by Palle Gravesen and Sten Lennart Jakobsen, Natural History Museum of Denmark. However, it was first discovered in 2013 by the amateur geologist Mogens Madsen, Fredericia, by acid dissolution of the collected material. The tooth is declared Danekræ (DK-734) and is stored in the collection of the Natural History Museum of Denmark (MGUH-30862).

The preserved tooth crown has a basoapical height of 20.4 mm and a basal maximum width of 14.5 mm (Fig. 3). A large, basoapically oriented crack in the enamel divides the tooth crown on the lingual side and continues also labially. Two other cracks are visible around the tooth, disturbing also the mesial

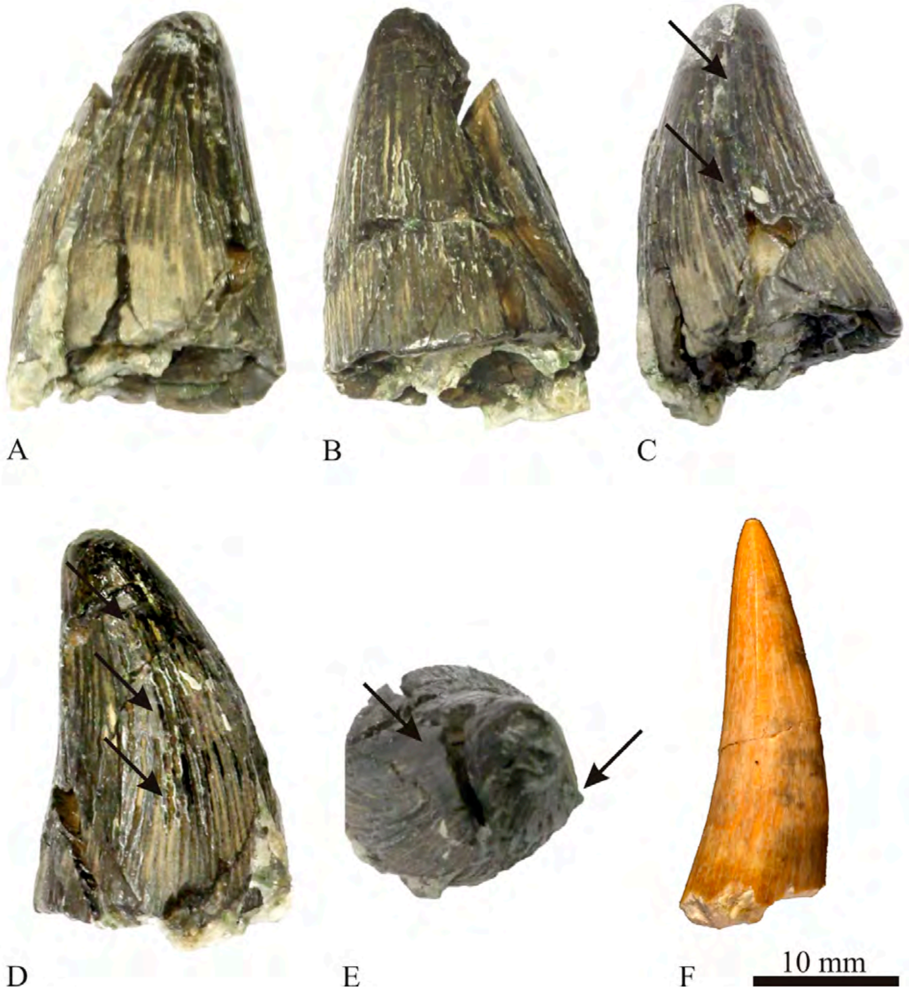

Fig. 3. Isolated crocodylian tooth from the basal conglomerate of the Lellinge Greensand Formation (Middle Paleocene) (MGUH-30862), **A**: Lingual view. **B**: Labial view. **C**: Mesial view. **D**: Distal view. **E**: In apical aspect. The weak carina (cutting edge) is visible in the mesial, distal and apical views, indicated by arrows. **F**: Thoracosaurid tooth from the Middle Danian of Faxe Quarry for comparison. Photos **A**–**E** by Heinrich Mallison. Photo **F** by Sten Lennart Jakobsen.

and distal carina. The cracks expose the underlying dentine.

The tooth crown is conical and blunt in habitus. The base of the tooth crown is circular, and the apex is narrowly rounded. The tooth crown is only very slightly labiolingually compressed and very slightly curved along the axis of its length. The lingual side of the tooth crown is slightly less convex than the labial side. Visible, but weak, carinae are present both on the medial and the distal side. The carinae start directly dorsally to the base of the tooth crown and fade ventrally towards its apex. The carinae are smooth and separated from the rest of the striated enamel only by their greater height and overall smoothness. The apex of the tooth crown is slightly worn, with the outermost layer of the enamel chipped off.

Both on the labial and on the lingual sides the enamel is strongly striated. This striation is produced by a pattern of deep grooves or flutes in the enamel. The numerous grooves extend straight from the base of the tooth crown until its apical part. Due to the tapering of the tooth crown, some of the grooves become wedged into the surrounding ones ending between them, but none of them swerve laterally to reach the carinae. The striae end lingually at the dorsal fifth of the tooth crown, but labially extend slightly higher, into the dorsal sixth of the crown.

Discussion and systematic assignment

The rounded cross section of the basis of the tooth crown together with the presence of weak, unserrated carinae and the striation of the enamel demonstrate that the isolated tooth belongs to a crocodyliform (Fig. 3). Secondary criteria for this assignment is the size of the tooth crown and its Middle Paleocene age (Selandian basal conglomerate), which excludes the marine reptiles such as sauropterygians or mosasaurs. Morphologically, the tooth can be characterised as rather generalistic, showing no specific dietary adaptations and lacking unambiguous features that would allow a closer taxonomic assignment. Determination of the tooth is also hampered by the overall rareness of Paleocene crocodylians in Europe (Efimov & Yarkov 1993; Buscalioni *et al*. 2003; Delfino *et al*. 2005; Buscalioni & Vullo 2008; Martin & Delfino 2010). Non-eusuchian crocodyliforms are not known from Europe after the Maastrichtian, and all known crocodyliforms of the Paleocene of Europe belong to Eusuchia (Buscalioni *et al*. 2003; Martin & Delfino 2010).

The sparse Scandinavian fossil record of Paleocene crocodylians comprises *Thoracosaurus* from the Danian limestone of the Limhamn quarry in southern Sweden (Lundgren 1890; Troedsson 1923, 1924), and skeletal fragments and loose teeth of possible thoracosaurid affinities from the Danian of the Faxe quarry, Denmark (Bendix-Almgreen 1972; Bonde *et al*. 2008). However, crocodylian bite traces, *Nihilichnu*s, in a turtle carapace fragment from the Faxe quarry (Milàn *et al.* 2011) suggest the presence of a crocodylian with more robust jaws than the extreme long, narrow and delicate jaws of *Thoracosaurs* which are unsuited for a chelonivorous diet.

Comparisons of the described tooth with non-eusuchian mesoeucrocodylians from the latest Cretaceous of Europe yield no similarities, and a taxonomic assignment to dyrosaurids (Buffetaut & Lauverjat 1978), *Doratodon* (Buffetaut 1979, 1980; Company *et al*. 2005), *Ischyrochampsa* (Vasse 1995), or *Theriosuchus* (Martin *et al*. 2010) can be excluded by differences in tooth morphology. The overall morphological similarity of the tooth from Gemmas Allé to those of the thalattosuchian *Machimosaurus* (Krebs 1967, 1968; Buffetaut 1982) is a convergence, because the youngest occurrence of *Machimosaurus* extends only as far as to the Early Cretaceous (Valanginian, Cornée & Buffetaut 1997). The stratigraphic age of the described specimen also strongly suggests its affiliation with the Eusuchia.

Among Late Cretaceous and Early Paleocene eusuchian crocodylians of Europe, *Thoracosaurus* is the only better known taxon from Scandinavia. The teeth of *Thoracosaurus scanicus* (= *Th. macrorhynchus*, Brochu 2004) from the Danian in Limhamn quarry (Troedsson 1924) differ from the described specimen by their more slender and acute, conical shape and differences in the striation pattern (Fig. 3F). *Thoracosaurus* teeth have a different ratio between crown height and basal width (between 1.9 and 3.3 in *Th. macrorhynchus* (Koken 1888; Troedsson 1924; Laurent *et al*. 2000; Brochu 2004) as compared to 1.4 in the specimen from Gemmas All*é*. The described tooth differs in its stouter morphology also from the teeth of other contemporary gavialoid crocodylians (Brochu 2004; Delfino *et al*. 2005) and it cannot be assigned to this group. Isolated crocodylian teeth from the Danian limestone at Limburg, Holland, are all referred to *Thoracosaurus* (Jagt *et al*. 2013); however one of them shows a much broader, stouter conical shape than typical *Thoracosaurus* teeth (Jagt *et al*. 2013, fig 19a).

Asiatosuchus should also be considered as a potential candidate for the bearer of the tooth. *Asiatosuchus* is primarily known from Asia (Mook 1940; Angielczyk & Gingerich 1998), but it has also been identified from the Paleocene of Russia (Efimov & Yarkov 1993) and from the Eocene locality of Messel in Germany (Berg 1966; Rossmann & Blume 1999). The teeth of *Asiatosuchus* generally have tooth crowns similar in shape to the tooth from Gemmas All*é*. However, they differ from the latter by the lateral expansion of the enamel striae onto the distinct carinae, which gives them a serrated appearance (Berg 1966; Angielczyk & Gingerich 1998) that is clearly absent in the specimen from Gemmas Allé.

Turning to late Cretaceous forms, the only other Scandinavian crocodylian is *Aigialosuchus villandensis.* This species was erected on the basis of fragmentary remains of the rostrum and preorbital region from the Campanian deposits at Blaksudden, Ivö, Sweden (Persson 1959). *Aigialosuchus* is a problematic taxon in need of revision (Martin & Delfino 2010). As pointed out by Martin & Delfino (2010), the contribution of the nasal to the posterior margin of the external naris in *Aigialosaurus* makes incorporation of this taxon into Gavialoidea unlikely. Its anatomical affinities could even place *Aigialosaurus* within the tomistomime Crocodyloidea, although the taxon then would be much older than the latter clade (Piras *et al.* 2007). Until a thorough taxonomic revision of this material is carried out, the systematic position of *Aigialosaurus* within the Crocodylomorpha will remain unclear. Although stratigraphically younger, the isolated tooth from Gemmas All*é* resembles in many aspects the description and figures of *Aigialosuchus villandensis* as "short, stout and slightly recurved; ... densely striated in an apico-basal direction and exhibit only slight indications of anterior and posterior carinal crests" (Persson 1959: p. 473). However, without a personal examination of the remains of *Aigialosaurus* by the first author, and considering the limited quality of the figures and data in Persson (1959), no certain assignment of the tooth from Gemmas All*é* to this taxon can be made at this point.

Among the late Cretaceous eusuchians from Europe, the alligatoroid *Acynodon* can be excluded because of its peculiar tooth morphology. Teeth of *Acynodon* are either slender and possessing a distinct carina, or slightly bulbous with striations which are replaced by a pattern of pustules on the enamel (Buscalioni *et al*. 1997; Martin 2007; Delfino *et al*. 2008b). The teeth of *Arenysuchus* from the Maastrichtian of Spain (Puértolas *et al*. 2011) are morphologically very similar to the tooth from Gemmas Allé. They differ mainly by their general lack of a striation pattern and a slightly lower crown height.

Overall morphological similarities to the described tooth are also present in other alligatoroid teeth from the late Cretaceous of Europe. *Allodaposuchus* teeth from southern Europe (Buscalioni *et al*. 2001; Delfino *et al*. 2008a; Martin 2010) seem to display a weaker pattern of striation, but stronger carinae than in the described tooth. *Musturzabalsuchus* from Spain (Buscalioni *et al*. 1997; Company *et al*. 2005) seems to possess teeth of both similar habit and striation in the posterior part of the dentary. However, the description and the figures are too poor to allow a certain assignment without personal examination of the material. Finally, from southern France, *Massaliasuchus* seems to possess rather identical teeth in the posterior part of maxilla and dentary (Martin & Buffetaut 2008). However, the description and illustrations of this material are of insufficient quality for a detailed comparison.

Because of the overall morphological similarity to some alligatoroid taxa, and because the alligatoroids are the most frequent crocodylians in the Upper Cretaceous deposits of Europe (Martin & Delfino 2010), we consider an assignment of the tooth from Gemmas Allé to the Alligatoroidea as the most plausible. However, the assignment is clearly uncertain.

Conclusion

The morphology and stratigraphic age (earliest Middle Paleocene) of the tooth from Gemmas Allé indicate that the specimen belongs to a eusuchian crocodyliform with a rather generalistic dentition. A more precise taxonomic assignment is extremely difficult as it is not known whether the striation pattern of the enamel is diagnostic or should be regarded as an acccidential variation. Two possibilities appear for a taxonomic assignment: 1), the tooth belongs to *Aigialosuchus*, a longirostrine eusuchian of uncertain systematic affinity, or 2), the tooth belongs to a member of the Alligatoroidea. The Alligatoroidea are the most common crocodylians in the Upper Cretaceous deposits of Europe. They form a highly diverse group including both more generalistic forms (*Allodaposuchus* or *Massaliasuchus*) and more specialized forms (*Acynodon).* Gavialoid crocodylians and in particular *Thoracosaurus*, can be excluded because of their deviating tooth morphology.

Regardless of its assignments, the tooth from Gemmas Allé is interesting in a stratigraphic context, as it constitutes one of the few Danian/Selandian records of crocodylians in Europe in general and in Scandinavia in particular. Together with body and trace fossil evidence from the Faxe quarry, the tooth demonstrates the existence of at least one other crocodylian taxon than *Thoracosaurus* in the Early and Middle Paleocene of Scandinavia. It clearly demonstrates that this part of the Paleocene of Northern Europe must have accommodated a more diverse crocodylian fauna than hitherto known.

Acknowledgements

We are grateful to Sten Lennart Jakobsen for help with photos of the now lost locality. Mogens Madsen is thanked for his work with dissolving the conglomerate and finding the tooth. Heinrich Mallison, Museum Für Naturkunde, Berlin, kindly provided detailed photos of the tooth. Inken Mueller-Töwe, Naturstyrelsen, provided location maps. Finn Surlyk provided useful discussion of the stratigraphy. The critical and constructive reviews by Claus Heilmann-Clausen and Erik Thomsen greatly helped to improve the manuscript.

References

Angielczyk, K.D. & Gingerich, P.D. 1998: New specimen of cf. *Asiatosuchus* (Crocodyloidea) from the Middle Eocene Drazinda Formation of the Sulaiman Range, Punjab (Pakistan). Contributions from the Museum of Paleontology, The University of Michigan 30, 163–189.

Bendix-Almgreen, S.E. 1972: Kæmpeøgler i Danmark?. VARV 1972(3), 66–73.

Berg, D.E. 1966: Die Krokodile, insbesondere *Asiatosuchus* und aff. *Sebecus*?, aus dem Eozän von Messel bei Darmstadt/Hessen. Abhandlungen des Hessischen Landesamtes für Bodenforschung 52, 1–105.

Berthelsen, O. 1962: Cheilostome Bryozoa in the Danian Deposits of East Denmark. Danmarks Geologiske Undersøgelse, II. Række 83, 290 pp.

Berthelsen, O. 1995: Fra det nordlige Sokkelund. Noget om geologi, teglværker, grusgravning og tørveskæring i Søllerød, Lyngby-Taarbæk, Gentofte og Gladsaxe kommuner. 71 pp, Danmarks og Grønlands Geologiske Undersøgelse, Miljø- og Energiministeriet.

Bonde, N., Andersen, S., Hald, N. & Jakobsen, S.L. 2008: Danekræ - Danmarks bedste fossiler, 226 pp. Copenhagen: Gyldendal.

Brochu, C.A. 2004: A new Late Cretaceous gavialoid crocodylian from eastern North America and the phylogenetic relationships of thoracosaurs. Journal of Vertebrate Paleontology 24, 610–633.

Buffetaut, E. 1979: Revision der Crocodylia (Reptilia) aus den Gosau-Schichten (Ober-Kreide) von Österreich. Beiträge zur Paläontologie von Österreich 6, 89–105.

Buffetaut, E. 1980: Crocodilians from the continental Upper Cretaceous of Europe: New finds and interpretations. Mesozoic Vertebrate Life 1, 5–14.

Buffetaut, E. 1982: Le crocodilien *Machimosaurus* von Meyer (Mesosuchia, Teleosauridae) dans le Kimmeridgien de l'Ain. Bulletin trimestre de la Société Géologique de la Normandie et Amis du Muséum du Havre LXIX, 17–26.

Buffetaut, E. & Lauverjat, J. 1978: Un Crocodilien d'un type particulier dans le Cénomanien de Nazarè. Comptes Rendus Sommaire des Seances de la Societe geologique de France 1978, 79–82.

Buscalioni, A.D. & Vullo, R. 2008: Three steps in the Cretaceous evolution of crocodylomorpha: example from Barremian to Maastrichtian diversity in the Iberian Peninsula, and what about mid-Cretaceous gap? In: Mazin, J.-M., Pouech, J., Hantzpergue, P. & Lacombe, V. (eds), Mid-Mesozoic Life and Environments. Documents des Laboratoires de Géologie de Lyon 164, 29–32.

Buscalioni, A.D., Ortega, F. & Vasse, D. 1997: New crocodiles (Eusuchia: Alligatoroidea) from the Upper Cretaceous of southern Europe. Comptes Rendu de l'Academie des Sciences, Paris, Sciences de la Terre et des Planètes 325, 525–530.

Buscalioni, A.D., Ortega, F., Weishampel, D.B. & Jianu, C.M. 2001: A revision of the crocodyliform *Allodaposuchus precedens* from the Upper Cretaceous of the Hateg Basin, Romania. Its relevance in the phylogeny of Eusuchia. Journal of Vertebrate Paleontology 21, 74–86.

Buscalioni, A.D., Pérez-Moreno, B.P. & Sanz, J.L. 2003: Pattern of biotic replacement in modern crocodiles during the Late Cretaceous. Coloquios de Paleontología 1, 77–93.

Christiansen, N. 2007: The Fauna of the Lellinge Greensand in the Hedeland area. Unpublished M.Sc. thesis, University of Copenhagen, 101 pp.

Clemmensen, A. & Thomsen, E. 2005: Palaeoenvironmental changes across the Danian–Selandian boundary in the North Sea Basin. Palaeogeography, Palaeoclimatology, Palaeoecology 219, 351–394.

Company, J., Superbiola, X.P., Ruiz-Omeñaca, J.I. & Buscalioni, A.D. 2005: A new species of Doratodon (Crocodyliformes: Ziphosuchia) from the Late Cretaceous of Spain. Journal of Vertebrate Paleontology 25, 343–353.

Cornée, J.-J. & Buffetaut, E. 1997: Découverte d'un Téléosauridé (Crocodylia Mesosuchia) dans le Valanginien supérieur du massif d'Allauch (sud-est de la France). Comptes Rendu de l'Academie des Sciences, Paris, Sèrie D 288, 1151–1154.

Deecke, W. 1899: Ueber eine als Diluvialesgeschiebe vorkommende Paleocäne Echinodermenbrecchie. Mitteilungen des Naturwissenschaftlichen Vereins für Vorpommern und Rügen 31, 67–76.

Delfino, M., Piras, P. & Smith, T. 2005: Anatomy and phylogeny of the gavialoid crocodylian Eosuchus lerichei from the Paleocene of Europe. Acta Palaeontologica Polonica 50, 565–580.

Delfino, M., Codrea, V., Folie, A., Dica, P., Godefroid, P. & Smith, T. 2008a: A complete skull of Allodaposuchus precedens Nopsca, 1928 (Eusuchia) and a reassessment of the morphology of the taxon based on the Romanian remains. Journal of Vertebrate Paleontology 28, 111–122.

Delfino, M., Martin, J.E. & Buffetaut, E. 2008b: A new species of *Acynodon* (Crocodylia) from the Upper Cretaceous (Santonian–Campanian) of Villaggio del Pescatore, Italy. Palaeontology 51, 1091–1106.

Efimov, M.B. & Yarkov, A.A. 1993: A Paleocene crocodile from the lower Volga Basin. Paleontological Journal 27, 114–118.

Franke, A. 1927: Die Foraminiferen und Ostracoden des Palaeocäns von Rugaard in Jütland und Sundkrogen bei Kopenhagen. Danmarks Geologiske Undersøgelse, II. Række 46, 49 pp.

Gravesen, P. 1993. Fossiliensammeln in Südskandinavien. 248 pp. Weinstadt: Goldschneck-Verlag.

Gravesen, P. 1994: Udgravningerne til Øresundsforbindelsen ved Tårnby på Amager 1994 – en kort beskrivelse. Lapidomanen 1994, 5pp.

Gravesen, P., & Jakobsen, S.L. 2012: Skrivekridtets Fossiler. 154 pp. Copenhagen: Gyldendal.

Grönwall, K.A. 1904: Forsteningsførende Blokke fra Langeland, Sydfyn og Ærø samt bemærkninger om de ældre Tertiærdannelser i det baltiske område. Danmarks Geologiske Undersøgelse, II. Række 15, 62 pp.

Gry, H. 1935: Petrology of the Paleocene sedimentary rocks of Denmark. Danmarks Geologiske Undersøgelse, II. Række 61, 171 pp.

Harder, P. 1922: Om Grænsen mellem Saltholmskalk og Lellinge Grønsand og nogle Bemærkninger om Inddelingen af Danmarks ældre Tertiær. Danmarks Geologiske Undersøgelse, II. Række 38, 108 pp.

Heilmann-Clausen, C., & Surlyk, F. 2006: Koralrev og Lerhav. In: Sand-Jensen, K. & Larsen, G. (eds), Naturen i Danmark, Geologien, 181–226. Copenhagen: Gyldendal.

Hucke-Voigt, K. 1967: Einführung in die Geschiebeforschung. (Sedimentärgeschiebe). Herausgegeben und erweitert von E. Voigt, 132 pp. Oldenzaal: Nederlandse Geologische Stichting.

Jagt, J.W.M., van Bakel, B.W.M., Cremers, G., Deckens, M.J.M., Dortangs, R.W., van Es, M., Fraaije, R.H.B., Kisters, P.J.M., van Knippenberg, P.H.M., Lemmens, H., Nieuwenhuis, E., Severijns, J. & Stroucken, J.W. 2013: Het Vroeg Paleoceen (Danien) van zuidelijk Limburg en aangrenzend gebied – nieuwe fauna´s en nieuwe inzichten. Afzettingen WTKG 34, 198–230.

Koken, E. 1888: *Thoracosaurus macrorhynchus* Bl. aus der Tuffkreide von Maastricht. Zeitschrift der Deutschen Geologischen Gesellschaft 40, 754–773.

Krebs, B. 1967: Der Jura-Krokodilier *Machimosaurus* H. v. Meyer. Paläontologische Zeitschrift 41, 46–59.

Krebs, B. 1968: Le crocodilien *Machimosaurus*. Memória dos Servicos Geológicos de Portugal (N.S.) 14, 21–53.

Laurent, Y., Buffetaut, E., & Le Loeuff, J. 2000: Un crane de thoracosaurine (Crocodylia, Crocodylidae) dans le Maastrichtien superieur du sud de la France. Oryctos 3, 19–27.

Lundgren, B. 1890: Ein Gavial aus dem Senon von Annetorp bei Malmö. Neues Jahrbuch für Mineralogie, Geologie und Paläontologie 2, 275.

Martin, J.E. 2007: New material of the Late Cretaceous globidontan *Acynodon iberoccitanus* (Crocodylia) from southern France. Journal of Vertebrate Paleontology 27, 362–372.

Martin, J.E. 2010: *Allodaposuchus* Nopsca, 1928 (Crocodylia, Eusuchia), from the Late Cretaceous of southern France and its relationships to Alligatoroidea. Journal of Vertebrate Paleontology 30, 756–767.

Martin, J.E. & Buffetaut, E. 2008: *Crocodilus affuvelensis* Matheron, 1969 from the Late Cretaceous of southern France: a reassessment. Zoological Journal of the Linnean Society 152, 567–580.

Martin, J.E. & Delfino, M. 2010: Recent advances in the comprehension of the biogeography of Cretaceous European eusuchians. Palaeogeography, Palaeoclimatology, Palaeoecology 293, 406–418.

Martin, J.E., Rabi, M. & Csiki, Z. 2010: Survival of *Theriosuchus* (Mesoeucrocodylia: Atoposauridae) in a Late Cretaceous archipelago: a new species from the Maastrichtian of Romania. Naturwissenschaften 97, 845–854.

Milàn, J., Lindow, B.E.K. & Lauridsen, B.W. 2011: Bite traces in a turtle carapace fragment from the middle Danian (Lower Paleocene) bryozoan limestone, Faxe, Denmark. Bulletin of the Geological Society of Denmark 59, 61–67.

Milthers, V. 1935: Nordøstsjællands Geologi. 2. edition. Danmarks Geologiske Undersøgelse, V. Række 3, 192 pp.

Mook, C.C. 1940: A new fossil crocodilian from Mongolia. American Museum Novitates 1097, 1–3.

Ørestadsselskabet I/S 2001: Metro. Gangtunnel ved Nørreport. Geologi. Datering af sand. Ravpindelag. Report by Cowi Consult, 5 pp. + appendices.

Persson, P.O. 1959: Reptiles from the Senonian (U. Cret.) of Scania (S. Sweden). Arkiv för Mineralogi och Geologi 2, 431–478.

Piras, P., Delfino, M., Favero, L.D. & Kotsakis, T. 2007: Phylogenetic position of the crocodylian *Megadontosuchus arduini* and tomistomine palaeobiogeography. Acta Palaeontologica Polonica 52, 315–328.

Puértolas, E., Canudo, J.I. & Cruzado-Caballero, P. 2011: A New Crocodylian from the Late Maastrichtian of Spain: Implications for the initial radiation of Crocodyloids. PLOS One 6, 1–12.

Ravn, J.P.J. 1939: Études sur les mollusques du Paléocène de Copenhague. Det Kongelige Danske Videnskabernes Selskab Biologiske Skrifter 1(1), 106 pp.

Rees, J. 2000: An Early Cretaceous scincomorph lizard dentary from Bornholm, Denmark. Bulletin of the Geological Society of Denmark 48, 105–109.

Rees, J. 2002: Shark fauna and depositional environment of the earliest Cretaceous Vitabäck Clays at Eriksdal, southern Sweden. Transactions of the Royal Society of Edinburgh, Earth Sciences 93, 59–71.

Reinecke, T. & Engelhard, P. 1997: The Selachian Fauna from Geschiebe of the Lower Selandian Basal Conglomerate in the Danish Subbasin. Erratica, Monographien zur Geschiebekunde 2, 32 pp.

Rohde, A. 2008: Auf Fossiliensuche an der Ostsee. 272 pp. Neumünster: Wachholtz Verlag.

Rørdam, K. 1897: Kridtformationen i Sjælland i Terrænet mellem København og Køge, og paa Saltholm. Avec Résumé en francais. Danmarks Geologiske Undersøgelse, II. Række 6, 152 pp.

Rørdam, K. 1899: Beskrivelse til Kaartbladene Kjøbenhavn og Roskilde i 1:100 000. Danmarks Geologiske Undersøgelse, I. Række 6, 107 pp. + plates.

Rosenkrantz, A. 1920a: Craniakalk fra Kjøbenhavns Sydhavn. Danmarks Geologiske Undersøgelse, II. Række 36, 79 pp.

Rosenkrantz, A. 1920b: En ny københavnsk Lokalitet for forsteningsførende Paleocæn. Meddelelser fra Dansk Geologisk Forening 5, 1–10.

Rosenkrantz, A. 1924: De københavnske Grønsandslag og deres Placering i den danske Lagrække. Meddelelser fra Dansk Geologisk Forening 6, 1–39.

Rosenkrantz, A. 1925. Undergrundens tektoniske Forhold i København og nærmeste Omegn. Meddelelser fra Dansk Geologisk Forening 6, 1–18.

Rosenkrantz, A. 1930: Den paleocæne Lagserie ved Vestre Gasværk. Meddelelser fra Dansk Geologisk Forening 7, 371–390.

Rosenkrantz, A. 1937: Bemærkninger om det østsjællandske Daniens Stratigrafi og Tektonik. Meddelelser fra Dansk Geologisk Forening 9, 199–212.

Rosenkrantz, A. 1942: Om de strukturelle Forhold i den prækvartære Undergrund i Østsjælland. Meddelelser fra Dansk Geologisk Forening 10, 152–158.

Rossmann, T. & Blume, M. 1999: Die Krokodil-Fauna der Fossillagerstätte Grube Messel: Ein aktueller Überblick. Natur und Museum 129, 261–270.

Rudolph, F., Bilz, W., & Pittermann, D. 2010: Fossilien an Nord- und Ostsee. 283 pp. Wiebelsheim: Quelle & Meyer.

Schmitz, B., Pujalte, V., Molina, E., Monechi, S. Orue-Etxebarria, X., Speijer, R.P., Alegrat, L., Apellaniniz, E., Arenillas, I., Aubry, M.-P., Baceta, J.-I., Berggren, W.A., Bernaola, G., Caballero, F., Clemmensen, A., Dinarés-Turell, J., Dupais, C., Heilmann-Clausen, C., Orús, A.H., Knox, R., Martin, R.M., Ortiz, S., Payros, A., Petrizzo, M.R., Salis, K., Sprong, J., Steurbbaut, E., & Thomsen, E. 2011: The Global Stratotype Sections and Points for the bases of the Selandian (Middle Paleocene) and Thanetian (Upper Paleocene) stages at Zumaia, Spain. Episodes 34, 220–243.

Schnetler, K.I. 2001: The Selandian (Paleocene) mollusc fauna from Copenhagen, Denmark: the Poul Harder 1920 collection. Danmarks og Grønlands Geologiske Undersøgelse (GEUS), Bulletin 37, 73 pp.

Schulz, W. 2003: Geologischer Führer für den norddeutschen Geschiebesammler. Cw Verlagsgruppe, Schwerin, 507 pp.

Schwarz-Wings, D., Rees, J. & Lindgren, J. 2009: Lower Cretaceous Mesoeucrocodylians from Scandinavia (Denmark and Sweden). Cretaceous Research 30, 1345–1355.

Schwarzhans, W. 2003: Fish otoliths from the Paleocene of Denmark. Geological Survey of Denmark and Greenland Bulletin 2, 94 pp.

Stenestad, E. 1976: Københavnsområdets geologi især baseret på citybaneundersøgelserne. Danmarks Geologiske Undersøgelse, III. Række 45, 149 pp.

Stouge, S., Hjortkjær, B.F., Rasmussen, J.A., Roncaglia, L. & Sheldon, E. 2000: Micro- and nannofossil biostratigraphy across the Danian/Selandian Stage boundary at Gemmas Allé, Copenhagen, Denmark. GFF 122, 161–162.

Troedsson, G.T. 1923: Om krokodilfyndan i Skånes yngsta Krita. GFF 45, 549–567.

Troedsson, G.T. 1924: On crocodilian remains from the Danian of Sweden. Lunds Universitets Årsskrift 2, 20, 1–75.

Vasse, D. 1995: *Ischyrochampsa meridionalis* n. g. n. sp., un crocodilien d'affinité gondwanienne dans le Crétacé supérieur du Sud de la France. Neues Jahrbuch für Geologie und Mineralogie, Monatshefte 1995, 501–512.

Manganiferous minerals of the epidote group from the Archaean basement of West Greenland

ANNA KATERINOPOULOU, TONCI BALIC-ZUNIC, JOCHEN KOLB, ALFONS BERGER
& KARSTEN SECHER

Katerinopoulou, A., Balic-Zunic, T., Kolb, J., Berger, A. & Secher, K. 2014. Manganiferous minerals of the epidote group from the Archaean basement of West Greenland. © 2014 by Bulletin of the Geological Society of Denmark, Vol. 62, pp. 27–37. ISSN 2245-7070. (www.2dgf.dk/publikationer/bulletin).

The chemical compositions and crystal structures of Mn^{3+}-containing minerals from the epidote group in Greenland rocks are investigated and described in detail. They occur in hydrothermally altered Archaean mafic sequences within the gneissic complex of the North Atlantic craton of West Greenland. The Mn-containing minerals have a characteristic red to pink colour. A detailed microchemical study shows a significant inter- and intra-sample variation in Mn content. The samples from different parageneses can be classified as Mn-bearing epidote and Mn-bearing clinozoisite. The intra-sample variation in the content of Al, Fe and Mn is on a very fine scale, but still allows for identification of a negative correlation between Mn and Fe. Textures indicate different stages of growth. Crystal chemical data are compared with literature data and illustrate the basic systematic differences between the influence of Fe and Mn on the crystal structure of the epidote group minerals.

Received 9 June 2014
Accepted in revised form
7 August 2014
Published online
6 October 2014

Keywords: Epidote, clinozoisite, Greenland, manganiferous minerals.

A. Katerinopoulou [annak@snm.ku.dk], Natural History Museum of Denmark, Øster Voldgade 5–7, DK-1350 Copenhagen K, Denmark; current address: [akat@topsoe.dk], Haldor Topsøe, Nymøllevej 55, DK-2800 Kgs. Lyngby, Denmark. T. Balic-Zunic [toncib@snm.ku.dk], Natural History Museum of Denmark, Øster Voldgade 5–7, DK-1350 Copenhagen K, Denmark. J. Kolb [jkol@geus.dk] and K. Secher [kse@geus.dk], Geological Survey of Denmark and Greenland (GEUS), Øster Voldgade 10, DK-1350 Copenhagen K, Denmark. A. Berger [ab@geo.ku.dk], Department of Geography and Geology, University of Copenhagen, Øster Voldgade 10, DK-1350 Copenhagen K, Denmark; current address: [alfons.berger@geo.unibe.ch], Institute of Geological Sciences, University of Bern, Switzerland.

Observations of Mn-containing minerals in Greenland have been scarce. Apart from a dubious determination in 1901 by Flink (Bøggild 1953, remark on p. 140) of rhodocrosite within the Proterozoic late Gardar alkaline Narssarsuk pegmatite, Thomassen & Krebs (2001) report manganiferous carbonate in East Greenland, associated with epithermal vein fillings related to the Palaeogene subvolcanic Flammefjeld intrusive complex. These carbonates are the only previously published observations. However, there have been some unpublished reports of pink-coloured minerals from Greenland tentatively described as "thulite", a pink Mn^{2+}-bearing variety of zoisite (O.V. Petersen, personal communication). Here we attempted to analyze in detail all of the known occurrences of the latter type of minerals from Greenland and provide their first full characterization. They all originate from Archean rocks.

Origin of the material and geological setting

The samples carrying manganiferous minerals were collected from three different locations in the areas of Maniitsoq, Tasiusarsuaq and Paamiut, West Greenland (Table 1, Fig. 1). All three areas lie within the Archaean North Atlantic craton which is mainly composed of grey gneisses and narrow belts of supracrustal rocks. The areas mainly comprise amphibolite and mafic granulite, as well as minor metasedimentary and ultramafic rocks (e.g. Windley & Garde 2009). Late-tectonic granitic intrusions are volumetrically minor (e.g.Windley & Garde 2009). The rocks underwent several stages of high-grade metamorphism in granulite and amphibolite facies and several stages of deformation during the Archaean (Friend & Nutman 2001). A mafic dyke swarm intruded the craton in the

Table 1. Origin and characteristics of samples

Sample	Location	Coordinates	Host rock	Manganiferous mineral
492571	Maniitsoq area	65°18.36'N, 51°35.70'W	Pegmatitic/aplitic granulite	Light pink Mn-containing clinozoisite
508347	Tasiusarsuaq terrane	63°56.46'N, 50°03.84'W	Amphibolite (meta-peridotite)	Purple Mn-rich epidote
177975	Paamiut area	62°00.78'N, 49°40.26'W	Amphibolite	Purple Mn-rich clinozoisite*

*Earlier described as 'thulite'

Proterozoic with NW–SE, E–W, and NE–SW orientations (Kalsbeek & Taylor 1985). The dykes intersect mutually and are themselves intersected by kilometre-scale faults and fault zones which are interpreted to be Proterozoic, based on intersection relationships (e.g. Smith & Dymek 1983).

The brittle to brittle–ductile faults are near-vertical and trend N–S, NW–SE, and W–E. They have a lateral displacement of marker horizons of up to 1 km. All faults show a halo of hydrothermal alteration, which for the larger faults may extend to several hundreds of metres (Kolb *et al.* 2009). The hydrothermal alteration is characterized by the greenschist facies assemblage of chlorite, epidote, muscovite and calcite (Kolb *et al.* 2009).

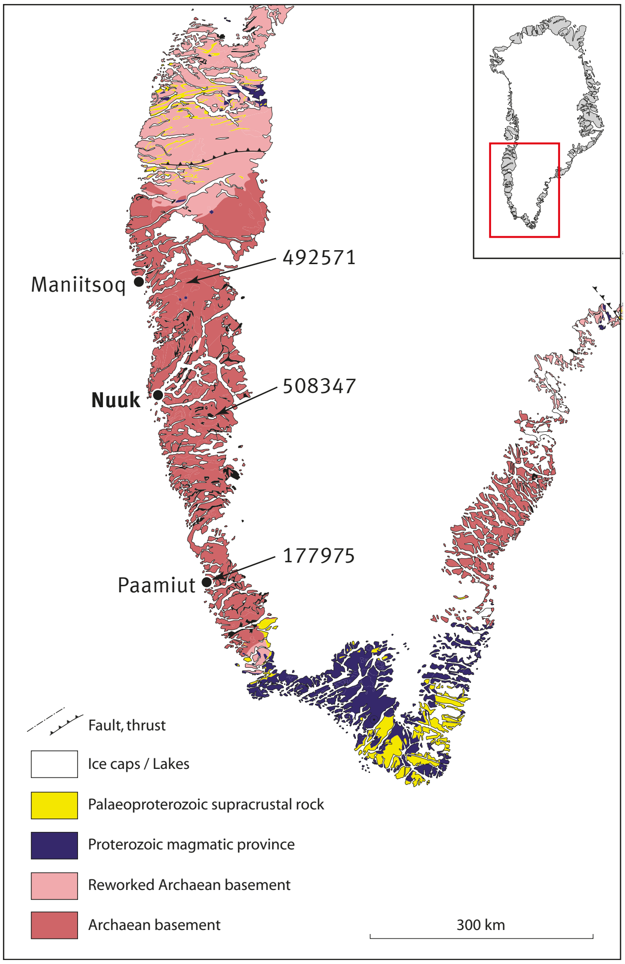

Fig. 1. Map of West Greenland showing the locations of the Mn-bearing mineral samples.

The hydrothermal alteration assemblage locally comprises pyrite and chalcopyrite. The sulphides are commonly oxidized and leached, as witnessed by the formation of hematite, bornite and covellite, which may be related to a later hydrothermal meteoric overprint. The occurrence of the manganiferous minerals analyzed here is restricted to hydrothermal alteration of fault zones in different host rocks.

Sample 492571 represents migmatitic gneiss from the Maniitsoq area. The gneisses have a granulite facies mineral assemblage of orthopyroxene + clinopyroxene + plagioclase + quartz ± magnetite, ilmentite, amphibole and biotite (Riciputi *et al.* 1990). Peak metamorphic conditions are estimated at 800 ± 50°C and 7.9 ± 1 kbar (Riciputi *et al.* 1990). Retrogression in amphibolite facies is widespread, whereas a greenschist facies overprint is restricted to fault zones (Riciputi *et al.* 1990; Windley & Garde 2009).

Sample 508347 represents a meta-ultramafic dyke or sill from the Tasiusarsuaq terrane (Kolb *et al.* 2012). Three rock types are distinguished in the locality: (1) a massive, medium-grained greenish to brownish weathering rock with a clinopyroxene + hornblende + orthopyroxene + magnetite ± garnet ± biotite ± olivine ± calcite ± cummingtonite ± pyrrhotite ± chalcopyrite assemblage; (2) a layered, medium-grained grey rock with centimetre-scale black hornblende ± quartz ± titanite ± calcite ± magnetite layers and grey hornblende + plagioclase layers; (3) a massive, medium-grained, black rock consisting of hornblende + clinopyroxene + orthopyroxene + pyrrhotite + magnetite. They represent meta-pyroxenites and meta-peridotites that were overprinted at 7–12 kbar and 750–840°C (Riciputi *et al.* 1990; Wells 1976). Retrograde amphibolite facies conditions are estimated at 7 kbar and 630°C (Riciputi *et al.* 1990; Wells 1976). A dilational jog south of Ameralik fjord is a few hundred metres wide and intensely altered and mineralized by a stockwork quartz vein system containing up to 25 ppm Ag and 2 wt% Cu (Appel *et al.* 2005; Kolb *et al.* 2009). The hydrothermal system is interpreted to be controlled by deformation along the faults. Focusing of fluids and stockwork-type veining and mineralization is controlled by regional anisotropies represented in this case by the dilational jog. Greenschist facies assemblages close to the fault zones comprise epidote + chlorite + quartz + serpentine + talc ± rutile ± titanite.

Sample 177975 from the Paamiut area is a chip from a large ice-transported boulder of more than 200 kg. This impressive piece of purple coloured float has never been unambiguously traced to an in-situ locality, although it probably originates from similar rocks containing purple epidote-like minerals that have been observed in the eastern part of the Paamiut area (F. Kalsbeek, personal communication). It is an amphibolite with a characteristic assemblage comprising hornblende + plagioclase + quartz ± garnet and minor titanite, magnetite, ilmenite and apatite. The boulder from which the sample was taken shows stockwork vein sets and a greenschist facies alteration assemblage of clinozoisite/epidote + albite + quartz.

Experimental

Mineral chemical analyses were performed on polished thin sections using a JEOL JXA8200 electron microprobe (EMP) located at the Department of Geography and Geology of the University of Copenhagen. Measuring conditions were 15 kV and 15 nA, all elements were measured with WDS using natural and synthetic oxides and silicates as standards. Corrections of the raw data were performed using the ZAF procedure.

Single crystals of reddish to pink colour were optically hand-picked from the rock samples for X-ray diffraction (XRD). Analyses were performed using a Bruker-AXS four-circle diffractometer equipped with a CCD area detector and a flat graphite monochromator, using MoKα radiation from a fine-focus sealed X-ray tube. A total of 2800 exposures per sample (step = 0.2°, time/step = 10 s) covering the full reciprocal sphere were collected. Data collection, intensity integration and absorption correction were carried out with the Bruker programs Smart, Saint and Sadabs respectively. After space group identification the structure was refined using the structure model of Dollase (1971) as starting model. Occupancies were refined and the mean electron number was used to elaborate on the composition of the samples. For sites A1 and A2 the number of electrons was 20 within standard deviation, and site populations were fixed to full Ca occupation. Refinement data are reported in Table 2.

Table 2. Refinement details for the three samples

Sample number	**492571**	**508347**	**177975**
Empirical formula (XRD+EMPA)*	$Ca_2Al_{2.78}Fe_{0.21}Mn_{0.02}Si_3O_{12}(OH)$	$Ca_2Al_{2.20}Fe_{0.60}Mn_{0.13}Si_3O_{12}(OH)$	$Ca_2Al_{2.51}Fe_{0.47}Mn_{0.02}Si_3O_{12}(OH)$
Formula weight M_r	965.6	884.7	966.5
Crystal System	monoclinic	monoclinic	monoclinic
Z	2	2	2
F(000)	477	438	478
μ(mm^{-1})	3.36	3.18	3.44
$\varrho\chi$ (gr cm^{-3})	3.52	3.20	3.51
Space group (no.)	P2(1)/m (11)	P2(1)/m (11)	P2(1)/m (11)
a (Å)	8.8790(9)	8.8891(5)	8.8890(7)
b (Å)	5.5947(1)	5.6255(3)	5.6149(5)
c (Å)	10.1570(9)	10.1605(5)	10.1601(8)
β (°)	115.483(6)	115.447(1)	115.439(2)
V (Å^3)	455.47	458.79	457.93
Number of reflections/Unique	4769/1463 (R_{int} = 0.0498)	4926/1525 (R_{int} = 0.0304)	5060/1524 (R_{int} = 0.0511)
Data/restraints/parameters	1463/0/119	1525/0/119	1524/0/119
Extinction coefficient *k*	0	0	0
Goodness-of-fit, S	0.807	0.767	0.824
R indices for I>2σ(I)	R_1 = 0.0355	R_1 = 0.0208	R_1 = 0.0390
R indices (all data)	R_1 = 0.0531	R_1 = 0.0225	R_1 = 0.0608
	wR_2 = 0.1131	wR_2 = 0.0861	wR_2 = 0.1256

$R_1 = \sum||Fo|-|Fc|| / \sum|Fo|$

$wR_2 = [\sum[w(Fo^2-Fc^2)^2] / \sum[w(Fo^2)^2]]^{0.5}$

*The proportions of Al, Fe and Mn are calculated on the basis of the m.e.n. (Table 4) by taking into account the Fe:Mn ratio calculated from the EMPA results (Table 3).

Table 3. Chemical compositions of epidote-group minerals.

Sample	**492571**			**492571**		
	High Fe			**Low Fe**		
	N=3			N=7		
	wt%	stdev	Range	wt%	stdev	Range
Al_2O_3	28.52	0.33	28.15 - 28.77	31.41	0.42	30.62 - 31.88
Fe_2O_3	5.76	0.31	5.50 - 6.10	2.20	0.28	1.92 - 2.70
CaO	23.86	0.20	0.01 - 0.02	24.50	0.37	24.05 - 25.01
MgO	0.02	0.01	0.01 - 0.02	0.11	0.03	0.05 - 0.16
SiO_2	39.01	0.33	0.00 - 0.21	39.39	0.35	38.78 - 39.80
Mn_2O_3	0.08	0.11	0.00 - 0.21	0.30	0.09	0.18 - 0.41
TiO_2	0.02	0.03	0.00 - 0.06	0.16	0.11	0.02 - 0.27
Total	97.27	0.91	96.24 - 97.96	98.07	0.88	96.63 - 99.24
Recalculation to cations on the basis of O = 12.5						
Al	2.64	0.01	2.64 - 2.65	2.84	0.02	2.82 - 2.85
Fe	0.38	0.02	0.36 - 0.40	0.14	0.02	0.12 - 0.18
Ti	0.00	0.00	0.00 - 0.00	0.01	0.01	0.00 - 0.02
Si	3.07	0.00	3.06 - 3.07	3.02	0.01	3.01 - 3.04
Mn	0.01	0.01	0.00 - 0.01	0.02	0.01	0.01 - 0.03
Ca	2.01	0.02	1.99 - 2.02	2.01	0.01	1.99 - 2.03
Mg	0.00	0.00	0.00 - 0.00	0.01	0.00	0.01 - 0.02
Total	8.11	0.00	0.00 - 8.11	8.05	0.01	8.04 - 8.06

Analyses of sample 492571 are categorized according to the Fe content

Sample	**508347**			**177975**		
	N=49			N=33		
	wt%	std dev	Range	wt%	std dev	Range
Al_2O_3	23.68	0.92	21.58 - 25.39	28.47	2.08	25.31 - 31.47
Fe_2O_3	11.74	2.07	8.33 - 15.55	4.53	3.24	1.00 - 11.06
TiO_2	0.05	0.05	0.00 - 0.22	0.06	0.06	0.00 - 0.21
Na_2O	0.01	0.01	0.00 - 0.04	0.02	0.05	0.00 - 0.28
SiO_2	37.67	0.29	36.96 - 38.19	38.34	0.59	37.40 - 39.47
Mn_2O_3	1.30	1.06	0.00 - 3.56	1.35	1.72	0.02 - 5.89
CaO	23.93	0.23	23.42 - 24.33	24.58	0.43	23.85 - 25.31
MgO	0.03	0.03	0.00 - 0.09	0.06	0.05	0.00 - 0.17
$Cr2O_3$	0.02	0.02	0.00 - 0.08	0.01	0.02	0.00 - 0.06
Total	98.43	0.61	96.91 - 99.57	97.43	0.73	96.15 - 99.38
Recalculation to cations on the basis of O = 12.5						
Al	2.21	0.08	2.02 - 2.34	2.62	0.17	2.34 - 2.85
Fe	0.70	0.12	0.50 - 0.93	0.27	0.19	0.06 - 0.65
Ti	0.00	0.00	0.00 - 0.01	0.00	0.00	0.00 - 0.01
Na	0.00	0.00	0.00 - 0.01	0.00	0.01	0.00 - 0.04
Si	2.99	0.01	2.95 - 3.01	2.99	0.02	2.95 - 3.03
Mn	0.08	0.06	0.00 - 0.22	0.08	0.10	0.00 - 0.35
Ca	2.03	0.02	1.98 - 2.08	2.05	0.02	2.01 - 2.10
Mg	0.00	0.00	0.00 - 0.01	0.01	0.01	0.00 - 0.02
Cr	0.00	0.00	0.00 - 0.00	0.00	0.00	0.00 - 0.00
Total	8.02	0.01	8.00 - 8.04	8.02	0.01	8.00 - 8.06

Results

Chemical compositions and mineral associations

The results of the microprobe analyses of the pink coloured minerals from the three investigated samples are presented in Table 3. X-ray diffraction results show that they all belong to the epidote group of minerals which is in accordance with their chemical composition. The measured variation of the Al→Fe,Mn substitution in sample 177975 indicates a continuous solid solution (Fig. 2), whereas this variation in sample 492571 lacks compositions within the proposed immiscibility gap of the clinozoisite-epidote series around 25% epidote (Raith 1976; Heuss-Aßbichler & Fehr 1997). Sample 508347 lies on the high-Fe side of the proposed immiscibility gap and is thus not indicative (Fig. 2).

The mineral assemblage determined by EMP analysis in sample 492571 (migmatitic gneiss from Maniitsoq) characterizes the greenschist facies and comprises coexisting clinozoisite and quartz, tremolite, titanite and zircon (Fig. 3a). Clinozoisite appears in masses of irregular grains, which consist of iron-rich rims (approx. 0.40 Fe apfu) and iron-poor cores (approx. 0.12 Fe apfu) (Fig. 3b). The cores are sometimes more complex with an euhedral zone with an intermediate (Fe+Mn)/Al ratio surrounded by an irregular second zone that is characterized by low (Fe+Mn)/Al ratio (Zones I and II, respectively on Fig. 3b). Fe-rich rims follow the grain boundaries or make lobate intrusions in the cores (Zone III on Fig. 3b). The appearance of zone III indicates a post-crystallization replacement process by a fluid richer in Fe. The apparent compositional gap is thus most probably due to this secondary enrichment in Fe which ceased at some time without subsequent homogenization of clinozoisite.

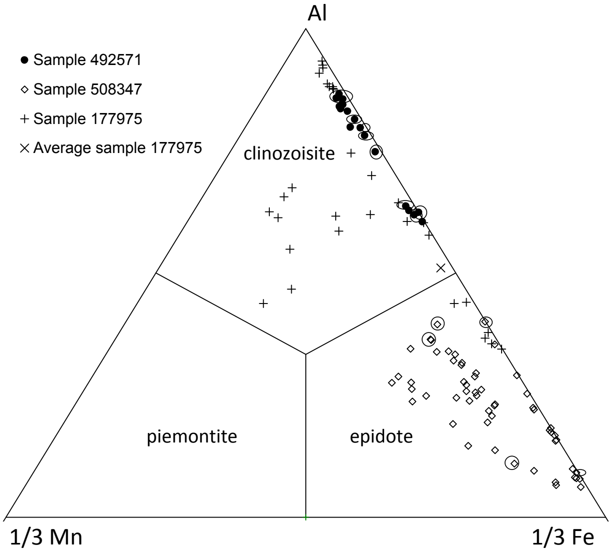

Fig. 2. Ternary diagram (Al–Mn–Fe) showing the octahedral cation population of epidote group minerals calculated from the results of microprobe analysis. Ellipses surround the compositions found for the 492571 and 508347 crystals investigated by XRD. The average composition of the crystal from 177975 is inferred from XRD results assuming 0.02 wt% Mn.

In sample 508347 (meta-peridotite), two textural types of epidote are observed: (1) euhedral grains ~100μm in size (Fig. 4a) and (2) massive aggregates of anhedral grains (Fig. 4b). These textural types do not have any distinctive compositional differences. Epidote shows variable amounts of Mn and Fe (Fig. 2). Compositions of the grains cover a broad range, extending from high Fe, low Mn and reaching close to the epidote-clinozoisite boundary with a wide scope

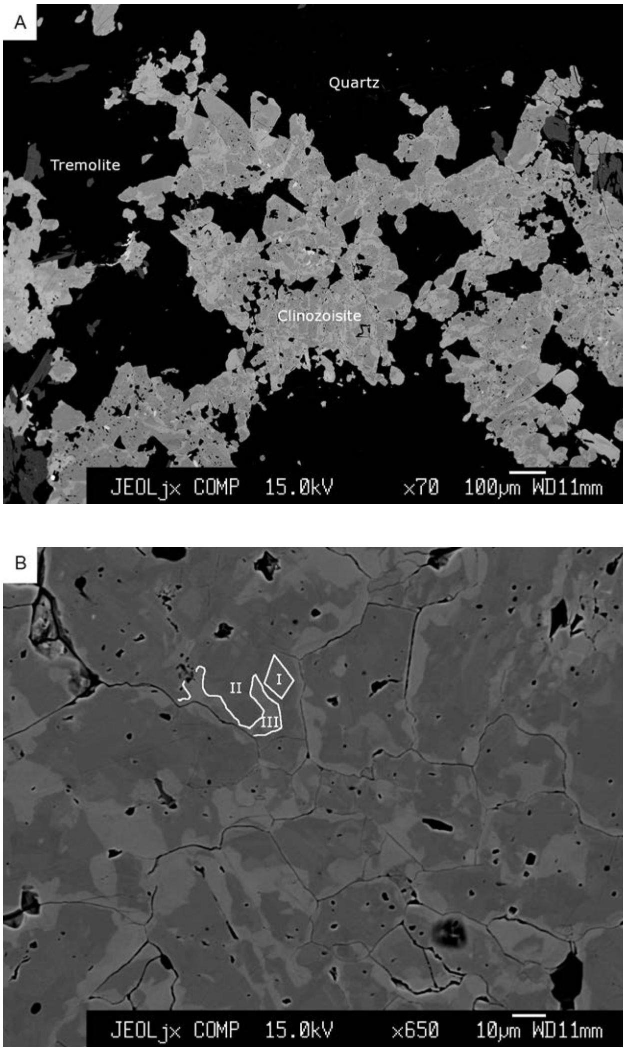

Fig. 3. Back-scattered electron images of sample 492571 (from felsic migmatitic gneiss). **A**: Clinozoisite in association with quartz and minor tremolite. **B**: Close-up of the clinozoisite assemblage with compositional zoning indicated, as described in the text.

of Mn content reaching up to 0.22 apfu. The enrichment in Mn is variable on a small scale and is generally negatively correlated with the Fe content. Several points with almost no Mn extend broadly along the epidote-clinozoisite join. It seems that the local variations in Mn during the growth of epidote caused a high degree of compositional inhomogeneity. One possible explanation is that the Mn content originates from the metamorphosed rock and depended on the distribution of primary Mn-containing minerals and their transformation paths.

In sample 177975 (amphibolite), the hydrothermal veins exhibit (1) clinozoisite selvages with 0.01–0.07 Fe apfu; (2) a fine-grained zone of mixed clinozoisite and epidote; (3) a broader zone dominated by larger crystals of subhedral Fe-rich clinozoisite (Fig. 5). There is a strong variation in the Mn-Fe content, sometimes even within the same crystal. The zonation is also optically detectable in the variable colour of the hand specimen. The content of Mn^{3+}, which is responsible for the red colour, has a range of 0-0.35 apfu in the sample (Fig. 2). This sample has on average the highest Mn-content of all the investigated samples.

It is interesting that the points with the lowest and highest Fe-contents show very small amounts of Mn, whereas those with intermediate compositions (corresponding to Fe-rich clinozoisite) show a large variation and sometimes significant enrichment in Mn (Fig. 2). Some parts are relatively enriched in manganese and reach the boundaries of the piemontite field. This enrichment occurs on a small scale and these crystals are in direct contact with Mn-poor areas. This illustrates the fact that even small amounts of Mn^{3+} are enough to give pink colouring, even in the presence of a high iron content.

Considering the large variations in compositions of clinozoisite and epidote in all three samples, the three crystals chosen for the crystal structure analysis were prepared for EMP analysis after the XRD measurement. Unfortunately, the crystal from 177975 was lost during the polishing process and its composition can only be reconstructed on the basis of its crystal structure. This shows that it has roughly average composition close to the clinozoisite-epidote boundary with a low Mn content (Fig. 2 and Table 2). The crystal from 492571 has an average composition of $Ca_2Al_{2.78}Fe_{0.21}Mn_{0.02}Si_3O_{12}(OH)$ determined from eight spot measurements with a relatively high variation in Al:Fe ratio from 62:37 to 81:12, encompassing

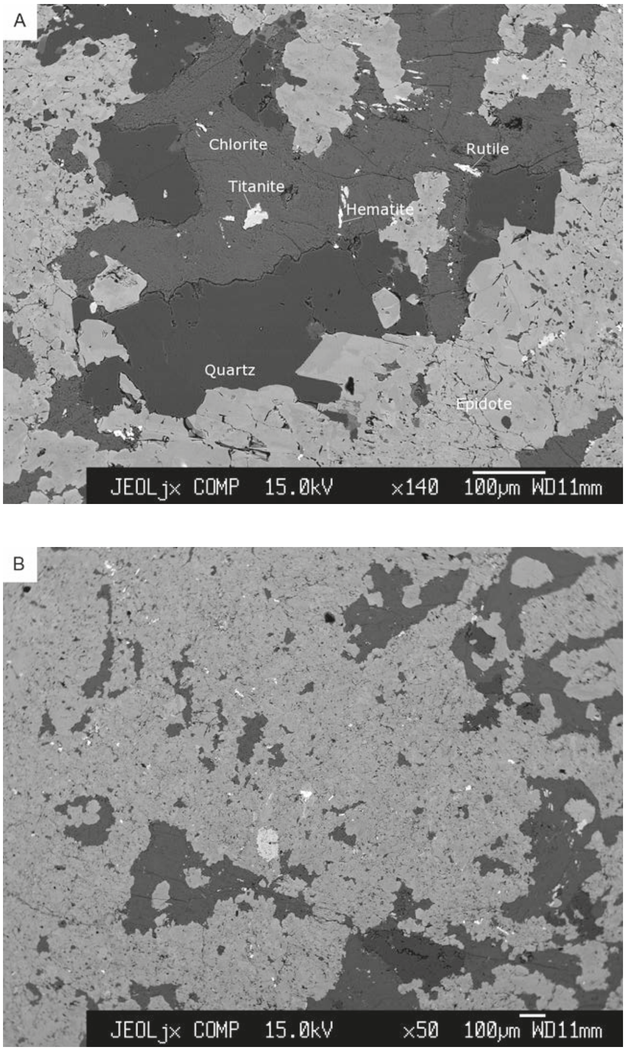

Fig. 4. Back-scattered electron images of sample 508347 (metaperidotite). **A**: Euhedral grains of epidote ranging into anhedral massive epidote in association with chlorite, quartz and accessory titanite and rutile. **B**: Massive anhedral epidote with interdispersed chlorite and minor quartz.

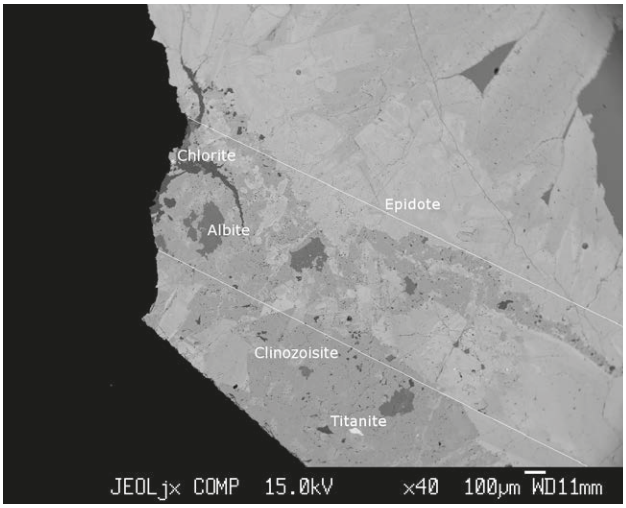

Fig. 5. Back-scattered electron image of sample 177975 (amphibolite). Lines are used as a guide to the eye to indicate the different zones within the sample.

Table 4. Atomic parameters and equivalent isotropic thermal factors U_{eq} for the three investigated samples

sample	492571	508347	177975
A1 (Ca)			
x	0.76082(11)	0.75837(6)	0.75933(12)
y	0.75	0.75	0.75
z	0.15481(9)	0.15276(5)	0.15336(11)
U	0.0120(2)	0.01080(13)	0.0087(3)
A2 (Ca)			
x	0.60639(11)	0.60516(6)	0.60581(12)
y	0.75	0.75	0.75
z	0.42342(9)	0.42398(5)	0.42368(11)
U	0.0135(2)	0.01331(14)	0.0109(3)
occ	Ca	Ca	Ca
M1 (Al)			
x	0	0	0
y	0	0	0
z	0	0	0
U	0.0081(3)	0.00652(15)	0.0028(5)
occ	Al	Al	Al
M2 (Al)			
x	0	0	0
y	0	0	0
z	0.5	0.5	0.5
U	0.0079(3)	0.00687(15)	0.0026(5)
occ	Al	Al	Al
M3			
x	0.28911(13)	0.29235(5)	0.29151(12)
y	0.25	0.25	0.25
z	0.22408(11)	0.22404(4)	0.22430(11)
U	0.0089(3)	0.00713(14)	0.0061(3)
m.e.n.	15.67(8) [15.47]	20.75(4) [21.77]	19.60(9) [19.35]
T1 (Si)			
x	0.33854(14)	0.33893(7)	0.33907(16)
y	0.75	0.75	0.75
z	0.04803(12)	0.04733(6)	0.04775(15)
U	0.0081(2)	0.00638(14)	0.0054(3)
T2 (Si)			
x	0.67930(14)	0.68243(7)	0.68143(16)
y	0.25	0.25	0.25
z	0.27523(12)	0.27499(6)	0.27509(15)
U	0.0080(2)	0.00679(14)	0.0052(3)
T3 (Si)			
x	0.18260(13)	0.18335(7)	0.18333(15)
y	0.75	0.75	0.75
z	0.31628(12)	0.31780(6)	0.31744(15)
U	0.0077(2)	0.00622(14)	0.0051(3)
O1			
x	0.2346(3)	0.23341(14)	0.2343(3)
y	0.9959(3)	0.99465(17)	0.9946(4)
z	0.0451(2)	0.04137(12)	0.0433(3)
U	0.0110(4)	0.0092(2)	0.0083(5)
O2			
x	0.3010(2)	0.30284(14)	0.3021(3)
y	0.9859(4)	0.98298(18)	0.9839(4)
z	0.3521(2)	0.35456(11)	0.3535(3)
U	0.0110(4)	0.0096(2)	0.0089(5)
O3			
x	0.7890(3)	0.79268(14)	0.7912(3)
y	0.0129(4)	0.01352(18)	0.0138(4)
z	0.3454(2)	0.34160(11)	0.3430(3)
U	0.0118(4)	0.0106(2)	0.0098(5)
O4			
x	0.0550(4)	0.0536(2)	0.0538(4)
y	0.25	0.25	0.25
z	0.1315(3)	0.13002(16)	0.1299(4)
U	0.0080(5)	0.0075(3)	0.0050(6)
O5			
x	0.0389(3)	0.04113(19)	0.0398(4)
y	0.75	0.75	0.75
z	0.1428(3)	0.14476(16)	0.1441(4)
U	0.0087(6)	0.0079(3)	0.0075(7)
O6			
x	0.0600(4)	0.06388(19)	0.0629(4)
y	0.75	0.75	0.75
z	0.4013(3)	0.40444(16)	0.4039(4)
U	0.0090(6)	0.0084(3)	0.0062(7)
O7			
x	0.5159(4)	0.5150(2)	0.5147(4)
y	0.75	0.75	0.75
z	0.1775(3)	0.17991(17)	0.1786(4)
U	0.0121(6)	0.0106(3)	0.0110(7)
O8			
x	0.5118(4)	0.5212(2)	0.5187(4)
y	0.25	0.25	0.25
z	0.2969(4)	0.30533(19)	0.3031(5)
U	0.0151(6)	0.0148(3)	0.0122(8)
O9			
x	0.6392(4)	0.6297(2)	0.6340(5)
y	0.25	0.25	0.25
z	0.1036(3)	0.10006(17)	0.1013(4)
U	0.0201(7)	0.0165(3)	0.0155(8)
O10			
x	0.0758(4)	0.08072(19)	0.0776(4)
y	0.25	0.25	0.25
z	0.4234(3)	0.42734(16)	0.4249(4)
U	0.0095(6)	0.0083(3)	0.0075(7)

A list of anisotropic thermal factors can be provided by the authors upon request. The occupancy of site M3 is represented by the refined mean electron number (m.e.n.) for this site. The m.e.n. calculated from EMPA is in [] brackets.

almost the entire range found in the large sample and representing both the Fe-poor core and Fe-rich rim. The crystal from 508347 has an average composition of $Ca_2Al_{2.20}Fe_{0.60}Mn_{0.13}Si_3O_{12}(OH)$ from five spot measurements. There is a large compositional variation within the crystal, which is immediately detectable in the backscatter image (Fig. 4). Part of the crystal has a composition with a very low Mn content (0.003 apfu) but a high Fe content, whereas other parts have Mn up to 0.11 apfu. The average composition of the crystal falls practically in the middle of the composition field for the sample (Fig. 2).

Crystallographic data

Single crystal X-ray diffraction of selected crystals confirms the clinozoisite-type structure for all three samples and substitution of Al, Fe and Mn, as expected for this structural family (Table 4). According to the structure refinement, Fe and Mn are exclusively present on the M3 site.

Identification of the proportion of Fe and Mn in the structure is not straightforward from X-ray diffraction data because the scattering factors of Fe and Mn are similar. It is, however, expected that the two have a different effect on the geometrical parameters of the crystal structure because of the Jahn–Teller effect of Mn^{3+} (Langer *et al.* 2002). The $3d^4$-configuration of M^{3+} in octahedral coordination causes splitting of the ^5E_g octahedral crystal-field ground state. The $3d^5$-configured Fe^{3+} behaves differently when incorporated in the structure and does not deviate from sphericity. The differences between Fe^{3+} and Mn^{3+} might influence the average bond distances and volumes and the distortion parameters of the coordination polyhedra. To explore this effect, we plotted data from crystal structures of synthetic and natural members of the epidote group of minerals (Dollase 1968; Gabe *et al.* 1973; Nozic *et al.* 1978; Stergiou *et al.* 1987; Comodi & Zanazzi 1997; Giuli *et al.* 1999; Nagashima & Akasaka 2004) with different substitution degrees of Fe and Mn. For the calculation of crystal chemical parameters we used the program IVTON (Balic-Zunic & Vickovic 1996).

Looking at the asphericity of the octahedra, i.e. the relative discrepancy of the ligands from the surface of the common sphere (Balic-Zunic & Makovicky 1996), it is clear that the asphericity can be expected to be significantly higher for Mn at the M3 site compared to Fe (Fig. 6a). Similar to the asphericity, the volume-based distortion (Makovicky & Balic-Zunic 1998) of the M3 site is larger for Mn-bearing samples than for Fe-bearing ones (Fig. 6b). Distortion seems to follow a linear trend with variation in chemistry, which changes at 0.6 apfu Fe in the clinozoisite–epidote series and 1 apfu Mn in the clinozoisite–piemontite series, representing the change of substitution mechanism with large Fe or Mn concentrations (Franz & Liebscher 2004). The trends are of decreasing asphericity and increasing volume distortion with increasing Fe or Mn content.

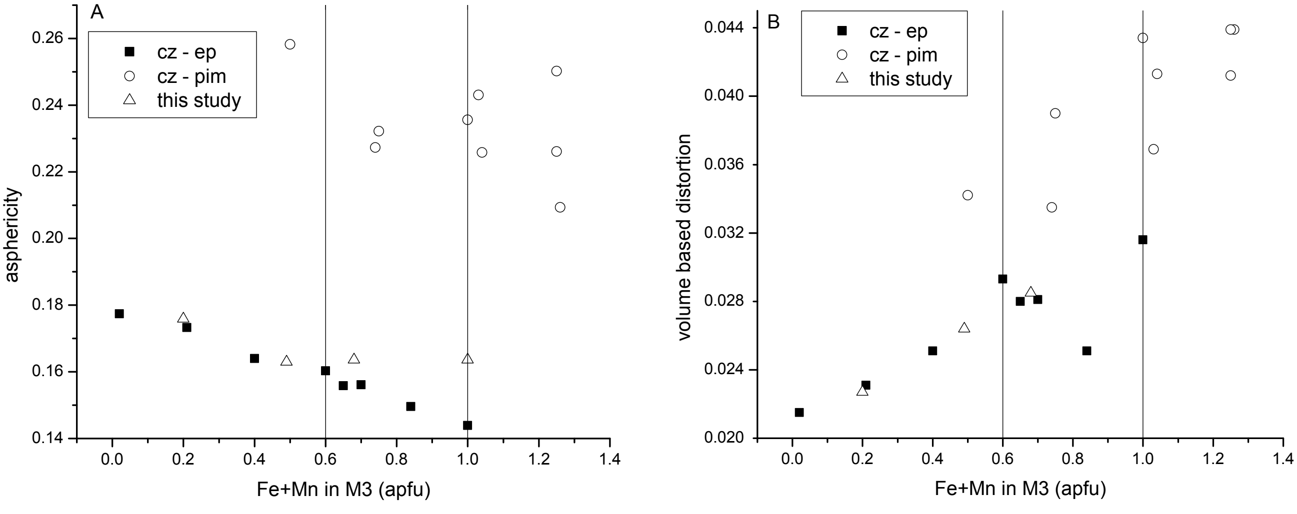

Fig. 6. Distortion parameters of the M3 polyhedron. **A**: Asphericity. **B**: Volume-based distortion. Cz: clinozoisite, ep: epidote, pim: piemontite. Clinozoisite–epidote data from Comodi & Zanazzi (1997), Dollase (1968, 1971), Gabe *et al.* (1973), Giuli *et al.* (1999) and Stergiou *et al.* (1987). Clinozoisite–piemontite data from Dollase (1969) and Nagashima & Akasaka (2004). Lines at 0.6 and 1 apfu mark the change in substitution mechanism for Fe and Mn, respectively.

Discussion

The crystal structure of the epidote group minerals with the general formula A1A2M1M2M3T_3O_{12}(OH) contains three types of octahedral sites: M1, M2 and M3. M1 octahedra share edges and form chains that run along the b axis. Individual M3 octahedra are attached to these chains on alternate sides, thus forming a zig-zag M1/M3 octahedral chain. M2 octahedra share edges and form separate simple chains that also run parallel to the b axis. The two types of octahedral chains are bridged by SiO_4 tetrahedra and Si_2O_7 groups (T in the general formula stands for the tetrahedral cation, in this case Si). In the spaces between the octahedral chains there are two crystallographically distinct sites, A1 and A2 coordinated by 9 and 10 oxygens, respectively. A-type sites are mainly occupied by Ca. The trivalent cations such as Al, Mn^{3+} and Fe^{3+} are distributed over the octahedral M sites. The classification rules for the solid solution series in the clinozoisite subgroup, where Ca occupies the A site, are based on the observation that the atomic substitutions take place predominately on the M3 sites. The M1 site accommodates some Fe and Mn only in samples with very high contents of these elements, whereas M2 remains practically a pure Al site. In accordance with this, the compositions which have a predominating content of Al in the M3 site are called clinozoisite, those with most Fe at this site are called epidote, and those that have Mn as the dominating cation are called piemontite (Armbruster *et al.* 2006). The M3 octahedron is located on the mirror plane. It is the largest and most distorted octahedron in the structure.

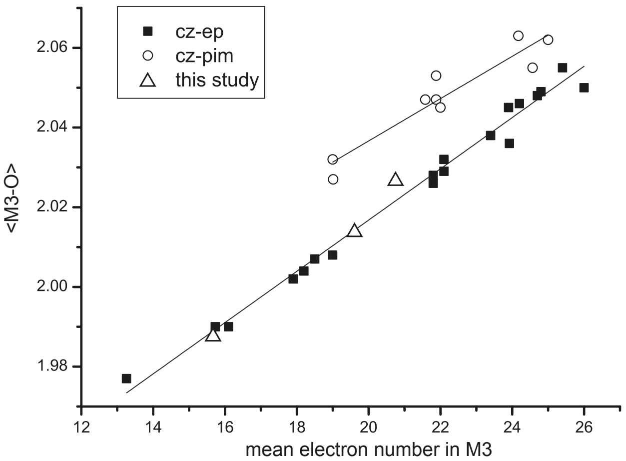

Fig. 7. Mean bond distance plotted against mean electron number for the M3 site. Cz: clinozoisite, ep: epidote, pim: piemontite. Clinozoisite–epidote data from Bonazzi & Menchetti (1995), Comodi & Zanazzi (1997), Dollase (1968, 1971), Gabe *et al.* (1973), Giuli *et al.* (1999), Langer *et al.* (2002) and Stergiou *et al.* (1987). Clinozoisite–piemontite data from Dollase (1969 and Nagashima & Akasaka (2004). Regression lines were fitted with a linear least squares function for each solid solution series.

Unlike M1 and M2 coordination octahedra, which form infinite chains by trans-edge sharing, the M3 polyhedron is only side-attached to the (M1) chain. This leaves a possibility to fill this site with a cation larger than Al. The bond distances and volume of the M3 polyhedron increase by rotation of the silicate tetrahedra with which the M3 polyhedron shares corners without influencing significantly the size of the M1 and M2 octahedral chains.

The incorporation of ions larger than Al in this site is therefore preferable. According to Bonazzi & Menchetti (1995) and Franz & Liebscher (2004), the volume of M3 increases with increasing Fe content, accompanied by the rotation of $T1O_4$ and $T2O_4$ tetrahedra with decreasing T1-O9-T2 angle. Nagashima & Akasaka (2004) observed the same structure changes with increasing Mn^{3+} content.

The substitution mechanism has been previously studied in natural and synthetic solid solutions along the clinozoisite-epidote join (Belov & Rumanova 1953, 1954; Ito *et al.* 1954; Dollase 1968, 1971; Gabe *et al.* 1973; Nozic *et al.* 1978; Stergiou *et al.* 1987; Comodi & Zanazzi 1997; Giuli *et al.* 1999; Langer *et al.* 2002) and the clinozoisite-piemontite join (Dollase 1969; Bonazzi & Menchetti 2004; Nagashima & Akasaka 2004, 2010). A change in substitution mechanism in these solid solutions at about 0.6 Fe pfu or 1 Mn pfu, respectively, has been suggested by Franz & Liebscher (2004). At concentrations higher than these, Fe or Mn are suggested to begin to enter the M1 site. It has also been proposed that small amounts of Fe^{2+} or Mn^{2+} can enter the A-sites in the clinozoisite sub-group (Bonazzi & Menchetti 2004; Nagashima & Akasaka 2010). There were no such indications from our X-ray diffraction data, in accordance with the results of the chemical analysis.

As regards the parameters of the M3 coordination polyhedron, only sample 508347 shows deviation from the pure clinozoisite-epidote trend and indication of the Mn content (Fig. 7). It is interesting that the distortion parameters do not indicate the point where the content of Mn seems to be insufficient to produce a significant deviation, whereas this is clearly visible in the bond lengths and size of the coordination polyhedra. Sample 492571 has only 1–2 mol% of Mn and it is not surprising that its influence cannot be observed. For sample 177975 we can conclude that the amount of Mn does not exceed a few mol% according to its crystal chemical parameters, but it is still sufficient to give the crystal its characteristic pink colour. Considering the large variation of the Mn content in this sample and due to the fact that the amount of Mn in the single crystal could not be experimentally determined, the Mn content ascribed to the crystal in Table 2 should be considered tentative.

The occurrence of the Mn-bearing minerals is related to vein formation within the West Greenland basement and the petrological implications point to a more widespread Mn- source introduced during the cratonic stages of Archaean Greenland.

There is a considerable variation in chemistry and texture of the manganiferous minerals described in this study. We could confirm by single-crystal X-ray diffraction and chemical analysis that they all belong to the epidote group of minerals and include both epidote and clinozoisite members enriched in Mn to varying degrees. The Mn content in the three analyzed samples varies significantly, although all of them have a similar appearance with a characteristic pink to purple colour. The mineral in the retrograde altered migmatitic gneiss (492571) is clinozoisite with a small amount of Mn (1 to 2 mol% in M3 site) which exhibits incomplete replacement of an original Fe-poor clinozoisite by a Fe-enriched variety in the last hydrothermal stage. The sample from the amphibolized meta-peridotite (508347) is epidote with a pronounced negative correlation in the content of Mn and Fe (Fig. 2). The sample from amphibolite (177975) locally shows the highest concentration of Mn of all three investigated samples and lies predominantly in the clinozoisite field, although the Fe-richest domains reach the epidote field. It is interesting that the medium-Fe portions of the sample typically show the highest Mn contents. A somewhat less clear negative correlation between Mn and Fe contents is observed in this sample (Fig. 2). However, the trends are difficult to define because the variation in content of Al, Fe and Mn is extensive and on a very fine scale. According to textural observations Mn has been mobilized in several stages, appearing both in larger euhedral grains and in fine grained anhedral material. The two textural types of epidote are similar in terms of Mn, Fe and Al variations, sometimes within the same crystal. They occur in veins produced by hydrothermal processes and their composition seems to depend strongly both on fluid composition and on the original chemical composition of the altered minerals.

The crystal chemical data available for the epidote group of minerals show discrepancies between synthetic and natural samples which can be attributed to the influence of quenching of the synthetic ones (Giuli *et al.* 1999). There is also a general lack of data from the natural samples with well documented chemical composition and crystal structure, especially for Mn-containing members of the group. Although this impedes the conclusion about the Mn/Fe ratios from the crystal structure analysis, we could document for the epidote sample the influence of around 10 mol% Mn on the crystal chemical parameters of the M3 site. Taking into account the speed of acquisition and accuracy of the new generation of single crystal diffractometers, we see this as an encouragement to use single-crystal diffraction in combination with chemical analysis for a routine, full characterisation of minerals from the epidote group. Our results show that minerals from this group achieve and retain a substantial chemical inhomogeneity without losing the structural homogeneity.

Acknowledgements

The authors thank O.V. Petersen and M. Ghisler for inspiring discussions during the preparation of this article and the referees Thomas Armbruster and J. Richard Wilson for their constructive comments. Our colleague, D. Schlatter, is thanked for alertness during the field collection. J. Kjærstrøm (Paamiut) noted the 'thulite' float in his backyard and is thanked for delivering samples of it to the Geological Museum, Copenhagen.

References

Appel, P.W.U., Coller, D., Coller, V., Heijlen, W., Moberg, E.D., Polat, A., Raith, J., Schjødt, F., Stendal, H. & Thomassen, B. 2005: Is there a gold province in the Nuuk region? Report from field work carried out in 2004. Rapport Danmarks og Grønlands Geologiske Undersøgelse 2005/27, 79 pp.

Armbruster, T., Bonazzi, P., Akasaka, M., Bermanec, V., Chopin, C., Gieré, R., Heuss-Assbichler, S., Liebscher, A., Menchetti, S., Pan, Y. & Pasero, M. 2006: Recommended nomenclature of epidote-group minerals. European Journal of Mineralogy 18 (5), 551–567.

Balic-Zunic, T. & Makovicky, E. 1996: Determination of the centroid or "the best centre" of a coordination polyhedron. Acta Crystallographica B52, 78–81.

Balic-Zunic, T. & Vickovic, I. 1996: IVTON - Program for the calculation of geometrical aspects of crystal structures and some crystal chemical applications. Journal of Applied Crystallography 29, 305–306.

Belov, N.V. & Rumanova, I.M. 1953: The crystal structure of epidote $Ca_2Al_2FeSi_3O_{12}(OH)$. Doklady Akademii Nauk SSSR 89, 853–856.

Belov, N.V. & Rumanova, I.M. 1954: The crystal sructure of epidote. Trudy Instituta Kristallografii, Akademiya Nauk SSSR 9, 103–163.

Bøggild, O.B. 1953: The mineralogy of Greenland. Meddelelser om Grønland 149 (3), 442 only.

Bonazzi, P. & Menchetti, S. 1995: Monoclinic members of the epidote group: effects of the Al–Fe^{3+}–Fe^{2+} substitution and of the entry of REE^{3+}. Mineralogy and Petrology 53, 133–153.

Bonazzi, P. & Menchetti, S. 2004: Manganese in monoclinic members of the epidote group: piemontite and related minerals. Reviews in Mineralogy and Geochemistry 56, 495–552.

Comodi, P. & Zanazzi, F. 1997: The pressure behavior of clinozoisite and zoisite: An X-ray diffraction study. American Mineralogist 82, 61–68.

Dollase W.A. 1968: Refinement and comparison of the structures of zoisite and clinozoisite. American Mineralogist 53, 1882–1898.

Dollase W.A. 1969: Crystal structure and cation ordering of piemontite. American Mineralogist 54, 710–717.

Dollase W.A. 1971: Refinement of the crystal structures of epidote, allanite and hancockite. American Mineralogist 56, 447–464.

Franz, G. & Liebscher, A. 2004: Physical and chemical properties of the epidote minerals–An introduction. Reviews in Mineralogy and Geochemistry 56, 1–80.

Friend, C.R.L. & Nutman, A.P. 2001: U-Pb zircon study of tectonically bounded blocks of 2940–2840 Ma crust with different metamorphic histories, Paamiut region, South-West Greenland: implications for the tectonic assembly of the North Atlantic craton. Precambrian Research 105 (2–4), 143–164.

Gabe, E.J., Portheine, J.C. & Whitlow, S.H. 1973: A reinvestigation of the epidote structure: Confirmation of the iron location. American Mineralogist 58, 218–223.

Giuli, G., Bonazzi, P. & Menchetti, S. 1999: Al–Fe disorder in synthetic epidotes: A single-crystal X-ray diffraction study. American Mineralogist 84, 933–936.

Heuss-Aßbichler, S. & Fehr, K.T. 1997: Intercrystalline exchange of A1 and Fe^{3+} between grossular–andradite and clinozoisite–epidote solid solutions. Neues Jahrbuch für Mineralogie, Abhandlungen 172 (1), 69–100.

Ito, T, Morimoto, N. & Sadanaga, R. 1954: On the structure of epidote. Acta Crystallographica 7, 53–59.

Kalsbeek, F. & Taylor, P. 1985: Age and origin of early Proterozoic dolerite dykes in South-West Greenland. Contributions to Mineralogy and Petrology 89 (4), 307–316.

Kolb, J., Stensgaard, B.M., Schlatter, D.M. & Dziggel, A. 2009: Controls of hydrothermal quartz vein mineralisation and wall rock alteration between Ameralik and Sermilik, southern West Greenland. Rapport Danmarks og Grønlands Geologiske Undersøgelse 2009/25, 76 pp.

Kolb, J., Kokfelt, T. & Dziggel, A. 2012: Deformation history of an Archaean terrane at mid-crustal level: the Tasiusarsuaq terrane of southern West Greenland. Precambrian Research 212–213, 34–56.

Langer, K., Tillmanns, E., Kersten, M., Almen, H. & Arni, R.K. 2002: The crystal chemistry of Mn^{3+} in the clino- and orthozoisite structure types, $Ca_2M^{3+}_3[OH/O/SiO_4/Si_2O_7]$: A structural and spectroscopic study of some natural piemontites and "thulites" and their synthetic equivalents. Zeitschrift für Kristallographie 217, 563–580.

Makovicky E. & Balic-Zunic, T. 1998: New measure of distortion for coordination polyhedra. Acta Crystallographica B54, 766–773.

Nagashima, M. & Akasaka, M. 2004: An X-ray Rietveld study of piemontite on the join $Ca_2Al_3Si_3O_{12}(OH)$–$Ca_2Mn_3^{3+}Si_3O_{12}(OH)$ formed by hydrothermal synthesis. American Mineralogist 89, 1119–1129.

Nagashima, M. & Akasaka, M. 2010: X-ray Rietveld and ^{57}Fe Mössbauer studies of epidote and piemontite on the join $Ca_2Al_2Fe^{3+}Si_3O_{12}(OH)$–$Ca_2Al_2Mn^{3+}Si_3O_{12}(OH)$ formed by hydrothermal synthesis. American Mineralogist 95, 1237–1246.

Nozic, Y.Z., Kanepit, V.N., Fykin, L.Y. & Makarov, Yu.S. 1978: A neutron-diffraction study of the structure of epidote. Geochemistry International 15, 66–69.

Raith, M. 1976: The Al-Fe(III)-epidote miscibility gap in a metamorphic profile through the Penninic series of the Tauern Window. Contributions to Mineralogy and Petrology 57, 99–117.

Riciputi, L.R., Valley, J.W. & McGregor, V.R. 1990: Conditions of Archean granulite metamorphism in the Godthab–Fiskenaesset region, southern West Greenland. Journal of Metamorphic Geology 8, 171–190.

Smith, G.M. & Dymek, R.F. 1983: A description and interpretation of the Proterozoic Kobbefjord Fault Zone, Godthåb district, West Greenland. Rapport Grønlands Geologiske Undersøgelse 112, 113–127.

Stergiou, A.C., Rentzeperis, P.J. & Sklavounos, S. 1987: Refinement of the crystal structure of a medium iron epidote. Zeitschrift für Kristallographie 178, 297–305.

Thomassen, B. & Krebs, J.D. 2001: Palaeogene gold- and silver-bearing epithermal veins at Amdrup Fjord, southern East Greenland. Rapport Danmarks og Grønlands Geologiske Undersøgelse 2001/133, 78 pp.

Wells, P. 1976: Late Archean metamorphism in the Buksefjorden region, Southwest Greenland. Contributions to Mineralogy and Petrology 56, 229–242.

Windley, B.F. & Garde, A.A. 2009: Arc-generated blocks with crustal sections in the North Atlantic craton of West Greenland: crustal growth in the Archean with modern analogues. Earth-Science Reviews 93 (1–2), 1–30.

A study of the sharks and rays from the Lillebælt Clay (Early–Middle Eocene) of Denmark, and their palaeoecology

AGNETE WEINREICH CARLSEN & GILLES CUNY

Carlsen, A.W. & Cuny, G. 2014. A study of the sharks and rays from the Lillebælt Clay (Early–Middle Eocene) of Denmark, and their palaeoecology. © 2014 by Bulletin of the Geological Society of Denmark, Vol. 62, pp. 39–88. ISSN 2245-7070. (www.2dgf.dk/publikationer/bulletin).

Received 25 February 2014
Accepted in revised form
13 August 2014

Elasmobranch assemblages from the Eocene Lillebælt Clay Formation (Late Ypresian to Middle Lutetian) at Trelde Næs in Denmark yielded teeth of 31 different genera/species from surface collecting as well as from bulk sampling. The fauna is dominated by lamniform pelagic sharks and deep-water genera like Hexanchiformes, *Centrophorus, Isistius, Echinorhinus* and *Pristiophorus*. *Coupatezia miretrainensis, Centrophorus* aff. *granulosus* and *Chlamydoselachus* cf. *fiedleri* are reported for the first time from the Ypresian. The record of *Coupatezia miretrainensis* extends its stratigraphic record from the Lutetian back to the Late Ypresian, whereas the record of *Centrophorus* aff. *granulosus* extends the origin of the *Centrophorus granulosus* group back to the Late Ypresian from its hitherto known origin in the Lutetian. The possible presence of the sparsely known Bartonian genus *Turania* awaits further sampling to be confirmed. The Ichthyofauna suggests deposition in a deep-water environment in subtropical to temperate waters on the middle or outer continental shelf and upper slope at water depth down to 350 m. This is in agreement with depositional depths inferred from fossil molluscs and fish otoliths from Trelde Næs.

Keywords: Denmark, Lillebælt Clay Formation, Eocene, Elasmobranchii, fossil teeth, palaeoecology.

Agnete Weinreich Carlsen [agnetecarlsen@mail.dk], Natural History Museum of Denmark, University of Copenhagen, Øster Voldgade 5-7, DK-1350 København K, Denmark. Gilles Cuny [gilles.cuny@gmail.com], Natural History Museum of Denmark, University of Copenhagen, Øster Voldgade 5–7, DK-1350 København K, Denmark; current address: UMR CNRS 5276 LGLTPE, Université Claude Bernard, Lyon 1, Campus de la Doua Bâtiment Géode, 2 rue Raphaël Dubois, F-69622 Villeurbanne Cedex, France.

The vertebrate fauna from the Eocene of Denmark is still imperfectly known. Bonde (1966) reported *Palaeohypotodus rutoti* under the name *Odontaspis rutoti* and *Striatolamia macrota* under the name *Odontaspis* (*Synodontaspis*) *macrota 'premut. striata'* and several fossils of bony fish from the Fur Formation (Early Eocene) in the Limfjord area in Northern Jutland. So far, very little information has been published about the vertebrate fossils from the Eocene Lillebælt Clay Formation in Eastern Jutland (see Hansen *et al*. 2013).

The Lillebælt Clay Formation has been described as sparsely fossiliferous, but a great deal of fossilised invertebrates has been found. Bonde (1968) reported echinoderms, molluscs, crustaceans, brachiopods, annelids, radiolarians and foraminifers from the Lillebælt Clay at Trelde Næs. The molluscan fauna from Trelde Næs has been described in detail by Schnetler and Heilmann-Clausen (2011). The fauna contains 75 species mostly embedded in concretions with a provenance from L4 to the lower part of the Søvind Marl Formation. This molluscan fauna suggests deposition depths between 100 and 300 m (Schnetler & Heilmann-Clausen 2011).

Associated skeletal and dental remains of a fossil odontaspidid shark have recently been described from Trelde Næs (Hansen *et al.* 2013). In spite of the rarity of macrofossils, intensive collecting by amateurs has resulted in the recovery of much material including many shark teeth and teeth of bony fish.

The aim of this paper is to describe the elasmobranch fossil teeth from the Lillebælt Clay Formation, Eocene of Denmark. This fauna, although well-known by avocational palaeontologists in Denmark, has rarely been described in the scientific literature. Moreover, the composition of the fauna gives information on the depositional environment of the Lillebælt

Clay Formation. Three private collections have been available for this study. Unfortunately, most of the material is collected from the surface of the beach and its exact provenance is therefore quite vague. Three collectors have also screen-washed bulk material from layer L2 of the Lillebælt Clay and the provenance of this material is therefore more precisely known, dating from the Late Ypresian. The material described by Hansen *et al.* (2013) comes from layer L5 and is therefore slightly younger (Lower Lutetian) than the assemblage from layer L2.

Geological setting

Trelde Næs is a peninsula in Eastern Jutland near the town of Fredericia (Fig. 1). During the Eocene, the Danish area was covered by the North Sea and clays and marls were deposited. When the Lillebælt Clay was deposited, a land bridge closed the North Sea from the warm Atlantic Ocean and pure clays were deposited at Trelde Næs (Heilmann-Clausen & Surlyk 2006, fig. 10-2). The fine-grained clays of the Lillebælt Clay Formation and the lower part of the Søvind Marl are exposed in outcrops on the SE-coast of Trelde Næs (Fig. 1) (Heilmann-Clausen *et al.* 1985). Small outcrops of Søvind Marl have been observed at Kirstinebjerg and Østerskov (Schnetler & Heilmann-Clausen 2011). Schnetler (1985) claimed to have observed small temporary exposures of the Late Oligocene Brejning Formation at Trelde Næs but gave no evidence for it. In wet periods large amounts of water are absorbed by the clay which becomes unstable and may form landslides. The Lillebælt Clay is generally poor in fossil material, but extensive sampling has revealed a great variety of fossils including snails, bivalves, crabs and shark teeth.

Stratigraphy

The Lillebælt Clay Formation has been extensively logged by Heilmann-Clausen *et al.* (1985) and it is formally divided into six lithological units named from the base L1 to L6. At Trelde Næs L2 to L6 is more or less exposed in outcrops and their stratigraphy is illustrated by Heilmann-Clausen *et al.* (1985, fig. 14). L2 is a grey-green extremely fine-grained, waxy, non-calcareous clay, probably deposited very slowly far from the coast (Heilmann-Clausen & Surlyk 2006). In

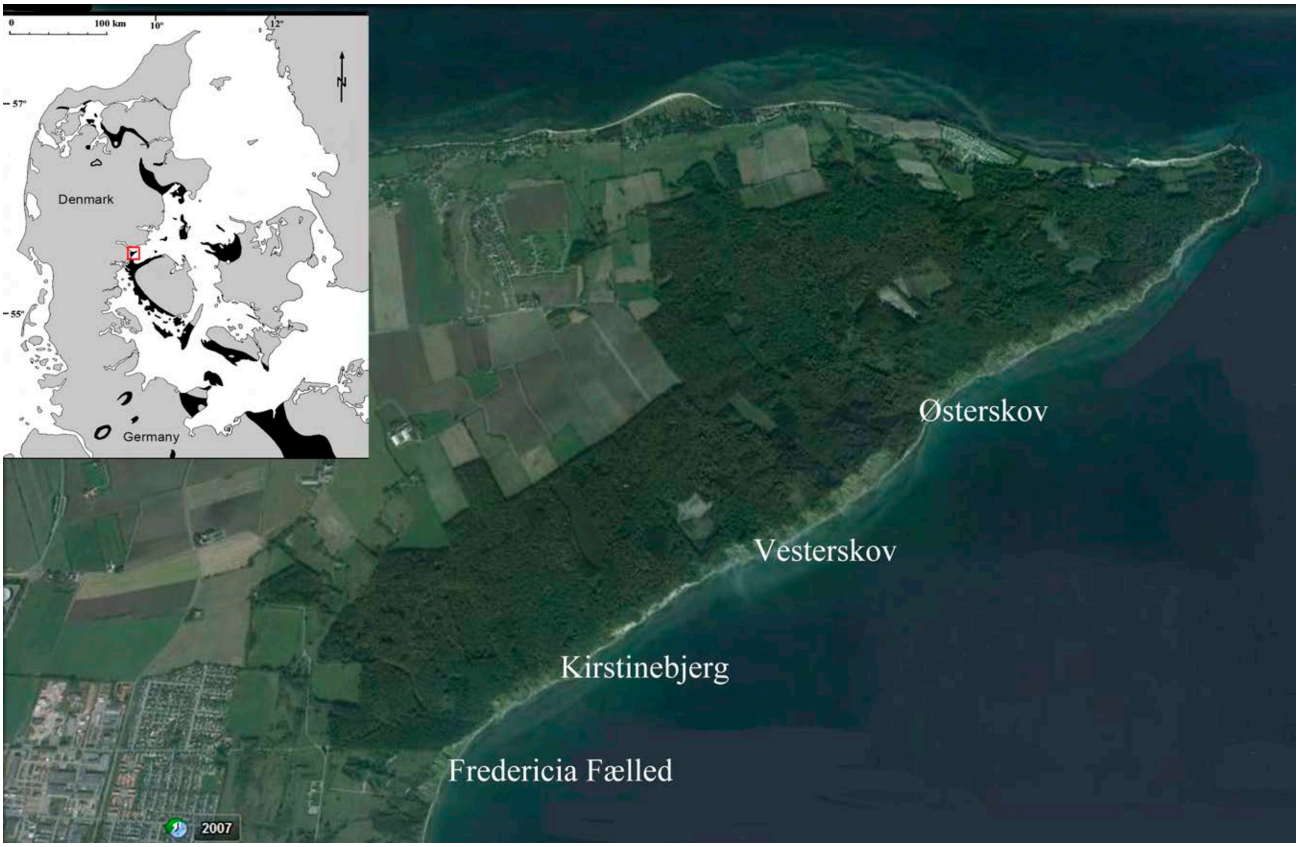

Fig. 1. The Trelde Næs peninsula showing the location of Kirstinebjerg, Fredericia Fælled, Vesterskov and Østerskov. The inserted map of Denmark shows the position of Trelde Næs (red square) and the Eocene outcrops (in black) below the Quaternary. Partly from Schnetler & Heilmann-Clausen (2011) and Hansen *et al.* 2013. Google map.

the lower part of L2, two black layers are seen. Both layers are rich in organic material and this could indicate anoxic bottom waters due to blooming of planktonic organisms. Two closely spaced ash layers just below the lowermost black layer form an important marker within L2. Layer L2 was deposited in the Late Ypresian. The transition to L3 is marked by a carbonate-cemented horizon with signs of bioturbation, which could indicate oxygen-rich bottom water. The boundary between L2 and L3 marks the transition to the Lutetian (Schnetler & Heilmann-Clausen 2011). L3 contains mainly red-brown clay beds and one ash bed. L4 consists of greenish clay and a concretionary layer is present near the base. L5 consists of dark grey-green, slightly calcareous clay. In L6, bioturbation is frequent and there are intervals of marls suggesting warmer waters. Several concretionary layers are present in L6. At Trelde Næs the Lillebælt Clay Formation is overlain by the lower part of the late Lutetian Søvind Marl Formation which has an increased calcareous content.

The Lillebælt Clay Formation in Jutland is usually glacially folded. At Kirstinebjerg the strata form an asymmetrical anticline (Fig. 2).

Palaeo-water depths

In the Lillebælt Clay Formation the grain-size is extremely small, with almost 90% in the clay fraction $< 63\mu$m (Heilmann-Clausen *et al.* 1985), indicating sedimentation in deep waters far from the coast. The distance to the nearest palaeo-coast in Sweden was about 300 km at the time (Thomsen *et al.* 2012). The water depth in the Danish area during the time period when the Trelde Næs sediments were deposited was probably decreasing from 500 to 400 m due to a global decrease in the sea level (Heilmann-Clausen & Surlyk 2006, fig. 10-2). The global sea level was, however, still high due to the ice free world (Heilmann-Clausen & Surlyk 2006). The North Sea Basin was divided into the Norwegian–Danish Basin and the north-west German Basin by the Precambrian Ringkøbing–Fyn High (Heilmann-Clausen & Surlyk 2006, fig 6-2). The Ringkøbing–Fyn High consists of a series of elevated basement blocks extending from the North Sea across Denmark to the Baltic Sea (Michelsen 1994). Trelde Næs is located on the northern border of this structure. Based on boreholes, Dinesen *et al.* (1977) constructed contour maps of the Eocene and Danian surface in Jutland and Fyn and found that the Danian as well as the Eocene surface in the Trelde Næs area was elevated by at least 150 m compared to central and north-western Jutland. There are no available data specifically on the Ypresian/Lutetian palaeo-bathymetry in the Fredericia area, but the paper mentioned above could support the idea that the water depth was lower in the Trelde Næs area than in central and north-western Jutland and probably in the North Sea Basin as a whole.

Stable isotope (δ^{13}C, δ^{18}O) and biostratigraphic data on benthic foraminifera from the Middle Ypresian Røsnæs Clay Formation at Albæk Hoved (situated 15 km north-east of Trelde Næs) suggest the palaeodepth to have been from 600 to 1000 m (Schmitz *et al.* 1996). The Røsnæs Clay was deposited in a period where the English Channel was open and the sea level was higher than when the Trelde Næs sediments were deposited (Heilmann-Clausen & Surlyk 2006, fig. 10-2).

Based on the molluscan fauna of Trelde Næs, Schnetler & Heilmann-Clausen (2011) suggested the palaeodepth to have been from 100 to 300 m.

Fig. 2. The locality at Kirstinebjerg. The first author and Mogens Madsen sampling from the upper black layer in L2.

Material and methods

The present study is based on four separate collections.

1) Ole Barsøe Hansen (OBH), Kolding, has collected shark teeth during the last 20–30 years. All the teeth were surface collected from between the pebbles on the beach at the foot of the steep clay banks along the south-east coast of Trelde Næs. The examined part of the collection consists of a total of 1931 teeth. The majority of the teeth (1748) are from Lamniformes. Of the total number of teeth, 39% are identified to genus or species, 30% are identified only to family or order, and the remaining 31% of the teeth are so damaged that identification was not attempted. The precise stratigraphic origin of these teeth is unknown but they are from layer L2 to L6 and Søvind Marl, the layers outcropping in the area.

2) Mogens Madsen (MM), Fredericia, has collected shark teeth during 4–5 years. His collection consists of 170 teeth of which 98 were hand collected from the beach and 72 were extracted from bulk samples taken from the Lillebælt Clay, layer L2 at Kirstinebjerg (GPS coordinates: 09°48'09.03''E, 55°35'52.6''N). The bulk material was collected over the years and a total of approximately 100 kg of clay has been processed. The clay was dried, dissolved in warm water and screen washed through a 1 mm sieve. The residues were dried and searched for teeth by MM using a binocular microscope. About 63 % of the teeth are identified to genus or species.

3) Sten Lennart Jakobsen (SL), Copenhagen, has taken a bulk sample of approximately 20 kg of clay also from L2 at Kirstinebjerg. The clay was dried, dissolved in warm water, treated with tetrasodiumpyrophosphate ($Na_4P_2O_7$) and screen washed through a 0.25 mm sieve. The dry residue was searched using a binocular microscope (Euromex) by the first author. Sixteen shark teeth were retrieved and of these 13 teeth are identified to genus or species.

4) The first author's (AWC) collection, Copenhagen. In 2012 a total bulk sample of 40.9 kg was taken from L2 at Kirstinebjerg (Fig. 2). The clay was dried, dissolved in warm water, treated with tetrasodiumpyrophosphate ($Na_4P_2O_7$) and screen washed through a 0.25 mm sieve. The clay from the black layer was difficult to disintegrate and was thereafter treated with hydrogen peroxide (H_2O_2). The dry residue was searched using a binocular microscope (Euromex) and 97 shark teeth and teeth fragments were retrieved. Of these, 31 teeth are identified to genus or species.

All illustrated teeth are housed in the Natural History Museum of Denmark in Copenhagen under the catalogue numbers DK728 (Mogens Madsen), DK729 (Ole Barsøe Hansen), DK730 (Sten Lennart Jakobsen) and DK731 (Agnete Weinreich Carlsen) after they have been declared 'Danekræ' in 2013 (Christensen & Hald 1991). The remaining teeth in Lot MM (Mogens Madsen), Lot OBH (Ole Barsøe Hansen), Lot SL (Sten Lennart Jakobsen) and Lot AWC (Agnete Weinreich Carlsen) are all housed in their respective private collections.

Teeth larger than 5 mm have been photographed with a Nikon D7000. Smaller teeth have been photographed with a JEOL Scanning Electron Microscope (SEM) JSM 6335F. A few small teeth were photographed with an Olympus digital image acquisition system DP12 mounted on an Olympus SZ40 binocular microscope.

Besides the shark teeth, the bulk samples contained a large amount of teeth and a few vertebrae of bony fish. They are not the subject of this work.

Systematic palaeontology

Class Chondrichthyes Huxley 1880

Subclass Elasmobranchii Bonaparte 1838

Subcohort Neoselachii Compagno 1977

Superorder Galeomorphii Compagno 1973

Order Lamniformes Berg 1958

Family Mitsukurinidae Jordan 1898

Genus *Anomotodon* Arambourg 1952

***Anomotodon sheppeyensis* Casier 1966**
Fig. 3A–F

Material. 73 anterior and 27 lateral teeth, including DK729aa, DK729ab and Lot OBH10.0.

Description. Forty-seven anterior teeth are severely worn out. Their ornamentation is probably lost and the cutting edges are indistinct, whereas 26 anterior teeth and 27 lateral teeth with triangular crowns are well preserved.

Anterior teeth measure 10 to 21 mm apico-basally, and 6 to 10 mm mesio-distally. The crown is slender, erect and more or less inclined lingually. The lingual face is strongly convex mesio-distally and ornamented with folds in the basal two thirds of the cusp. The folds are parallel in the basal part and become more interdigitated nearer to the apex. The lingual crown–root junction is characterised by a very marked depressed neck. The labial face is smooth and slightly convex mesio-distally. At the labial crown–root junction there is a small median crest. The enameloid expands over the upper labial part of the root lobes. The cutting edges are well developed and expand down along the short oblique heels. The root height is one third of the total height. The lobes are close and symmetric with an angle between them of about 70° in the most anterior teeth, widening to 110° in the more posterior teeth where the lobes are getting more asymmetric. The mesial lobe is longer, more pointed and more labio-lingually flattened than the distal lobe. The lingual protuberance is strong and a deep, long nutritive groove is present.

Twenty-seven teeth have a triangular crown and are considered to be laterals. They measure 6–10 mm apico-basally and 6–10 mm mesio-distally. Fourteen are from the upper jaw and thirteen from the lower jaw. The upper teeth have a triangular, asymmetric crown, whereas the lower teeth have a triangular symmetric crown (Cunningham 2000). The cutting edges are well developed and expand over the long,

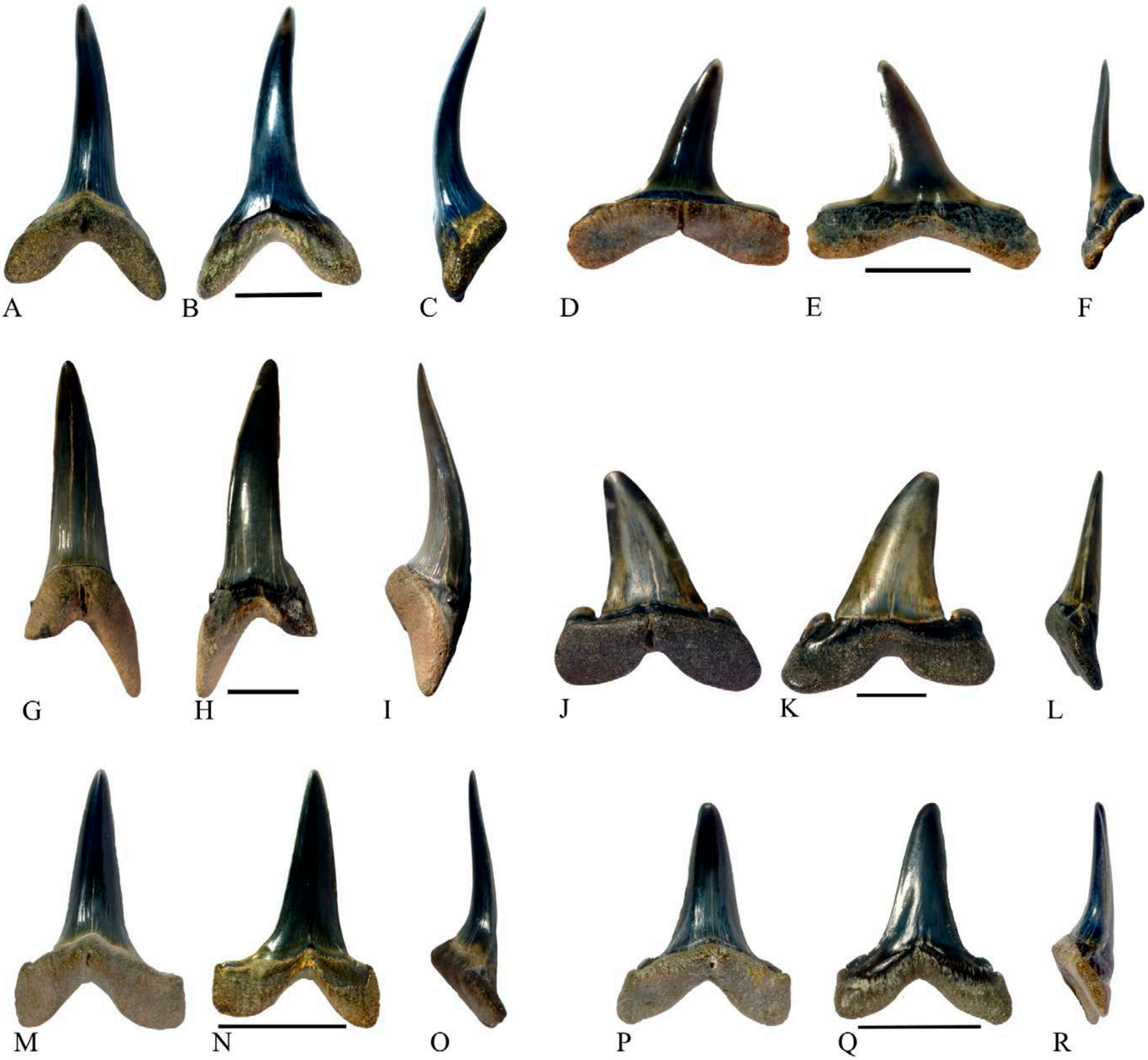

Fig. 3. **A**–**F**, *Anomotodon sheppeyensis*. **A**–**C**, anterior tooth DK729aa. **A**, lingual view; **B**, labial view; **C**, distal view**. D**–**F**, lateral tooth DK729ab. **D**, lingual view; **E**, labial view; **F**, mesial view. Scale bars 5 mm. **G**–**L**, *Striatolamia macrota***. G**–**I**, anterior tooth DK729ba. **G**, lingual view; **H**, labial view; **I**, mesial view. **J**–**L**, lateral tooth DK729bb. **J**, lingual view; **K**, labial view; **L**, mesial view. Scale bars 10 mm. **M**–**R**, *Woellsteinia kozlovi*. **M**–**O**, anterior tooth DK729ca. **M**, lingual view; **N**, labial view; **O**, distal view. **P**–**R**, lateral tooth DK729cb. **P**, lingual view; **Q**, labial view; **R**, distal view. Scale bars 10 mm.

low horizontal heels. On the upper teeth, the mesial cutting edge has a sinusoidal shape, concave in the basal half and convex in the apical part. The distal cutting edge is strongly concave near the base and almost straight apically. The root lobes are widely spread with straight mesial and distal edges in the upper teeth and more rounded edges in the lower teeth. The linguo-basal face of the root is flat in most of the teeth and the basal edge is arc-shaped. The lingual protuberance is strong with a nutritive groove.

Comparison. Among Mitsukurinidae and Odontaspididae, the presence of lingual ornamentation can be observed in teeth of *Mitsukurina* Jordan 1898, *Woellsteinia* Reinecke, Stapf & Raisch 2001, *Striatolamia* Glikman 1964b and *Turania* Kozlov 2001. However, lateral teeth of *Mitsukurina* and anterior and lateral teeth of *Striatolamia* and *Turania* have cusplets (Cappetta 2012). The morphology of teeth of *Woellsteinia* is close to the Trelde Næs teeth, but they are significantly larger and have a more robust crown (Reinecke *et al.* 2001) than teeth of *Anomotodon* (Cappetta 1976).

The type species of *Anomotodon, A. plicatus* Arambourg 1952, is recorded from the late Cretaceous. Its teeth are smaller (less than 11 mm apico-basally in the anterior teeth) than the Trelde Næs teeth (Arambourg 1952). *Anomotodon novus* Winkler 1876b is known from the Eocene of the Paris Basin and the Paleogene of the North Sea Basin in Germany (Dutheil *et al.* 2006; Diedrich 2012). Teeth of *A. novus* are separated from the Trelde Næs teeth by their smaller size and often smooth lingual face (Cappetta 1976; Eeckhaut and De Schutter 2009) whereas another Eocene species, *A. multidenticulatus* Long 1992, is separated by having teeth with small cusplets on the heels (Long 1992). The Trelde Næs teeth are significantly smaller than teeth of the Cretaceous *A. hermani* Siverson 1992, which are up to 30 mm high and have strong folds covering most of the lingual face (Siverson 1992). Cappetta (1976) redescribed teeth of *Anomotodon sheppeyensis* from the Eocene (Ypresian) of the London Clay. The Trelde Næs teeth agree with the teeth of the latter species (Rayner *et al.* 2009, p. 114).

Genus *Striatolamia* Glikman 1964b

***Striatolamia macrota* (Agassiz 1843)**
Fig. 3G–L

Material. 14 anterior, 14 antero-lateral and 18 lateral teeth, including DK729ba, DK729bb and Lot OBH11.0.

Description. Long and slender teeth with a sigmoidal profile of the crown in mesial or distal view are supposed to be from anterior files. They measure up to 50 mm apico-basally and up to 16 mm mesio-distally. Most of the teeth lack parts of the root lobes. The lingual crown face is strongly convex mesio-distally. The labial face is convex at the base and almost flat in the apical part. The lingual face is ornamented with fine parallel folds in the basal three fourths. The folds are missing close to the cutting edges. In some of the teeth, the ornamentation is missing. The cutting edges are well developed and do not reach the crown base. Very small (about 0.5 mm high) lateral cusplets appear on both sides of the main cusp. The cusplets are pointed and well separated from the main cusp when seen in labial view. The enameloid is interrupted between the cusp and the cusplet. The root is strong and represents two fifth of the total tooth height. The root lobes are long and pointed with a mesio-distal flattening and an acute angle between the lobes. The lingual protuberance is pronounced and bears a shallow furrow.

The teeth supposed to be from the antero-lateral files are better preserved than the anterior teeth. They are shorter apico-basally, the cusp is more or less inclined distally and the root lobes are with an obtuse angle, increasing in the more lateral positions. The lingual root face is almost flat in mesial view. Most of the teeth are ornamented in the same way as the anterior teeth. The cutting edges are longer and almost reach the crown base. The cusplets are still very small (about 0.5 mm high) and the cutting edge between the cusp and the cusplets is interrupted.

The teeth supposed to be from the lateral files have a triangular labio-lingually flattened and distally inclined crown. The largest tooth measures 30 mm apico-basally and 30 mm mesio-distally. Only a few teeth are faintly ornamented; the cutting edges are well developed and reach the crown base. On the labial face, there is a triangular depression at the base of the crown and the crown–root boundary is straight. The cusplets are proportionally larger than in the anterior teeth. They are rounded and clearly pectinated. In labial view they are clearly separated from the main cusp and the cutting edge between the cusp and the cusplet is interrupted. In one tooth there are two distal cusplets not fully separated. The roots are robust with widely spread lobes separated by a rounded indentation. The root lobes are more or less rectangular. The lingual protuberance is weak and bears a shallow groove, sometimes with a foramen.

Comparison. The Trelde Næs teeth resemble teeth of *Carcharias* Rafinesque 1810 in many ways, but the very small cusplets on the anterior teeth are characteristic of teeth of *Striatolamia* (Ferrusquia-Villafranca *et al.* 1999; Cunningham 2000). The cutting edges remain on the border of the teeth of *Striatolamia*, whereas in teeth of *Carcharias* they are labially displaced at the base

(Mannering & Hiller 2008). Teeth of *Anomotodon* and *Woellsteinia* are also ornamented but their teeth are considerably smaller and do not have cusplets. Teeth of *Mitsukurina* have ornamentation but no cusplets on the anterior teeth.

Striatolamia striata Winkler 1876a is reported from the Upper Paleocene in the Paris Basin in France (Dutheil *et al.* 2006) and *Striatolamia macrota* is reported from the Lower Eocene (Ypresian) of the Isle of Sheppey, England (Agassiz 1843), France (Adnet 2006a; Dutheil *et al.* 2006), the German North See Basin (Diedrich 2012), Antarctica (Long 1992) and Belgium (Eeckhaut & De Schutter 2009). The well-developed ornamentation on teeth of *Striatolamia striata* (Cappetta 2012) separates them from the Trelde Næs teeth. The Trelde Næs teeth are similar to those of *Striatolamia macrota*.

The taxonomic relationships of *Striatolamia macrota* have been debated. Adnet (2006a) and Eeckhaut & De Schutter (2009) place these teeth in their own genus *Striatolamia* in the family Odontaspididae, but often as Odontaspididae *incertae sedis*, although they give no reasons for this. Long (1992) and Purdy (1998) argue for the genus *Carcharias* because of their morphology close to teeth of *Carcharias taurus* and Long (1992) finds no reason for retaining the genus *Striatolamia*. Siverson (1995), however, points out that the similarities between teeth of *Striatolamia macrota* and those of the extant *Carcharias taurus* Rafinesque 1810 could be the result of convergent evolution. With the discovery of the oldest species of *Striatolamia*, *Striatolamia cederstroemi* (Siverson 1995; Upper Danian from Sweden), which had teeth with small cusplets only on the anterior teeth, the traditional assignment of *Striatolamia* to the Odontaspididae became less well supported. Cappetta and Nolf (2005) relate *Striatolamia* to the family Mitsukurinidae because of the ornamentation pattern of the teeth. It all depends on which characters are considered most important: the tooth shape and cusplets or the ornamentation. We follow here Cappetta and Nolf (2005) as well as Siverson (1995) and assign *Striatolamia* to the family Mitsukurinidae.

Genus *Woellsteinia* Reinecke, Stapf & Raisch 2001

Woellsteinia kozlovi Adnet 2006a

Fig. 3M–R

Material. 8 anterior and 14 lateral teeth, including DK729ca, DK729cb and Lot OBH12.0.

Description. Anterior teeth measure up to 22 mm apico-basally and 14 mm mesio-distally. One of the teeth is very small (14 mm apico-distally) and could be a parasymphyseal tooth. The crown is robust with a broad base and is narrowing towards the apex. The crown is erect or inclined slightly distally. In mesial view the crown is straight except in three cases where the tip is slightly lingually inclined. The labial face is smooth and slightly convex. The enameloid extends like an apron over the proximal half of the labial face of the root lobes and in the best preserved teeth; this apron is ornamented with vertical ridges. The labial crown–root junction has an upright median V-shaped depression pointing towards the crown tip. The lingual face is strongly convex. In the basal two thirds, it is ornamented with longitudinal folds. A narrow dental rim is present at the crown base. The cutting edges are well developed and extend over the short oblique heels, in some cases with irregular bumps on the heels. Real cusplets are not present. The root height is approximately one third of the total height. It has two slightly asymmetric lobes; the distal one is longer and more rounded than the mesial one. The angle between the lobes is about 90°. The lingual protuberance is large with a nutritive foramen in a poorly developed groove.

The lateral teeth are smaller than the anterior teeth. They measure up to 17 mm apico-basally and up to 16 mm mesio-distally. They have a more triangular and robust crown which is straight in mesial view. The lingual ornamentation is less pronounced than in the anterior teeth and missing in the more worn teeth. The crown is distally inclined in the lower laterals with a concave distal cutting edge. The heels are long and almost horizontal and the cutting edges expand over the heels. The root is robust and the root lobes are well separated with an obtuse angle. Some of the root lobes are ear-shaped and some are more rectangular. They are all flattened labio-lingually. The lingual protuberance is less developed than in the anterior teeth and the nutritive groove is shallow.

Comparison. When compared to teeth of Odontaspididae, the teeth from Trelde Næs separate easily because they do not have lateral cusplets (Cappetta 2012). The presence of lingual ornamentation can be observed in teeth of *Anomotodon, Mitsukurina, Woellsteinia, Striatolamia* and *Turania*. However teeth of *Mitsukurina*, *Striatolamia* and *Turania* have cusplets (Cappetta 2012). The morphology of the Trelde Næs teeth is close to teeth of *Anomotodon* but the Trelde Næs teeth are larger and have a more robust crown. The ornamented labial apron is only described in teeth of *Woellsteinia* (Reinecke *et al.* 2001).

Two species are reported from the Eocene; *Woellsteinia kozlovi* Adnet 2006a and *Woellsteinia hermani* (Zhelezko & Kozlov 1999). The last species has no folds on the teeth (Mannering & Hiller 2008). The Trelde Næs teeth have folds and seem therefore closest to teeth of *Woellsteinia kozlovi* which also have a more robust crown than teeth of *Woellsteinia hermani* (Reinecke *et al.* 2001). The genus *Woellsteinia* has been reported from Germany (Reinecke *et al.* 2001), south-western France (Adnet 2006a) and Asia (Zhelezko & Kozlov 1999).

Family Lamnidae Müller and Henle 1838

Genus *Isurolamna* Cappetta 1976

***Isurolamna affinis* (Casier 1946)**
Fig. 4A–F

Material. 45 anterior and 171 lateral teeth, including DK729da, DK729db and Lot OBH13.0.

Description. The anterior teeth measure from 13 to 20 mm apico-basally and from 9 to 11 mm mesio-distally. The crown is slender and lingually inclined in 28 teeth, whereas it is slightly distally inclined in 17 teeth. The lingual face is strongly convex, the labial face almost flat with a median depression adjacent to the almost straight crown–root junction. The enameloid is smooth on both faces. The cutting edges are worn, but when preserved they stop before the base of the crown. There is one pair of very small cusplets. In one of the best preserved teeth they are triangular, divergent and separated from the main cusp. The root shows two rounded lobes and the angle between the lobes varies from 90° to 120°. The basal root edge is arcuate. The lingual protuberance is marked and has a shallow, short nutritive groove or a round foramen.

The lateral teeth measure from 8 to 12 mm apico-basally and from 8 to 12 mm mesio-distally. The crown is triangular and straight in some of them and distally inclined in others. The crown is flattened labio-lingually with a convex lingual face and a flat labial face. The labial crown–root junction is straight. The cutting edges are well preserved and reach the base of the crown. On most of the teeth there is one pair of well-developed triangular cusplets, well separated from the main cusp in lingual view. On twenty teeth, the cusplets are doubled. The root lobes are rectangular or rounded, often with straight mesial and distal edges. The basal root edge is arcuate or straight with a small depression medially. The lingual protuberance is low and a shallow short nutritive groove is present on most of the teeth.

Comparison. The genus *Isurolamna* is characterized by a strong heterodonty, anterior teeth being of isuroid morphology and lateral teeth of lamnid morphology (Cappetta 1976). The Trelde Næs anterior teeth are separated from teeth of Odontaspididae because of the very vestigial or lacking nutritive groove. They resemble teeth of *Isurus* Rafinesque 1810. The lateral teeth resemble teeth of Lamnidae because of the shallow and short nutritive groove. The Trelde Næs teeth are very similar to teeth of *Isurolamna* (Adnet 2006a). Two species are known from the Lower Eocene, *Isurolamna inflata* Leriche 1905 and *Isurolamna affinis* (Cappetta 2012). Teeth of *Isurolamna affinis* have very vestigial or lacking lateral cusplets on the anterior teeth and have a tendency to doubling of the cusplets on the lateral teeth, whereas teeth of *Isurolamna inflata* have regular but small cusplets on the anterior teeth and just one pair of cusplets on the lateral teeth (Adnet 2006a). *Isurolamna bajarunsai* Glikman & Zhelezko 1985 is known from the Middle Eocene of Kazakhstan. Its teeth differ from the Trelde Næs teeth by being significantly larger (Adnet 2006a). The Trelde Næs teeth seem closest to teeth of *Isurolamna affinis* and are similar to teeth figured by Casier (1966) and Cappetta (2012 fig. 203A–G).

Isurolamna affinis is known from the Ypresian of England (Casier 1966), the Eocene of south-western France (Adnet 2006a), the Eocene of Belgium (Nolf 1988; Eeckhaut & De Schutter 2009) and the Ypresian/Lutetian of North Germany (Diedrich 2012).

Genus *Macrorhizodus* Glikman 1964b

***Macrorhizodus* cf. *nolfi* Zhelezko 1999 in Zhelezko & Kozlov (1999)**
Fig. 4G–L

Material. 20 anterior, 34 antero-lateral and 45 lateral teeth, including DK729ea, DK729eb and Lot OBH14.0.

Description. Specimens from the anterior files are long and robust. They measure from 30 to 48 mm apico-basally and from 15 to 23 mm mesio-distally. The cusp is stout with a lingual inclination in mesial view. The labial face is smooth and slightly convex, flatter at the base. The crown–root junction is curved and the enameloid extends a little over the labial root lobes. On most of the teeth there is a slight overhang of the enameloid to the root. The lingual face is strongly convex and smooth. The neck is narrow but marked and on half of the teeth there is a small crest basal to the neck. The cutting edges are marked and extend to the base of the crown. The root is very strong. The root lobes are long and the angle between the lobes varies from 45° to 90°. The root lobes are pointed and on the best preserved tooth there is a crest along the lingual margins of the root. In mesial view the root lobes are arched with the concavity located lingually. The lingual protuberance is strong and a single foramen is present on the best preserved teeth.

In teeth from the antero-lateral files the cusp is erect in mesial view and more triangular and shorter than in the anterior teeth. The specimens, which are probably from the antero-lateral files, are up to 28 mm apico-distally and up to 21 mm mesio-distally. The root lobes are more separated and of unequal length; the mesial lobe is longer and more pointed than the distal lobe.

The upper lateral teeth have a distally inclined crown with a concave distal cutting edge, and the lower lateral teeth have a symmetric crown with almost straight cutting edges (Shimada 2005). The crown is considerably lower (22 mm apico-distally) in the lateral teeth compared to the anterior teeth. It is triangular with some concavity at the labial base. In mesial view, the crown is straight. Most of the teeth have a short heel and the cutting edge follows that heel. In a few of them, there are vestigial cusplets or a bump on the heel. The labial crown–root junction is straight with a little overhang of the enameloid. The root is strong, the linguo-basal and the labial faces are flat and the lobes are widely spread and almost rectilinear. The basal edge is more or less concave. The lingual protuberance is weak and a foramen is present on the best preserved teeth.

Comparison. The Trelde Næs teeth have no cusplets which excludes them from the Odontaspididae. They have a robust design which excludes them from the Mitsukurinidae, and the enameloid is smooth as in teeth of Lamnidae (Cappetta 2012). *Macrorhizodus* was considered as a synonym of *Isurus* by Cappetta (1987), but its tooth design and morphology is different from the latter. The cutting edge is complete in teeth of *Macrorhizodus* whereas in teeth of *Isurus* it generally does not reach the base (Cappetta 2012). The Trelde Næs teeth compare very well with teeth of *Macrorhizodus*.

Macrorhizodus nolfi is described from the Lower Eocene (Zhelezko & Kozlov 1999; Rayner *et al.* 2009) and *Macrorhizodus praecursor* from the Eocene of Belgium (Leriche 1905). *Macrorhizodus* (*Oxyrhina*) *praecursor* was described by Leriche (1905) as the Eocene variation of the Oligocene *Macrorhizodus (Oxyrhina) desori* (Agassiz 1843), although there is no illustration of these teeth presented by the latter author. *Macrorhizodus nolfi* is the only species characterised by teeth with very small and vestigial lateral cusplets or bumps on the heels of the lateral teeth (Adnet 2006a). A few of the lateral teeth from Trelde Næs have very small cusplets or bumps on the heel and it is therefore suggested that they are close to teeth of *Macrorhizodus nolfi.* This is in

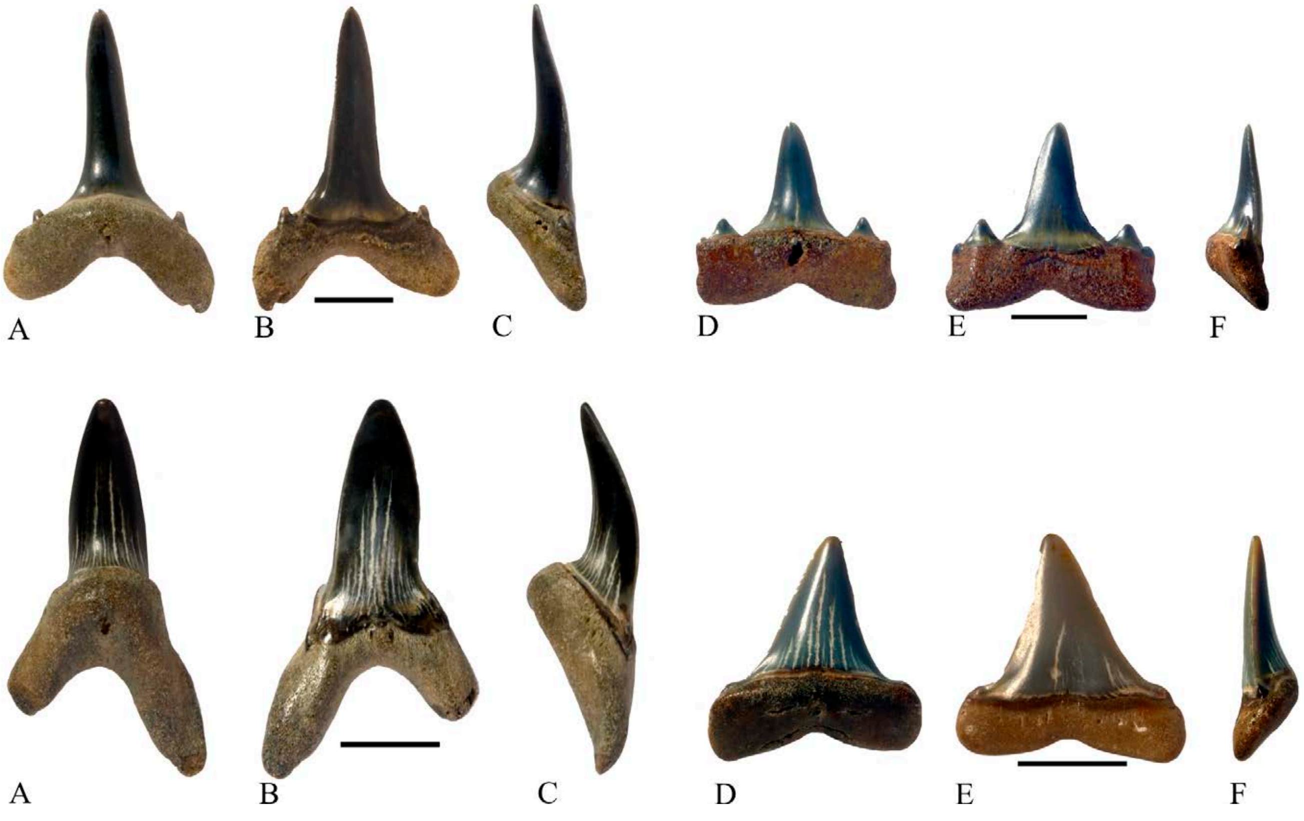

Fig. 4. **A**–**F**, *Isurolamna affinis*. **A**–**C**, anterior tooth DK729da. **A**, lingual view; **B**, labial view; **C**, mesial view. **D**–**F**, lateral tooth DK729db. **D**, lingual view; **E**, labial view; **F**, mesial view. Scale bars 5 mm. **G**–**L,** *Macrorhizodus* cf. *noldi*. **G**–**I**, anterior tooth DK729ea. **G**, lingual view; **H**, labial view; **I**, mesial view. **J**–**L**, lateral tooth DK729eb. **J**, lingual view; **K**, labial view; **L**, mesial view. Scale bars 10 mm.

accordance with the age of the Lillebælt Clay Layer 2 to 6 interval which is dated to Ypresian/Lutetian (Heilmann-Clausen *et al.* 1985). However, the provenance of the Trelde Næs teeth is not known precisely because they were sampled from the beach. *Macrorhizodus nolfi* has been recorded in the Lower Eocene of the London Clay (Casier 1966; Rayner *et al.* 2009) and the Ypresian of Kazakhstan (Zhelezko & Kozlov 1999).

Family Xiphodolamiidae Glickman 1964a

Genus *Xiphodolamia* Leidy 1877

Xiphodolamia ensis Leidy 1877
Fig. 5A–C

Material. DK729f, one antero-lateral tooth.

Description. The tooth measures 13 mm apico-basally and 7 mm mesio-distally. The crown is slightly lingually inclined and bent distally at about 30°. The crown is slender with smooth enamel. The lingual face is strongly convex, the labial face slightly convex. The mesial cutting edge is partly worn, but it reaches the crown foot. The distal cutting edge is located only on the apical half of the tooth. A short distal heel is present. There are no cusplets.

The root is strong and high (5 mm apico-basally), wider mesio-distally than the base of the cusp and divided into two well defined square lobes. The distal lobe is twice the size of the mesial lobe measured mesio-distally. The lobes are close together. The lingual protuberance is marked and with a small foramen. The linguo-basal face of the root is flat as well as the labial face. The basal edges of the root lobes are straight.

Comparison. The square shape of the root of DK729f separates it from teeth of other lamniform sharks. The position of the cutting edges is unique in teeth of *Xiphodolamia* (Adnet *et al.* 2009). Five species of *Xiphodolamia* are mentioned by Cappetta (2012); *Xiphodolamia ensis, Xiphodolamia barbadica, Xiphodolamia eocaena, Xiphodolamia zignoi* and *Xiphodolamia serrata.* They are probably synonyms except for *Xiphodolamia serrata,* which possesses serrated cutting edges (Adnet *et al.* 2009; Cappetta 2012). DK729f is probably from one of the antero-lateral files because of the complete mesial cutting edge and the apically placed distal cutting edge (Adnet *et al.* 2009). DK729f separates from teeth of *Xiphodolamia serrata* by the absence of serration on the cutting edges. It resembles teeth figured as *Xiphodolamia ensis* by Woodward (1899 pl. 1 fig. 8), Adnet *et al.* (2009, fig. 2) and Rayner *et al.* (2009 p. 105). *Xiphodolamia ensis* is known for instance from the Early Ypresian London Clay (Rayner *et al.* 2009), the Eocene of Belgium (Eeckhaut & De Schutter 2009) and the Ypresian/Lutetian of North Germany (Diedrich 2012).

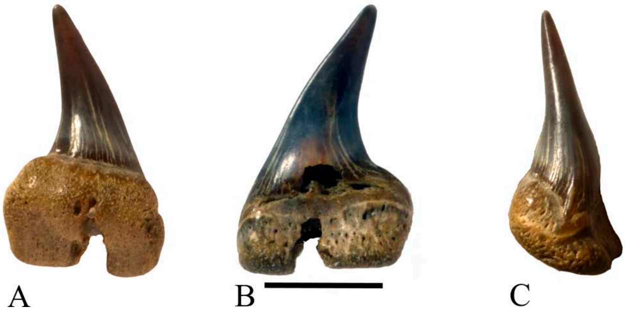

Fig. 5. **A**–**C**, *Xiphodolamia ensis*. Antero-lateral tooth DK729f. **A**, lingual view; **B**, labial view; **C**, mesial view. Scale bar 5 mm.

Family Alopiidae Bonaparte 1838

Genus *Alopias* Rafinesque 1810

Alopias crochardi Ward 1978
Fig. 6A–F

Material. 24 anterior and 24 lateral teeth, including DK-729ga, DK729gb, MM0070, MM0058 and Lot OBH16.0.

Description. Teeth measure up to 13 mm apico-basally and 11 mm mesio-distally. The cusp is pointed, symmetric and slender with a lingual inclination in the anterior teeth. The lingual face is smooth and convex. The lingual crown–root junction is marked by a pronounced neck. Labially the crown enameloid expands in a thin layer over the root lobes. The labial crown face is slightly convex and in some teeth there is a medial depression basally. In most of the teeth the cutting edges are worn, but when they are present they are sharp and reach the base of the crown and become fainter over the short heels. The root is bi-lobed with a semi-circular basal face. The lobes are slim and rounded. The lingual protuberance is strong with a shallow nutritive groove.

The lateral teeth are smaller in size and straighter in mesial view and the crown is more triangular and bent distally compared to the anterior teeth. The mesial border in the most lateral teeth has a sinusoidal shape with a small bump over the heel. The distal border is strongly concave at the base and slightly convex near the apex. There are no cusplets but in a few teeth the heels have low callosities. The root is bi-lobed with a semi-circular basal edge in most of the teeth. The lobes are linguo-labially flattened and the mesial lobe is the longest. The linguo-basal face of the root is flat. The lingual protuberance is well developed and in most of the teeth the nutritive groove is long and deep.

Comparison. The Trelde Næs teeth have no cusplets which separates them from teeth of Odontaspididae and *Usakias* Zhelezko & Kozlov 1999. The crown face is smooth unlike on most of the teeth of Mitsukurinidae (Cappetta 2012). The teeth compare well to the general description of teeth of *Alopias* by Ward (1978).

There are three living species of *Alopias*: *Alopias superciliosus* Lowe 1841, *Alopias vulpinus* Bonnaterre, 1788 and *Alopias pelagicus* Nakamura 1935. *Alopias superciliosus* has teeth with a slender gracile crown and a well-developed lingual groove on the root, *Alopias vulpinus* has teeth with a broader triangular crown and no lingual groove on the root, and *Alopias pelagicus* has teeth with small denticles on the distal heel (Ward 1978). The teeth from Trelde Næs are closest to the *Superciliosus* group.

At least four species have been described from the lower Eocene: *Alopias crochardi* Ward 1978, *Alopias leeensis* Ward 1978, *Alopias denticulatus* Cappetta 1981 and *Alopias alabamensis* White 1956. Teeth of *Alopias denticulatus* have small vestigial cusplets, and teeth of *Alopias alabamensis*, *Alopias latidens alabamensis* and *Alopias leeensis* have a broad crown (Ward 1978; Zalmout *et al.* 2012 fig. 4 AA and BB). The teeth from Trelde Næs are very similar to teeth of *Alopias crochardi* (Rayner *et al.* 2009, p. 113), but we cannot rule out the possibility that some of the teeth attributed to *Alopias crochardi* represent worn teeth of *Alopias denticulatus* (see the discussion below on the teeth of *Usakias* sp.).

Genus *Usakias* Zhelezko & Kozlov 1999

Usakias sp.
Fig. 6G–L

Material. 47 anterior and antero-lateral and 16 lateral teeth, including DK729ha, DK729hb and Lot OBH17.0. All the teeth are more or less worn.

Description. The anterior and antero-lateral teeth measure up to 14 mm apico-basally and up to 11 mm mesio-distally. The anterior teeth have a straight crown in lingual view and the antero-lateral teeth are slightly inclined distally. The crown is slim, triangular and lingually inclined, but not of sigmoidal shape. The lingual face is strongly convex, the labial face is slightly convex often with a basal triangular depression. The enameloid is smooth on both faces. On the labial face the enameloid extends over the apical part of the root lobes. The lingual crown–root junction is well marked by a depressed neck. At the labial crown–root junction, the enameloid is overhanging the root, sometimes as a bulge. The cutting edges, when preserved, are sharp and stop well before the crown base. There is one pair of small cusplets emerging from the labial extension over the root lobes. They are worn on most of the teeth, but when well-preserved they are pointed and hook-shaped.

The root is bi-lobed and symmetric in the anterior teeth and slightly asymmetrical in the antero-lateral

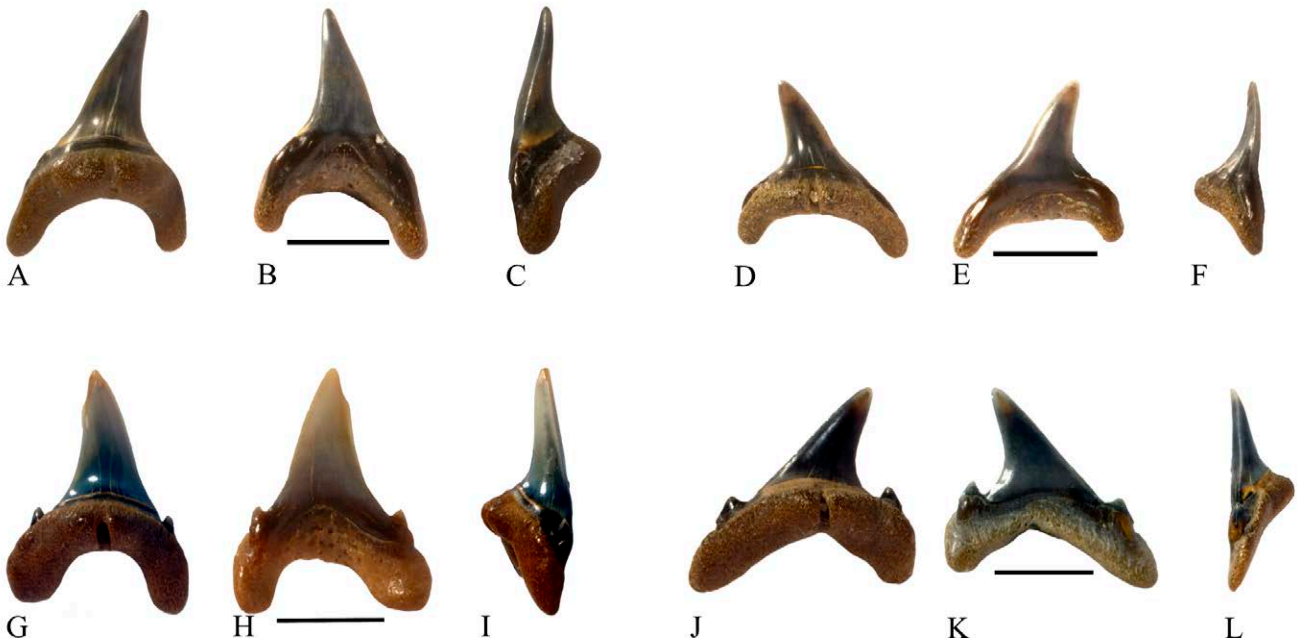

Fig. 6. **A**–**F**, *Alopias crochardi.* **A**–**C**, anterior tooth DK729ga. **A**, lingual view; **B**, labial view; **C**, mesial view. **D**–**F**, lateral tooth DK729gb. **D**, lingual view; **E**, labial view; **F**, mesial view. **G**–**L**, *Usakias* sp. **G**–**I**, anterior tooth DK729ha. **G**, lingual view; **H**, labial view; **I**, mesial view. **J**–**K**, lateral tooth DK729hb. **J**, lingual view; **K**, labial view; **L**, mesial view. All scale bars 5 mm.

teeth, the mesial lobe being longer than the distal one. The root lobes are slim and rounded, and the basal root edge is semi-circular. The lingual protuberance is strong with a long and sometimes deep nutritive groove.

The lateral teeth are of the same size and have a distally inclined crown which is straight in mesial view. The cutting edges run to the base of the crown where they are in continuity with the cutting edge of the low broad cusplets. The root lobes are more spread out and the lingual protuberance is weaker than in the anterior and antero-lateral teeth; they still bear a nutritive groove.

Comparison. The Trelde Næs teeth morphology is typical for teeth of Alopiidae with a labial enameloid extension over the root and a C-shaped root. They separate from teeth of *Alopias* by having well developed cusplets and incomplete cutting edges on the anterior teeth. *Alopias denticulatus* also has cusplets, but they are vestigial and not hook-shaped (Adnet 2006a), contrary to the teeth from Trelde Næs which all have well developed cusplets. Zhelezko & Kozlov (1999) erected the genus *Usakias* for alopiid teeth with cusplets and included *Alopias denticulatus* but excluded *Alopias crochardi* where cusplets are not present. However, Adnet (2006a) preferred to retain *Alopias denticulatus* as different from *Usakias* based on the size and shape of the cusplets.

The Trelde Næs teeth are worn and it is not possible to assign them with confidence to a specific species and particularly to *Usakias asiaticus* Kozlov 2000, the unique species in the Lower Eocene, and it is even possible that some of them are teeth of *Alopias denticulatus*.

Usakias is known from the Lower and Middle Eocene of Kazakhstan (Zhelezko & Kozlov 1999), North Germany (Diedrich 2012) and Belgium (Eeckhaut & De Schutter 2009).

Family Otodontidae Glikman 1964b

Genus *Carcharocles* Jordan and Hannibal 1923

Carcharocles auriculatus (Blainville 1818)

Fig. 7A–F

Material. 26 teeth, most of them fragmentary, including DK729ia, DK729ib, Lot OBH18.0 and Lot MM10.0.

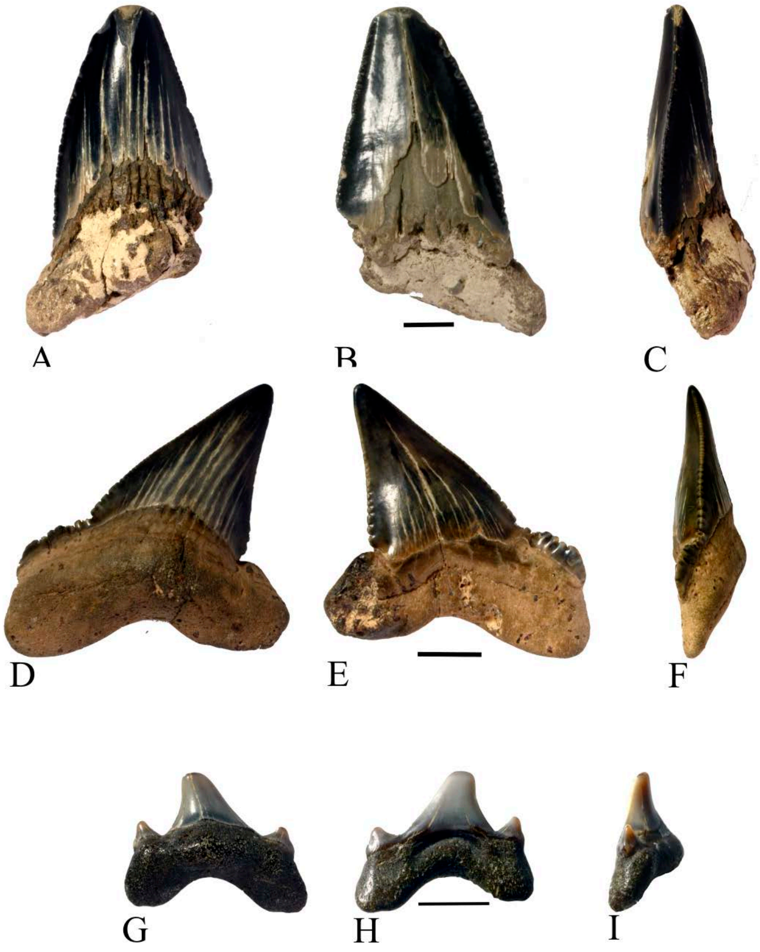

Fig. 7. **A**–**F**, *Carcharocles auriculatus*. **A**–**C**, anterior tooth DK729ia. **A**, lingual view; **B**, labial view; **C**, mesial view. **D**–**F**, lateral tooth DK729ib. **D**, lingual view; **E**, labial view; **F**, mesial view. Scale bars 10 mm. **G**–**I**, *Otodus* cf. *obliquus*. Lateral tooth DK729j. **G**, lingual view; **H**, labial view; **I**, mesial view. Scale bar 5 mm.

Description. The largest tooth measures approximately 65 mm apico-basally. One of the root lobes and the cusplets are missing. The intact tooth would have been about 45 mm mesio-distally. Both crown faces are smooth and convex, the lingual face more so than the labial face. The crown is rather narrow and almost symmetrical, very robust and triangular. The cutting edges are irregularly serrated from the apex to the base of the crown. On the lingual face, the band at the base of the crown is clearly chevron-shaped. This tooth is believed to be from the anterior files because of its symmetrical shape.

The best preserved tooth measures 38 mm apico-distally and 42 mm mesio-distally. Only a small part of the distal lobe of the root is missing on the labial side. The crown is robust, triangular and inclined 45° distally. The lingual face is more convex than the labial face, especially near the base. The crown is more linguo-labially compressed than in the anterior tooth. The cutting edges are irregularly serrated from the base to the apex. The mesial cutting edge is convex, whereas the distal one is slightly concave. At the base of the mesial cutting edge, there is a broad cusplet with six irregular serrations. The distal cusplet is worn out. On the lingual face, the band at the base of the crown is clearly chevron-shaped. The root is nearly half the size of the total height of the tooth. It shows two widely separated rounded lobes. The mesial lobe is larger and thicker than the distal lobe. The basal edge is arc-shaped in lingual view. The lingual protuberance is not very salient and lacks a nutritive foramen. This tooth is believed to be from the lateral files because of its asymmetric crown.

Two smaller teeth (18–20 mm apico-basally) have an even more inclined crown and their lingual band is not clearly chevron-shaped. These teeth are believed to be from the posterior files.

Comparison. The teeth are very large and thereby separated from most other teeth just by their size. Teeth of *Otodus obliquus* Agassiz 1843 are also large, but they are not serrated as the Trelde Næs teeth are. The only genus with teeth similar to these teeth is *Carcharocles*.

It is believed by most authors (Cappetta 2012) that *Carcharocles* belongs to the Otodontidae, but still a few authors refer these very large teeth to the Lamnids (Purdy *et al.* 2001). Cappetta (2012) considers *Carcharocles* to be a subgenus of *Otodus*. In our opinion this is to make it more complicated than necessary. The transition from the non-serrated teeth of *Otodus obliquus* to the regularly serrated teeth of *Carcharocles megalodon* Agassiz 1843 is best described by the acquisition of partial serration in teeth of *Otodus subserratus* (Agassiz 1843) to full irregular serration in teeth of *Carcharocles auriculatus* and subsequent loss of the side cusplets in teeth of *Carcharocles megalodon* where the serration is regular. Teeth with fine but irregular partial serration have been called *Otodus obliquus* var. *mugodzharicus* Zhelezko in Zhelezko & Kozlov 1999, but they are probably synonymous with *Carcharocles aksuaticus* Menner 1928, which occupies the morphospace between *Otodus obliquus* and *Carcharocles auriculatus* (http://www.elasmo.com/). The Trelde Næs teeth are separated from the partially serrated teeth of *Otodus obliquus* var. *mugodzharicus* by their completely serrated cutting edges. They seem closest to teeth of *Carcharocles auriculatus* because of the narrow crown in the anterior teeth, their broad cusplets and the complete and irregular serration of the cutting edges on the main cusp as well as on the cusplets (Cappetta 2012). *Carcharocles auriculatus* is known from the Early to Late Eocene (Ward & Wiest 1990; Long 1992; Eeckhaut & De Schutter 2009; Diedrich 2012).

Genus *Otodus* Agassiz 1843

Otodus cf. *obliquus* Agassiz 1843

Fig. 7G–I

Material. 3 worn lateral teeth, including DK729j and Lot OBH19.0.

Description. The teeth measure about 11 mm apico-basally and 13 mm mesio-distally. The crown is triangular, broad and inclined distally at about 20°. In mesial view it is almost straight. The lingual face is strongly convex, the labial face almost flat. The enameloid is smooth. The cutting edges are not serrated and reach the base of the crown. The labial crown–root junction is arcuate and the enameloid overhangs the root slightly. The lingual crown–root junction is marked by a broad, slightly chevron-shaped neck. There is one pair of cusplets; they are 2mm high, diverging and pyramid-shaped. The root is very strong (about 50% of the total height of the tooth). The lobes are round, more or less spread out and with labio-lingually flattened extremities. The basal root edge is C-shaped. The lingual protuberance is not very marked and there is no nutritive groove, but a small foramen is present.

Comparison. The Trelde Næs teeth resemble teeth of *Cretalamna* Glikman 1958, but they have a more robust root and a wider crown. The Trelde Næs teeth compare well with teeth of *Otodus*. They are much worn and cannot be identified to species level with confidence.

Otodus appeared in the lower Paleocene (Zhelezko & Kozlov 1999) and is known from the Ypresian of the London Clay in England (Rayner *et al.* 2009) and from northern Africa in Morocco (Arambourg 1952; Noubhani & Cappetta 1997). *Otodus obliquus* is mostly

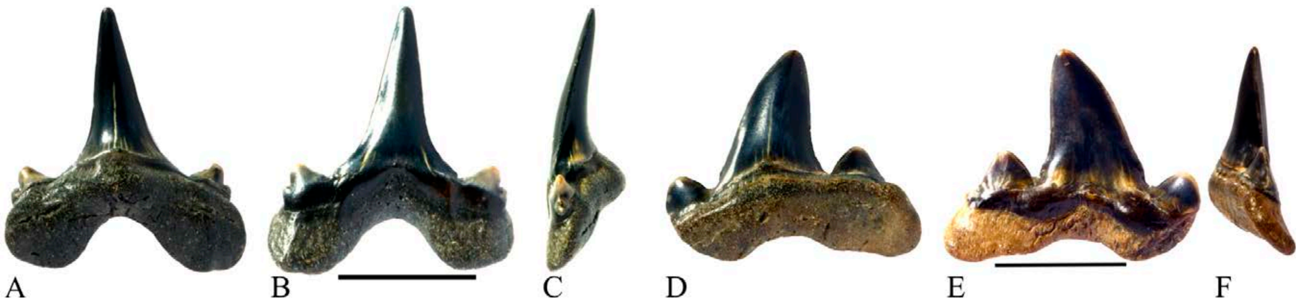

Fig. 8. **A**–**F**, *Cretalamna* aff. *appendiculata*. **A**–**C**, anterior tooth DK729ra. **A**, lingual view; **B**, labial view; **C**, distal view. **D**–**F**, lateral tooth DK729rb. **D**, lingual view; **E**, labial view; **F**, distal view. Scale bars 10 mm.

restricted to the Eocene but has also been mentioned from the Late Paleocene of Kazakhstan (Kordikova *et al.* 2001) and Denmark (Reinecke & Engelhard 1997).

Genus *Cretalamna* Glikman 1958

Cretalamna aff. *appendiculata* (Agassiz 1843)

Fig. 8A–F

Material. 1 anterior and 2 worn lateral teeth, including DK729ra, DK729rb and Lot OBH29.0.

Description. The anterior tooth measures 19 mm apico-basally and 17 mm mesio-distally. The crown is not very broad, triangular and upright in lingual view and with a slight lingual inclination. The lingual face is convex, the labial face less so with a shallow depression basally. The enameloid is smooth. There are two pairs of low cusplets. The inner ones are triangular and diverging, the outer ones vestigial and not fully separated from the inner ones. The root is low with two rounded lobes. The basal edge of the root is U-shaped. The lingual protuberance is not very strong and there is no nutritive groove.

The lateral teeth measure 11 to 16 mm apico-basally and 9 to 18 mm mesio-distally. The crown is stout with a strongly convex lingual face; the labial face is slightly convex in the apical half and with a median depression in the basal part. The crown is inclined at about 10° distally. The mesial cutting edge is convex, the distal one straight. The cutting edges are not serrated and reach the base of the crown. The enameloid is smooth. There is one pair of 2–3 mm high diverging cusplets which are triangular and pectinated with cutting edges. The lingual crown–root junction is marked and slightly chevron shaped. The labial crown–root junction is medially concave. The enameloid covers and overhangs the apical third of the root under the cusplets. The root is low with widely spread round root lobes. The tip of the mesial root lobe is missing on the largest tooth. The basal edge of the root is medially concave and U-shaped. The lingual protuberance is not very prominent and there is no sign of a nutritive groove or foramen.

Comparison. The Trelde Næs teeth resemble teeth of *Otodus obliquus* but are considerably smaller. *Otodus* is characterized by a robust root and a wide crown in contrast to teeth of *Cretalamna* where the root is lower and the cusp more narrow (Ward personal communication 2013). The morphology of the Trelde Næs teeth shares with those of *Cretalamna* a narrow crown on the anterior tooth, a broad triangular cusplets and a lack of a nutritive groove on the low root (Shimada 2007). Teeth of *Cretalamna appendiculata* have one pair of cusplets whereas teeth of *Cretalamna maroccana* Arambourg 1935 have two pairs of cusplets. However, isolated teeth of *Cretalamna appendiculata* type are notoriously difficult to identify at species level (Siverson *et al.* in press).

Traditionally *Cretalamna* is assigned to the family Cretoxyrhinidae but its exact relationships are uncertain; it has been suggested (Siverson 1999; Shimada 2007; Underwood & Cumbaa 2010; Siverson *et al.* in press) that *Cretalamna* should instead be assigned to the Otodontidae, based on the striking similarities in the tooth morphology between the *Otodus obliquus* group and the Late Cretaceous *Cretalamna*. *Cretalamna* is known from the Lower Cretaceous to the Priabonian, and in the Lower Eocene chiefly by the species *Cretalamna appendiculata* (Cappetta 2012) which has been reported from the Early Ypresian London Clay (Rayner *et al.* 2009), the Ypresian/Lutetian of south-western France (Adnet 2006a) and the Ypresian/Lutetian of Morocco (Noubhani & Cappetta 1997). However, the species *Cretalamna appendiculata* appears to be restricted to the Late Cretaceous (Siverson *et al.* in press) and the Eocene specimens are likely to belong to a different species, not yet named.

Family Odontaspididae Müller & Henle 1839

Genus *Palaeohypotodus* Glikman 1964b

***Palaeohypotodus rutoti* (Winkler 1876a)**
Fig. 9A–F

Material. Two teeth: DK729ka and DK729kb.

Description. The anterior tooth (DK729ka) measures 22 mm apico-basally and 8 mm mesio-distally. The crown is slender and very slightly distally inclined in labial view and lingually inclined with a sigmoidal shape. The cutting edges stop just before the base of the main cusp and are labially displaced near the base. There are coarse striations at the base of the labial face along the crown–root junction. Otherwise the enameloid is smooth. There are two cusplets separated from the main cusp on the mesial side. On the distal side, the root and the cusplets are not preserved. The inner cusplet is high (3 mm), pointed and lingually inclined. The outer cusplet is smaller and hook-shaped. The preserved root lobe is long, almost vertical, and mesio-distally compressed. The lingual protuberance is strong with a long deep nutritive groove.

The lateral tooth (DK729kb) measures 8 mm apico-basally and 8 mm mesio-distally. The crown is slender, triangular and upright. It is lingually inclined in mesial view. The lingual face is more convex than the labial face. The cutting edges are not serrated and do not reach the base of the cusp. Two cusplets are present

Fig. 9. **A**–**J**, *Palaeohypotodus rutoti*. **A**–**C**, anterior tooth DK729ka. **A**, lingual view; **B**, labial view; **C**, mesial view. **D**–**F**, lateral tooth DK729kb. **D**, lingual view; **E**, labial view; **F**, distal view. **G**–**L**, *Odontaspis* cf. *winkleri*. **G**–**I**, anterior tooth DK729la. **G**, lingual view; **H**, labial view; **I**, mesial view. **J**–**L**, lateral tooth DK729lb. **J**, lingual view; **K**, labial view; **L**, mesial view. All scale bars 5 mm.

on each side of the main cusp. The inner ones are high (almost half the height of the main cusp) and pointed, bending lingually. The outer ones are very small and diverge from the main cusp. Several vertical bulges or strong folds are present at the labial base of the cusp and the cusplets, otherwise the enameloid is smooth. The root is high, half the total height of the tooth. The lobes are long and rounded and the basal edge is arc-shaped. The lingual protuberance is marked and bears a deep nutritive groove.

Comparison. Basal labial ridges are seen on teeth of *Hispidaspis* Sokolov 1978 and *Cenocarcharias* Cappetta & Case 1999 but DK729ka–b can be separated from these by their very high cusplets (Cappetta 2012). Teeth of *Johnlongia* Siverson 1996 also have labial coarse ornamentation and high cusplets but separate from DK729ka–b because their ornamentation, contrary to the latter, covers a great part of the labial face of the cusp (Cappetta 2012). Labial ornamentation can sometimes be seen on teeth of *Odontaspis,* but it is never as coarse as in DK729ka–b (Cappetta & Nolf 2005; Mannering & Hiller 2008).

It is always difficult to identify a genus from just two teeth, but DK729ka–b seem very close to *Palaeohypotodus*. Cappetta & Nolf (2005) refer to this genus as being monospecific.

Palaeohypotodus rutoti has been described from the Early Eocene of Belgium (Iserbyt & De Schutter 2012), the Paleocene and Eocene of France (Cappetta & Nolf 2005), the Late Paleocene of North America (Ward & Wiest 1990), the Upper Danian of Greenland (Bendix-Almgreen 1969), the Early Eocene London Clay of England (Rayner *et al.* 2009) and the Eocene of Antarctica (Long 1992).

Genus *Odontaspis* Agassiz 1838

Odontaspis cf. *winkleri* Leriche 1905

Fig. 9G–L

Material. 6 anterior and 3 lateral teeth, including DK729la, DK729lb and Lot OBH21.0.

Description. The teeth measure from 10 to 25 mm apico-basally and from 8 to 15 mm mesio-distally. The crown is very slim, upright in lingual view and lingually inclined in mesial view. The lingual face is more convex than the labial face. The cutting edges are not serrated and do not reach the base of the crown on the six anterior teeth. On the three lateral teeth, they stop just at the base of the crown and there are coarse serrations on the basal 1 mm of the cutting edge. The lingual crown face is smooth. The enameloid on the labial crown face expands over the apical part of the root lobes and on three teeth there are faint vertical folds in the enameloid extension at the base of the cusplets. There are two pairs of cusplets; the inner ones are high (2–4 mm) and the outer ones vestigial. The inner cusplets are pointed, slightly lingually inclined, without cutting edges and circular at the base.

The root lobes are long and slim with an arcuate basal edge. The angle between the lobes varies from 80° to 110°. The lingual protuberance is very marked and there is a deep nutritive groove with one foramen.

Comparison. When compared with those of other odontaspidids, the Trelde Næs teeth separate from those of *Carcharias*, *Jaekelotodus* Menner 1928, *Hypotodus* Jaekel 1895 and *Sylvestrilamia* Cappetta & Nolf 2005, which never possess cusplets as high as the Trelde Næs ones. Well-developed cusplets are present in teeth of *Odontaspis*, *Brachycarcharias* Cappetta & Nolf 2005, *Orpodon* Cappetta & Nolf 2005 and *Palaeohypotodus* (Cappetta 2012). However, teeth of *Brachycarcharias* have a broader crown and a lingually ornamented crown face (Cappetta & Nolf 2005) and teeth of *Orpodon* are much smaller. Teeth of *Palaeohypotodus* have a pronounced coarse labial ornamentation at the base of the crown (Cappetta 2012), whereas the labial ornamentation on the Trelde Næs teeth is faint and restricted to the base of the cusplets. The incomplete cutting edges are characteristic of anterior teeth of *Odontaspis* (Mannering & Hiller 2008). Basal serrations on the cutting edge are present on teeth of *Mennerotodus* Zhelezko 1994, *Hispidaspis*, *Palaeohypotodus* and *Jaekelotodus* (Cappetta 2012), but can also be seen on the lateral teeth of *Odontaspis winkleri* (Ward personal communication 2013). The slender crown, relatively high cusplets, short cutting edges and labial folds are seen on teeth of *Odontaspis winkleri* and *Odontaspis speyeri* Dartevelle & Casier 1943; however the more slender teeth of *Odontaspis winkleri* compare best to the Trelde Næs teeth (Leriche 1905, Arambourg 1952, Mannering & Hiller 2008).

Odontaspis winkleri is known from the Eocene of Belgium (Leriche 1905; Nolf 1988; Eeckhaut & De Schutter 2009), the Lower Eocene of England (Casier 1966, Rayner *et al.* 2009), the Ypresian/Lutetian of France (Adnet 2006a; Dutheil *et al.* 2006) and North Germany (Diedrich 2012).

Genus *Jaekelotodus* Menner 1928

Jaekelotodus robustus (Leriche 1921)

Fig. 10A–F

Material. 5 anterior and 6 lateral teeth, including DK729ma, DK729mb and Lot OBH22.0.

Description. The anterior teeth measure from 24 to 33 mm apico-basally and from 16 to 20 mm mesio-distally. The crown is triangular, symmetric, stout and slightly lingually inclined. The lingual face is strongly convex, the labial face almost flat with a basal median depression. The enameloid expands over the apical part of the root lobes on the labial face and the enameloid overhangs the root. The labial crown–root junction is V-shaped. The cutting edges are sharp and reach the crown base. There are two pairs of cusplets on three teeth, one pair on the other two teeth. The cusplets are 2–3 mm high, pointed, hook-shaped and inclined lingually. When present the second pair of cusplets is very small and not completely separated from the inner cusplets.

The lateral teeth measure from 16 to 22 mm apico-basally, and from 17 to 22 mm mesio-distally. The crown is erect in mesial view and more or less distally inclined. The lingual face is convex, the labial face flat with a basal median depression. The enameloid is overhanging the root on the labial face. The crown–root junction is concave in its median part. The cutting edges are sharp and reach the crown base. The distal edge is concave, the mesial one straight or convex.

There are two pairs of cusplets on all the lateral teeth. The inner ones are pointed and lingually inclined; the outer ones are vestigial and not completely separated from the inner ones. The root has two widely spread rounded lobes, labio-lingually flattened at their extremities. The basal root edge is arcuate with a median concavity in three specimens. The lingual protuberance is not very prominent and there is a shallow nutritive groove with a small foramen.

Comparison. The cusplets are short on the Trelde Næs teeth and thereby they are separated from teeth of *Odontaspis*, *Orpodon*, *Palaeohypotodus* and *Brachycarcharias*. Teeth of *Hypotodus* also have one or two pairs of hooked short cusplets, but they differ from the Trelde Næs teeth by their cutting edge, which never reaches the crown base (Cappetta 2012). The very robust crown and the complete cutting edge are only seen in teeth of *Jaekelotodus*. Two species of *Jaekelotodus* are described from the Paleogene (Nolf 1988; Cappetta & Nolf 2005), *Jaekelotodus trigonalis* Jaekel 1895 and *Jaekelotodus robustus*. Teeth of *Jaekelotodus trigonalis* separate from teeth of *Jaekelotodus robustus* by always having two pairs of cusplets on the anterior teeth and having higher cusplets on the lateral teeth (Cappetta and Nolf 2005). The Trelde Næs teeth have one or two

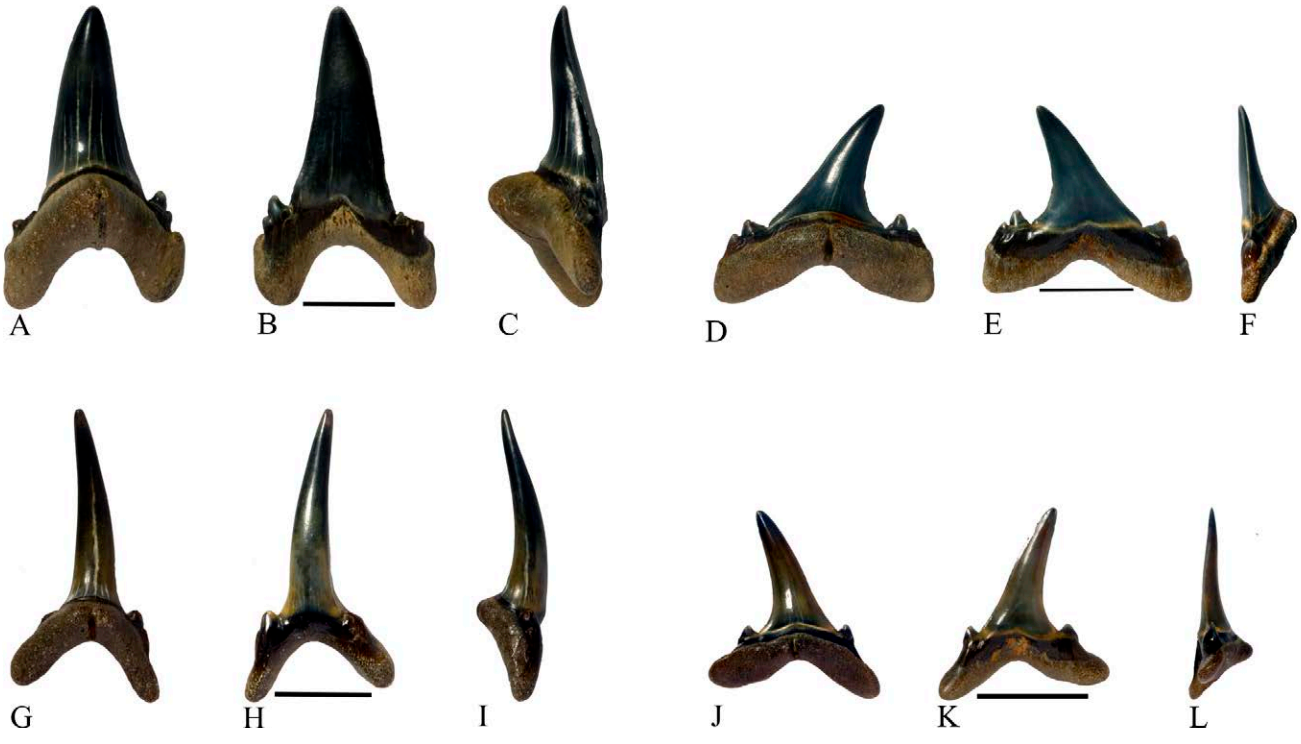

Fig. 10. **A**–**F**, *Jaekelotodus robustus*. **A**–**C**, anterior tooth DK729ma. **A**, lingual view; **B**, labial view; **C**, distal view. **D**–**F**, lateral tooth DK729mb. **D**, lingual view; **E**, labial view; **F**, mesial view. **G**–**L**, *Carcharias* sp. *sensu* Cappetta & Nolf 2005. **G**–**I**, anterior tooth DK729na. **G**, lingual view; **H**, labial view; **I**, mesial view. **J**–**L**, lateral tooth DK729nb. **J**, lingual view; **K**, labial view; **L**, distal view. All scale bars 10 mm.

cusplets on the anterior teeth and seem closest to teeth of *Jaekelotodus robustus*.

Jaekelotodus robustus is known from the Eocene of Belgium (Nolf 1988; Eeckhaut & De Schutter 2009), the Eocene of North Germany (Diedrich 2012) and the Eocene of England (Casier 1966; Rayner *et al*. 2009).

Genus *Carcharias* Rafinesque 1810

Carcharias sp. *sensu* Cappetta & Nolf 2005

Fig. 10G–L

Material. 8 anterior and 6 lateral teeth, including DK729na, DK729nb and Lot OBH23.0.

Description. The anterior teeth measure from 12 to 32 mm apico-basally and from 7 to 15 mm mesio-distally. Two teeth are significantly smaller and better preserved than the other ones, which are worn. The crown is high and narrow, almost upright in labial view and more or less lingually inclined. The lingual face is strongly convex, the labial face slightly convex. The enameloid is smooth except for one tooth where there are faint signs of ornamentation on the lingual face. The cutting edges are worn on most of the teeth, but when preserved they are sharp and do not reach the base of the crown. There is one pair of small cusplets which are pointed, hook-shaped and lingually inclined. The lingual crown–root junction is marked by a distinct neck, the labial enameloid overhangs the root to some degree and the junction is arcuate. The enameloid extends over the apical part of the labial root lobes. The root is with two long rounded lobes, the angle between which is about 90°. The lingual protuberance is marked and with a long nutritive groove. The two small teeth are either from a juvenile or from the upper intermediate file.

The lateral teeth are almost the same size and measure about 15 mm apico-basally and 15 mm mesio-distally. They are better preserved than the anterior teeth. The crown is more or less distally inclined and the labial face is almost flat. On one tooth, there are very fine lingual striations. In mesial view the crown is straight. The cutting edges reach the base of the crown. The cusplets are triangular in labial view, pointed and slightly lingually inclined. On the best preserved tooth, there is no interruption of the cutting edge between the main cusp and the cusplets. The root is low with widely spread symmetric and rounded lobes. The lingual protuberance is not very strong and there is a long deep nutritive groove.

Comparison. The Trelde Næs teeth differ from teeth of most other Odontaspididae because of the lingual ornamentation which is only seen on teeth of *Turania*, *Brachycarcharias*, *Sylvestrilamia* and sometimes *Carcharias*. Teeth of *Brachycarcharias* have a more robust crown and longer cusplets than the Trelde Næs teeth, and anterior teeth of *Sylvestrilamia* are less than 20 mm high (Cappetta & Nolf 2005). Teeth of *Turania* have strong ornamentation covering most of the lingual crown face (Cappetta 2012). The Trelde Næs teeth are close to the teeth described as *Carcharias* sp. by Cappetta & Nolf (2005). They have only faint ornamentation, which probably results from wear. The cutting edges are fairly long on the Trelde Næs teeth and thereby differ from the Miocene *Carcharias acutissima* Agassiz 1843 figured by Cappetta (2012, fig. 183) where the cutting edges are short. The genus *Carcharias* is known from the Late Cretaceous to the Recent (Cappetta 2012).

Genus *Turania* Kozlov 2001

Turania sp.

Fig. 11A–F

Material. 4 anterior and 1 lateral teeth, including DK729oa, DK729ob and Lot OBH24.0.

Description. The anterior teeth measure from 23 to 27 mm apico-basally and from 14 to 15 mm mesio-distally. The crown is very slender and upright in labial view and lingually inclined in mesial view. The lingual face is convex, whereas the labial face is slightly convex with a slight median depression basally. The enameloid on the lingual face is ornamented with strong longitudinal folds covering most of the crown except the tip. The labial face is smooth. The cutting edges are well developed and reach the base of the crown on one tooth and stop before the base on three teeth. The lingual crown–root junction is marked with a distinct neck. On the labial face, the enameloid expands basally over the root lobes, overhangs the root, and the crown–root junction is V-shaped. There is one pair of well separated small pointed cusplets slightly diverging and lingually bent. There are no cutting edges on the cusplets. The root has two long symmetrical lobes; the angle between the lobes varies from 70° to 90°. The lobe extremities are pointed and flattened labio-lingually. The lingual protuberance is well developed and there is a deep nutritive groove.

The lateral tooth measures 16 mm apico-basally and 12 mm mesio-distally. The crown is upright in labial view and slightly lingually bent. The cutting edges reach the base of the crown. The lingual crown face is ornamented, the labial face is smooth. The lingual crown–root junction is marked with a distinct neck, the labial one is straight. There is one pair of cusplets, which are well separated from the crown and of triangular shape with signs of worn cutting edges. The root is low with two widely spread rounded flat root lobes. The lingual protuberance is low with a shallow nutritive groove and one foramen.

Comparison. The Trelde Næs teeth differ from teeth of most other Odontaspididae because of the lingual ornamentation which is only seen on teeth of *Turania*, *Sylvestrilamia*, *Brachycarcharias* and sometimes *Carcharias*. Teeth of *Brachycarcharias* have a more robust crown and longer cusplets than the Trelde Næs teeth, and anterior teeth of *Sylvestrilamia* are less than 20 mm high (Cappetta & Nolf 2005). The Trelde Næs teeth are close to the teeth described as *Turania* (Cappetta 2012). They are also close to teeth of *Striatolamia*, but these teeth have very small cusplets and weaker ornamentation. *Turania* is described from the Lower Bartonian of Kazakhstan (Kozlov 2001). Cappetta (2012) consider that the validity of the genus is not established with certainty.

Genus *Hypotodus* Jaekel 1895

***Hypotodus verticalis* (Agassiz 1843)**
Fig. 11G–L

Material. 6 antero-lateral and 1 lateral teeth, including DK729pa, DK729pb and Lot OBH25.0

Description. The antero-lateral teeth measure from 17 to 24 mm apico-basally and from 12 to 14 mm mesio-distally. The crown is triangular, upright and in two specimens lingually inclined. The enameloid is smooth on both faces. The lingual face is convex, the labial face less so, sometimes with a small short basal median ridge. The cutting edges are marked and they almost reach the base of the crown. The labial crown–root junction is concave apically. There is no significant enameloid overhang of the root. There is one pair of cusplets. They are small (1–2 mm high), hook-shaped, pointed and directed lingually and in

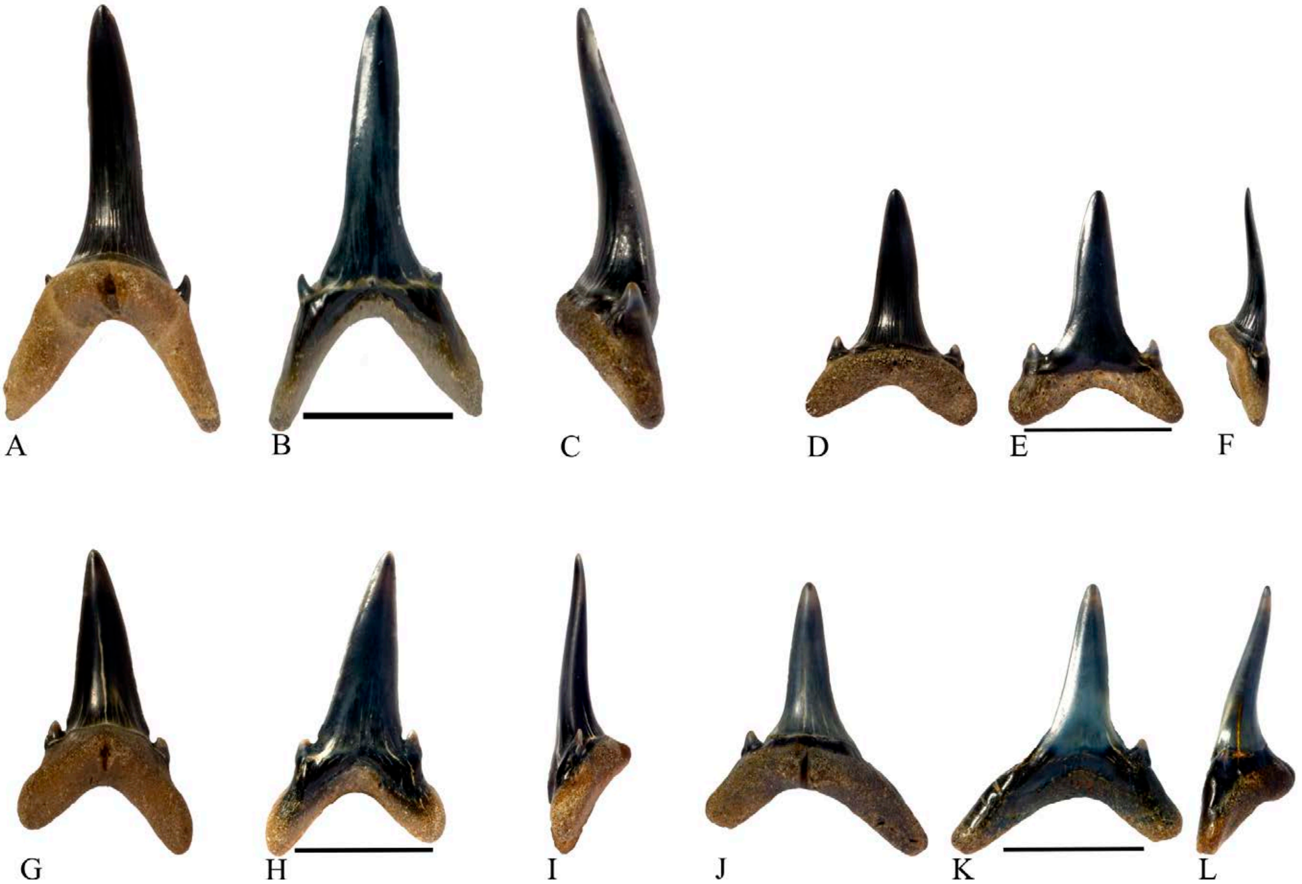

Fig. 11. **A**–**F**, *Turania* sp. **A**–**C**, anterior tooth DK729oa. **A**, lingual view; **B**, labial view; **C** mesial view. **D**–**F**, lateral tooth DK729ob. **D**, lingual view; **E**, labial view; **F**, mesial view. **G**–**L**, *Hypotodus verticalis.* **G**–**I**, anterior tooth DK729pa. **G**, lingual view; **H**, labial view; **I,** distal view. **J**–**L**, lateral tooth DK729pb. **J**, lingual view; **K**, labial view; **L**, distal view. All scale bars 10 mm.

some teeth medially. The cusplets are separated from the main cusp by a deep and narrow notch in lingual view. The root lobes are asymmetric, long and flattened in the extremities. The angle between the lobes varies from 80° to 110°. The basal root edge is more or less angled. The lingual protuberance is marked and has a long and shallow nutritive groove.

The lateral tooth measures 18 mm apico-basally and 13 mm mesio-distally. The crown is triangular, upright in lingual view and straight in mesial view. The lingual face is convex, the labial face almost flat and slightly hollowed at the base with a vertical small ridge. The cutting edges almost reach the base of the crown. The distal cusplet is worn away; the mesial one is small, pointed and triangular. The cusplet is separated from the crown by a notch.

The root lobes are long and asymmetrical. The distal lobe is the longest. The angle between the lobes is about 120°. The lobes are round and the basal root edge is arcuate. The lingual protuberance is marked and there is a long and deep nutritive groove.

Comparison. The Trelde Næs teeth have small cusplets and thereby separate from teeth of *Odontaspis*, *Orpodon*, *Brachycarcharias* and *Palaeohypotodus*. They also have smooth enameloid and thereby separate from teeth of *Carcharias*, *Turania*, *Brachycarcharias*, *Sylvestrilamia* and most Mitsukurinidae. The cutting edges stop before the base of the crown in the Trelde Næs teeth whereas they reach the base in teeth of *Jaekelotodus*, *Isurolamna*, *Sylvestrilamia* and *Brachycarcharias*. Teeth of *Hypotodus* are characterized by small hook-shaped cusplets which are separated by a deep notch from the crown, smooth enameloid and cutting edges not reaching the base (Cappetta 2012).

Cappetta & Nolf (2005) revised the Odontaspididae and restricted the genus *Hypotodus* to only one species *Hypotodus verticalis*. *Hypotodus verticalis* is known from the Lower Eocene (Ypresian) of England (Agassiz 1843; Casier 1966, Rayner *et al.* 2009), the Eocene of Belgium (Nolf 1988; Eeckhaut & De Schutter 2009) and the Ypresian of France (Adnet 2006a; Dutheil *et al.* 2006; Adnet & Cappetta 2008).

Odontaspididae genus and species indet. 1
Fig. 12A–C

Material. 6 anterior teeth, including DK729qa and Lot OBH26.0.

Description. The teeth measure from 21 to 34 mm apico-basally and from 10 to 17 mm mesio-distally. The crown is very slim and inclined lingually and not of sigmoidal shape. The lingual and labial faces are strongly convex and smooth, so that the crown is almost circular at its base. There is a small vertical ridge at the base of the labial face. The cutting edges are blunt and indistinct. The cusplets are high (up to 5 mm). They are slim, pointed and inclined lingually.

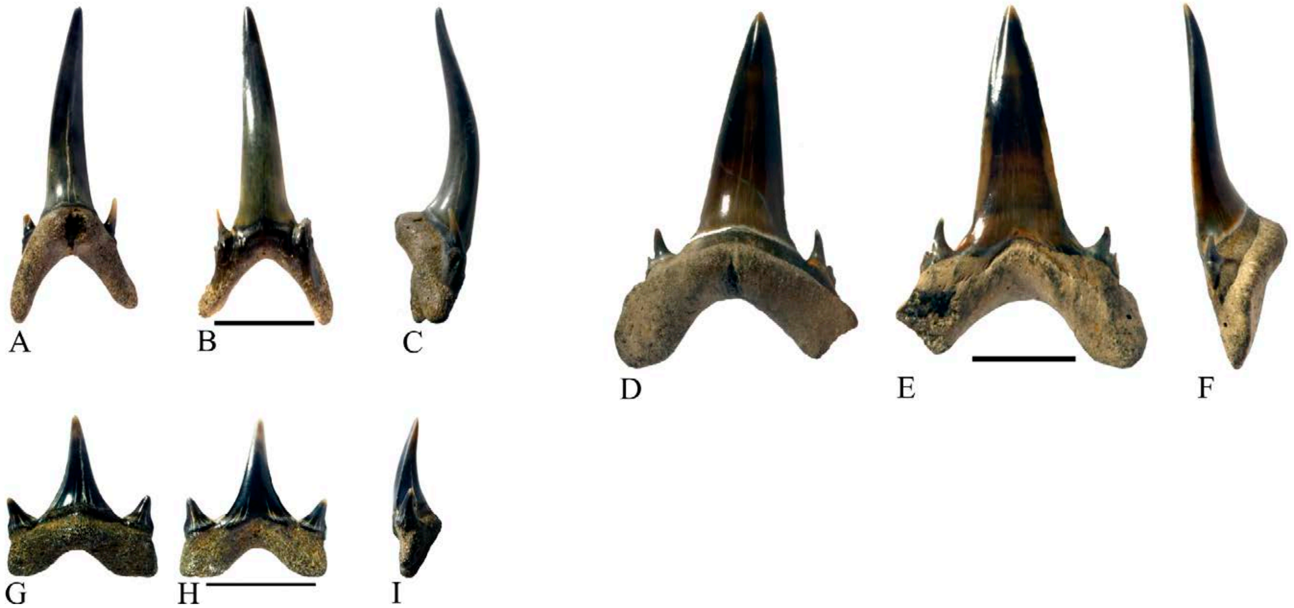

Fig. 12. **A**–**C,** Odontaspididae genus et species indet. 1, anterior tooth DK729qa. **A**, lingual view; **B**, labial view; **C**, distal view. **D**–**F**, Odontaspididae genus et species indet. 2, anterior tooth DK729qc. **D**, lingual view; **E**, labial view; **F**, mesio-distal view. **G**–**I**, Lamniformes family indet., lateral tooth DK729qb. **G**, lingual view; **H**, labial view; **I**, mesio-distal view. All scale bars 10 mm.

They have no cutting edges and are circular at the base. On two teeth, there seems to have been an accessory cusplet. On one tooth there are, labially, very coarse vertical folds at the base of the cusp and the cusplets. The root is symmetrical with long slender root lobes with an angle between the lobes of 70° to 90°. The lingual protuberance is strong with a deep nutritive groove.

Comparison. The Trelde Næs anterior teeth cannot with confidence be placed in a specific genus. They are without doubt of odontaspidid morphology. They bear some resemblance to *Odontaspis*, but the crown lacks clear cutting edges.

Odontaspididae genus and species indet. 2
Fig. 12D–F

Material. 1 anterior tooth, DK729qc.

Description. The tooth measures 35 mm apico-basally and 25 mm mesio-distally. The crown is labio–lingually flattened, triangular, symmetrical and slightly sigmoidal in mesial view. The lingual face is convex, whereas the labial face is flat with a shallow median depression at the base and no overhang of the root. The enameloid is smooth. The cutting edges are almost straight, very sharp and stop just before the base of the crown. The labial crown–root junction is slightly V-shaped and the lingual one is marked by a broad neck. There are two pairs of cusplets. The inner ones are 4 mm high, slender with cutting edges and inclined lingually. The outer cusplets are vestigial and not fully separated from the inner ones. The root has two rounded lobes with flattened extremities. The tip of one of the root lobes is not preserved. The angle between the root lobes is 90° and the basal root edge is arc-shaped. The lingual protuberance is not very strong and there is a deep nutritive groove.

Comparison. The Trelde Næs tooth is without doubt of odontaspidid morphology. It resembles teeth of *Jaekelotodus*, but the crown is flatter and the root less strong (Cappetta 2012). It cannot be identified with confidence at genus or species level.

Odontaspididae genus and species indet. 2 is easily separated from Odontaspididae genus and species indet. 1 by the robustness its crown compared with the gracile, clutching-piercing teeth of Odontaspididae genus and species indet. 1.

Lamniformes family indet.

Fig. 12G–I

Material. 12 lateral teeth, including DK729qb and Lot OBH28.0.

Description. The teeth measure from 10 to 18 mm apico-basally and from 11 to 14 mm mesio-distally. The crown is low, triangular and inclined distally in five teeth. The remaining teeth have erect crowns in

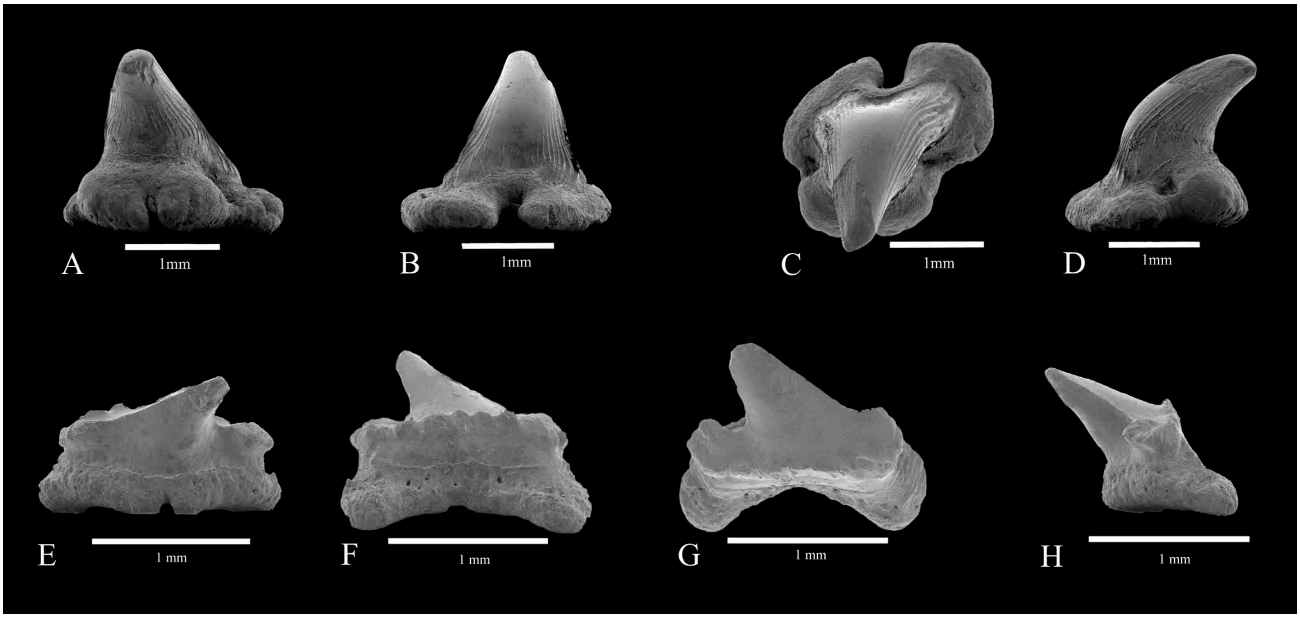

Fig. 13. **A**–**D**, *Megascyliorhinus cooperi*. Anterior tooth DK728a. **A**, lingual view; **B**, labial view; **C**, apical view; **D**, mesio-distal view. **E**–**H**, *Foumtizia* sp. Lateral tooth DK728b. **E**, lingual view; **F**, labial view; **G**, apical view; **H**, distal view.

labial view and slightly lingually inclined crowns in mesial view. The enameloid is smooth. The lingual face is convex, the labial face less so with a median basal triangular depression. The cutting edges are sharp and reach the base of the crown. There is one pair of cusplets on seven teeth and two pairs on five teeth. The cusplets are up to 2 mm high, triangular, diverging and with a sharp cutting edge. When the cusplets are doubled, the outer ones are vestigial and not separated from the inner one. The lobes of the root are rounded and more or less spread out. The basal root edge is angled in some teeth and arc-shaped in others. The lingual protuberance is not very strong; there is no nutritive groove, but on some of the teeth a small foramen is present.

Comparison. The teeth could have some affinity to Lamnidae and Otodontidae, which often lack a distinct furrow on their teeth (Cappetta 2012). However, teeth of Otodontidae have a more robust root than the Trelde Næs teeth. The cusplets on teeth of Lamnidae are not as developed as on the Trelde Næs teeth (Cappetta 2012). These lateral teeth cannot therefore be ascribed with confidence to a specific family.

Order Carcharhiniformes Compagno 1973

Family Scyliorhinidae Gill 1862

Subfamily Megascyliorhininae Pfeil 1984

Genus *Megascyliorhinus* Cappetta & Ward 1977

Megascyliorhinus cooperi **Cappetta & Ward 1977**
Fig. 13A–D

Material. 1 anterior tooth (DK728a) and 1 lateral tooth (MM3110).

Description. DK728a measures 3 mm apico-basally, but the tip of the crown is missing, and 2.5 mm mesio-distally. The crown is stout and strongly inclined lingually. The labial face is convex and in the basal part there is a depression at the crown–root junction. The enameloid is ornamented with parallel folds at the base and in the mesial and distal regions of the crown. The central part of the labial face is smooth. There are no visible cutting edges. The lingual face of the crown is strongly convex and ornamented in the basal half.

The root is divided into two lobes by a deep groove. The root base is flat and broader than the base of the cusp. The labial part of the root has asymmetric rounded lobes; the lingual part is more narrow and continuous with a strong lingual protuberance. The limit between the lingual and the labial part of the root is marked by a narrow depression with a deep hole on the mesial as well as on the distal side of the root. This is best seen in apical view. There are no cusplets.

MM3110 measures 2 mm apico-basally and 1.8 mm mesio-distally. The crown is almost symmetrical. It is stout, conical, pointed and inclined lingually. The lingual face is convex and worn without visible ornamentation. The labial face is strongly convex with a bulge in the basal part of the crown and a depression at the crown–root junction. The enameloid has folds on the basal one third, especially in the mesial and distal regions of the cusp. The cusp has no visible cutting edges. There is one slender, pointed, 1 mm long cusplet which is well separated from the main cusp. It is lingually bent. The other cusplet is broken off together with a part of the root.

The root is low with a flat basal face divided into two rounded lobes by a lingual groove. The labial half of the root is broader than the lingual half, which is continuous with a pronounced lingual protuberance. The limit between the lingual and the labial part of the root is marked by a deep narrow lateral depression with a deep oval hole.

Comparison. The subfamily Megascyliorhininae is characterised by teeth with a high conical cusp with little marked cutting edges and ornamentation on the labial and lingual faces of the cusp. Cusplets are often present on the lateral teeth. The basal root face is flat with a deep furrow (Cappetta & Ward 1977). Teeth of *Megascyliorhinus miocaenicus* Antunes & Jonet 1970 from the Miocene of France are close to the Trelde Næs teeth but have a stouter crown with lesser lingual inclination (Cappetta & Ward 1977). Teeth of *Megascyliorhinus trelewensis* Cione 1986 from the Oligocene of Argentina differ from the Trelde Næs teeth by being larger with an incomplete basal furrow and the presence of lateral cutting edges (Cione 1986). The Trelde Næs teeth closely resemble teeth of *Megascyliorhinus cooperi* known from the Ypresian of the London Clay in England (Cappetta & Ward 1977; Rayner *et al.* 2009) and from the Middle Eocene of France (Adnet 2006a, Plate 31). *Megascyliorhinus cooperi* is also known from the Oligocene to Pliocene of New Zealand (Keyes 1984).

Scyliorhinidae incerta subfamilia

Genus *Foumtizia* Noubhani & Cappetta 1997

Foumtizia **sp.**
Fig. 13E–H

Material. 1 well preserved tooth (DK728b) and 1 tooth lacking the crown (MM0072).

Description. DK728b measures 1.5 mm mesio-distally and 1.5 mm apico-basally, whereas MM0072 measures 2 mm mesio-distally and 1.5 mm apico-basally. DK728b has a triangular stout crown slightly bent distally and lingually inclined. The cutting edges reach the base of the crown and are continuous with one low cusplet on each side of the crown. The distal cutting edge is concave, the mesial one almost straight. The cusplets are worn. The lingual crown face is smooth and strongly convex. The crown–root junction is marked and almost straight. The labial crown face is moderately convex and at the crown–root junction and under the heels there are eight coarse vertical folds on a prominent horizontal crest which overhangs the root. The ornamentation does not extend to the crown face. These folds are worn on MM0072 but the crest is preserved.

The root is strong with a strong lingual protuberance and divided into two lobes by a deep furrow. The root lobes are kidney-shaped in basal view and slightly concave. Seen in labial view, the basal border of the root is concave on both teeth; seen apically the labial border is concave as well. There are several foramina along the basal margin on the labial face of the root.

Comparison. The Trelde Næs teeth are probably from the lateral files because of their distally inclined cusp (Cappetta 1976). They are separated from other scyliorhinid teeth by the presence of coarse folds at the base of the labial crown face. This character is also seen on teeth of *Premontreia* Cappetta 1992, but these teeth are larger and have a lower and more rectangular root contrary to the Trelde Næs teeth where the root is with rounded lobes (Cappetta 2012). The Trelde Næs teeth are assigned to the genus *Foumtizia* because of the confinement of the ornamentation to the base of the crown combined with the rounded root lobes (Cappetta 2012).

Teeth of *Foumtizia poudenxae* Adnet 2006a and *Foumtizia zhelezkoi* Malyshkina 2006 differ from the Trelde Næs teeth by having folds on both sides of the cusp. Teeth of *Foumtizia arba* Noubhani & Cappetta 1997 are significantly smaller and lack folds on the labial crest at the crown-root junction. Teeth of *Foumtizia gadaensis* Noubhani & Cappetta 1997 differ from the Trelde Næs teeth by having a more lingually inclined crown and more cusplets which are situated higher on the crown (Noubhani & Cappetta 1997). The Trelde Næs teeth resemble teeth of *Foumtizia abdouni* Noubhani & Cappetta 1997 as well as of *Foumtizia pattersoni* Cappetta 1976, but with only two more or less well preserved lateral teeth it is not possible to assign the Trelde Næs teeth to a specific species.

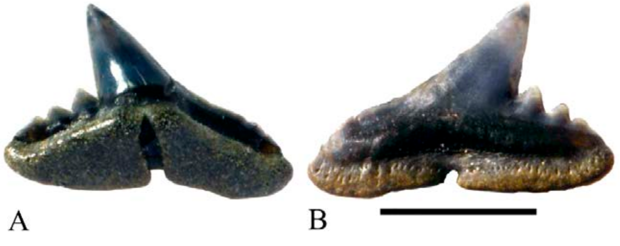

Fig. 14. **A**–**B**, *Physogaleus* cf. *secundus*, upper lateral tooth DK729s. **A**, lingual view; **B**, labial view. Scale bar 5 mm.

Foumtizia is known from the Early Eocene London Clay (Rayner *et al.* 2009), the Ypresian/Lutetian of south-western France (Adnet 2006a), the Ypresian Paris Basin in France (Dutheil *et al.* 2006) and the Ypresian/Lutetian of Morocco (Noubhani & Cappetta 1997).

Family Carcharhinidae Jordan & Everman 1896

Genus *Physogaleus* Cappetta 1980a

Physogaleus cf. _secundus_ Winkler 1876b
Fig. 14A–B

Material. 3 lower and 8 upper teeth, including DK729s (upper lateral tooth), MM0053 (upper lateral tooth) and Lot OBH30.0.

Description. DK729s measures 9 mm mesio-distally, 7 mm apico-basally and 3 mm labio-lingually. The tooth is labio-lingually compressed. The main cusp is triangular and inclined distally at about 65° to the crown–root boundary. The mesial edge is long and almost straight with two small irregular bumps. In the middle of the cutting edge, a small part is missing due to wear. The mesial third of the cutting edge has faint signs of serration. The distal cutting edge is straight and short, creating a notch with the distal heel. The heel is marked and three triangular cusplets are present, decreasing in size distally. The lingual face of the main cusp is convex, whereas the labial face is almost flat in the apical half and convex basally along the straight crown–root junction. The enameloid is smooth. The root is low with a slightly concave basal face. It is divided into two almost triangular (in basal view) lobes by a deep furrow. The lingual protuberance is marked. In labial view the root is rectangular.

The three lower antero-lateral teeth measure 10 mm mesio-distally, 10 mm apico-basally and 4 mm labio-lingually. The crown is high and inclined about 45° distally. The mesial heel is long and the shape of the mesial cutting edge is sinusoidal without serration. The distal cutting edge is concave and there are three cusplets on the distal heel. The lingual face of the crown is strongly convex, the labial face is slightly convex and the enameloid overhangs the root. The root is bulky with a pronounced lingual protuberance. It is divided into two lobes by a long deep furrow. Seen basally the root lobes are triangular. The basal edge of the root is almost straight in labial view.

The eight upper lateral teeth differ from the lower teeth in having a wider triangular and more robust crown and the basal edge of the root is slightly concave.

Comparison. The Trelde Næs teeth separate from teeth of *Scoliodon* Müller & Henle 1837 by having cusplets on the distal heel and from teeth of *Rhizoprionodon* Whitley 1929 which are smaller (less than 4 mm) and also lack cusplets on the distal heel (Cappetta 1980a). Teeth of *Galeocerdo* Müller & Henle 1837 and *Carcharhinus* Blainville 1816 are larger than the Trelde Næs teeth and also differ by having complete serrated cutting edges, whereas teeth of *Abdounia* Cappetta 1980a have mesial as well as distal cusplets (Cappetta 2012). The Trelde Næs teeth fit well with the description of teeth of the genus *Physogaleus* (Cappetta 1980a). The position of the figured Trelde Næs tooth in the jaws is interpreted from Cappetta (2012, fig. 297).

Three species of *Physogaleus* have been reported from the Paleogene of Europe (Dutheil *et al.* 2002; Adnet 2006a): *Physogaleus secundus*, *Physogaleus tertius* Winkler 1874 and *Physogaleus latus* Storms 1894. The teeth of the three species are almost similar and can probably only be separated by their size. Teeth of *Physogaleus secundus* are rather large and have more developed distal cusplets compared to *Physogaleus tertius*; Teeth of *Physogaleus latus* are close to teeth of *Physogaleus secundus* but are two or three times larger. The Trelde Næs teeth seem closest to teeth of *Physogaleus secundus*.

Superorder Squalomorphii Compagno 1973

Order Hexanchiformes Berg 1940

Suborder Chlamydoselachoidei Berg 1958

Family Chlamydoselachidae Garman 1884

Genus *Chlamydoselachus* Garman 1884

Chlamydoselachus cf. *fiedleri* Pfeil 1983

Fig. 15A–F

Material. 1 antero-lateral tooth (DK728c).

Description. DK728c measures 3 mm apico-basally. The distal cusp is lacking. The median cusp is slightly

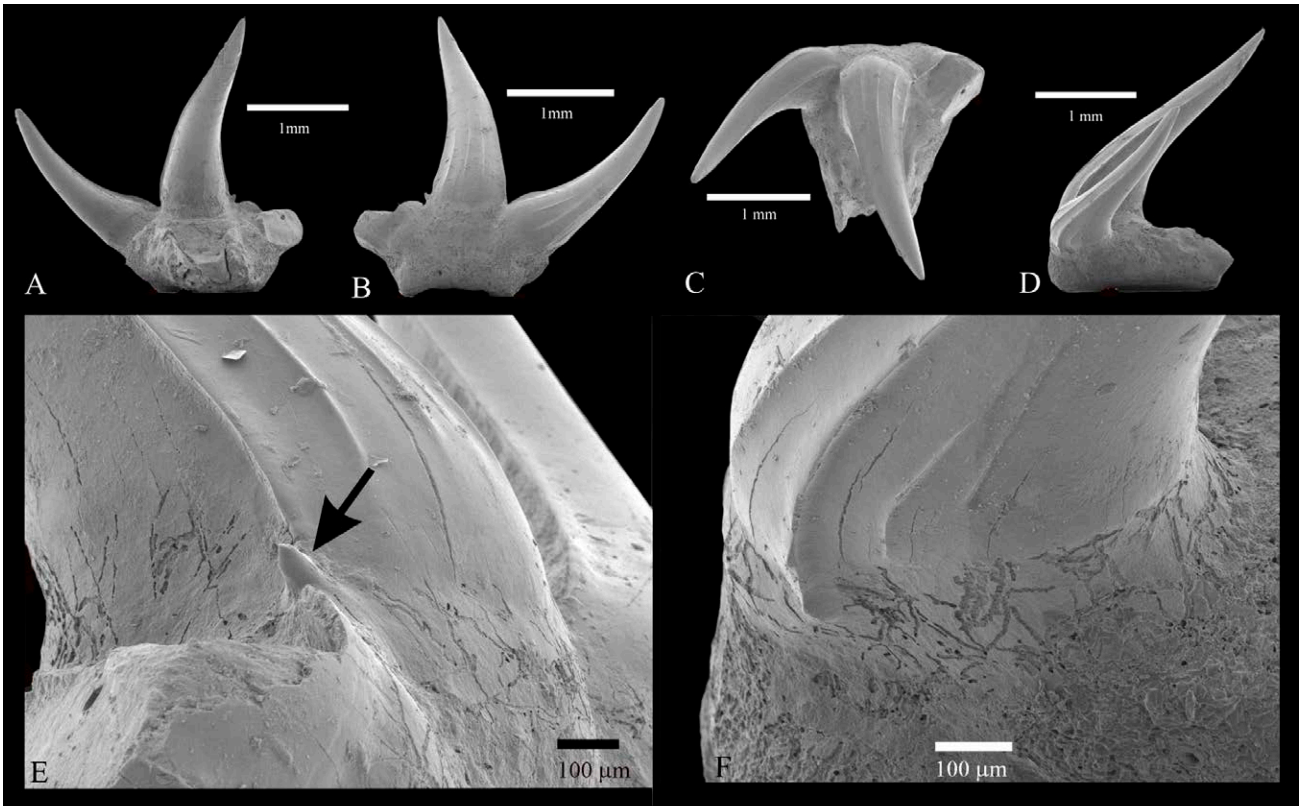

Fig. 15. **A**–**F**, *Chlamydoselachus* cf. *fiedleri*. Antero-lateral tooth DK728c. **A**, lingual view; **B**, labial view; **C**, apical view; **D**, mesial view; **E**, detail of intermediary cusplet; **F**, detail of microborings.

sigmoidal in lingual view and the angle between the median cusp and the base of the root is about 60° in mesial view. The mesial cusp is slightly more lingually inclined. The angle between the median cusp and the preserved mesial cusp is about 45° in lingual view. The lingual face of the cusps is strongly convex with a smooth enameloid. Four almost parallel sharp longitudinal ridges are present on the basal half of the labial face of the cusps. The cutting edges are sharp and reach the base of the crown on both cusps. There is no gap between the base of the median and lateral cusps and a very small intermediate cusp is present distally at the base of the median cusp. The crown–root junction on the lingual face of the median cusp is marked by a broad neck. There are many microborings at the base of the mesial cusp.

The root measures 1.8 mm labio-lingually and 1.2 mm mesio-distally. It is low and broader labially than lingually. The apical surface of the root is divided by a deep trough flanked by a marked mesial and distal crest. The lingual edge has a broad shallow incision forming two short lobes. The basal surface of the root is almost flat in the lingual part and is slightly concave in the labial part, forming a shallow depression when seen in labial view. Several very small foramina are present on the basal surface of the root, none on the apical surface.

Comparison. Chlamydoselachidae contains two genera; *Chlamydoselachus* and *Proteothrinax* (former *Thrinax* Pfeil 1983). Absence of intermediate cusplets is seen in teeth of *Proteothrinax* (Pfeil 1983; Cappetta 2012) and *Chlamydoselachus goliath* Antunes & Cappetta 2002 from the Late Cretaceous of Angola (Antunes & Cappetta 2002), *Chlamydoselachus keyesi* from the Paleocene of New Zealand (Mannering & Hiller 2008), *Chlamydoselachus lawleyi* Davis 1887 from the Pliocene of Italy (Pfeil 1983) and sometimes in the recent *Chlamydoselachus anguineus* Garman 1884. DK728c separates from *Proteothrinax* by having an ornamented crown with full cutting edges. Teeth of *Chlamydoselachus goliath* are significantly larger than DK728c and have upright cusps which lack ornamentation (Antunes & Cappetta 2002). Teeth of *Chlamydoselachus lawleyi* differ from DK728c by having a gap between the median cusp and the lateral cusps (Pfeil 1983). Teeth of *Chlamydoselachus*

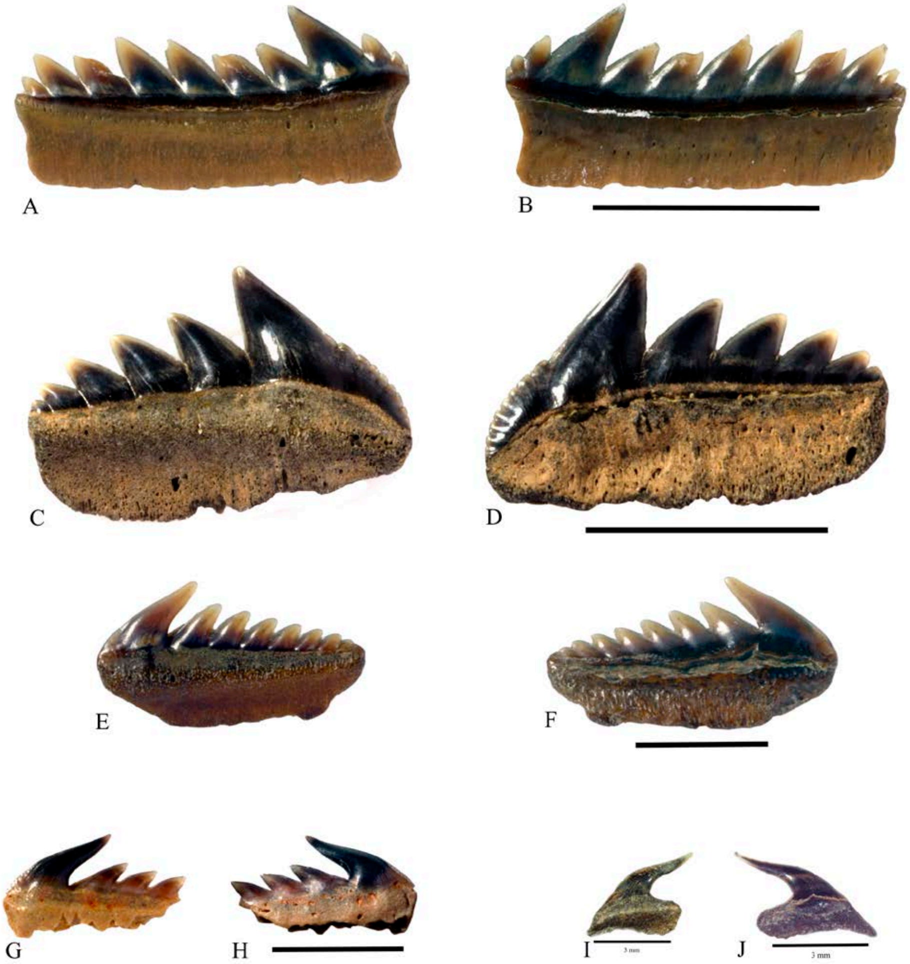

Fig. 16. **A–B**, *Heptranchias howelli*. Lower tooth DK729t. **A**, lingual view; **B**, labial view. Scale bar 10 mm. **C–D**, *Notorynchus serratissimus*. Lower tooth DK729u. **C**, lingual view; **D**, labial view. Scale bar 10 mm. **E–F**, *Hexanchus* cf. *agassizi*. Lower tooth DK729v. **E**, lingual view; **F**, labial view. Scale bar 5 mm. **G–J**, *Weltonia burnhamensis*. **G–H**, lower tooth DK729x. **G**, lingual view; **H**, labial view. Scale bar 5 mm. **I–J**, upper tooth DK728d. **I**, lingual view; **J**, labial view. Scale bar 3 mm.

fiedleri from the Lutetian of Austria and Denmark have intermediary cusplets. However Pfeil (1983, fig 54) describe a juvenile tooth of *Chlamydoselachus fiedleri* of very small size, lacking intermediary cusplets and only striated on the labial face of the cusps. It differs from DK728c only by having a labio-lingually shorter root. Teeth of *Chlamydoselachus keyesi* from the Paleocene of New Zealand (Mannering & Hiller 2008) are also close to DK728c as they lack intermediate cusps, are coarsely striated on the labial face of the cusps and have lingually bent cusps. However their root is different from DK728c, being shorter labio-lingually, and the teeth are significantly larger. DK728c is very small and could represent a tooth from a juvenile. It has characters common with *Chlamydoselachus fiedleri* as well as with *Chlamydoselachus keyesi*. Because of its short root, it cannot be assigned with confidence to one of these two species, but it seems closest to *Chlamydoselachus fiedleri.*

Chlamydoselachus thompsoni Richter & Ward 1990 is known from the Cretaceous of Antarctica and differs from DK728c by its larger size and ornamentation of both faces of the crown. The genus *Chlamydoselachus* is known from the Late Cretaceous of Antarctica and Angola (Richter & Ward 1990; Antunes & Cappetta 2002), the Paleocene of New Zealand (Consoli 2008; Mannering & Hiller 2008) until recent. The species *Chlamydoselachus fiedleri* has been reported from the Eocene (Lutetian) of Austria and Denmark (Pfeil 1983).

Suborder Hexanchoidei Garman 1913

Family Heptranchidae Barnard 1925

Genus *Heptranchias* Rafinesque 1810

Heptranchias howelli Reed 1946
Fig. 16A–B

Material: 1 complete lower tooth (DK729t), 17 lower teeth of which one is complete (Lot OBH31.0), 1 broken tooth (MM5012b).

Description. The largest tooth measures 17.5 mm mesio-distally, 8.5 mm apico-basally and 4.5 mm labio-lingually. The teeth have one primary cusp and five to seven accessory cusps. The primary cusp is significantly larger in height than the other cusps. The accessory cusps increase in height distally until the third and fourth one, which are similar in size. The last three cusps decrease in height distally. Small cusplets are seen at the base of the mesial cutting edge of the primary cusp, increasing in size apically. Their number varies from one to three. The mesial cutting edge on the primary cusp is slightly convex and the distal cutting edge is straight. The cutting edges on the accessory cusps are slightly convex. The lingual face is convex, whereas the labial face is almost flat. All the cusps are inclined about 45° distally. The crown–root junction is distinct and almost parallel to the root base. The root height is 5 mm in the largest tooth and the root is rectangular with a straight basal edge. There is a relatively deep depression in the mesial edge seen in labial view, whereas the distal one is straight or convex. The root is compressed linguo-labially. The labial face of the root is flat with many small foramina. The lingual face is composed of two concave faces forming a longitudinal protuberance at their junction. In the mesial part, three small, but distinct foramina open on the lingual face. In apical view the tooth is slightly concave to the lingual side.

Comparison. The teeth are believed to come from an antero-lateral file of the lower jaw because of their comb-shape. The Trelde Næs teeth separate from those of Hexanchidae by the irregular decrease in size of the accessory cusps. This is typical for Heptranchidae (Cappetta 2012). The Trelde Næs teeth are typical for teeth of *Heptranchias* and separate easily from those of the very different *Paraheptranchias* Pfeil 1981 where small cusplets are present between the main cusps (Cappetta 2012).

Teeth of *Heptranchias perlo* Bonnaterre, 1788 usually have a single mesial cusplet on the upper teeth (Long 1992) and two or more mesial cusplets on the lower lateral teeth (Compagno *et al.* 2005). Teeth of the Oligocene *Heptranchias ezoensis* Applegate & Uyeno 1968 and *Heptranchias tenuidens* Leriche 1938 differ from the Trelde Næs teeth by their reduced number and considerable size of mesial cusplets (Cappetta 1981). *Heptranchias howelli*, which has teeth with up to five mesial cusplets, is known from the Eocene (Cappetta 1981; Long 1992; Noubhani & Cappetta 1997; Kriwet 2005; Adnet 2006a). The Trelde Næs teeth, having one to three mesial cusplets, are very similar to the teeth described from Morocco as teeth of *Heptranchias howelli* (Cappetta 1981). Siverson (1995) describes teeth of *Heptranchias sp.* from the Danian of Sweden. His figures and description are also close to the Trelde Næs teeth but the Swedish teeth look more compact with a deeper root.

Family Hexanchidae Gray 1851

Genus *Notorynchus* Ayres 1855

Notorynchus serratissimus (Agassiz 1843)
Fig. 16C–D

Material. 24 lower teeth, 7 of which are well preserved, including DK729u, MM5012a and Lot OBH32.0.

Description. The best preserved tooth measures 20 mm mesio-distally and 12 mm apico-distally. The teeth are linguo-labially flattened and comb-shaped. The main cusp is larger than the accessory cusps which gradually decrease in size distally. On the basal half of the mesial edge of the main cusp, a long heel bears five to ten small cusplets which decrease in size mesially. There are four to five accessory cusps. The cutting edges of the main cusp are both straight. On the accessory cusps, the mesial cutting edges are convex and the distal ones straight. All the cusps lean distally. The main cusp is the most upright with an angle between the cusp and the root base measuring more than 45°. The accessory cusps lean more distally the further distally they are situated. The lingual face of the cusps is more convex than the labial face. The root–crown junction is distinct and concave towards the root base. The root is high and almost rectangular. The mesial and distal edges of the root are straight or with a small depression in labial view. The labial face of the root is flat with many small, mostly oval openings. The lingual root face has a pronounced lingual protuberance parallel to the basal edge, and several openings of various sizes are present on the linguo-basal face. Seen apically most of the teeth are slightly oblique with a lingual concavity.

Comparison. The Trelde Næs teeth are from the lower jaw because of their comb-shape. They have a regular decrease in size of the accessory cusps and thereby separate from teeth of Heptranchidae (Cappetta 2012). They have a mesial heel with small cusplets which separates them from teeth of *Hexanchus* Rafinesque 1810 where the basal half of the mesial edge of the main cusp is more or less serrated and no heel is present (Ward 1979). Teeth of *Pachyhexanchus* Cappetta 1990a also have a long mesial heel, but it is never serrated (Cappetta 2012). Teeth of the Cretaceous *Gladioserratus* Underwood *et al.* 2011a are close to the Trelde Næs teeth, but differ by having serrae of even size on the mesial heel whereas the serrae on the Trelde Næs teeth decrease in size mesially.

The Trelde Næs teeth separate from teeth of the Oligocene *Notorynchus kempi* Ward 1979 which is larger and has finer mesial serrations and more accessory cusplets, and from teeth of the Oligocene–Miocene *Notorynchus primigenius* Agassiz 1843 that are even larger with a more pointed and upright main cusp (Ward 1979). The Trelde Næs teeth closely resemble teeth of *Notorynchus serratissimus*, which has been reported from the Early Eocene of England (Casier 1966; Cappetta 1976; Rayner *et al.* 2009) and Belgium (Leriche 1905; Nolf 1988; Eeckhaut & De Schutter 2009).

Genus *Hexanchus* Rafinesque 1810

Hexanchus cf. *agassizi* Cappetta 1976

Fig. 16E–F

Material. 6 teeth from the lower jaw, including DK729v, Lot OBH33.0 and Lot MM0078.

Description. The best preserved tooth measures 11 mm mesio-distally, 6 mm apico-basally and 1.7 mm labio-lingually. The tooth is worn. It is comb-shaped with a main cusp and seven accessory cusps regularly decreasing in size distally. All cusps are leaning apico-distally. The mesial cutting edge of the main cusp has no serration and no heel. It is convex in the basal two thirds and straight near the apex. The distal cutting edge is concave in the basal part and convex in the apical part. The lingual face is convex, the labial face almost flat. The main cusp is slightly larger than the first accessory cusp. The accessory cusps have convex mesial and almost straight distal cutting edges. The root–crown junction is distinct and parallel to the moderately developed lingual protuberance. On the mesial edge of the root there is a small depression. The distal edge is incomplete. The labial face of the root is flat. On the lingual protuberance there are two small foramina opening basally to the main and the first accessory cusp. The basal edge of the root is straight.

Comparison. The Trelde Næs teeth separate from teeth of Heptranchidae by the regularly decreasing size of the accessory cusps (Cappetta 2012). Teeth of *Notorynchus* always have cusplets on the mesial heel, whereas the mesial serration on teeth of *Hexanchus* are less developed or even missing (Ward 1979). Teeth of *Pachyhexanchus* have a mesial non-serrated heel, contrary to *Hexanchus* where no heel is present (Cappetta 2012). The Trelde Næs teeth have no visible serration, but this could partly be a result of wear. The acrocone cusp on the Trelde Næs teeth is larger than the first accessory cusp, but not as large as in teeth of *Weltonia* Ward 1979, where it is at least 50% larger than the first accessory cusp (Ward 1979).

Ward (1979) describes the teeth of *Hexanchus agassizi*, *Hexanchus collinsonae* and *Hexanchus hookeri* from the Lower Eocene of England. Teeth of *Hexanchus collinsonae* and *Hexanchus hookeri* separate from teeth of *Hexanchus agassizi* by their stouter roots and coarser serration (Ward 1979). *Hexanchus collinsonae* and *Hexanchus hookeri* may be ontogenetic states of *Hexanchus agassizi* (Adnet 2006b). The Trelde Næs teeth are most likely lower teeth of *Hexanchus agassizi* having no visible serration. *Hexanchus agassizi* is known from south-western France and from the London Clay of England (Adnet 2006a; Rayner *et al.* 2009).

Genus *Weltonia* Ward 1979

Weltonia burnhamensis Ward 1979
Fig. 16G–J

Material. 1 lower tooth (DK728c) and 1 upper tooth (DK728d).

Description. DK728c is comb-shaped and thus probably from the lower jaw. The main cusp and three accessory cusps are preserved. The tooth is 7 mm long mesio-distally and 4 mm high apico-basally. The basal half of the root and the distal part of the tooth is missing so that the tooth was probably larger than the given measurements. The main cusp is of sigmoidal shape. The basal two thirds of its mesial cutting edge are convex with coarse serration on its basal half. The apical one third is concave. The basal one third of the distal cutting edge is strongly concave, the apical two thirds slightly convex. The lingual face is convex, the labial face almost flat. The main cusp is significantly larger than the first accessory cusp and the two cusps are well separated. The main cusp is distally inclined at about 45°. The three accessory cusps decrease regularly in size distally and all lean about 45° distally. The mesial cutting edges are convex, the distal ones almost straight. The lingual faces are convex, the labial faces almost flat. The basal part of the root is missing but a week longitudinal lingual protuberance parallel to the crown–root boundary is preserved. The preserved labial root face is flat. The mesial edge of the root is depressed. Several foramens of various sizes are seen on both root surfaces.

DK728d measures 3 mm apico-basally and 4 mm mesio-distally. There is one slender, very sigmoidal cusp, which is inclined distally at about 70°. Both faces of the cusp are convex. The mesial cutting edge is sharp, the distal one blunt. The root is flat with a moderate lingual protuberance. On the labial face, the crown–root junction is marked by a deep depression in the middle part of the tooth. This tooth is with only one cusp and thereby probably from the upper jaw.

Comparison. The lower tooth is typical of Hexanchidae because of the regular decrease of the size of the accessory cusps (Cappetta 2012). It is separated from teeth of *Hexanchus*, *Notorynchus* and *Pachyhexanchus* by its high sigmoidal main cusp which is well separated from the second cusp (Ward 1979). Two species of *Weltonia* are described: *Weltonia burnhamensis* and *Weltonia ancistrodon* Arambourg 1952. The Trelde Næs tooth separates from teeth of *Weltonia ancistrodon* which have a very high main cusp (Arambourg 1952; Cappetta 2012, fig. 85G). On the other hand it agrees well with teeth of *Weltonia burnhamensis*. This species is known from the Ypresian of England (Casier 1966; Rayner *et al.* 2009).

Order Squatiniformes Buen 1926

Family Squatinidae Bonaparte 1838

Genus *Squatina* Dumeril 1806

Squatina cf. _prima_ Winkler 1874
Fig. 17A–C

Material. 1 well-preserved tooth (DK729y) and 3 worn teeth (Lot OBH35.0).

Description. The best preserved tooth is broader than high: 11 mm mesio-distally and 4 mm apico-basally. The cusp is slender, erect, triangular and symmetric in labial view. The labial as well as the lingual face of the cusp are convex and smooth. The labial face is extended basally in a small rounded apron. The lingual protuberance is strong and covered with enameloid medially forming a triangular uvula. The cutting edges on the crown are sharp and expand over the long, low heels. The root is flat and perpendicular to the cusp and of triangular shape in basal view. The root is hollowed in its labial median area where one opening is present. The medio-lingual duct is covered and a medio-lingual foramen opens at the extremity of the lingual protuberance. Below the crown–root boundary there are several small foramina on the lingual face of the root. The root vascularisation is hemiaulacorhize. This means that there is a connection between the central foramen on the root base

Fig. 17. **A**–**C**, *Squatina* cf. *prima*. Lateral tooth DK729y. **A**, lingual view; **B**, labial view; **C**, apical view. Scale bar 5 mm.

and the foramen on the lingual protuberance via the medio-internal canal which runs parallel to the surface (Cappetta 2012).

The other three teeth are smaller with a relatively higher and slightly lingually inclined cusp. The basal face of the root is concave in two teeth.

Comparison. The Trelde Næs teeth separate from teeth of *Pseudorhina* Jaekel 1898, which are very small, less than 1.5 mm in total width, and with a much wider labial apron (Cappetta 2012). Teeth of *Squatina* are also similar to teeth of *Orectolobus* Bonaparte 1834 but the heels are elevated and sometimes form distal denticles in the latter (Long 1992).

The Trelde Næs teeth belong to the genus *Squatina* because of their triangular root, their rounded labial apron, their long heels with sharp cutting edges and their triangular crown. The conservative nature of the *Squatina* dentition makes it difficult to identify isolated teeth at species level and their stratigraphic position becomes of importance. *Squatina hassei* Leriche 1929 is the preferred identification for the Cretaceous sharks. Teeth of this species are small (5 mm) with a short cusp and steeply sloping shoulders. *Squatina prima* is the Paleogene species employed for this genus. Its teeth have a slender crown and low shoulders (Casier 1966; Adnet 2006a). *Squatina subserrata* Münster 1846 is the Pliocene–Miocene species and is characterized by robust teeth (http:/elasmo.com). The Trelde Næs teeth are very similar to teeth of *Squatina prima* because of the slender crown, the low shoulders and the medium size (Casier 1966; Adnet 2006a).

Order Squaliformes Goodrich 1909

Family Centrophoridae Bleeker 1859

Genus *Centrophorus* Müller & Henle 1837

Centrophorus aff. *granulosus* Bloch & Schneider 1801

Fig. 18A–D

Material. 22 teeth, including DK731, Lot AWC10.0, Lot SL0001 and Lot MM3118.0

Description. The teeth are small, less than 3 mm apico-basally. The height (apico-basally) is larger than the width (mesio-distally). The teeth are labio-lingually flattened with a very distally inclined triangular crown. The labial and lingual faces are slightly convex with smooth enameloid. The mesial cutting edge is slightly sigmoid and coarsely serrated, whereas the distal one is straight without serrae. The distal heel is low and rounded and separated from the crown by a deep notch. A flat apron on the labial face extends down over the root, not reaching the base of the root. The apron is triangular and thick with distinct edges. On the lingual face the uvula is marked and of triangular shape. The root is labio-lingually compressed. The basal edge is more or less straight. The mesial edge is curved with a depression in which the adjacent mesial tooth is interlocked. In the bottom of the depression a wear facet is present in the largest teeth. The distal edge of the root is rounded to accom-

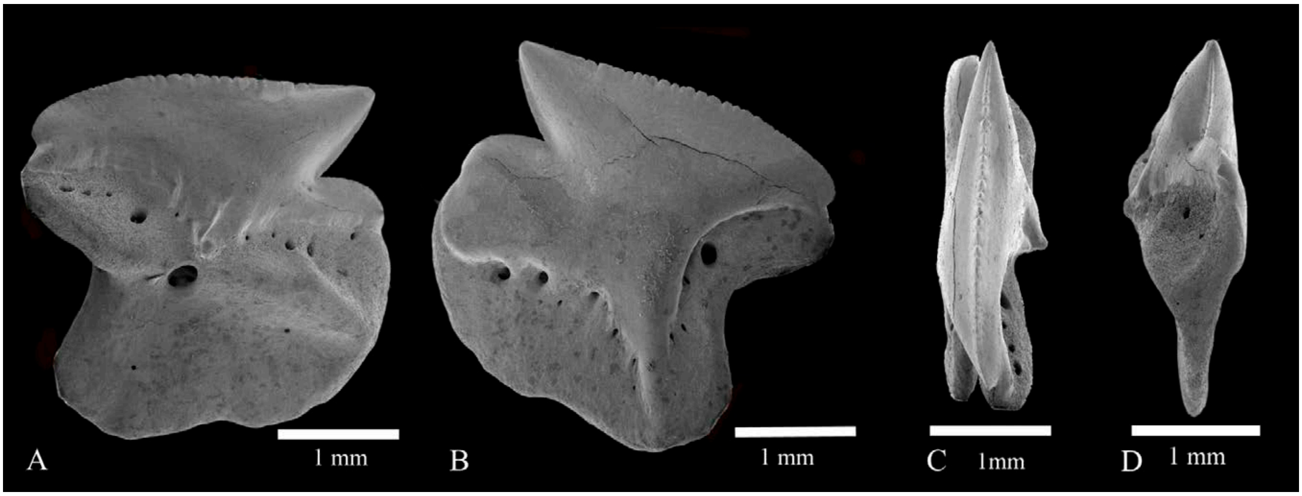

Fig 18. **A**–**D**, *Centrophorus* aff. *granulosus*. DK731. **A**, lingual view; **B**, labial view; **C**, apical view; **D**, distal view.

modate the adjacent distal tooth. The labial root face is flat and several large foramina open close to the crown–root junction. The lingual root face is divided by a prominent longitudinal protuberance parallel to the crown base. The uvula extends basally to the protuberance and a large foramen opens just basal to the tip of the uvula. From this foramen, a shallow furrow is present in mesio-basal direction, reaching the root base. On both sides of the uvula, the root has a shallow depression and a few foramina open on the lingual face of the root.

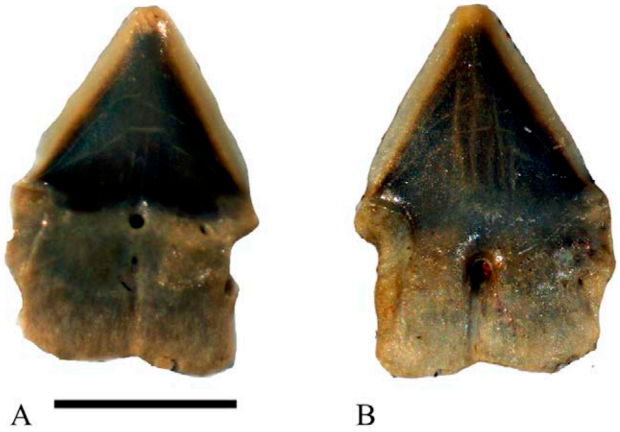

Fig. 19. **A**–**B**, *Isistius trituratus*. Anterior tooth DK730. **A**, lingual view. **B**, labial view. Scale bar 2 mm.

Comparison. The basal root compression, the shape and size of the labial apron and the lingual protuberance separates the Trelde Næs teeth from those of all the squaliform families except Centrophoridae, which includes the genus *Centrophorus* and *Deania* Jordan & Snyder 1902 (Cappetta 2012). The Trelde Næs teeth have serrated mesial cutting edges and only one opening, an infundibulum, just below the tip of the uvula, whereas teeth of *Deania* have unserrated cutting edges and two lingual openings (De Schutter & Wijnker 2002).

Many species of the genus *Centrophorus* have been described. The recent species *Centrophorus squamosus* Bonnaterre, 1788 has teeth with ornamentation on the uvula and serration on the mesial as well as the distal cutting edge (Marsili & Tabanelli 2007), whereas the Trelde Næs teeth are only serrated on the mesial cutting edge. The Trelde Næs teeth closely resemble teeth of *Centrophorus granulosus* as figured by Cappetta (2012, fig. 98 F–G) and *Centrophorus* aff. *granulosus* as figured by Adnet (2006a, Plate 4, fig. 4–7). *Centrophorus* is known from the Upper Cretaceous to recent (Adnet & Cappetta 2001; Klug & Kriwet 2010). *Centrophorus* aff. *granulosus* is known from the Lutetian of south-western France (Adnet 2006a).

Family Dalatiidae Gray 1851

Genus *Isistius* Gill 1865

***Isistius trituratus* Winkler 1876b**
Fig. 19A–B

Material. 9 lower teeth, including DK730 (1 well preserved tooth), Lot MM0002 (5 well preserved teeth) and Lot AWC11.0 (3 fragmentary teeth).

Description. The largest tooth is 4 mm high apico-basally, 3 mm broad mesio-distally and strongly flattened labio-lingually. The crown is symmetric and triangular with unserrated cutting edges and without heels. Both faces are slightly convex. On the labial face a thin apron is present with a poorly marked basal boundary near the ‘button-hole’. This hole is an oval infundibulum, and a furrow reaches from its basal edge to the basal edge of the root. The labial root face is flat. The basal margin of the root is slightly indented in the centre. The root is square with straight mesial and distal margins. The lingual face is flat and at the crown–root boundary there is a poorly developed lingual protuberance parallel with the root base. Two axial foramina open lingually, a round one just below the crown and an oval one in the middle of the root. A shallow furrow stretches from this hole to the base of the root. The overlap depressions on the mesial and the distal root edges that accommodate the adjacent tooth are long and marked; especially the mesial one is deep. All teeth are from the lower jaw because of their triangular crown.

Comparison. The Trelde Næs teeth are placed in the Dalatiidae because of their triangular crown and their ‘button-hole’. The genus *Isistius* is the only genus with teeth with a symmetric crown without heels and a square root. Two fossil species of *Isistius* have been described from the Eocene to Lower Pliocene; *Isistius trituratus* and *Isistius triangulus* Probst 1879 (Cappetta 2012). From the most ancient to the most recent species, the opening of the ‘button-hole’ seems to have a successively lower position on the labial face of the root, and the root becomes higher (Cappetta 2012). The Trelde Næs teeth have smooth cutting edges on the crown and thereby separate from teeth of *Isistius triangulus* which have serrated cutting edges (Longbottom 1979; Adnet 2006a). Teeth of living *Isistius brasiliensis* Quoy & Gaimard 1824 have higher roots than those of *Isistius trituratus* (Arambourg 1952). The Trelde Næs teeth are very similar to teeth of *Isistius trituratus*, which lack serration (Arambourg 1952).

Isistius trituratus is known from the Lower Eocene of England (Casier 1966; Cooper 1977; Rayner *et al.*

2009), the Eocene of Belgium (Nolf 1988; Eeckhaut & De Schutter 2009; Iserbyt & De Schutter 2012) and Morocco (Arambourg 1952; Ward & Wiest 1990; Noubhani & Cappetta 1997) and the Lutetian of France (Adnet 2006a).

Order Echinorhiniformes Buen 1926

Family Echinorhinidae Gill 1862

Genus *Echinorhinus* Blainville 1816

Echinorhinus cf. *priscus* Arambourg 1952

Fig. 20A–F

Material. 39 teeth, including DK728e, DK728f, Lot AWC12.0, Lot MM0067.0 and Lot SL0006.

Description. The largest and best preserved tooth measures 6 mm mesio-distally, 3.5 mm apico-basally and 0.5 mm labio-lingually. The crown is triangular and bent distally. The most mesial part of the cutting edge is convex, the middle part is straight and the distal part is slightly concave. The distal cutting edge is slightly convex. The distal heel is low and short and separated from the main cusp by a deep notch. The cutting edges are worn but faint signs of irregular serration are preserved in most of the teeth. Both labial and lingual crown faces are slightly convex. In most of the teeth the crown tip extends beyond the distal border of the root. The root is strongly compressed labio-lingually. In labial view it is rectangular with straight distal, mesial and basal borders. The crown–root junction is almost straight on both sides of the tooth. The labial root face is flat and there are several small foramina opening along the crown–root junction. The lingual root face is flat and the crown–root junction forms a longitudinal shallow protuberance with many small foramina. In most of the teeth there is a vertical furrow in the central part of the lingual root face; a few teeth have two parallel furrows.

Comparison. The Trelde Næs teeth belong to Echinorhiniformes because of their strong labio-lingual compression and their simple, distally inclined cusp and no overlapping of the teeth (Cappetta 2012). They differ from teeth of *Pseudoechinorhinus* Pfeil 1983 and *Paraechinorhinus* Pfeil 1983 where the cusp is more upright and not bent (Cappetta 2012, fig. 94). Teeth of

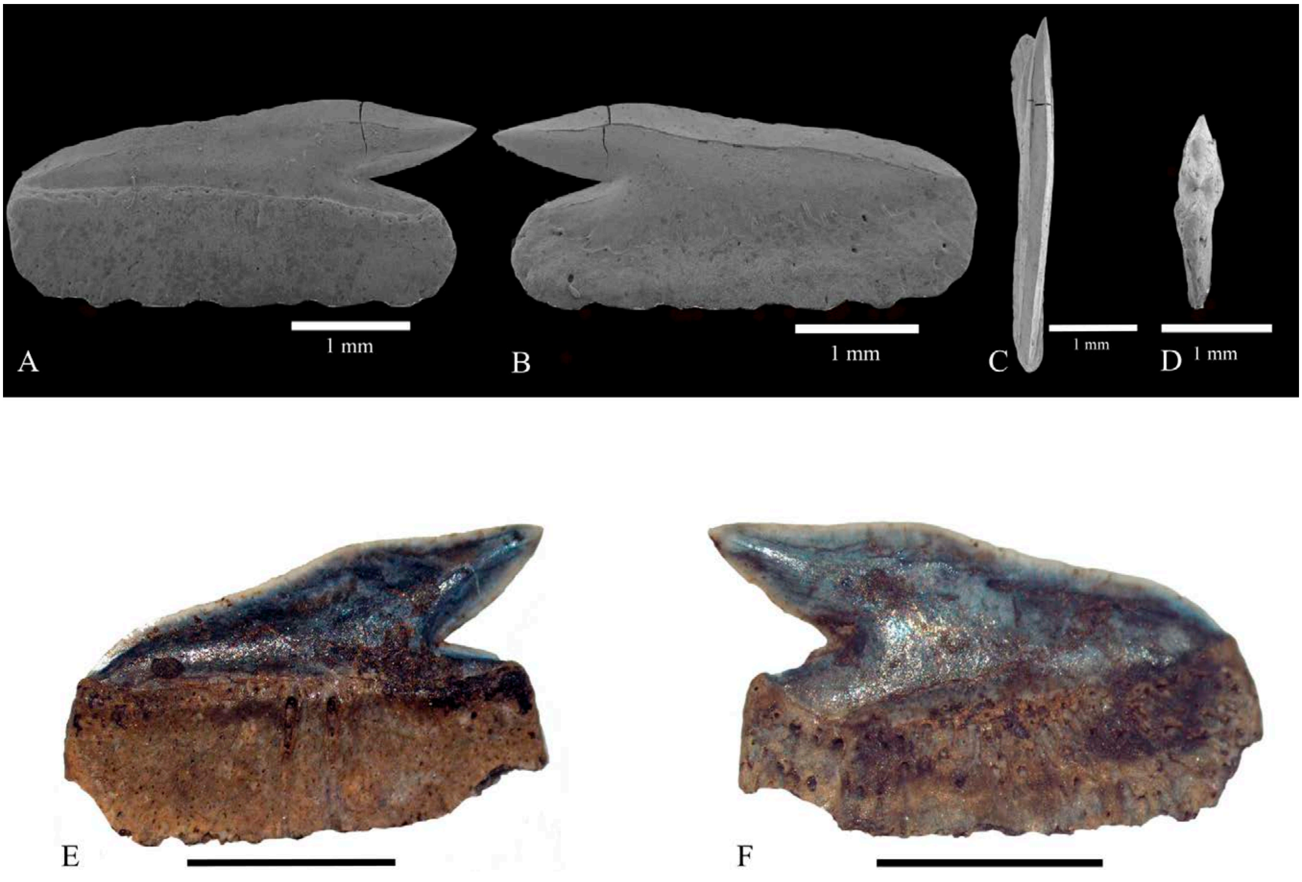

Fig. 20. **A**–**D**, *Echinorhinus* cf. *priscus*. Lateral tooth DK728e. **A**, lingual view; **B**, labial view; **C**, apical view; **D**, distal view. **E**–**F**, *Echinorhinus* cf. *priscus*. Anterolateral tooth DK728f. **E**, lingual view; **F**, labial view.

Gibbechinorhinus Cappetta 1990b are very large (up to 24 mm mesio-distally) and *Orthechinorhinus* Adnet 2006a have very small (less than 3 mm mesio-distally) teeth of tearing type (Cappetta 2012).

The Trelde Næs teeth separate easily from teeth of the living *Echinorhinus brucus* Bonnaterre, 1788 and *Echinorhinus cookei* Pietschmann 1928 which have cusplets on the mesial side of the main cusp and on the heel.

Pfeil (1983) gave exhaustive descriptions of known species of *Echinorhinus*. Most of the Cretaceous species lack cusplets (Adnet *et al.* 2012). Among the Tertiary species only teeth of *Echinorhinus priscus* known from the Lower Eocene of Morocco and Austria (Noubhani & Cappetta 1997; Pfeil 1983) and *Echinorhinus weltoni* Pfeil 1983 known from the Upper Eocene always lack side cusplets. All the Oligocene, Miocene and Pliocene species have teeth with either mesial or distal cusplets or both (Pfeil 1983). The Trelde Næs teeth are serrated in a way similar to teeth of *Echinorhinus weltoni* but differ from the latter by having longer distal crown tips extending beyond the root (Pfeil 1983). The Trelde Næs teeth are also close to teeth of *Echinorhinus priscus*, but in the latter no serration has been described (Arambourg 1952; Pfeil 1983). It seems therefore that the Trelde Næs teeth possess characters from both Eocene species but they seem closest to teeth of *Echinorhinus priscus* where long distal crown tips are described (Pfeil 1983).

Order Pristiophoriformes Berg 1958

Family Pristiophoridae Bleeker 1859

Genus *Pristiophorus* Müller **& Henle 1837**

***Pristiophorus* cf. *lanceolatus* Davis 1888**

Fig. 21A–D

Material. 1 rostral tooth, DK729z.

Description. DK729z is an almost intact rostral tooth where a tiny part of the apex of the enameloid cap is missing. The tooth is worn. The total height from apex to base is 4.5 mm: 2.5 mm for the cap and 2 mm for the peduncle. The cap is dorso-ventrally flattened with slightly convex dorsal and ventral faces. The base of the peduncle is perpendicular to the cap. The enameloid is smooth and the cutting edges are rounded and almost parallel in dorsal view, except for the apical fifth where they gradually taper to the apex. The tooth lacks transverse ridges. At the cap–peduncle junction there is a bulge forming a collar above the constricted peduncle.

The peduncle widens rapidly basally and measures 3.1 mm (antero-posteriorly) at the flat base. Seen basally there is a deep anterior–posterior rectangular groove opening to the pulp cavity. The posterior margin is concave and slightly bi-lobed (one of the lobes is missing). The anterior margin is convex and there is a deep furrow from the central hole to the front of the peduncle.

Comparison. DK729z is a rostral tooth of Pristiophoridae because of its lack of transverse ridges and its open pulp cavity that separate it from rostral teeth of Pristoidei (Slaughter & Springer 1968; Cappetta 2012). Rostral teeth of Sclerorhynchoidei are, like the rostral teeth of Pristiophoridae, not imbedded in alveoli, but teeth of the former have a closed basal face (Cappetta 2012).

Three genera of Pristiophoridae have been described. Rostral teeth of *Pristiophorus* differ from rostral teeth of the extant *Pliotrema* Regan 1906 and the extinct *Ikamauius* Keyes 1979 by lacking barbs on the cutting edges (Keyes 1982). DK729z does not have parallel crown edges like rostral teeth of *Pristiophorus lineatus* Applegate & Uyono 1968 but slightly tapering

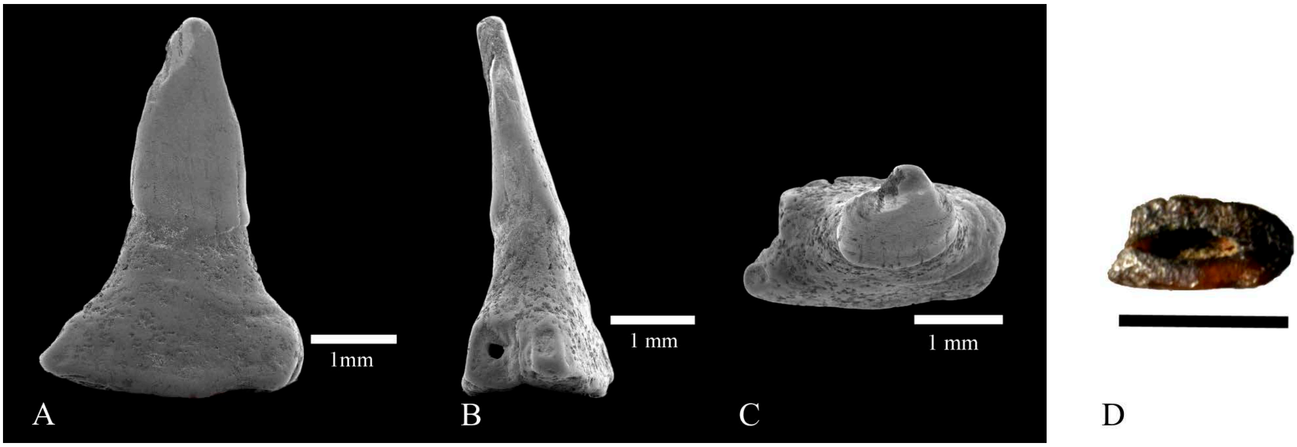

Fig. 21. **A**–**D**, *Pristiophorus* cf. *lanceolatus*. Rostral tooth DK729z. **A**, dorsal view; **B**, posterior view; **C**, apical view; **D**, basal view.

crown edges, and it lacks ornamentation on the crown like rostral teeth of *Pristiophorus lanceolatus* (Keyes 1982). It separates from rostral teeth of the Cretaceous Pristiophorus *tumidens* Woodward 1932, the Miocene *Pristiophorus suevicus* Jaekel 1890 and the Eocene *Pristiophorus lapicidinensis* Adnet 2006a which all have ornamentation on the crown (Long 1992; Gottfried & Rabarison 1997; Adnet 2006a).

Comparisons are difficult because of the low number of figured teeth for the different species in the literature and the fact that only one worn tooth is available from Trelde Næs. *Pristiophorus lineatus* is known from the Oligocene of Japan (Cappetta 2012), and *Pristiophorus lanceolatus* is known from the Eocene of Antarctica (Long 1992; Kriwet 2005) and the Oligocene of New Zealand (Keyes 1982). The Trelde Næs rostral tooth is closest to teeth of *Pristiophorus lanceolatus.* Similar teeth have been found in the Eocene of Oregon (Welton 1972), the Eocene of Antarctica (Long 1992) and the Pliocene of Italy (Cigala-Fulgosi 1986).

Superorder Batomorphii Cappetta 1980b

Order Myliobatiformes Compagno 1973

Superfamily Dasyatoidea Jordan 1888

Family *incertae sedis*

Genus *Coupatezia* Cappetta 1982

Coupatezia miretrainensis Adnet 2006a
Fig. 22A–D

Material. 3 lateral male teeth, including DK728g, MM1010 and MM0046.

Description. The teeth are very small and measure about 2 mm mesio-distally, 2 mm labio-lingually and 1.8 mm apico-basally. They have a slender, pointed lingually and slightly distally inclined cusp. The labial

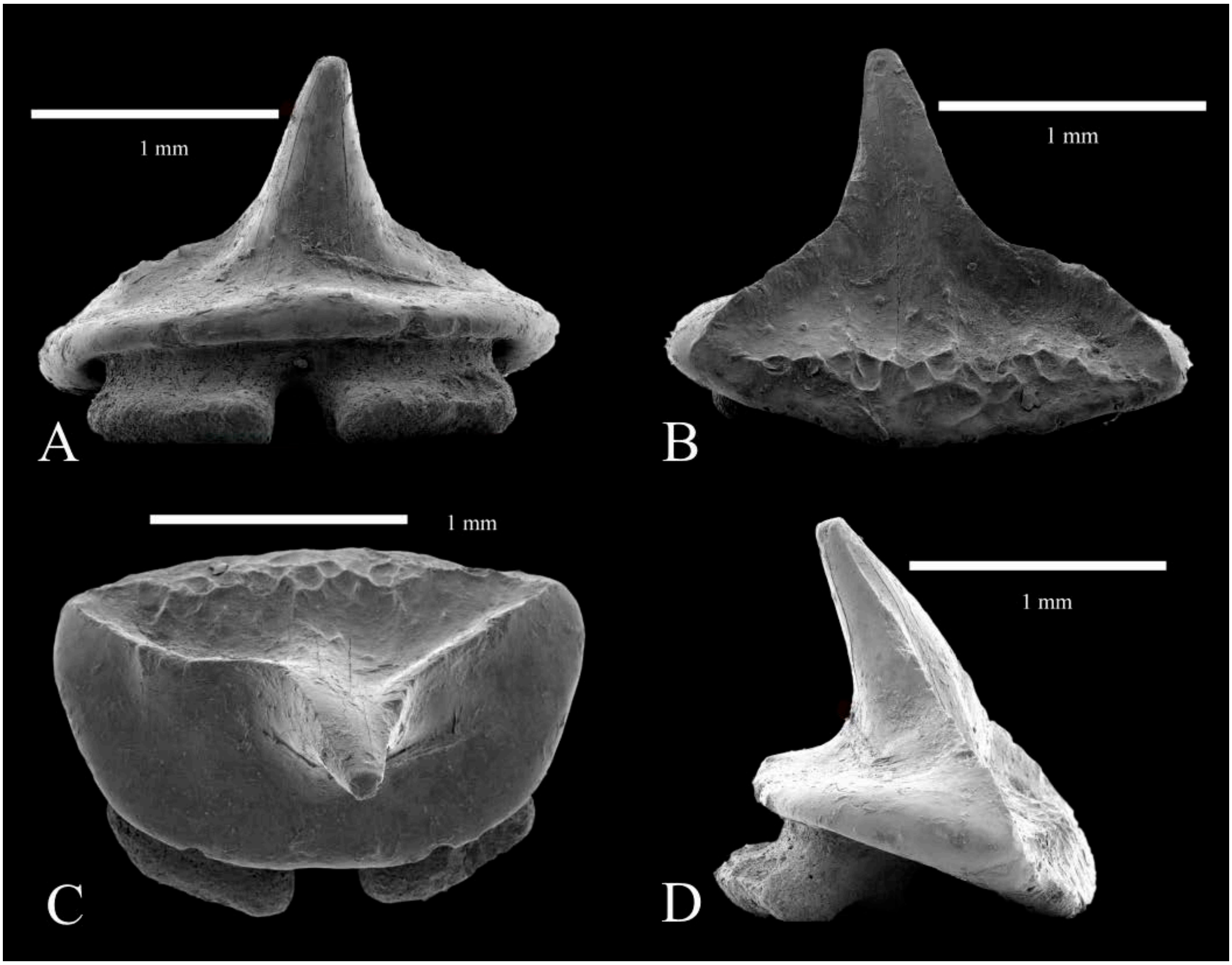

Fig. 22. **A**–**D**, *Coupatezia miretrainensis*. Male lateral tooth DK728g. **A**, lingual view; **B**, labial view; **C**, apical view; **D**, mesio-distal view.

face of the cusp is flat in the upper part and slightly concave in the basal part and without a median ridge. The edge of the labial visor is convex, broad and rounded with a flat horizontal basal face. The enameloid on the basal part of the labial face and the visor has coarse, vermicular and irregular ornamentation. The lingual crown face is strongly convex mesiodistally with 10–15 very faint longitudinal ridges or cracks on the enameloid, which are possibly a result of wear. The lingual visor is short and semi-circular when seen in apical view. The labial and lingual crown faces are separated by labially displaced and very prominent cutting edges which reach the crown base.

The root is low and displaced lingually. Its basal face is flat. It is divided in two triangular lobes by a deep and broad furrow with a large central foramen. The lingual edges of the root extend slightly beyond the crown foot and are visible in apical view. The lingual and the labial borders of the root are respectively oblique and parallel.

Comparison. The Trelde Næs teeth separate from teeth of *Raja* Agassiz 1843 by having ornamentation on the labial face of the cusp (Ward 1984). Furthermore the root is more developed in teeth of *Raja* and the basal side of the labial visor is convex. The Trelde Næs teeth also differ from teeth of *Torpedo* Forskål, 1775 and *Narcine* Henle 1834 by having ornamentation (Adnet 2006a). The Trelde Næs teeth have some resemblance with teeth of *Taeniura lymna* Forskål, 1775 known from the Miocene to the recent (Cappetta 2012) but they differ by having ornamentation near and on the basal labial margin of the cusp (Cappetta 2012). Labial ornamentation is seen on teeth of *Merabatis* Arambourg 1952 but these teeth are characterized by the complete concealment of the root by the visors in apical view, contrary to teeth of *Coupatezia* where the root is visible in apical view. Furthermore, teeth of *Raja* and *Merabatis* have a more or less sharp median labial vertical crest which is not present on the Trelde Næs teeth. *Coupatezia* has been described from the Upper Cretaceous of Morocco (Arambourg 1952; Noubhani & Cappetta 1997) to the Lutetian and Bartonian of France (Adnet 2006a). The species *Coupatezia miretrainensis* differ from the other species by its vermicular labial ornamentation and its relatively thin labial visor (Adnet 2006a). The Trelde Næs teeth are similar to lateral male teeth of *Coupatezia miretrainensis* figured by Adnet (2006a, plate 37, fig. 4a–4c). The Trelde Næs teeth are believed to be from male individuals because of the pointed cusp, contrary to the low cusp in female teeth. The slightly asymmetric cusp suggests a lateral position in the jaw.

Table 1. List of elasmobranchs found at Trelde Næs. Numbers indicate the number of teeth used in the descriptions

	Surface material Lillebælt Clay layer L2–L6 and Søvind Marl	Bulk material Lillebælt Clay layer L2
Superorder Galeomorphii		
Order Lamniformes		
Anomotodon sheppeyensis	100	
Striatolamia macrota	46	
Woellsteinia kozlovi	22	
Isurolamna affinis	216	
Macrorhizodus cf. *nolfi*	99	
Xiphodolamia ensis	1	
Alopias crochardi	46	2
Usakias sp.	63	
Carcharocles auriculatus	34	
Otodus cf. *obliquus*	3	
Palaeohypotodus rutoti	2	
Odontaspis cf. *winkleri*	9	
Jaekelotodus robustus	11	
Carcharias sp. *sensu* Cappetta & Nolf 2005	14	
Turania sp.	5	
Hypotodus verticalis	7	
Odontaspididae genus indet. 1	6	
Odontaspididae genus indet. 2	1	
Cretalamna aff. *appendiculata*	3	
Lamniformes family indet.	12	
Order Carchariniformes		
Megascyliorhinus cooperi	2	
Foumtizia sp.		2
Physogaleus cf. *secundus*	10	1
Superorder Squalomorphii		
Order Hexanchiformes		
Chlamydoselachus cf. *fiedleri*		1
Heptranchias howelli	18	1
Notorynchus serratissimus	23	1
Hexanchus cf. *agassizi*	4	2
Weltonia burnhamensis	1	1
Order Squatiniformes		
Squatina cf. *prima*	4	
Order Squaliformes		
Centrophorus aff. *granulosus*		22
Isistius trituratus		9
Order Echinorhiniformes		
Echinorhinus cf. *priscus*		39
Order Pristiophoriformes		
Pristiophorus cf. *lanceolatus*	1	
Superorder Batomorphii		
Order Myliobatiformes		
Coupatezia miretrainensis		3

Palaeoecology and palaeoenvironment

Inferences on the palaeoecology of the Trelde Næs sharks and rays may be made by considering the occurrence and behaviour of related living forms, based on information in the literature (Compagno 2003; Compagno et al. 2005; http://www.fishbase.com). Of the 31 identified genera recorded from Trelde Næs so far, twelve genera are represented by extant genera, and fourteen are members of extant families. The last five are members of extinct families and can only be related to modern superfamily or order. When there are no close living relatives, the palaeoecology may be considered exclusively from the tooth morphology and the fossil record.

The Trelde Næs shark and ray teeth material is divided into two sets according to the sampling method (Table 1): 1) Teeth retrieved from screen washed bulk samples where the provenance is known to be from the Lillebælt Clay Formation layer L2; 2) Teeth retrieved from surface sampling whose origin can therefore only be delimited to the Lillebælt Clay Formation layer L2 to L6 and the Lower Søvind Marl Formation.

For the purpose of this project, deep-water chondrichthyans have been defined as those sharks and rays whose distribution is predominantly at, are restricted to, or spend the majority of their lifecycle at depths below 200 m. This depth is generally recognized as the continental and insular shelf edge, and therefore deep-water species are those occurring on or over the continental and insular slopes and beyond, including the abyssal plains and oceanic seamounts (Kyne & Simpfendorfer 2007).

Screen washed material

This material (Table 1) contains only small teeth of Lamniformes, Carchariniformes, Hexanchiformes, Squaliformes, Echinorhiniformes and Myliobatiformes, and includes thirteen different genera retrieved from a relatively small bulk size of approximately 160 kg.

Lamniformes are represented by two teeth of *Alopias crochardi*. The tooth morphology of the fossil species *Alopias crochardi* is closest to that of *Alopias superciliosus*. These pelagic sharks live worldwide in warm to temperate oceans and have been observed down to a depth of 730 m (http://www.fishbase.org).

Carchariniformes are represented by *Megascyliorhinus cooperi*, *Foumtizia* sp. and *Physogaleus* cf. *secundus*. These genera have no close living relatives.

Megascyliorhinus cooperi is described as belonging to the family Scyliorhinidae (Cappetta & Ward 1977) in the extinct subfamily Megascyliorhininae. Teeth of *Megascyliorhinus* differ from teeth of other Scyliorhinids by lacking cusplets on the anterior teeth, but Cappetta & Ward (1977) pointed out broad similarities between the teeth of *Megascyliorhinus* and the teeth of *Scyliorhinus* Blainville 1816. The latter genus is benthic and nocturnal with a depth range from 10 to 780 m (http://www.fishbase.org). Cappetta & Ward (1977) suggested a depth range of 150 to 200 m for *Megascyliorhinus*, whereas Adnet (2006a) suggested it

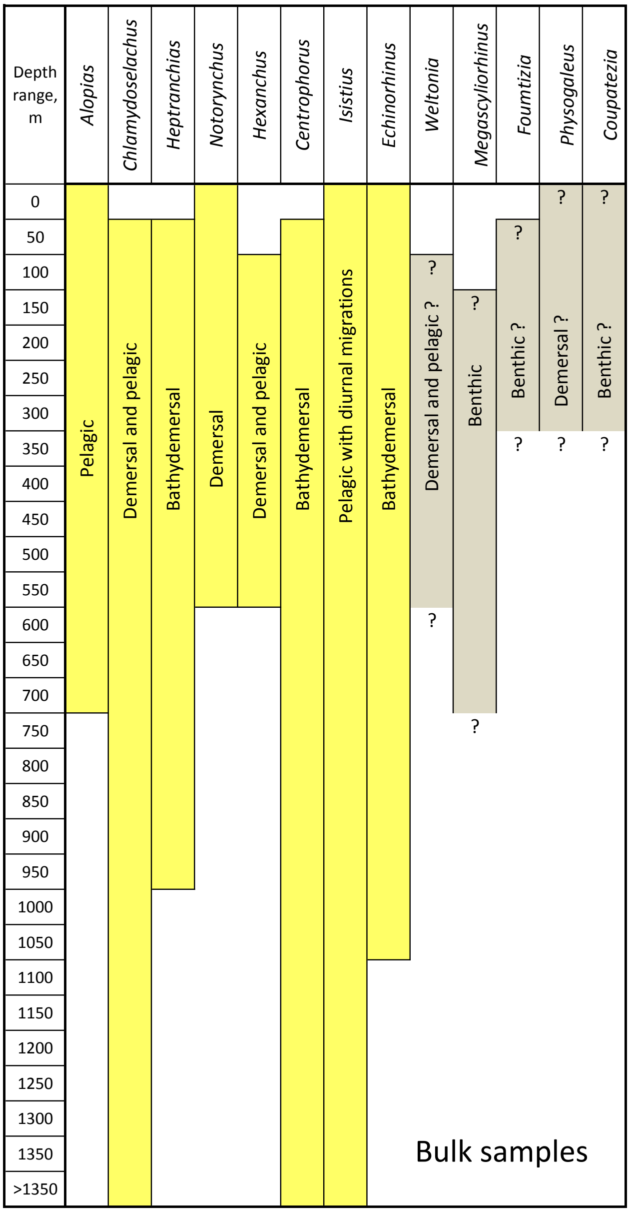

Fig. 23. Suggested depth range (metres) of the sharks and rays found in the Lillebælt Clay Formation layer L2 (bulk samples). The yellow columns indicate recent genera. The grey columns indicate fossil genera without close living relatives and where the depth range is uncertain.

to be deeper as it has been found together with other deep-water species.

Teeth of *Foumtizia* have ornamented crowns with small cusplets and a pronounced horizontal labial crest, characters found among Scyliorhinidae and Triakidae (Compagno 2003). The habitat of *Foumtizia* is unknown, but the fact that it has been found together with other deep-water genera such as *Centrophorus* in south-western France (Adnet 2006a) could suggest a depth range of a few hundred metres.

Physogaleus cf. *secundus* is described as belonging to the family Carcharhinidae. Cappetta (1980a) suggested that *Physogaleus* might be an ancestor to *Scoliodon*, *Rhizoprionodon* and *Loxodon*, but the morphology of its teeth seems closest to that of *Rhizoprionodon* (Compagno *et al.* 2005, drawings p. 317–320). *Rhizoprionodon* probably lives near the bottom and is very common in coastal water and on continental shelves with a depth range down to 350 m (Compagno *et al.* 2005).

Hexanchiformes are represented by *Chlamydoselachus* cf. *fiedleri*, *Heptranchias howelli*, *Notorynchus serratissimus*, *Hexanchus* cf. *agassizi* and *Weltonia burnhamensis*.

The recent species of *Chlamydoselachus* live near the bottom as well as in the midwaters with a depth range of 50 to 1200 m and they have been found on the continental shelf and upper slopes (http://www.fishbase.org). *Heptranchias perlo* is the only recent species of the genus *Heptranchias*. It is found near the bottom on the outer continental and insular shelves and upper slopes in depths of 50 to 400 m, as well as inshore, down to 1000 m (http://www.fishbase.org). *Notorynchus cepedianus* is the only recent species of the genus *Notorynchus*. It is found on the continental shelf, often in shallow water, but its depth range is from 1 to 570 m. It lives near the bottom but can also be seen near the surface (http://www.fishbase.org).

There are two recent species of *Hexanchus*. They both live near the bottom and in open waters, occasionally moving to the surface at night. Their depth range is usually from 90 to 600 m (http://www.fishbase.org). *Weltonia* is described as belonging to the family Hexanchidae and has no living relatives at genus level. There are two fossil species of *Weltonia*: *Weltonia burnhamensis* and *Weltonia ancistrodon,* known respectively from the London Clay (Casier 1966; Ward 1979) and Morocco (Arambourg 1952; Noubhani & Cappetta 1997). The fact that *Weltonia* has been found together with other hexanchids in the above-mentioned locations justifies the assumption that *Weltonia* was also living in deep waters.

Squaliformes are represented by *Centrophorus* aff. *granulosus* and *Isistius trituratus*. The recent species of *Centrophorus* are all deep-water species living on the outer slope near the bottom. The depth range varies, but the common range is 100 to 800 m although some species have been found at depths of 2400 m (http://www.fishbase.org).

The recent species of *Isistius* are also deep-water species down to over 1350 m, found in tropical to temperate waters with diurnal migration to the surface at night (http://www.fishbase.org).

Echinorhiniformes are represented by *Echinorhinus* cf. *priscus*. The modern species of *Echinorhinus* are deep-water sharks, found on continental and insular shelves and upper slopes and sometimes also in shallow water. They live in temperate water down to 900 m. (http://www.fishbase.org).

Only one species of Batomorphii was found: *Coupatezia miretrainensis*. The tooth morphology of *Coupatezia* has some similarities to teeth of Dasyatidae, in particular *Dasyatis pastinaca* (common stingray) (Cappetta 2012). This species lives today on muddy bottoms down to 200 m in subtropical waters (http://www.fishbase.org). Teeth of *Coupatezia* also show some similarities with teeth of *Taeniura* (Cappetta 2012, fig. 414), but this genus is reef-related in tropical waters (http:/www.fishbase.org).

Adnet (2006a) suggested that some species of *Coupatezia* were living in deep waters, and the fact that teeth of *Coupatezia* have been found in deep-water sediments together with teeth of several other deep-water genera (Adnet *et al.* 2008) supports this idea. It was probably found down to about 350 m, but this remains uncertain.

Summary. All the species with recent close relatives present in layer L2 can be found in water depths down to 600 m or more (Fig. 23). The pelagic species (*Alopias* and *Isistius*) give no information on the water depth because they feed at various depths in the water column. The demersal and bathydemersal species (*Chlamydoselachus*, *Heptranchias*, *Notorynchus*, *Hexanchus, Centrophorus* and *Echinorhinus*) all live and feed near the bottom and thereby suggest a maximum water depth about 600 m, but they are also found in shallower waters. This agrees with the water depth in the Danish area given in Heilmann-Clausen & Surlyk (2006) as probably being about 500 m during the Late Ypresian. The habitat and depth range of the five genera without close living relatives (*Weltonia*, *Megascyliorhinus*, *Foumtizia*, *Physogaleus* and *Coupatezia*) is difficult to infer with confidence. We consider them all to have been benthic or demersal. It seems that the depositional environment for the teeth from the bulk sample was a marine deep-water environment with depth below 100 m but probably not deeper than 350 m (Fig. 23). This agrees with the water depth of 100 to 300 m inferred from the molluscan fauna from Trelde Næs (Schnetler & Heilmann-Clausen 2011). An explanation for the discrepancy between the depth given by Heilmann-Clausen & Surlyk (2006) and the present fossil record could be that Trelde Næs is located in the vicinity of the Ringkøbing–Fyn High in the North Sea Basin. Another explanation for the difference from the expected 500 m would be that teeth of *Foumtizia, Physogaleus* and *Coupatezia* have been transported by currents from shallower waters out into a deeper basin. This explanation seems less probable because the nearest coastline was about 300 km from the deposition site at Trelde Næs (Thomsen *et al.* 2012).

Surface collected material

This material consists mainly of teeth of Lamniformes (about 90%). There are only very few small teeth in this material, probably because of the collecting method, but this does not mean that the small and very small teeth are absent from the sediments. The far most abundant teeth are from Mitsukurinidae, Lamnidae and Alopiidae (Table1).

Seventeen species of Lamniformes in seven families were identified. Mitsukurinidae are represented by *Anomotodon sheppeyensis*, *Striatolamia macrota* and *Woellsteinia kozlovi*. There is only one living species in this family, *Mitsukurina owstoni* Jordan1898. This shark is a pelagic shark with a worldwide distribution in tropical and warm waters with a depth range from 30 to1300 m. It has been found on outer continental shelves and upper slopes, but rarely in shallow water close inshore (http://www.fishbase.org). Teeth of *Anomotodon sheppeyensis* have been found in the London Clay deep-water sediments (Rayner *et al.* 2009) and the deep-water sediments of south-western France (Adnet 2006a). However, teeth of other species of *Anomotodon* have been found in shallow-water deposits in Antarctica (Kriwet 2005) and Southern Chile (Otero *et al.* 2012). Teeth of *Striatolamia macrota* are known from the Early Ypresian London Clay (Rayner *et al.* 2009), the Ypresian/Lutetian of south-western France (Adnet 2006a; Adnet *et al.* 2008) and the Ypresian/Lutetian of North Germany (Diedrich 2012). All these environments are considered to be deep-water environments. However, teeth of *Striatolamia macrota* have also been found in marine shallow-water deposits of the Eocene of Belgium (Nolf 1988), Antarctica (Kriwet 2005), Southern Chile (Otero *et al.* 2012) and Maryland, USA (Ward & Wiest 1990). Teeth of *Woellsteinia* have only been found in deep-water deposits from south-western France (Adnet 2006a) and from New Zealand (Mannering & Hiller 2008). The fossil record of the Mitsukurinidae suggests therefore a pelagic behaviour and a worldwide distribution of fossil genera.

Lamnidae are represented by *Isurolamna affinis* and *Macrorhizodus* cf. *nolfi*. Today, the family encompasses *Carcharodon*, *Isurus* and *Lamna*. They are all pelagic with a depth range from 0 to 750 m, but sometimes visit temperate shallower waters (http://www.fishbase.org).

Teeth of *Isurolamna affinis* have been found in deep-water sediments from the London Clay (Rayner *et al.* 2009), south-western France (Adnet 2006a), North Germany (Diedrich 2012) and shallow open marine waters from Belgium (Nolf 1988; Eeckhaut & De Schutter 2009). Teeth of *Macrorhizodus nolfi* have been found in the deep-water sediments from the Early Ypresian London Clay (Rayner *et al.* 2009) and also in Ypresian deposits of Kazakhstan (Zhelezko & Kozlov 1999), for which the palaeobathymetry is not known. Teeth of *Macrorhizodus praecursor* have been found in deep-water deposits in south-western France (Adnet 2006a), Germany (Diedrich 2012) as well as in shallow open marine water deposits in Belgium (Nolf 1988), Egypt (Underwood *et al.* 2011b), Antarctica (Kriwet 2005) and Chile (Otero *et al.* 2012). This suggests that *Isurolamna* as well as *Macrorhizodus* were pelagic sharks like the recent lamnids.

Xiphodolamiidae are represented by *Xiphodolamia ensis* which has no recent relatives. Adnet *et al.* (2009) considered this genus as Lamnidae *incertae sedis*, but Cappetta (2012) has elevated the subfamily Xiphodolaminae Glikman 1964a to the rank of family because of its very special dental morphology. Adnet *et al.* (2009) regarded *Xiphodolamia* as an old lineage derived from the stem group of Lamnidae, close to the Isuroid sharks. Fossil teeth of *Xiphodolamia* are rare in coastal deposits but occur in deep-water deposits like the London Clay (Rayner *et al.* 2009), North Germany (Diedrich 2012), but also in shallow-marine water in Belgium (Nolf 1988; Eeckhaut & De Schutter 2009). This led Adnet *et al.* (2009) to suggest that *Xiphodolamia* probably lived in rather deep and/or open waters.

Alopiidae are represented by *Alopias crochardi* and *Usakias* sp. The closest recent relative to *Alopias crochardi* is presumed to be *Alopias superciliosus,* which is a pelagic species distributed worldwide in warm and temperate waters down to 730 m (http://www.fishbase.org). Teeth of *Usakias* are morphologically close to teeth of *Alopias* and there is no reason to think that its habitat differed from the habitat of *Alopias*. Teeth of *Usakias* have been found in deep-water sediments in North Germany (Diedrich 2012) and shallow-marine water sediments in Belgium (Eeckhaut & De Schutter 2009).

Otodontidae is an extinct family represented by *Carcharocles auriculatus* and *Otodus* cf. *obliquus*. Based on the size and morphology of teeth of *Carcharocles auriculatus*, this shark must have been a very large predator. Its teeth have been found worldwide (Cappetta 2012). This suggests that it had a pelagic behaviour and its teeth have been found in deep as well as shallow-marine deposits. Teeth of *Otodus* cf. *obliquus* are morphologically very close to teeth of *Carcharocles* and it is parsimonious to infer a similar habitat. *Otodus* had the same distribution as *Carcharocles* (Cappetta 2012) and has been found in deep-water sediments in the London Clay (Rayner *et al.* 2009), the Paris Basin in France (Dutheil *et al.* 2006) and North Germany (Diedrich 2012).

Cretalamna aff. *appendiculata*. From the morphology and size of their teeth, they are believed to have been large predatory sharks, and their teeth have been found worldwide (Cappetta 2012). Teeth of *Cretalamna* aff. *appendiculata* have been found in deep-water sediments from the Northern hemisphere in the London Clay (Rayner *et al.* 2009), southwestern France (Adnet 2006a) and sediments from Morocco (Noubhani & Cappetta 1997).

Odontaspididae are represented by six different genera: *Palaeohypotodus, Odontaspis, Jaekelotodus, Carcharias, Turania* and *Hypotodus*, whereas the family encompasses today only *Odontaspis* and *Carcharias*.

Odontaspis is found on or near the bottom of the continental and insular shelves and upper slopes and are considered deep-water species, possibly pelagic (Compagno *et al.* 2005), with a depth range from 1 to over 1000 m (http://www.fishbase.org).

Carcharias lives in the neritic zone in water depth down to 200 m. It is a common littoral shark found inshore from the surf zone and in shallow bays to the outer continental shelves. It often occurs on or near the bottom but also in midwaters or at the surface. It is known to migrate between oceans, moving to cooler water in summer, and is distributed worldwide in the subtropical zone (http://www.fishbase.org).

The different lifestyles of *Odontaspis* and *Carcharias* lead Cvancara & Hoganson (1993) to place *Carcharias*

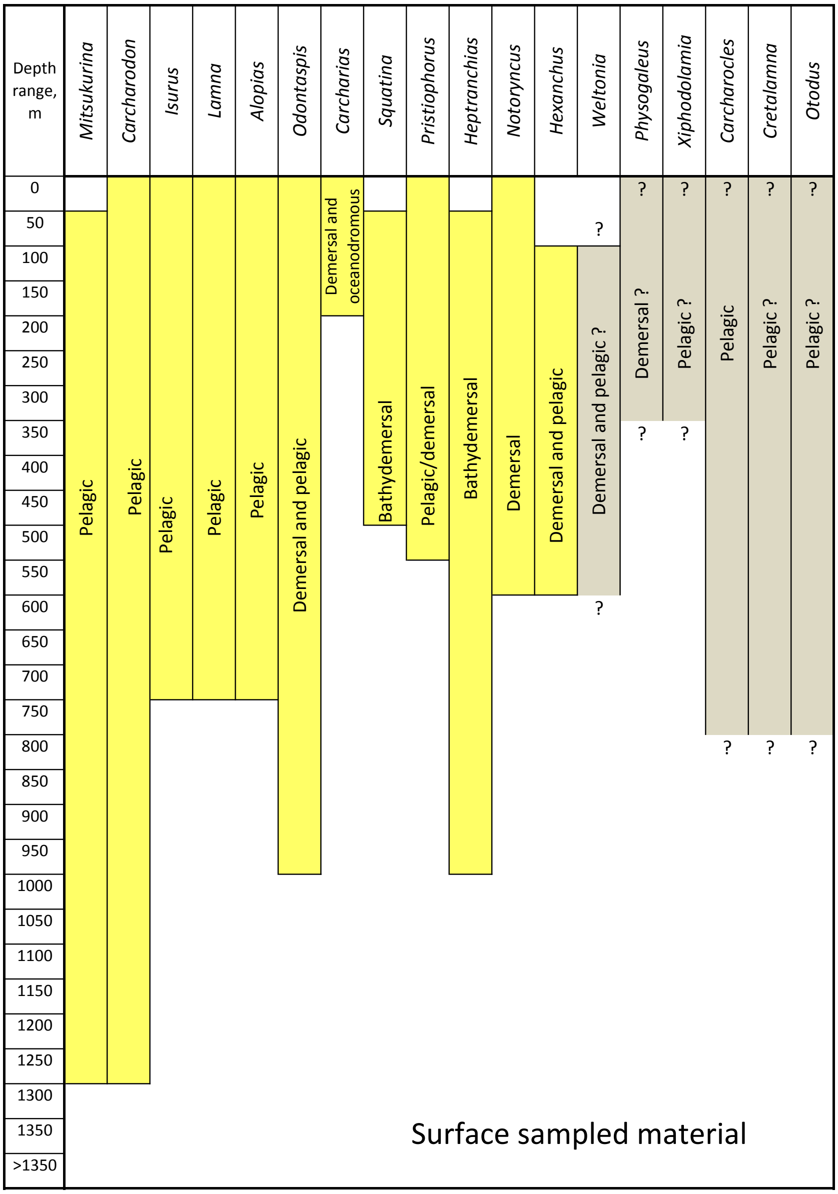

Fig. 24. Suggested depth range (metres) of the sharks found in the Lillebælt Clay Formation layers L2 to L6 and Lower Søvind Marl Formation (surface samples). The yellow columns indicate recent genera. The grey columns indicate fossil genera without close living relatives and where the depth range is uncertain.

in its own family Carchariidae. This has recently been confirmed by molecular DNA-studies which found that *Odontaspis* and *Carcharias* are not closely related (Vélez-Zuazo & Agnarsson 2011). However, these results have not yet been commonly accepted, and we conservatively keep all six genera in the family Odontaspididae.

Teeth of *Palaeohypotodus*, *Jaekelotodus*, and *Hypotodus* have morphology close to teeth of *Odontaspis* and probably lived in the same type of habitat as deep-water demersal species. *Palaeohypotodus* has been found in deep- and shallow-marine sediments from both hemispheres, whereas *Jaekelotodus* and *Hypotodus* have only been found in sediments from the Northern hemisphere (Cappetta 2012). Teeth of *Carcharias* sp. *sensu* Cappetta & Nolf 2005 have been found in deep-water sediments (Cooper 1977; Adnet 2006a; Dutheil *et al.* 2006; Mannering & Hiller 2008; Diedrich 2012) as well as in shallow-water sediments (Eeckhaut & De Schutter 2009) from both hemispheres. Teeth of *Turania* have so far only been found in Bartonian sediments (the deposition depth of which is unknown) in Kazakhstan (Kozlov 2001), but this taxon must be considered with caution as discussed above.

It is concluded that the fossil Odontaspididae were all deep-water species, possibly pelagic, and lived near the bottom in the epicontinental seas and in the open sea. Fossil teeth of *Carcharias* are not uncommon in deep-water sediments and it is a possibility that the genus today has adapted to shallower water than was the case in the Eocene.

Hexanchiformes (except *Chlamydoselachus*) and *Physogaleus* cf. *secundus* were present in the surface sample as well as in the bulk samples.

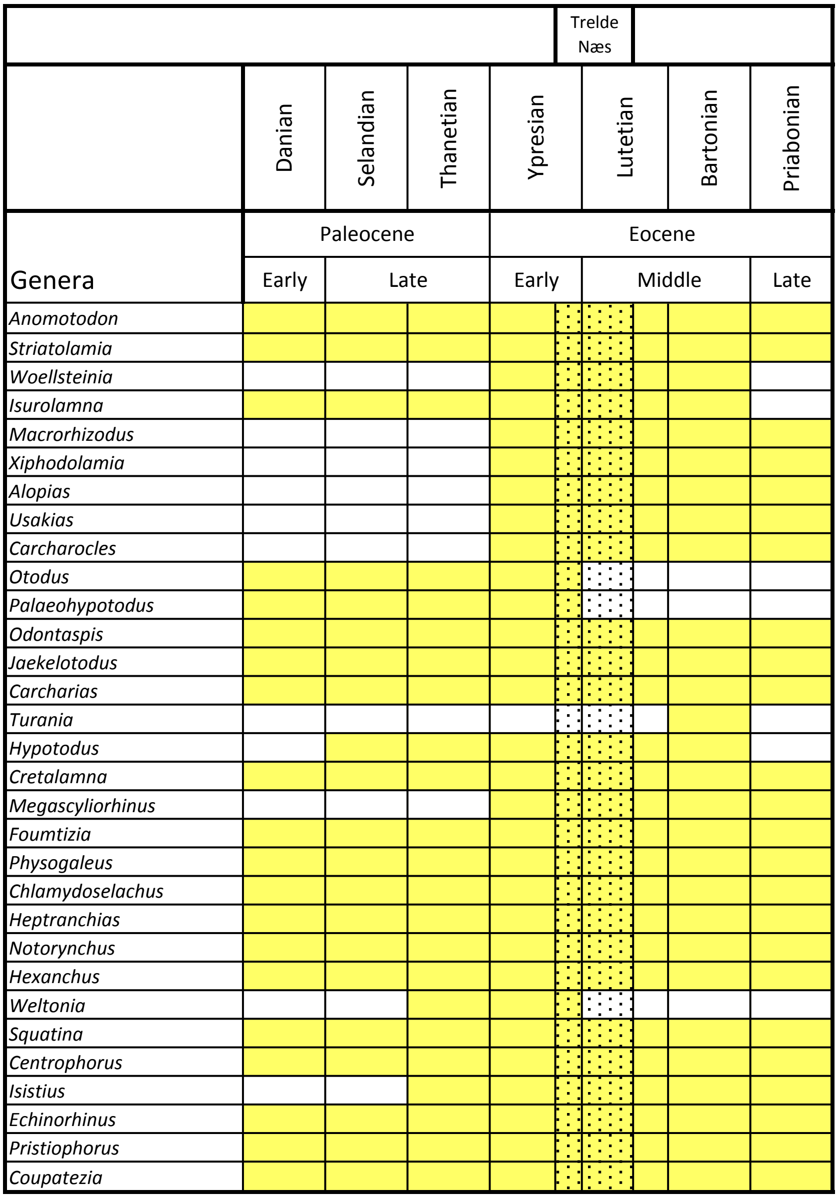

				Trelde Næs			
	Danian	Selandian	Thanetian	Ypresian	Lutetian	Bartonian	Priabonian
	Paleocene			Eocene			
Genera	Early	Late		Early	Middle		Late
Anomotodon	🟨	🟨	🟨	🟨	🟨	🟨	🟨
Striatolamia	🟨	🟨	🟨	🟨	🟨	🟨	🟨
Woellsteinia				🟨	🟨	🟨	
Isurolamna	🟨	🟨	🟨	🟨	🟨	🟨	
Macrorhizodus				🟨	🟨	🟨	🟨
Xiphodolamia				🟨	🟨	🟨	🟨
Alopias				🟨	🟨	🟨	🟨
Usakias				🟨	🟨	🟨	🟨
Carcharocles				🟨	🟨	🟨	🟨
Otodus	🟨	🟨	🟨	🟨			
Palaeohypotodus	🟨	🟨	🟨	🟨			
Odontaspis	🟨	🟨	🟨	🟨	🟨	🟨	🟨
Jaekelotodus	🟨	🟨	🟨	🟨	🟨	🟨	🟨
Carcharias	🟨	🟨	🟨	🟨	🟨	🟨	🟨
Turania						🟨	
Hypotodus		🟨	🟨	🟨	🟨	🟨	
Cretalamna	🟨	🟨	🟨	🟨	🟨	🟨	🟨
Megascyliorhinus				🟨	🟨	🟨	🟨
Foumtizia	🟨	🟨	🟨	🟨	🟨	🟨	🟨
Physogaleus	🟨	🟨	🟨	🟨	🟨	🟨	🟨
Chlamydoselachus	🟨	🟨	🟨	🟨	🟨	🟨	🟨
Heptranchias	🟨	🟨	🟨	🟨	🟨	🟨	🟨
Notorynchus	🟨	🟨	🟨	🟨	🟨	🟨	🟨
Hexanchus	🟨	🟨	🟨	🟨	🟨	🟨	🟨
Weltonia			🟨	🟨			
Squatina	🟨	🟨	🟨	🟨	🟨	🟨	🟨
Centrophorus	🟨	🟨	🟨	🟨	🟨	🟨	🟨
Isistius			🟨	🟨	🟨	🟨	🟨
Echinorhinus	🟨	🟨	🟨	🟨	🟨	🟨	🟨
Pristiophorus	🟨	🟨	🟨	🟨	🟨	🟨	🟨
Coupatezia	🟨	🟨	🟨	🟨	🟨	🟨	🟨

Fig. 25. Known stratigraphic distribution of the genera present in the total Trelde Næs fauna during the Paleocene and the Eocene. Data from Cappetta (2012).

Squatiniformes are represented by *Squatina* cf. *prima*. The recent species of *Squatina,* except *Squatina dumeril,* live on the continental shelf and the upper slope near or on the bottom with a depth range of approximately 10–500 m (http://www.fishbase.org). Fossil teeth of *Squatina* have been found in deep-sea and shallow-marine sediments worldwide (Nolf 1988; Ward & Wiest 1990; Noubhani & Cappetta 1997; Kriwet 2005; Adnet 2006a; Dutheil *et al.* 2006; Eeckhaut & De Schutter 2009; Rayner *et al*. 2009; Underwood *et al.* 2011b). This shark first appeared in the upper Jurassic and has had a very long time to spread worldwide in spite of its benthic behavior.

Pristiophoriformes are represented by one rostral tooth of *Pristiophorus* cf. *lanceolatus*. The recent species of *Pristiophorus* all live on the continental shelf and the upper slope. Two species are pelagic, the others are demersal and live on or near the bottom. The depth range of the genus is approximately 0–500 m (http://www.fishbase.org). In the fossil record, *Pristiophorus* has a worldwide distribution (Compagno *et al*. 2005). The genus has been found in the deep-water sediments of southwestern France (Adnet 2006a) and shallow-marine sediments of Egypt (Underwood *et al.* 2011b) and Antarctica (Kriwet 2005). *Pristiophorus lanceolatus* has been described from Antarctica (Long 1992), but may have been distributed worldwide (Long 1992).

Summary. The teeth from the surface material (Fig. 24) come from a long time period (about 5.1 Ma), from the Upper Ypresian to the Middle Lutetian.

Mitsukurina, *Carcharodon*, *Isurus*, *Lamna* and *Alopias* are pelagic and cannot contribute to estimation of

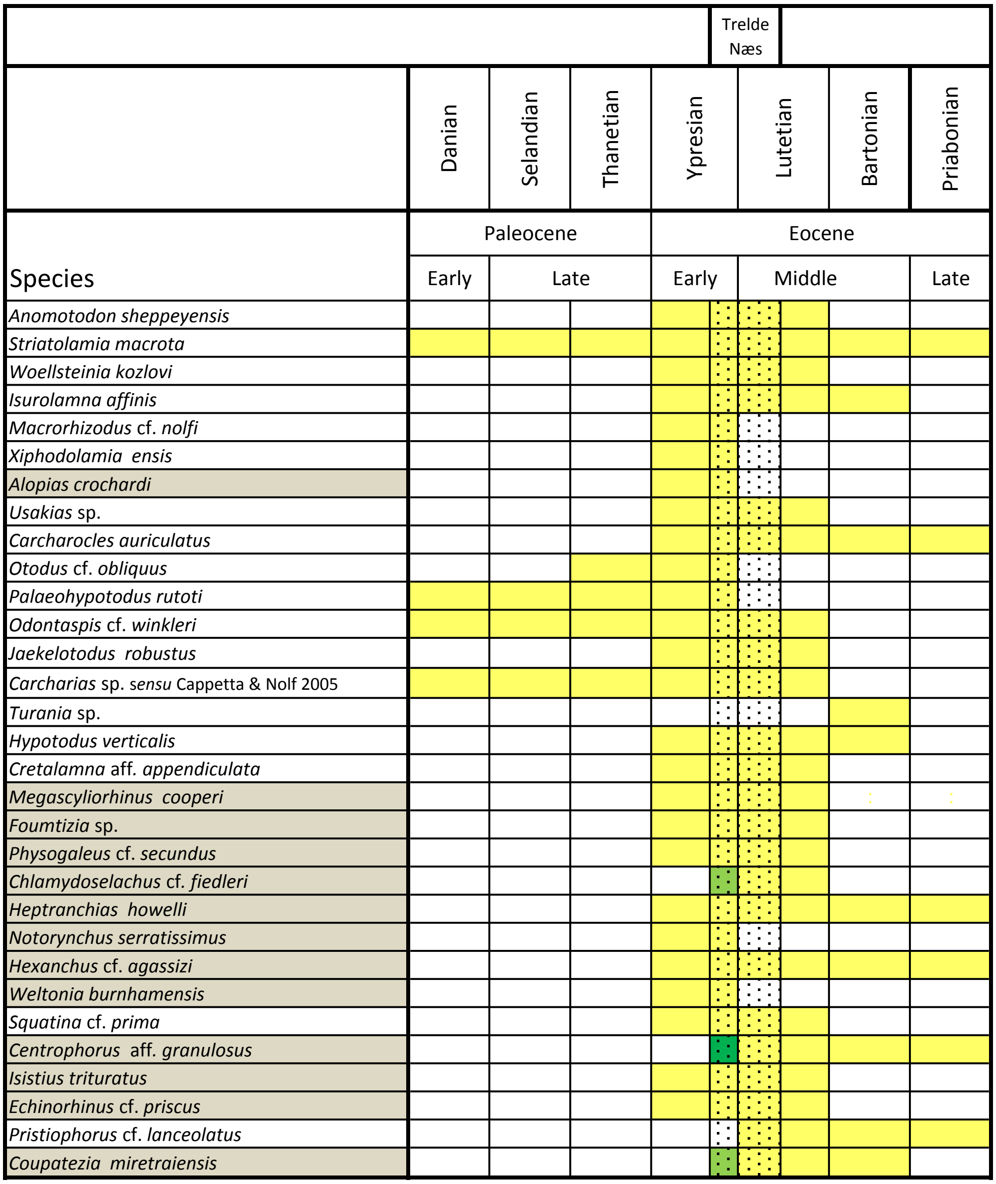

					Trelde Næs				
	Danian	Selandian	Thanetian	Ypresian		Lutetian		Bartonian	Priabonian
	Paleocene			Eocene					
Species	Early	Late		Early		Middle			Late
Anomotodon sheppeyensis				🟨	🟨	🟨	🟨		
Striatolamia macrota	🟨	🟨	🟨	🟨	🟨	🟨	🟨	🟨	🟨
Woellsteinia kozlovi				🟨	🟨	🟨	🟨		
Isurolamna affinis				🟨	🟨	🟨	🟨	🟨	
Macrorhizodus cf. *nolfi*				🟨	🟨				
Xiphodolamia ensis				🟨	🟨				
▨ *Alopias crochardi*				🟨	🟨				
Usakias sp.				🟨	🟨	🟨	🟨		
Carcharocles auriculatus				🟨	🟨	🟨	🟨	🟨	🟨
Otodus cf. *obliquus*			🟨	🟨	🟨				
Palaeohypotodus rutoti	🟨	🟨	🟨	🟨	🟨				
Odontaspis cf. *winkleri*	🟨	🟨	🟨	🟨	🟨	🟨	🟨		
Jaekelotodus robustus				🟨	🟨	🟨	🟨		
Carcharias sp. *sensu* Cappetta & Nolf 2005	🟨	🟨	🟨	🟨	🟨	🟨	🟨		
Turania sp.								🟨	
Hypotodus verticalis				🟨	🟨	🟨	🟨	🟨	
Cretalamna aff. *appendiculata*				🟨	🟨	🟨	🟨		
▨ *Megascyliorhinus cooperi*				🟨	🟨	🟨	🟨		
▨ *Foumtizia* sp.				🟨	🟨	🟨	🟨		
▨ *Physogaleus* cf. *secundus*				🟨	🟨	🟨	🟨		
▨ *Chlamydoselachus* cf. *fiedleri*					🟩	🟨	🟨		
▨ *Heptranchias howelli*				🟨	🟨	🟨	🟨	🟨	🟨
▨ *Notorynchus serratissimus*				🟨	🟨				
▨ *Hexanchus* cf. *agassizi*				🟨	🟨	🟨	🟨	🟨	🟨
▨ *Weltonia burnhamensis*				🟨	🟨				
Squatina cf. *prima*				🟨	🟨	🟨	🟨		
▨ *Centrophorus* aff. *granulosus*					🟩	🟨	🟨	🟨	🟨
▨ *Isistius trituratus*				🟨	🟨	🟨	🟨		
▨ *Echinorhinus* cf. *priscus*				🟨	🟨	🟨	🟨		
Pristiophorus cf. *lanceolatus*						🟨	🟨	🟨	🟨
▨ *Coupatezia miretraiensis*					🟩	🟨	🟨	🟨	

Fig. 26. Stratigraphic distribution of the Trelde Næs species. Yellow colour indicates stratigraphic distribution of the species known from the literature. Grey colour indicates species found in the bulk samples. Green colour indicates presence only known from Trelde Næs.

the water depth at which the sediment was deposited because they feed at various depths in the water column. *Odontaspis*, *Squatina*, *Pristiophorus*, *Heptranchias*, *Notorynchus* and *Hexanchus* are demersal in waters down at least to 500 m. This could agree with the water depth in the Danish area given in Heilmann-Clausen & Surlyk (2006) as probably around 500 m, with the exception of *Carcharias* which today lives in shallower water. It is in this connection notable that *Carcharias* has been found in several deep-water deposits, and the presence of *Carcharias* can therefore not be considered as a contradiction to the water depth given by Heilmann-Clausen & Surlyk (2006).

The habitat of the six fossil genera without close living relatives (*Weltonia*, *Physogaleus*, *Xiphodolamia*, *Cretalamna*, *Carcharocles* and *Otodus*) is difficult to infer with confidence (Fig. 24). It appears likely that the teeth from the surface sample were deposited in a marine

	Anomotodon sheppeyensis	*Striatolamia macrota*	*Woellsteinia kozlovi*	*Isurolamna affinis*	*Macrorhizodus* cf. *nolfi*	*Xiphodolamia ensis*	*Alopias crochardi*	*Usakias* sp.	*Carcharocles auriculatus*	*Otodus* (*Otodus*) cf. *obliquus*	*Palaeohypotodus rutoti*	*Odontaspis* cf. *winkleri*	*Jaekelotodus robustus*	*Carcharias* sp.	*Turania* sp.	*Hypotodus verticalis*	*Cretalamna* aff. *appendiculata*	*Megascyliorhinus cooperi*	*Foumtizia* sp.	*Physogaleus* cf. *secundus*	*Chlamydoselachus* aff. *fiedleri*	*Heptranchias howelli*	*Notorhyncus serratissimus*	*Hexanchus* cf. *agassizi*	*Weltonia burnhamensis*	*Squatina* cf. *prima*	*Centrophorus* aff. *granulosus*	*Isistius trituratus*	*Echinorhinus* cf. *priscus*	*Pristiophorus* cf. *lanceolatus*	*Coupatezia miretrainensis*	
	Lamniformes																	Carchariniformes			Hexanchiformes											
Trelde Næs Ypresian/Lutetian	100	46	22	216	99	1	48	63	34	3	2	9	11	14	5	7	3	2	2	11	1	19	24	6	2	4	22	9	39	1	3	31
(a) London Clay Early-Middle Ypresian	●	●		●	●	●	●			●	●	●	●	●		●	●	●	●	●			●	●	●	●		●				21
(b) SW France Ypresian/Lutetian	●	●	●	●								●				●	●	●	●			●		●		●	●	●			●	15
(c) Belgium Eocene		●		●		●		●	●		●	●	●	●		●				●			●			●		●				14
(d) North Germany Ypresian/Lutetian		●		●		●		●	●	●		●	●	●		●																10
(e) France Paris Basin Early Ypresian										●	●	●		●		●																5
(f) Morocco Ypresian/Lutetian		●								●		●		●		●	●			●		●				●		●	●			11

Fig. 27. List of faunas used for comparison on species level. (a): Rayner *et al.* (2009); Cooper (1977). (b): Adnet (2006a); Adnet *et al.* (2008). (c): Nolf (1988); Eeckhaut & De Schutter (2009). (d) : Diedrich (2012). (e): Dutheil *et al.* (2006). (f): Ward & Wiest (1990); Noubhani & Cappetta (1997). Numbers in row 3 indicate the number of teeth used for description/identification in the Trelde Næs fauna. ● indicates presence of the same species as in the Trelde Næs fauna. Numbers in the right column indicate the sum of the species in common with the Trelde Næs fauna.

	Anomotodon	*Striatolamia*	*Woellsteinia*	*Isurolamna*	*Macrorhizodus*	*Xiphodolamia*	*Alopias*	*Usakias*	*Carcharocles*	*Otodus* (*Otodus*)	*Palaeohypotodus*	*Odontaspis*	*Jaekelotodus*	*Carcharias*	*Turania*	*Hypotodus*	*Cretalamna*	*Megascyliorhinus*	*Foumtizia*	*Physogaleus*	*Chlamydoselachus*	*Heptranchias*	*Notorhyncus*	*Hexanchus*	*Weltonia*	*Squatina*	*Centrophorus*	*Isistius*	*Echinorhinus*	*Pristiophorus*	*Coupatezia*	
	Lamniformes																	Carchariniformes			Hexanchiformes											
Trelde Næs Ypresian/Lutetian	100	46	22	216	99	1	48	63	34	3	2	9	11	14	5	7	3	2	2	11	1	19	24	6	2	4	22	9	39	1	3	31
(a) London Clay Early-Middle Ypresian	●	●		●	●	●	●		●	●	●	●	●	●		●	●	●	●	●			●	●	●	●		●				22
(b) SW France Ypresian/Lutetian	●	●	●	●	●		●		●			●				●	●	●	●	●	●	●		●		●	●	●	●	●	●	22
(c) Belgium Eocene	●	●		●	●	●		●	●		●	●	●	●		●				●			●			●		●			●	17
(d) North Germany Ypresian/Lutetian	●	●		●	●	●		●	●	●		●	●	●		●																12
(e) France Paris Basin Early Ypresian	●	●		●						●	●	●		●		●			●							●						10
(f) Morocco Ypresian/Lutetian		●		●			●			●		●		●		●	●		●	●		●		●	●	●		●	●		●	17

Fig. 28. List of faunas used for comparison on genus level. (a) Rayner *et al.* (2009); Cooper (1977). (b): Adnet (2006a); Adnet *et al.* (2008). (c): Nolf (1988); Eeckhaut & De Schutter (2009). (d): Diedrich (2012). (e): Dutheil *et al.* (2006). (f): Ward & Wiest (1990); Noubhani & Cappetta (1997). Numbers in row 3 indicate the number of teeth used for description/identification in the Trelde Næs fauna. ● indicates presence of the same genus as in the Trelde Næs fauna. Numbers in the right column indicate the sum of the genera in common with the Trelde Næs fauna.

deep-sea environment below 100 m. The precise depth is unknown, but a depth between 100 and 350 m will satisfy almost all the species present in the studied surface sample. Based on the molluscan fauna from Trelde Næs, Schnetler & Heilmann-Clausen (2011) suggested deposition of the Lillebælt Clay in water depth between 100 and 300 m, which agrees with the data based on shark teeth distribution. The discrepancy between the water depth given by Heilmann-Clausen & Surlyk (2006) and the present work and the work of Schnetler & Heilmann-Clausen (2011) might be explained by the localisation of Trelde Næs in the vicinity of the Ringkøbing-Fyn High if this structure was expressed as an elevation of the sea floor.

It is concluded that in the period when the Lillebælt Clay Formation layers L2–L6 and the lower Søvind Marl Formation were deposited, the elasmobranch fauna was dominated by pelagic species and deep-water species living in warm to temperate water on the middle or outer continental shelf and upper slope. The average water depth in the period is estimated to have been between 100 and 350 m. It must be emphasized that the data on the species without close living relatives are uncertain. The fall in the sea level in the Danish area as given by Heilmann-Clausen & Surlyk (2006, fig 10-2) to have been about 100 m, from 500 m to 400 m in the actual period, cannot be confirmed by the present work, probably due to the sparsely known habitat of the fossil species without close living relatives.

Biostratigraphy

During the Late Ypresian and the Lutetian, the North Sea Basin was covered by a large epicontinental sea which covered Denmark, southeast England, northwest Germany, Holland, Belgium and part of France. From the Arctic Sea, a seaway opened into central Asia via the Turgai Strait.

Many of the genera present in the Trelde Næs fauna were already established in the Paleocene, see Fig. 25 (Cappetta 2012), and could have spread via the open seaways. In the Late Ypresian and Early Lutetian, a land bridge between the European continent and Great Britain blocked the direct passage between the North Sea and the Atlantic Ocean (Heilmann-Clausen & Surlyk 2006, fig 10-2), giving possibility for development of allopatric species of the same genera in the Trelde Næs fauna and in the faunas close to the Atlantic Sea.

Woellsteinia, Macrorhizodus, Xiphodolamia, Alopias, Usakias, Carcharocles and *Megascyliorhinus* first appeared at the beginning of the Eocene. *Weltonia* is restricted to the Thanetian and the Ypresian. *Isistius* first appeared in the Late Paleocene. *Turania*, if valid, has only been reported from the Bartonian. *Otodus, Palaeohypotodus* and *Weltonia* became extinct at the end of the Ypresian (Cappetta 2012).

The bulk sample from Trelde Næs has a known provenance from the Late Ypresian layer L2. It is seen from Fig. 26 that 10 of the recorded 13 species from L2 are known from the literature to be present in the Ypresian. Three species: *Chlamydoselachus* cf. *fiedleri*, *Coupatezia miretrainensis* and *Centrophorus* aff. *granulosus* have not earlier been described from the Ypresian.

The genus *Chlamydoselachus* is known from the Late Cretaceous to the present (Cappetta 2012), but, as the identification of the species *Chlamydoselachus* cf. *fiedleri* is tentative, it does not seem justified to extend the stratigraphic distribution of this species to the Ypresian; however if we consider that this species occurred in the Lutetian of Denmark (Pfeil 1983) it will not be unexpected to find this taxon in the Upper Ypresian too.

Coupatezia is also a genus that goes back to the Late Cretaceous. The presence of the species *Coupatezia miretrainensis* was so far restricted to the Lutetian (Adnet 2006a). Its discovery in L2 therefore extends its stratigraphic distribution to the Late Ypresian.

Adnet (2006a) described teeth of *Centrophorus* aff. *granulosus* from the Lutetian of southwestern France and suggested they were at the origin of the *Centrophorus granulosus* group. These teeth are similar to the Trelde Næs teeth and based on this similarity it seems justified to extend the origin of the *Centrophorus granulosus* group back to the Late Ypresian.

From Fig. 26 it can be seen that *Pristiophorus* cf. *lanceolatus* appeared in the Lutetian and therefore probably has come from L3–L6 or the Søvind Marl.

Turania is a doubtful genus which has until now only been known from Bartonian sediments (Kozlov 2001). Its presence in the Trelde Næs surface sample is difficult to explain. One possibility is that the five teeth in reality belongs to *Carcharias*, another possibility is that Trelde Næs contains sediments from the Bartonian. The latter seems less probable because extensive logging at Trelde Næs has never revealed Bartonian sediments (Heilmann-Clausen *et al.* 1985). Schnetler (1985) claimed to have observed small temporary exposures of the Late Oligocene Brejning Formation, but gave no evidence for it. In the present state of our knowledge, an extension of the stratigraphic distribution of *Turania* cannot be demonstrated. All the remaining species are already known from the Ypresian.

Macrorhizodus nolfi, Xiphodolamia ensis, Alopias crochardi, Otodus obliquus, Palaeohypotodus rutoti, Notorynchus serratissimus and *Weltonia burnhamensis* became extinct at the end of the Ypresian and therefore their teeth must have been washed out from the Late Ypresian layer L2 for them to appear in the surface sample.

Anomotodon sheppeyensis, Striatolamia macrota, Woellsteinia kozlovi, Isurolamna affinis, Usakias sp., *Carcharocles auriculatus, Odontaspis* cf. *winkleri, Jaekelotodus robustus, Carcharias* sp. *sensu* Cappetta & Nolf 2005, *Hypotodus verticalis, Cretalamna* aff. *appendiculata, Physogaleus* cf. *secundus* and *Squatina* cf. *prima* are all present in the surface sample. These species are known from the Lutetian as well as from the Ypresian (Fig. 26). These teeth could have been washed out from any of the layers at Trelde Næs, and the idea that some of the sediments are of Lutetian age (Heilmann-Clausen *et al.* 1985) can be supported.

Palaeogeography

The teeth of the Trelde Næs fauna were deposited in a 5.1 My long period from the Late Ypresian to the Middle Lutetian. It is therefore compared with other faunas deposited during approximately the same time span. It does not seem justified to consider the two samples from Trelde Næs separately.

Fossil North European Eocene elasmobranch faunas are reported form the London Clay(Cooper 1977; Rayner *et al.* 2009); France (Adnet 2006a; Dutheil *et al.* 2006; Adnet *et al.* 2008); North Germany (Diedrich 2012) and Belgium (Nolf 1988; Eeckhaut & De Schutter 2009). In the Mediterranean area, the Tethys Sea sediments have yielded elasmobranch faunas from Morocco (Arambourg 1952; Noubhani & Cappetta 1997). Figs. 27–28 give an overview of the species and genera in common with the Trelde Næs fauna.

North European faunas

Of the 31 different species found at Trelde Næs, 21 species (Fig. 27) and 22 genera (Fig. 28) are in common with species and genera in the Early/Middle Ypresian London Clay (Cooper 1977; Rayner *et al.* 2009). Nine of the Trelde Næs genera are not recorded from the London Clay. *Chlamydoselachus, Heptranchias, Centrophorus, Echinorhinus*, *Pristiophorus* and *Coupatezia* are all considered demersal/benthic deep-water genera and their absence in the London Clay may suggest that the London Clay was deposited in shallower (but still deep) waters than the Trelde Næs fauna. This opinion is supported by Schwartzhans (2007) who examined the fossil fish otoliths from Trelde Næs layer L3–L6 and found the deposition depth to have been shallower in the London Clay and even shallower in the Belgian Eocene than at Trelde Næs. *Anomotodon* and *Woellsteinia* have a very similar dental morphology and the absence of *Woellsteinia* in the London Clay does not seem significant. The same can be said about *Usakias* which is close to *Alopias*. Teeth of *Carcharocles auriculatus* are not present in the London Clay where *Carcharocles* is represented by *Carcharocles aksuaticus* under the name *Otodus obliquus* var. *mugodzharicus* (Rayner *et al.* 2009). This is not surprising because the London Clay species is the precursor of *Carcharocles auriculatus* and the London Clay is from the Early/Middle Ypresian when *Carcharocles aksuaticus* was representing the genus (http:/elasmo.com/). *Carcharias* sp. *sensu* Cappetta & Nolf 2005 and *Turania* sp. have a very similar dental morphology and appeared respectively in the Paleocene and the Bartonian. *Carcharias* sp. *sensu* Cappetta & Nolf 2005 is present in the London Clay (Cooper 1977), where it was described under the name *Synodontaspis hopei*. It is not surprising that *Turania* is absent from the older London Clay. *Turania* is a little known genus, and it has so far only been described from the Bartonian of Kazakhstan (Kozlov 2001). It was probably a migrating shark and could have spread from the North Sea to Asia via the Turgai Strait, but the presence of *Turania* at Trelde Næs requires further proof to be reliable.

The Ypresian/Lutetian deep-water fauna from southwestern France (Adnet 2006a; Adnet *et al.* 2008) has 15 species (Fig. 27) and 22 genera (Fig. 28) in common with the Trelde Næs fauna. The deep-water genera *Chlamydoselachus, Heptranchias, Hexanchus, Centrophorus, Echinorhinus, Coupatezia and Pristiophorus* are present; this suggests deposition in deep water with a depth similar to that of Trelde Næs.

The Eocene fauna from Belgium (Nolf 1988; Eeckhaut & De Schutter 2009) has 14 species (Fig. 27) and 17 genera (Fig. 28) in common with the Trelde Næs fauna. Most of the pelagic Lamniformes are present, but most of the deep-sea species are missing from the Belgian fauna; this could suggest deposition in shallower marine waters than at Trelde Næs, as Schwartzhans (2007) also inferred based on the fish otoliths from Trelde Næs.

The Ypresian/Lutetian North German fauna (Diedrich 2012) is characterised by Lamniformes of which 12 are in common with the 17 lamniform genera of the Trelde Næs fauna (Fig. 28). There are no small teeth in the German fauna which is probably due to the sampling method (sieving with a mesh size of 4 mm).

The Ypresian fauna from the Paris Basin (Dutheil *et al.* 2006) is dominated by Lamniformes, *Foumtizia* and *Squatina* (Fig. 28). Most of the deep-sea genera are missing. This may again suggest deposition in shallower waters than at Trelde Næs.

It is remarkable that the Trelde Næs fauna contains 39 teeth of *Echinorhinus* which is otherwise only found in the Ypresian/Lutetian of southwestern France (Adnet 2006a) and in Austria (Pfeil 1983) and Morocco in the Tethys Sea (Arambourg 1952; Noubhani & Cappetta 1997).

Tethyan fauna

In the Moroccan fauna from the southern Tethys Sea (Ward & Wiest 1990; Noubhani & Cappetta 1997), 11 species (Fig. 27) and 17 genera (Fig. 28) are in common with the Trelde Næs fauna. Most of the lamniform genera and deep-sea genera are represented, some of them as different species. This could be caused by the considerable distance between the locations.

Summary

In summary, the Trelde Næs fauna seems most similar to the fauna from the Early/Middle Ypresian London Clay and the fauna from the Ypresian/Lutetian deposits in southwestern France. The deep-water sharks are less common in the London Clay sediments than in the Trelde Næs and the southwestern France sediments. This could support the idea that the water depth was lower, at about 200 m, during deposition of the London Clay as suggested by Casier (1966). Trelde Næs is considered to have been far from the coast (Heilmann-Clausen & Surlyk 2006) and probably the London Clay was deposited closer to the coast line. This view is supported by the higher content of sand in the London Clay deposits (Casier 1966). The Trelde Næs fauna also has a strong affinity to the southwestern France fauna where the deposition depth seems to have been similar. At genus level there is also a relative strong affinity to the other North European faunas and to the fauna from Morocco. Differences in faunal associations are not only governed by phylogenetic evolution but also by sea level differences, salinity and availability of suitable prey to sustain the predatory sharks and rays.

Conclusions

Bulk samples and surface samples from Trelde Næs sediments have yielded 30 different genera/species of sharks and one species of ray (*Coupatezia miretrainensis*).

The vast majority of the teeth come from lamniform sharks, but this is probably due to sampling bias.

Teeth of 18 demersal/benthic deep-water genera are present.

Based on the elasmobranch fauna, the deposition depth was probably between 100 and 350 m.

The Trelde Næs fauna is most similar to the fauna from the Early/Middle Ypresian London Clay. The two faunas have 22 genera and 21 species in common. Six of the deep-water genera at Trelde Næs are missing in the London Clay. This suggests a shallower depositional environment of the London Clay compared to Trelde Næs.

The Trelde Næs fauna is also close to the Ypresian/Lutetian fauna from southwestern France. The two faunas have 22 genera and 15 species in common. Fourteen deep-water genera are present in southwestern France. This suggests a depositional environment similar to that of Trelde Næs.

A tooth of *Chlamydoselachus* cf. *fiedleri* is reported for the first time in the Late Ypresian of Denmark. The identification of the species is still to be considered with caution and it is not justified to extend the stratigraphic distribution of this species to the Late Ypresian.

Coupatezia miretrainensis is reported for the first time in the Late Ypresian of Denmark, extending its stratigraphic distribution from the Lutetian to the Late Ypresian.

Centrophorus aff. *granulosus* is reported for the first time in the Late Ypresian of Denmark. On the basis of similar teeth described by Adnet (2006) it seems justified to extend the origin of the *Centrophorus granulosus* group back to the Late Ypresian from its hitherto known origin in the Lutetian.

The presence of teeth of *Turania* in the Ypresian/Lutetian of Denmark, hitherto only known from the Bartonian, is puzzling. Further sampling from the Trelde Næs sediments might allow confirmation or disprovement of its presence.

The faunal assemblage from Trelde Næs confirms an Ypresian age of layer L2 in the Lillebælt Clay Formation.

The faunal assemblage from Trelde Næs confirms that the Lillebælt Clay Formation probably also contains sediments of Lutetian age.

Acknowledgements

This work has only been possible by the kindness of Mogens Madsen (Fredericia) and Ole Barsøe Hansen (Kolding) who generously made their private collections available to the authors. David Ward (Orpington, England) has helped with the identification of some of the teeth. Sten Lennart Jakobsen (Copenhagen) provided help with the photographic work and processing of the sediment.

References

Adnet, S. 2006a: Nouvelles faune de sélaciens (Elasmobranchii, Neoselachii) de l'Eocéne Moyen des Landes (Sud-Ouest, France). Implication de la connaissance des communautés d'eaux profondes. Paleo Ichthyologica 10, 1–128.

Adnet, S. 2006b: Biometric analysis of the teeth of fossil and recent hexanchid sharks and its taxonomic implications. Acta Palaeontologica Polonica 51(3), 477–488.

Adnet, S. & Cappetta, H. 2001: A paleontological and phylogenetic analysis of squaliform sharks (Chondrichthyes: Squaliformes) based on dental characters. Lethaia 34, 234–248.

Adnet, S. & Cappetta, H. 2008: New fossil triakid sharks from the early Eocene of Prémontré, France, and comments on fossil record of the family. Acta Paleontologica Polonica 53(3), 433–448.

Adnet, S., Cappetta, H. & Reynders, J. 2008: Contribution of Eocene sharks and rays from Southern France to the history of deep-sea selachians. Acta Geologica Polonica 58(2), 257–260.

Adnet, S., Guinot, G., Cappetta, H. & Welcomme, J.-L. 2012: Oldest evidence of bramble sharks (Elasmobranchii, Echinorhinidae) in the Lower Cretaceous of southeast France and the evolutionary history of orbitostylic sharks. Cretaceous Research 35, 81–87.

Adnet, S., Hosseinzadeh, R., Antunes, M.T., Balbino, A. C., Kozlov, V.A. & Cappetta, H. 2009: Review of the enigmatic Eocene shark genus *Xiphodolamia* (Chondrichthyes, Lamniformes) and description of a new species recovered from Angola, Iran and Jordan. Journal of African Earth sciences 55, 197–204.

Agassiz, L. 1833–1844: Recherches sur les poissons fossiles. Tome 3 contenant l'histoire des placoïdes, 422 pp. Petitpierre, Neuchâtel et Soleure.

Antunes, M.T. & Cappetta, H. 2002: Sélaciens du Crétacé (Albien–Maastrichtien) d'Angola. Palaeontographica Abteilung A 264(5–6), 85–146.

Antunes, M.T. & Jonet, S. 1970: Requins de l`Helvétien supérieur et du Tortonien de Lisbonne. Revista Faculdades Ciências naturais. Universidade Lisboa 16(1), 119–280.

Applegate, S.P. & Uyeno, T. 1968: The first discovery of a fossil tooth belonging to the shark genus Heptranchias, with a new Pristiophorus spine, both from the Oligocene of Japan. Bulletin of the National Science Museum, Ser. C (Geol. & Paleont.) 11(1), 195–200.

Arambourg, C. 1935: Note préliminaire sur les vertébrés fossiles des phosphates du Maroc. Bulletin de la Société géologique de France 5(5), 413–439.

Arambourg, C. 1952: Les vértebrés fossiles des gisements de phosphates (Maroc-Algérie-Tunisie). Notes et Mémoire. Service géologique de Maroc 92, 1–372.

Ayres, W.O. 1855: Description of new species of California fishes. Proceedings of the California Academy of Natural Science 1(1), 23–77.

Barnard, K.H. 1925: Monograph of the fishes of South Africa Part 1. Annals of South African Museum 21(1), 1–418.

Bendix-Almgreen, S.E. 1969: Notes on the upper Cretaceous and lower Tertiary fish faunas of Northern West Greenland. Bulletin of the Geological Society of Denmark 19, 204–217.

Berg, L.S. 1940: Classification of fishes, both recent and fossil. Travaux de L'Institut Zoologique de l'Academie des Sciences de l'URSS Tome V, 2, 87–345.

Berg, L.S. 1958: System der Rezenten und Fossilen Fischartigen und Fische. Hochschulbücher für Biologie XI+ 310 pp. Berlin.

Blainville, H.M.D. de 1816: Prodromes d'une nouvelle distribution systématique du règne animal. Bulletin de la Société Pholomathique de Paris 8, 105–112 + 121–124.

Blainville, H.M.D. de 1818: Sur les ichthyolites ou les poissons fossiles. Nouveau Dictionnaire d'Histoire Naturelle 27, 310–395. Deterville, Paris.

Bleeker, P. 1859: Enumeratio specierum piscium hucusque in Archipeloga indico observatum, adjectis habitionibus citationibusque, ubi descriptiones earum recentiores reperiuntur, nec non speciebus Musei Bleekeriani Bengalensibus, Japonicis, Capensibus Tasmanicisque. Acta Societas Scientiarum Indo-Neerlandicae 6, p. I–XXXVI + 1–176.

Bloch, H.M. & Schneider, J.G. 1801: M. E. Blochii Systema Ichthyologiae iconibus ex illustratum. Post obitum auctoris opus inchoatum absolvit, correxit, interpolavit Jo. Gottlob Schneider, Saxo. 584 pp.; Berolini (Sumtibus Austoris Impressum et Bibliopolio Sanderiano Commissum).

Bonaparte, C.L. 1834: Iconografia della fauna italica per le quattro classi degli animali vertebrati. Tomo III. Pesci. Roma: Fasc. 12–14, puntata 59–79.

Bonaparte, C.L. 1838: Selachorum tabula analytica. Nuovi annali delle scienze naturali, Bologna 2, 195–214.

Bonde, N. 1966: The fishes of the Mo-Clay Formation. Meddelelser fra Dansk Geologisk Forening 16, 198–202.

Bonde, N. 1968: Nyligt fundne fossiler fra det 'plastiske ler'. Meddelelser fra Dansk Geologisk Forening 18, 148–151.

Bonnaterre, J.P. 1788: Ichthyologie. Tableau encyclopédique et méthodique des trois règnes de la nature. Paris, 215 pp., pl. A–B + 1–100.

Buen, F. de 1926. Catálogo ictiológico del Mediterráneo Español y de Marruecos, recopilando lo publicado sobre peces de las costas mediterráneas y próximas del Atlántico (Mar de España). Resultados de las Campañas Realizadas por Acuerdos Internacionales, Instituto Español de Oceanografía 2, 1–221.

Cappetta, H. 1976: Sélaciens nouveaux du London Clay de L'Essex (Yprésien du Basin du Londre). Geobios 9(5), 551–575.

Cappetta, H. 1980a: Modification du statut générique de quelques espèces de sélaciens crétacés et tertiaires. Palaeovertebrata 10(1), 29–42.

Cappetta, H. 1980b: Les Sélaciens supérieur du Liban. I. Requins. Palaeontographica Abt. A 168(1–4), 69–148.

Cappetta, H. 1981: Addition a la faune de sélachiens fossiles du Maroc.1: Sur la présence des genres *Heptranchias*, *Alopias* et *Odontorhytis* dans L`Ypresien des Ouled Abdoun. Géobios 14(5), 563–575.

Capetta, H. 1982: Révision de *Cestracion duponti* Winkler 1874 (Selachii, Batomorphii) du Bruxellien de Woluwe-Saint-Lambert

(Eocène moyen de Belgique). Meddelingen Van De Werkgroep Voor Tertiaire En Kwartaire Geologie 19(4), 113–125.

Cappetta, H. 1987: Chondrichthyes II: Mesozoic and Cenozoic elasmobranchii. In: Schulze, H-P (ed.): Handbook of paleoichthyology 3B. 193 pp. Gustav Fischer Verlag, Stuttgart and New York.

Cappetta, H. 1990a: Hexanchiforme nouveau (Neoselachii) du Crétacé inférieur du Sud de la France. Palaeovertebrata 20(1), 33–54.

Cappetta, H. 1990b: Echinorhinidae nouveau (Neoselachii, Squaliformes) du Crétacé supérieur du Negev (Israël). Neues Jahrbuch für Geologie und Palaontologie, Monatshefte 1990(12), 741–749.

Cappetta, H. 1992: Carcharhiniformes nouveaux (Chondrichthyes, Neoselachii) de l'Yprésien du Bassin de Paris. Géobios 25(5), 639–646.

Cappetta, H. 2012: Chondrichthyes – Mesozoic and Cenozoic Elasmobranchii: Teeth. In: Schultze, H-P (ed.): Handbook of Paleoichthyology 3E, 512 pp. Verlag Dr. Friedrich Pfeil, München.

Cappetta, H. & Case, G.R. 1999: Additions aux faunes de sélaciens du Crétacé du Texas (Albien supérieur–Campanien). Palaeo Ichthyologica 9, 5–111.

Cappetta, H. & Nolf. D. 2005: Révision de quelque Odontaspididae (Neoselachi: Lamniformes) du Paléocène et de l'Eocène du Bassin de la mer du Nord. Bulletin de l'Institut Royal des Sciences Naturelles de Belgique, Sciences de la Terre 75, 237–266.

Cappetta, H. & Ward, D. 1977: *Megascyliorhinus cooperi* gen. nov. sp. nov., a new shark from the London Clay (Eocene) of Essex, England. Palaeontology 20(1), 195–202.

Casier, E. 1946: La faune ichthyologique de l'Ypresien de la Belgique. Mémoires du Musée Royal d'Histoire Naturelle de Belgique 104, 1–267.

Casier, E. 1966: Faune ichthyolgique du London Clay. 496 pp. London : British Museum of Natural History.

Christensen, E.J. & Hald, N. 1991: Danekræ, et nyt begreb i dansk museumslovgivning. Arkæologiske Udgravninger i Danmark 1990, 7–16.

Cigala-Fulgosi, F. 1986: A deep water elasmobranch fauna from a lower Pliocene outcropping (Northern Italy). In: Uyeno, T., Arai, R., Taniuchi, T. & Matsura, K. (eds): Proceedings of the second international conference on Indo-Pacific fishes. Ichthyological Society of Japan, Tokyo: 133–139.

Cione, A.L. 1986: A new *Megascyliorhinus* (Chondrichthyes, Galeomorphii) from the Middle Tertiary of Patagonia. Journal of Vertebrate Paleontology 6(2), 105-112.

Compagno, L.J.V. 1973: Interrelationships of living elasmobranchs. In: Greenwood, P.H., Miles, R.S. & Patterson, C. (eds.): Interrelationships of fishes. Zoological Journal of the Linnean Society 53 Suppl. 1, 15–61.

Compagno, L.J.V. 1977: Phyletic relationships of living sharks and rays. American Zoologist 17, 303–322.

Compagno, L.J.V. 2003: Sharks of the order Carcharhiniformes, 486 pp. The Blackburn Press.

Compagno, L.J.V., Dando, M. & Fowler, S. 2005: Sharks of the world. 368 pp. Princeton University Press, Princeton and Oxford.

Consoli, C.P. 2008: A rare Danian (Early Paleocene) *Chlamydoselachus* (Chondrichthyes: Elasmobranchii) from the Takatika Grit, Chatham Islands, New Zealand. Journal of Vertebrate Paleontology 28(2), 285–290.

Cooper, J. 1977: The palaeontology of the London Clay (Lower Eocene) of the Herne Bay coastal section, Kent, England. Proceedings of the Geological Association 88(3), 163–178.

Cunningham, S.B. 2000: A comparison of isolated teeth of early Eocene *Striatolamia macrota* (Chondrichthyes, Lamniformes), with those of a Recent sand shark, *Carcharias taurus*. Tertiary Research 20(1–4), 17–34.

Cvancara, A.M. & Hoganson, J.W. 1993: Vertebrates of the Cannonball Formation (Paleocene) in North and South Dakota. Journal of Vertebrate Paleontology 13(1), 1–23.

Dartevelle, E. & Casier, E. 1943: Les poissons fossiles du Bas-Congo et des régions voisines. Annales du Musée du Congo Belge, Sér. A (Minéralogie Géologie, Paléontologie) 3, 2(1), 1–200.

Davis, J.W. 1887: Note on a fossil species of Chlamydoselachus. Proceedings of the Zoological Society of London 1887, 542–544.

Davis, J.W. 1888: On fossil fish-remains from the Tertiary and Cretaceo-Tertiary formations of New-Zealand. Scientific transactions of the Royal Dublin Society 4(2), 1–48.

De Schutter, P.J. & Wijnker, E. 2002: Large *Centrophorus* (Chondrichthyes, Squaliformes) of the Belgian Neogene continental shelf. Geologica Belgica 15(1–2), 26–36.

Diedrich, C.G. 2012: Eocene (Lutetian) Shark-rich coastal paleoenvironments of the Southern North Sea Basin in Europe: Biodiversity of the Marine Fürstenau Formation including early white and megatooth Sharks. International Journal of Oceanography 2012, 1–22.

Dinesen, A., Michelsen, O. & Lieberkind, K. 1977: A survey of the Paleocene and Eocene deposits in Jylland and Fyn. Geological Survey of Denmark, series B (1), 1–14.

Dumeril, A.H.A. 1806: Zoologie analytique, ou méthode naturelle de classification des animaux. Paris, 1–344.

Dutheil, D.B., Moreau, F. & Delhaye-Prat, V. 2002: Cycle sédimentaire et vertébrés d'une formation peu connue du Bassin de Paris, l'unité des Sables de Bourguillemont (Oise, France) (Paléocène supérieur). Geodiversitas 24(4), 753–764.

Dutheil, D.B., Moreau, F. & De Plöeg, G. 2006: Les ichthyofaunes du gisement à ambre de Le Quesnoy (Paléocène et Éocène du bassin de Paris, France). Cossmanniana 11(1–4), 1–13.

Eeckhaut, G. & De Schutter, P. 2009: The elasmobranch fauna of the Lede Sand Formation at Oosterzele (Lutetian, Middle Eocene of Belgium). Palaeofocus 1, 1–57.

Ferrusquia-Villafranca, I., Applegate, P.S. & Espinosa-Arrubarrena, L. 1999: First Paleogene selachifauna of the Middle American–Caribbean–Antillean Region, La Mesa de Copoya, West-Central Chiapas – Mexico. Systematics and paleontogical significance. Revista Mexicans de Ciencias Geológicas 16(1), 155–174.

Forskål, P. 1775: Descriptiones animalium, avium, amphibiorum, piscium, insectorum, vermium / quae in itinere orientali observavit Petrus Forskål. 1–20 + i–xxxiv + 1–164. Hauniae (ex officina Mölleri).

Garman, S. 1884: An extraordinary shark. Bulletin of the Essex Institute 16, 47–55.

Garman, S. 1913: The Plagiostomia (sharks, skates and rays). Memories of the Museum of Comparative Zoology at Harvard College 36, XIII + 528 pp.

Gill, T.N. 1862: Analytical synopsis of the order of Squali; a revision of the nomenclature of the genera. Annals of the Lyceum of the Natural History of New York 7, 371–408.

Gill, T.N. 1865: Synopsis of the eastern American sharks. Proceedings of Academy of Natural Sciences of Philadelphia 16(5), 258–265.

Glikman, L.S. 1958: [Rates of evolution in Lamnoid sharks]. Doklady Akademii Nauk SSSR 123(3), 568–571 (in Russian).

Glikman, L.S. 1964a: [Subclass Elasmobranchii]. In: Obruchev. D.V. (ed.): Osnovi Paleontologii (Agnatha, Pisces), 195–237 , Moscow (Nauka) (in Russian).

Glikman, L.S. 1964b: [Sharks of the Palaeogene and their stratigraphic significance]. Doklady Akademii Nauk SSSR, Moscow, 228 pp. (in Russian).

Glikman, L.S. & Zhelezko, V.I. 1985: [Paleogene sharks of the Mangyschlak Plateau and the Eocene/Oligocene boundary]. Bulletin MOIP. Otdelenie geologicheskoe 60(5), 86–99. (in Russian).

Goodrich, E.S. 1909: Vertebrata Craniata. 1. Cyclostomes and fishes. In: Lankester E.R. (ed.), A Treatise on Zoology, part 9, XVI + 518 pp.. London: Adam a. Charles Black.

Gottfried, M.D. & Rabarison, J.A. 1997: First Mesozoic Gondwanan record of a sawshark (Chondrichthyes, Pristiophoriformes), from the Late Cretaceous of Madagascar. Journal of Vertebrate Paleontology 17(4), 750–751.

Gray, J.E. 1851: List of the specimens of fish in the collection of the British Museum. Part I. Chondropterygii. X + 160 pp. British Museum (Natural History), London.

Hansen, B.B., Cuny, G., Rasmussen, B.W., Shimada, K., Jacobs, P. & Heilmann-Clausen, C. 2013: Associated skeletal and dental remains of a fossil odontaspidid shark (Elasmobranchii: Lamniformes) from the Middle Eocene Lillebælt Clay Formation in Denmark. Bulletin of the Geological Society of Denmark 61, 37–46.

Heilmann-Clausen, C. & Surlyk, F. 2006: Koralrev og lerhav. In: Larsen, G. (ed.) Naturen i Danmark, Geologien, 549 pp. Copenhagen: Gyldendal.

Heilmann-Clausen, C., Nielsen, O.B. & Gersner, F. 1985: Lithostratigraphy and depositional environments in the Upper Paleocene and Eocene of Denmark. Bulletin of the Geological Society of Denmark 33, 287–323.

Henle, F.G.J. 1834: Ueber *Narcine*, eine neue Gattung electrischer Rochen nebst einer Synopsis der electrischen Rochen, 44 pp. Berlin: G. Eichler.

Huxley, T.H. 1880: On the application of the laws of evolution to the arrangement of the Vertebrata, and more particularly of the Mammalia. Proceedings of the Zoological Society of London 1880, 649–662.

Iserbyt, A. & De Schutter, P.J. 2012: Quantitative analysis of Elasmobranch assemblages from two successive Ypresian (early Eocene) facies at Marke, Western Belgium. Geologica Belgica 15(3), 146–153.

Jaekel, O. 1890: Über die systematische Stellung und über fossile Reste der Gattung Pristiophorus. Zeitschrift der Deutschen Geologischen Gesellschaft 42, 86–120.

Jaekel, O. 1895: Unter-tertäre Salachier aus Südrussland. Mémoirs du Comité geologique de St. Petersburg 9(4), 19–35.

Jaekel, O. 1898: Ueber die verschiedenen Rochentypen. Sitzungsberichte der Gesellschaft naturforschender Freunde zu Berlin 1898, 44–53.

Jordan, D.S. 1888: Description of two new species of fishes from South America. Proceedings of the Academy of Natural Sciences of Philadelphia 39, 387–388.

Jordan, D.S. 1898: Description of a species of fish (*Mitsukurina owstoni*) from Japan, the type of a distinct family of lamnoid sharks. Proceedings of the California Academy of Science (3) 1 (6), 199–202.

Jordan, D.S. & Evermann, B.W. 1896: The fishes of North and Middle America, a descriptive catalogue of the species of fish-like vertebrates found in the waters of North America, north of the isthmus of Panama. Part I. Bulletin of the United States National Museum 47, I–LX + 1–1240.

Jordan, D.S. & Hannibal, H. 1923: Fossil sharks and rays of the Pacific slope of North America. Bulletin of the Southern California Academy of Science 22, 27–63.

Jordan, D.S. & Snyder, J.O. 1902: Descriptions of two new species of squaloid sharks from Japan. Proceedings of the United States National Museum 25, 79–81.

Keyes, I.W. 1979: *Ikamauius*, a new genus of fossil sawshark (Order Selachii: Family Pristiophoridae) from the Cenozoic of New Zealand. New Zealand Journal of Geology and Geophysics 22(1), 125–129.

Keyes, I.W. 1982: The Cenozoic sawshark *Pristiophorus lanceolatus* (Davis) (Order Selachii) of New Zealand and Australia, with a review of the phylogeny and distribution of world fossil and extant Pristiophoridae. New Zealand Journal of Geology and Geophysics 25(4), 459–474.

Keyes, I.W. 1984: New records of fossil elasmobranch genera *Megascyliorhinus, Centrophorus*, and *Dalatias* (Order Selachii) in New Zealand. New Zealand Journal of Geology and Geophysics 27(2), 203–216.

Klug, S. & Kriwet, J. 2010: Timing of deep-sea adaptation in dogfish sharks: insights from a supertree of extinct and extant taxa. Zoologica Scripta 39(4), 331–342.

Kordikova, E.G., Polly, P.D., Alifanov, V.A., Rocek, Z., Gunnell, G.F. & Averianof, A.O. 2001: Small vertebrates from the Late Cretaceous and Early Tertiary of the Northeastern Aral Sea region, Kazakhstan. Journal of Paleontology 75, 390–400.

Kozlov, V.A. 2000: [Systematics and evolution of sharks from the family Alopiidae (based on the materials from Palaeogene deposits of Middle Asia and western Kazakhstan)]. Materialy po stratigrafii i Paleontologii Urals 4, 142–147 (in Russian).

Kozlov, V.A. 2001: Additions to the Paleogene elasmobranch fauna of western Kazakhstan. *Turania*, a new shark genus (Odontaspididae) and a new ray species (genus *Archaeomanta*, Mobulidae). Russian Academy of Science, Urals Branch, 83–86 (in Russian).

Kriwet, J. 2005: Additions to the Eocene selachian fauna of Antarctica with comments on Antarctic selachian diversity. Journal of Vertebrate Paleontology 25(1), 1–7.

Kyne, P.M. & Simpfendorfer, A.C. 2007: A Collation and summarization of available data on deepwater Chondrichthyans: Biodiversity, Life History and Fisheries. IUCN SSC Shark Specialist Group for the Marine Conservation, Biology Institute, 1–137.

Leidy, J. 1877: Description of vertebrate remains, chiefly from the Phosphate Beds of South Carolina. Journal of the Academy of Natural Sciences of Philadelphia 8(2), 209–261.

Leriche, M. 1905: Les poissons Eocène de la Belgique. Mémoires de Musée Royal d´Histoire Naturelle de Belgique 3(3), 59–228.

Leriche, M. 1921: Sur les restes de Poissons remaniés dans le Néogène de la Belgique. Leur signification au point de vue de l'histoire géologique de la Belgique pendant le tertiaire supérieur. Bulletin de la Sociéte Belge de Géologie 30, 115–120.

Leriche, M. 1929: Sur une forme nouvelle du genre *Chlamydoselachus* (*C. tobleri*) rejetée par le volcan de boue de Chagonary (île de la Trinité, Petites-Antilles). Bulletin de la Société Belge de Géologié, de Paléontologie et d'Hydrologie 38(1), 55–58.

Leriche, M. 1938: Contribution à l'étude des poissons fossiles des pays riverains de la Méditerranée américaine (Venezuela, Trinité, Antilles, Mexique). Mémoires de la Société Paléontologique Suisse 61(1), 42 pp.

Long, D.J. 1992: Sharks from the La Meseta Formation (Eocene), Seymour Island, Antarctic Peninsula. Journal of Vertebrate Paleontology 12(1), 11–32.

Longbottom, A.E. 1979: Miocene shark's teeth from Ecuador. Bulletin of the British Museum (Natural History), (Geology) 32(1), 57–70.

Lowe, R.T. 1841: A paper from the Rev. R.T. Lowe, M.A., describing certain new species of Madeiran fishes, and containing additional information relating to those already described. Proceedings of the Zoological Society of London 8, 36–39.

Malyshkina, T. 2006: Late Eocene scyliorhinid sharks from the Trans-Urals, Russia. Acta Palaeontologica Polonia 51(3), 465–475.

Mannering, A.A. & Hiller, N. 2008: An early Cenozoic neoselachian shark fauna from the Southwest Pacific. Palaeontology 51(6), 1341–1365.

Marsili, S. & Tabanelli, C. 2007: Bathyal sharks from the middle Pliocene of the Romagna Apennines (Italy). Neues Jahrbuch für Geologie und Paläontologie, Abhandlungen 244(2), 247–255.

Menner, V.V. 1928: [Les sélaciens du Paléogène de Manghyschlack d'Emba et du versant oriental d'Oural]. Bulletin de la Société imperiale des Naturalistes de Moscou. Section géologique 6(3-4), 292–338. (in Russian with French summary).

Michelsen, O. 1994: Stratigraphic correlation of the Danish onshore and offshore Tertiary successions based on sequence stratigraphy. Bulletin of the Geological Society of Denmark 41, 145–161.

Müller, J. & Henle, F.G.J. 1837: Gattungen der Haifische und Rochen, nach einer von ihm mit Herrn Henle unternommenen gemeinschaftlichen Arbeit über die Naturgeschichte der Knorpelfische. Berichte Akademie der Wissenschaften 1837(2), 111–118.

Müller, J. & Henle, F.G.J. 1838–41: Systematische Beschreibung der Plagiostomen, 200 pp. Veit & Co., Berlin.

Münster G. Von. 1846: Ueber die in der Tertiär-Formation des Wiener Beckens vorkommenden Fisch-Ueberreste, mit Beschreibung einiger neuen merkwürdigen Arten. Beiträge zur Petrefaktenkunde 7, 1–31.

Nakamura, H. 1935: On the two species of the thresher shark from Formosan waters. Memoirs Faculty Science Taihoku Imperial University Formosa 14(1), 1–6.

Nolf, D. 1988: Fossiles de Belgique. Dent de requins et de raies du Tertiaire de la Belgique. 188 pp. Brussels: Institut royal des sciences naturelles de Belgique.

Noubhani, A. & Cappetta, H. 1997: Les Orectolobiformes, Carcharhiniformes et Myliobatiformes (Elasmobranchii, Neoselachii) des bassins à phosphate du Maroc. (Maastrichtien–Lutétien basal). Systématique, biostratigraphie, évolution et dynamique des faunes. Palaeo Ichthyologica 8, 1–327.

Otero, R.A., Torres, T., Le Roux, J.P., Hervé, F., Fanning, C.M., Yury-Yáñez, R.E. & Rubilar-Rogers D. 2012: A Late Eocene age proposal for the Loreto Formation (Brunswick Peninsula, southernmost Chile), based on fossil cartilaginous fishes, paleobotany and radiometric evidence. Andean Geology 39(1), 180–200.

Pfeil, F.H. 1981: Eine nektonische Fischfauna aus dem unterooligozänen Schönecker Fischschiefer des Galon-Grabens in Oberbayern. Geologica Bavarica 82, 357–388.

Pfeil, F.H. 1983: Zahnmorphologische Untersuchungen an rezenten und fossilen Haien der Ordnungen Chlamydoselachiformes und Echinorhiniformes. Palaeo Ichthyologica 1, 1–315.

Pfeil, F.H. 1984: Neoselachian teeth collected from phosphorite-bearing greensand on Chatham Rise east of New Zealand. Geologisches Jahrbuch 65, 107–115.

Pietschmann, V. 1928: Neue Fischarten aus dem Pazifischen Ozean. Anzeiger der Akademie der Wissenschaften in Wien, 65(27), 297–298.

Probst, J. 1879: Beiträge zur Kenntniss der fossilen Fische aus der Molasse von Baltringen. Hayfische. Jahreshefte des Vereins für vaterländische Naturkunde in Württemberg 35, 127–191.

Purdy, R.W. 1998: Chondrichthyan fishes from the Paleocene of South Carolina. Transactions of the American Philosophical Society 88, 122–146.

Purdy, R.W., Schneider, V.P., Applegate, S.P., McLellan, J.H., Meyer, R.L., & Slaughter, B.H. 2001: The neogene sharks, rays and bony fishes from Lee Creek Mine, Aurora, North Carolina. Smithsonian contributions to paleobiology 90, 71–202.

Quoy, J.R.C. & Gaimard, J.P. 1824: Description des Poissons. Chapître IX. In: Freycinet, L. de, Voyage autour du Monde entrepris par ordre du roi, exécuté sur les corvettes de L. M. "L'Uranie" et "La Physicienne," pendant les années 1817, 1818, 1819 et 1820. Paris. Description des Poissons. Chapter IX.: 192–401 [1–328 in 1824; 329–616 in 1825].

Rafinesque, C.S. 1810: Caratteri di alcuni nuovi generi e nuovi spedie di animali e piante della Sicilia, con varie osservazione sopra i medesimi. Part 1. I–IV + 3–69 p. Palermo (Sanfilippo).

Rayner, R., Mitchell, T., Rayner, M. & Clouter, F. 2009: London Clay fossils of Kent and Essex, 228 pp. Medway Fossil and Mineral Society.

Reed, M.D. 1946: A new species of fossil shark from New Jersey. Notula Naturae of the Academy of Natural Sciences of Philadelphia 172, 1–3.

Regan, C.T. 1906: Descriptions of new or little known fishes from the coast of Natal. Annals of the Natal Government Museum 1(1), 1–6.

Reinecke, T. & Engelhard, P. 1997: The selachian fauna from Geschiebe of the Lower Selandian basal conglomerate (Thanetian, Late Paleocene) in the Danish subbasin (Sealand, Scania, western Baltic Sea). Erratica 2, 3–45.

Reinecke, T., Stapf, H. & Raisch, M. 2001: Die Selachier und Chimären des Unteren Meeressandes und Schleisandes im Mainzer Becken (Rupelium, Unteres Oligozän). Paleontos 1, 1–73.

Richter, M. & Ward, D.J. 1990: Fish remains from the Santa Marta Formation (Late Cretaceous) of James Ross Island, Antarctica. Antarctic Science 2(1), 67–76.

Schmitz, B., Heilmann-Clausen, C., King, C., Steurbaut, E., Andreasson, F.P., Corfield, R.M. & Cartlidge, J.E. 1996: Stable isotope and biotic evolution in the North Sea during the early Eocene: the Albæk Hoved section Denmark. Special Publication, Geological Society (London) 101, 275–306.

Schnetler, K.I. 1985: Two new Upper Oligocene gastropods from the North Sea Basin. Bulletin of the Geological Society of Denmark 34, 199–204.

Schnetler, K.I. & Heilmann-Clausen, C. 2011: The molluscan fauna of the Eocene Lillebælt Clay, Denmark. Cainozoic Research 8(1–2), 41–99.

Schwartzhans, W. 2007: Otoliths from casts from the Eocene Lillebælt Clay Formation of Trelde Næs near Fredericia (Denmark), with remarks on the diet of stomatopods. Neues Jahrbuch für Geologie und Paläontologie 246(1), 69–81.

Shimada, K. 2005: Phylogeny of lamniform sharks (Chondrichthyes: Elasmobranchii) and the contribution of dental characters to lamniform systematics. Paleontological Research 9(1), 55–72.

Shimada, K. 2007: Skeletal and Dental Anatomy of Lamniform Shark, *Cretalamna appendiculata*, from Upper Cretaceous Niobrara Chalk of Kansas. Journal of Vertebrate Paleontology 27(3), 584–602.

Siverson, M. 1992: Biology, dental morphology and taxonomy of lamniform sharks from the Campanian of the Kristianstad Basin, Sweden. Palaeontology 35(3), 519–554.

Siverson, M. 1995: Revision of the Danian Cow Sharks, Sand Tiger Sharks, and Goblin Sharks (Hexanchidae, Odontaspididae and Mitsukurinidae) from Southern Sweden. Journal of Vertebrate Paleontology 15(1), 1–12.

Siverson, M. 1996: Lamniform sharks of the mid Cretaceous Alinga Formation and Beedagong Claystone, Western Australia. Palaeontology 39(4), 813–849.

Siverson, M. 1999: A new large lamniform shark from the uppermost Gearle Siltstone (Cenomanian, Late Cretaceous) of Western Australia. Transactions of the Royal Society of Edinburgh: Earth Sciences 90, 49–65.

Siverson, M., Lindgren, J., Newbrey, M.G., Cederström, P. & Cook T.D. 2014: Late Cretaceous (Cenomanian–Campanian) mid-palaeolatitude sharks of *Cretalamna appendiculata* type. Acta Palaeontologica Polonica, in press, 1–49.

Slaughter, B.H. & Springer, S. 1968: Replacement of Rostral Teeth in Sawfishes and Sawsharks. Copeia 1968(3), 499–506.

Sokolov, M.1978: Sharks as guide-fossils for the zonation and subdivision of the Cretaceous beds of Tourousk. Nedra, Moskva 61, 1–60.

Storms, R. 1894: Troisième note sur les poissons du terrain rupélien. Bulletin de la Société Belge de Géologié, de Paléontologie et d'Hydrologie 8, 67–82.

Thomsen, E., Abrahamsen, N., Heilmann-Clausen, C., King, C. & Nielsen, O.B. 2012: Middle Eocene to earliest Oligocene development in the eastern North Sea Basin: Biostratigraphy, magnetostratigraphy and palaeoenvironment of the Kysing-4 borehole, Denmark. Palaeogeography, Palaeoclimatology, Palaeoecology 350–352, 212–235.

Underwood C.J. & Cumbaa S.L. 2010: Chondrichthyans from a Cenomanian (Late Cretaceous) bonebed, Saskatchewan, Canada. Palaeontology 53(4), 903–944.

Underwood, C.J., Goswami, A., Prasad, G.V.R., Omkar, V. & Flynn, J.J. 2011a: Marine vertebrates from the "Middle" Cretaceous (Early Cenomanian) of South India. Journal of Paleontology 31(3), 539–552.

Underwood, C.J., Ward, D.J., King, C., Antar, S.M., Zalmout, I.S. & Gingerich, P.D. 2011b: Shark and ray faunas in the Middle and Late Eocene of the Fayum Area, Egypt. Proceedings of the Geologists' Association 122, 47–66.

Vélez-Zuazo, X. & Agnarsson, I. 2011: Shark tales: A molecular species-level phylogeny of sharks (Selachimorpha, Chondrichthyes). Molecular Phylogenetics and Evolution 58, 207–217.

Ward, D.J. 1978: Additions to the fish fauna of the English Palaeocene. 1. Two new species of *Alopias* (Tresher Shark) from the English Eocene. Tertiary Research 2(1), 23–28.

Ward, D.J. 1979: Additions to the fish fauna of the English Paleogene. 3. A review of the Hexanchid sharks with a description of four new species. Tertiary Research 2(3), 111–129.

Ward, D.J. 1984: Additions to the fish fauna of the English Palaeogene. 5. A new species of *Raja* from the London Clay. Tertiary Research 6(2), 65–68.

Ward, D.J. & Wiest, R.L. 1990: A Checklist of Paleocene and Eocene sharks and rays (Chondrichthyes) from the Pamunkey Group, Maryland and Virginia, USA. Tertiary Research 12(2), 81–88.

Welton, B.J. 1972: Fossil sharks in Oregon. The Ore Bin 34(10), 161–172.

White, E.I. 1956: The Eocene fishes of Alabama. Bulletins of American Paleontology 36(156), 123–150.

Whitley, G.P. 1929: Additions to the check-list of the fishes of New South Wales. No. 2. Australian Zoologist 5(4), 353–357.

Winkler, T.C. 1874: Mémoire sur des dents de poissons du terrain bruxellien. Archives du Musée Teyler 3(4), 295–304.

Winkler, T.C. 1876a : Mémoire sur quelques restes de poissons du système heersien. Archives du Musée Teyler 4(1), 1–15.

Winkler, T.C. 1876b: Deuxième mémoire sur des dents de poissons fossiles du terrain bruxellien. Archives du Musée Teyler 4(1), 16–48.

Woodward, A.S. 1899: Notes on the teeth of sharks and skates from English Eocene formations. Proceedings of the Geologists' Association 16, 1–14.

Woodward, A.S. 1932: A Cretaceous pristiophorid shark. Annals and Magazine of Natural History, (Series 10) 10, 476–479.

Zalmout, I.S.A., Antar, M.S.M., Shafy, A.E., Metwally, M.H., Hatab, E.E. & Gingerich, P.D. 2012: Priabonian sharks and rays (Late Eocene: Neoselachii) from Minqar Tabaghbagh in the Western Qattara Depression, Egypt. Contributions from the Museum of Paleontology, University of Michigan 32(6), 71–90.

Zhelezko, V.I. 1994: Sharks of family Jaekelotodontidae of European and middle Asian paleobiogeographic provinces. Bulletin Moscow Society of Naturalists 69(6), 47–62 (in Russian).

Zhelezko, V.I. & Kozlov, V.A. 1999: Elasmobranchii and Paleogene biostratigraphy of Transurals and central Asia. Russian Academy of Sciences, Urals Branch 3, 1–323 (in Russian).

Web sites

http://www.elasmo.com/
http://www.fishbase.org/

The lower Maastrichtian Hvidskud succession, Møns Klint, Denmark: calcareous nannofossil biostratigraphy, carbon isotope stratigraphy, and bulk and brachiopod oxygen isotopes

MADS ENGHOLM JELBY, NICOLAS THIBAULT, FINN SURLYK, CLEMENS V. ULLMANN, RIKKE HARLOU & CHRISTOPH KORTE

Jelby, M.E., Thibault, N., Surlyk, F., Ullmann, C.V., Harlou, R. & Korte, C. 2014: The lower Maastrichtian Hvidskud succession, Møns Klint, Denmark: calcareous nannofossil biostratigraphy, carbon isotope stratigraphy, and bulk and brachiopod oxygen isotopes. © 2014 by Bulletin of the Geological Society of Denmark, Vol. 62, pp. 89–104. ISSN 2245-7070. (www.2dgf.dk/publikationer/bulletin).

Received 13 May 2014
Accepted in revised form
31 October 2014
Published online
28 November 2014

A new calcareous nannofossil and $\delta^{13}C$ stratigraphy is established for the chalk exposed in the lower Maastrichtian Hvidskud succession, Møns Klint, Denmark. It is based on 21 nannofossil samples and analysis of 82 stable isotope samples, allowing correlation with a previously established brachiopod zonation. The succession, which belongs to the brachiopod *spinosa-subtilis* to *pulchellus-pulchellus* zones, extends upwards from calcareous nannofossil subzone UC16ii to UC19ii and encompasses $\delta^{13}C$ events M1+ to M2+. A new chronostratigraphic and geochronological age model is proposed based on correlation with the cored boreholes Stevns-1 (Denmark) and ODP Site 762C (Indian Ocean). Hvidskud encompasses the 405 kyr eccentricity cycles $Ma_{405}13$ – $Ma_{405}11$ within magnetochron C31r. A sedimentation rate of 5.0 cm kyr^{-1} can be inferred from correlation to geochronological tie-points in ODP 762C, suggesting an age of ~70.9 Ma for the base of the succession and a duration of >680 kyr for the investigated interval. The Hvidskud succession is well-exposed, easily accessible, and the new stratigraphic framework and precise age model suggest that it can be used as a key locality for stratigraphic correlation of the lower Maastrichtian in north-western Europe. Information on palaeo-seawater temperatures can be drawn from oxygen isotope records obtained from bulk rock samples and 24 micromorphic brachiopod specimens (*Terebratulina faujasii*). The brachiopod data show a clear diagenetic trend but point to an upper range of unaltered values between –0.4 and –0.6‰. Assuming a $\delta^{18}O$ value of –1‰ for seawater in a Cretaceous ice-free world, this would indicate bottom water temperatures of 13.6 to 14.3°C of the Danish Chalk Sea (45°N) during the early Maastrichtian cooling.

Keywords: lower Maastrichtian, calcareous nannofossil biostratigraphy, $\delta^{13}C$ stratigraphy, Danish Basin, brachiopod zonation, oxygen isotopes, Hvidskud.

Mads Engholm Jelby [madsjelby@hotmail.com], Nicolas Thibault [nt@ign.ku.dk], Finn Surlyk [finns@ign.ku.dk], Clemens V. Ullmann [cu@ign.ku.dk], Rikke Harlou [rikke@harlou.dk], Christoph Korte [korte@ign.ku.dk], Department of Geosciences and Natural Resource Management, University of Copenhagen, Øster Voldgade 10, DK-1350 Copenhagen K, Denmark.

The coastal cliff Møns Klint, situated in eastern Denmark at the south-eastern margin of the Danish Basin, is an important locality for the study of the Maastrichtian of northern Europe (Fig. 1). The 6 km long and up to 130 m high cliff is composed of large glaciotectonic thrust sheets of white chalk and Quaternary deposits.

The Hvidskud thrust sheet, situated in the southern part of the cliff, exposes the thickest succession at Møns Klint comprising *c*. 60 m of lower Maastrichtian white chalk with flint bands and nodules, and abundant *Thalassinoides* burrows (Figs 2, 3). Previous stratigraphic studies of the succession are based on foraminifera, coccoliths, dinoflagellates, belemnites and brachiopods (Birkelund 1957; Steinich 1965; Surlyk 1970, 1979, 1982, 1984; Surlyk & Birkelund 1977; Schulz 1979). In particular, a detailed zonation was established on the basis of micromorphic brachiopods obtained from washed bulk samples (Surlyk 1969, 1970, 1979, 1982, 1984). Many of these species have a limited vertical distribution, occur in great numbers and have proved to be useful for biostratigraphic zonation and correlation of the chalk in north-western Europe (Steinich 1965; Surlyk 1970, 1984; Johansen & Surlyk 1990).

Many of the stratigraphically important microfossils from low latitudes are either absent or rare in the Maastrichtian chalk of north-western Europe, making it difficult to correlate precisely the Danish Maastrichtian brachiopod zonation with the newest Maastrichtian time scale (Thibault *et al.* 2012a, b). Recently, the Danish Maastrichtian has been correlated with the δ^{13}C stratigraphy and calcareous nannofossil biostratigraphy of north-western Europe (Voigt *et al.* 2010, 2012; Thibault *et al.* 2012a, b; Surlyk *et al.* 2013). Along with the development of an astronomical Maastrichtian time scale (Husson *et al.* 2011; Thibault *et al.* 2012b), this allows the establishment of an age model for the Hvidskud succession within the framework of the δ^{13}C and nannofossil stratigraphies established for the Danish lower Maastrichtian.

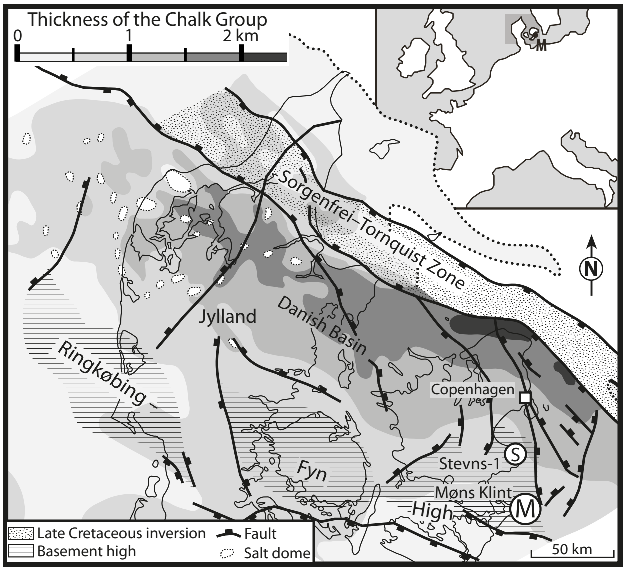

Fig. 1. Map of the Danish Basin showing the thickness of the Upper Cretaceous – Danian Chalk Group. Circled M, Møns Klint; Circled S, Stevns-1 drill hole. Modified from Stemmerik *et al.* (2006).

Fig. 2. Photograph of the upper part of the Hvidskud succession, Møns Klint, exposing glacially thrusted lower Maastrichtian white chalk with bands and nodules of black flint. Person standing next to the prominent flint band at 25.5 m, *c.* 8.5 m below the thin hardground.

The aim of the study is to establish a new calcareous nannofossil and δ^{13}C stratigraphy for the Hvidskud succession and to correlate these data with the brachiopod zonation of Surlyk (1984). An age model is proposed for the Hvidskud succession based on these results combined with δ^{13}C and nannofossil data for north-western Europe (Voigt *et al.* 2010, 2012; Thibault *et al.* 2012a, b) and the new astronomical time scale for the Maastrichtian (Husson *et al.* 2011; Thibault *et al.* 2012b). Additionally, climatic implications can be drawn for bottom waters of the lower Maastrichtian in the Danish Basin based on new isotopic results from micromorphic brachiopods.

Regional setting and stratigraphy

The Danish Basin is NW–SE elongated and is limited to the NE by the inverted and faulted Sorgenfrei–Tornquist Zone and to the S by the Ringkøbing–Fyn High. Møns Klint is situated over the eastern end of the high (Fig. 1). During the Cretaceous the basin was characterised by regional subsidence, interrupted by phases of inversion and relative uplift of the Sorgenfrei–Tornquist Zone (Liboriussen *et al.* 1987; Håkansson & Surlyk 1997; Vejbæk & Andersen 2002; Mogensen & Korstgård 2003). The Late Cretaceous experienced an ongoing sea-level rise, culminating in one of the globally highest sea-level stands during the Phanerozoic, resulting in the flooding of much of northern Europe (e.g. Haq *et al.* 1988; Kominz *et al.* 2008). The chalk, which is essentially a pelagic sediment, was deposited throughout the late Cenomanian to Maastrichtian, and the Campanian–Maastrichtian interval reaches thicknesses of up to several hundreds of metres in the Danish Basin (Stenestad 1972; Surlyk & Lykke-Andersen 2007; Rasmussen & Surlyk 2012; Surlyk *et al.* 2013). Monotonous, benthos-poor chalk was deposited in relatively deep water in the central parts of the basin. On the other hand, abundant minor omission surfaces and rich benthic fossil assemblages in parts of the Maastrichtian chalk of Møns Klint, including the Hvidskud succession, indicate that deposition occurred in relatively shallower water above the Ringkøbing–Fyn High, however still well below the photic zone and storm wave base (Fig. 3; Surlyk & Birkelund 1977).

The Hvidskud succession comprises the *spinosa-*

Table 1. Stratigraphic heights of brachiopod bio-events (first occurrences, FOs) in the Hvidskud succession, Møns Klint. Heights from Surlyk (1979).

Bio-events (FOs)	**m**	**Maastrichtian substage**	**Brachiopod zones (Surlyk 1984)**
Trigonosemus pulchellus	31.5	Base upper lower	*pulchellus-pulchellus*
Terebratulina subtilis	22.7	lower lower	*subtilis-pulchellus*

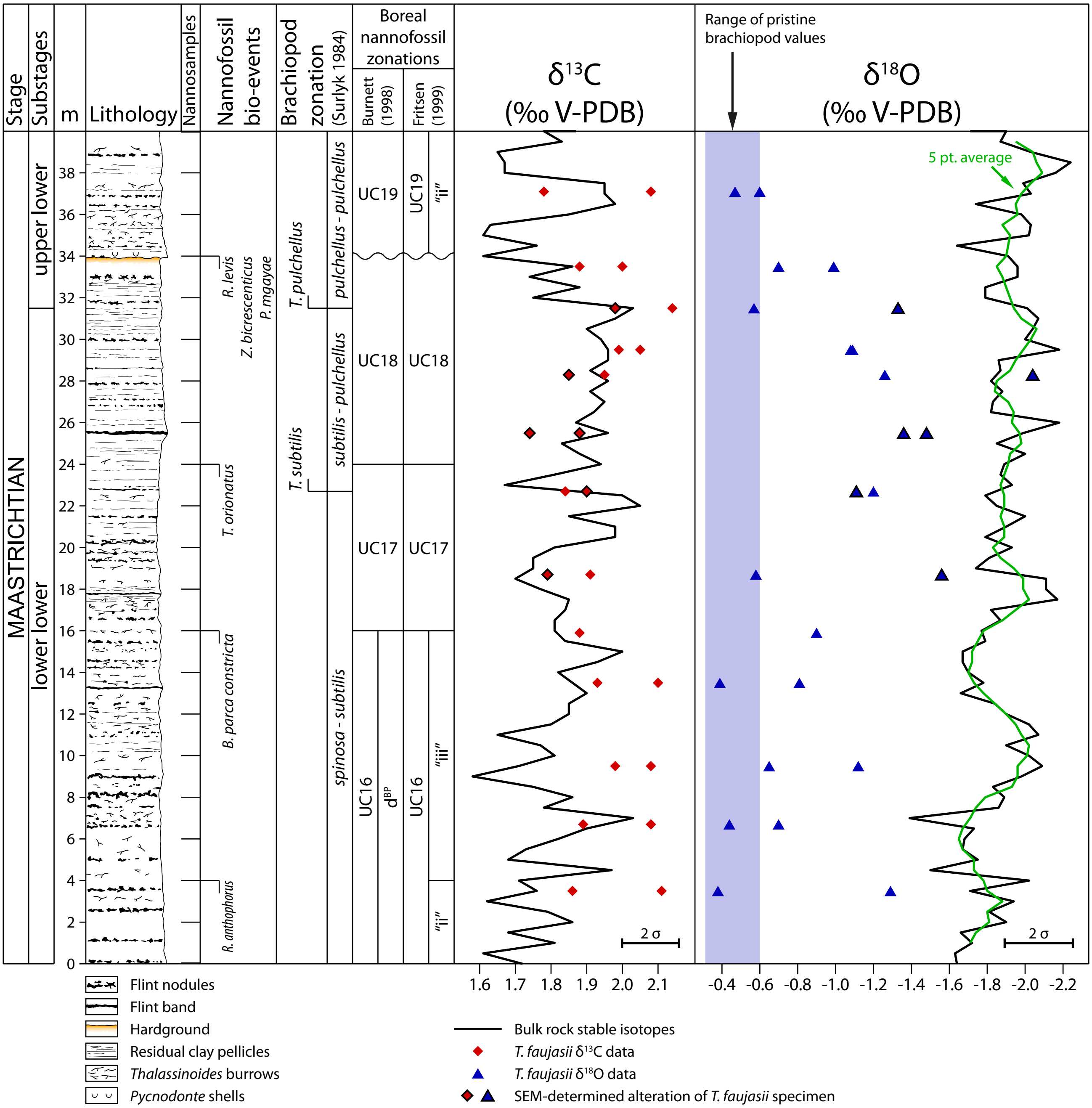

Fig. 3. Correlation of brachiopod and nannofossil zonations with bulk rock stable isotope profiles of the Hvidskud succession together with stable isotope data from the micromorphic brachiopod *Terebratulina faujasii*. Calcareous nannofossil and stable isotope data from this study. The range of pristine brachiopod $\delta^{18}O$ values represents the least altered signal for bottom water conditions and may thus be used to estimate the minimum palaeotemperature of bottom waters of the Chalk Sea in the Danish Basin. Note the relatively light stable isotope values of the brachiopod specimens considered to be altered from SEM inspection. Error bars represent the reproducibility (2σ) of in-house reference material. Log after Surlyk & Birkelund (1977).

subtilis, *subtilis-pulchellus* and *pulchellus-pulchellus* brachiopod zones of Surlyk (1984). The base of the *pulchellus-pulchellus* zone defines the boundary between the lower lower and the upper lower Maastrichtian in the Boreal Realm (Table 1; Surlyk 1969, 1970).

Material and methods

The measured section of Surlyk (1970, 1984) was extended downwards by *c.* 3.5 m and upwards by 1 m, resulting in a total thickness of 40 m. The exposed succession in the cliff is *c.* 60 m thick but the lower part is tectonically disturbed and was not included in the study. Nannoplankton biostratigraphy and stable isotope analyses were based on 82 samples with a resolution of 50 cm (Tables 2, 3). In addition, stable isotope, trace element and scanning electron microscope (SEM) analyses were performed on micromorphic brachiopods (Table 4) from the collection of F. Surlyk in order to synthesise climatic implications from both planktonic and benthic species.

Sample preparation

Bulk samples were dried at 40°C for 48 hours in order to extract possible interstitial fluids from the chalk.

Preparation of microbrachiopods

In order to retrieve monospecific stable isotope and trace element signals, 24 micromorphic brachiopods (distributed over 13 sample levels) of the species *Terebratulina faujasii* were prepared. This species was chosen for analysis as it occurs throughout the succession. Two samples were prepared for each stratigraphic level with one exception where the amount of shell material only allowed preparation of a single sample (Table 4). Articulate brachiopod shells are composed of an outer finely granular primary layer and an interior fibrous or lamellar secondary layer, both consisting of low-Mg calcite (e.g. Griesshaber *et al.* 2007). They may develop an additional prismatic tertiary layer (Parkinson *et al.* 2005). The secondary layer is very resistant to diagenesis (e.g. Veizer *et al.* 1999; Korte *et al.* 2008), and it has been documented that this layer, in contrast to the primary layer, is commonly precipitated in or close to isotopic equilibrium with seawater (Carpenter & Lohmann 1995; Parkinson *et al.* 2005). In order to remove the primary layer and possible attached chalk from the brachiopod shells, the following method was developed by R. Harlou at the Department of Geosciences and Natural Resource Management, University of Copenhagen. The brachiopod shells were carefully cleaned by alternate leaching with 1M acetic acid (CH_3COOH) and cleaning/neutralising with deionised water (MilliQ H_2O).

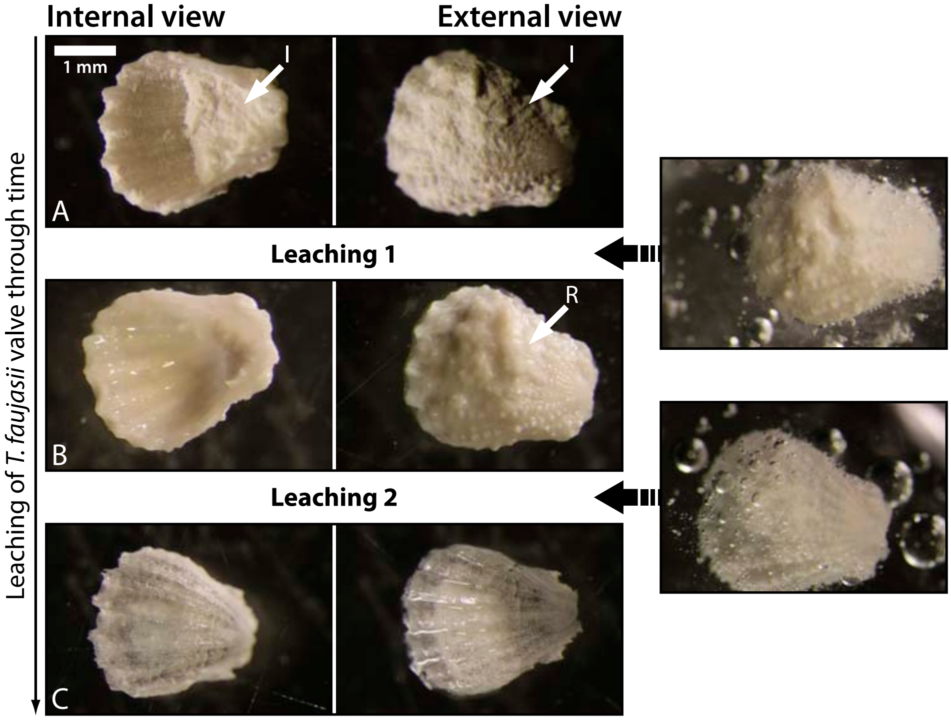

Fig. 4. Representative pictures of the multi-stepped leaching process developed by R. Harlou at the Department of Geosciences and Natural Resource Management, University of Copenhagen. The example presented here is a dorsal valve from the micromorphic brachiopod *Terebratulina faujasii*. Both external and internal views of the valve are included in order to ease comparison between each step. Note how the valve is progressively cleaned throughout the leaching process. **A**: The initial condition with adhering chalk (I) on both the internal and external sides of the valve. **B**: A cleaner valve after the first leaching with only residual chalk (R) on the external side of the valve. **C**: The outer primary layer has been removed from the valve after the second leaching. 1 mm scale bar applies to all pictures. Sample A4 (1), 33.5 m.

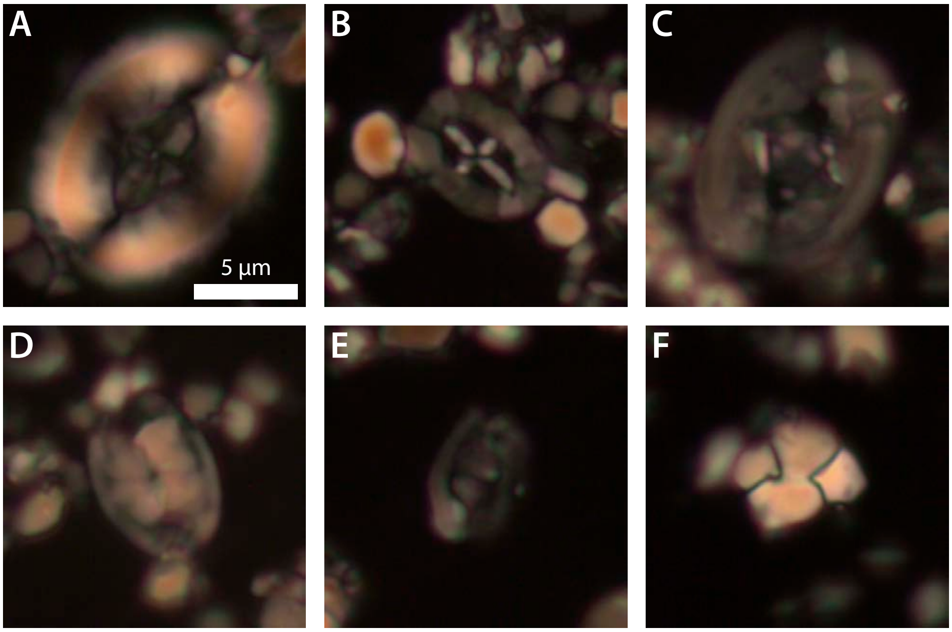

Fig. 5. Main calcareous nannofossils used for biostratigraphic subdivision of the Hvidskud succession, Møns Klint (A–E), and an additional important species found in the succession (F). **A**: *Broinsonia parca constricta*, 14.0 m. **B**: *Prediscosphaera mgayae*, 24.0 m. **C**: *Reinhardtites levis*, 8.0 m. **D**: *Tranolithus orionatus*, 24.0 m. **E**: *Zeugrhabdotus bicrescenticus*, 6.0 m. **F**: *Calculites obscurus*, 0.0 m. 5 µm scale bar applies to all pictures.

The latter also stopped the process of leaching if added in excess. This treatment is excellent for cleaning the shell surfaces and removing the primary layers of articulate brachiopods when preparing for isotope measurements (Fig. 4). The shells were subsequently dried at 40°C for 24 hours in order to extract residual interstitial fluids from the carbonate.

Calcareous nannofossil biostratigraphy

Dried bulk samples were gently disaggregated in a mortar and 50 mg (±0.5 mg) of the treated sediment was dispersed in 50 ml of deionised water buffered with diluted ammonium to avoid dissolution. The suspension was homogenised by treating it in an ultrasonic bath for 10 s and subsequently stirred with a magnet before aliquots of 0.75 ml of the suspension were evenly distributed on microscope slides by using a micropipette (see Koch & Young 2007). A total of 21 slides were produced, covering the complete succession and representing a stratigraphic resolution of 2 m.

Stratigraphic distribution

A semiquantitative analysis of the stratigraphic distribution of calcareous nannofossils was performed (Table 2) based on counting of species abundances (randomly counting of specimens at a magnification of ×1600). Counting was performed on >150 fields of view (FOVs) for each microscope slide. Counts were determined as follows: a species is common (C) if one to 10 specimens were observed in each FOV; there are few (F) if one specimen was observed in every two to 10 FOVs; a species is rare (R) if one specimen was observed in 11 to 100 FOVs and very rare (VR) if one specimen was observed in 100 to 200 FOVs; single (S) means that only one specimen was observed during the entire investigation of a single slide. The nannofossil biozonations are established using the last occurrence (LO) of key nannofossil markers (Fig. 5; Table 2). The biozonations of Burnett (1998) and Fritsen (1999) are applied (Fig. 6).

The Upper Cretaceous chalk of the North Sea and Danish Basin suffered from considerable redeposi-

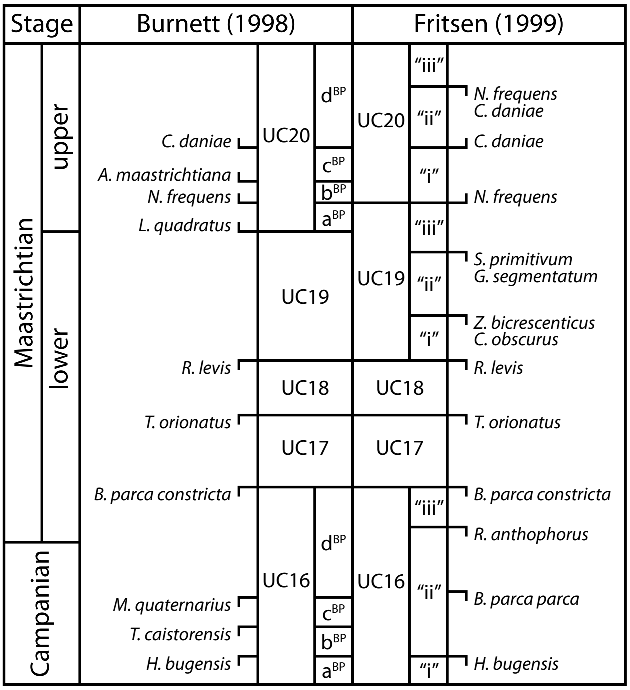

Fig. 6. Main nannofossil bio-events and biozonation schemes of Burnett (1998) and Fritsen (1999) for the upper Campanian – Maastrichtian of the Boreal Realm.

tion (e.g. Esmerode *et al.* 2008; Anderskouv & Surlyk 2011), suggesting that the precision of first and last occurrences of calcareous nannofossil markers may sometimes be disturbed and lead to uncertainties (Thibault *et al.* 2012a). Single spotty occurrences were therefore discarded as these are more likely to be reworked than *in situ*. Additional FOVs, up to an entire traverse of a slide, were examined to document rare species. Three modes of preservation of calcareous nannofossils (very poor, poor and good) have been considered, using the visual criteria of Roth (1983) for etching and overgrowth.

Stable isotope analyses

Approximately 200 to 900 μg of brachiopod shell fragments and bulk rock carbonate samples were transferred into glass vials (3.5 ml), sealed with rubber septa, and flushed with clean helium for 240 s. The aliquots were subsequently treated with ~0.05 ml anhydrous orthophosphoric acid (>100%) and equilibrated for >100 min at 70°C using a multiflow unit. The resultant CO_2 was analysed for carbon and oxygen isotopic compositions using the Micromass Iso Prime Isotope Ratio Mass Spectrometer at the Department of Geosciences and Natural Resource Management, University of Copenhagen. The raw data were corrected for weight dependent effects by measuring the Copenhagen in-house reference material (LEO: Carrara marble), covering the weight ranges of the analysed sample sets. Carbon and oxygen isotope values are expressed in per mil relative to the V-PDB reference (Tables 3, 4). The reproducibility (2sd) of the analysis, controlled by multiple measurements of the in-house reference material, was 0.18‰ for oxygen and 0.08‰ for carbon over a period of one year (2011, n = 649). For more analytical details see Ullmann *et al.* (2013).

Table 2. Distribution chart of selected calcareous nannofossil bio-events (last occurrences) in the Hvidskud succession, Møns Klint

Sample numbers	*Stratigraphic height (m)*	*Prediscosphaera stoveri*	*Kamptnerius magnificus*	*Arkhangelskiella cymbiformis* var. N	*Calculites obscurus*	*Biscutum coronum*	*Biscutum magnum*	*Zeugrhabdotus bicrescenticus*	*Reinhardtites levis*	*Prediscosphaera mgayae*	*Tranolithus orionatus*	*Broinsonia parca constricta*	*Reinhardtites anthophorus*	Preservation	UC Zones	
															Burnett (1998)	Fritsen (1999)
81	40	C	F	F	R		R			S				P	UC19	UC19ii
77	38	R	F	R	R		R							VP	UC19	UC19ii
73	36	R	C	R			R							VP	UC19	UC19ii
69	34	F	F	F	R			F	R	R				VP	UC18	UC18
65	32	F	F	R				C	R					VP	UC18	UC18
61	30	F	F	R	R			F	R	R				P	UC18	UC18
57	28	F	C	F				C	R	F				G	UC18	UC18
53	26	C	F	R				C	F	F				P	UC18	UC18
49	24	F	C	R				C	R	R	R			P	UC17	UC17
45	22	F	F	F				C	F	R				G	UC17	UC17
41	20	F	C	R				C	R	F				G	UC17	UC17
37	18	F	F	F				R	R	S				G	UC17	UC17
33	16	C	F	C				F	R	F		R		G	UC16d	16iii
29	14	F	F	R					F	R	R	R		G	UC16d	16iii
25	12	C	F	R	R		R	R	F			VR		G	UC16d	16iii
21	10	F	F	F	R		F	F	F	VR				G	UC16d	16iii
17	8	F	F	C	F		R	C	F	VR				G	UC16d	16iii
13	6	R	C	F	R		R	F	R	R				VP	UC16d	16iii
9	4	C	F	F	R		R	F	F	R			R	P	UC16d	16ii
5	2	C	R	F	R		R	R	R	R			R	G	UC16d	16ii
1	0	R	F	R	F	VR	VR	F		R		R		G	UC16d	16ii

C, Common (= 1–10 specimens/FOV); F, Few (= 1 specimen/2–10 FOVs); R, Rare (1 specimen/11–100 FOVs); VR, Very Rare (1 specimen/100–200 FOVs); S, Single specimen

Brachiopod element ratios

Remains of the reacted sample aliquots from the mass spectrometric analysis were used for element ratio measurements of the brachiopod shells. All samples were diluted to a nominal Ca concentration of 25 µg/g using 2% HNO_3. Samples were measured using a Perkin Elmer Optima 7000 DV ICP-OES at the Department of Geosciences and Natural Resource Management, University of Copenhagen, using a

Table 3. Bulk rock stable isotope data and stratigraphic position of samples

Height (m)	Maastrichtian substage	Boreal nannofossil zonations		δ^{13}C (‰ V-PDB)	δ^{18}O (‰ V-PDB)
		Burnett (1998)	Fritsen (1999)		
40.0	upper lower	UC19	UC19ii	1.87	–1.71
40.0	upper lower	UC19	UC19ii	1.78	–1.90
39.5	upper lower	UC19	UC19ii	1.83	–1.87
39.0	upper lower	UC19	UC19ii	1.65	–2.03
38.5	upper lower	UC19	UC19ii	1.67	–2.24
38.0	upper lower	UC19	UC19ii	1.67	–2.16
37.5	upper lower	UC19	UC19ii	1.95	–1.99
37.0	upper lower	UC19	UC19ii	1.95	–2.03
36.5	upper lower	UC19	UC19ii	1.98	–1.74
36.0	upper lower	UC19	UC19ii	1.85	–1.98
35.5	upper lower	UC19	UC19ii	1.63	–2.03
35.0	upper lower	UC19	UC19ii	1.61	–2.02
34.5	upper lower	UC19	UC19ii	1.76	–1.64
34.0	upper lower	Base UC19	Base UC19ii	1.61	–1.91
33.5	upper lower	UC18	UC18	1.86	–1.96
33.0	upper lower	UC18	UC18	1.74	–1.96
32.5	upper lower	UC18	UC18	1.88	–1.79
32.0	upper lower	UC18	UC18	1.75	–1.79
31.5	Base upper lower	UC18	UC18	2.03	–2.01
31.0	lower lower	UC18	UC18	1.98	–2.07
30.5	lower lower	UC18	UC18	1.90	–2.04
30.0	lower lower	UC18	UC18	1.94	–2.00
29.5	lower lower	UC18	UC18	1.96	–2.18
29.0	lower lower	UC18	UC18	1.96	–1.86
28.5	lower lower	UC18	UC18	1.91	–1.87
28.0	lower lower	UC18	UC18	1.96	–1.82
27.5	lower lower	UC18	UC18	1.91	–1.88
27.0	lower lower	UC18	UC18	1.95	–1.83
26.5	lower lower	UC18	UC18	1.92	–1.82
26.0	lower lower	UC18	UC18	1.87	–2.18
25.5	lower lower	UC18	UC18	1.96	–1.99
25.0	lower lower	UC18	UC18	1.83	–1.85
24.5	lower lower	UC18	UC18	1.88	–2.00
24.0	lower lower	Base UC18	Base UC18	1.94	–1.89
23.5	lower lower	UC17	UC17	1.81	–1.87
23.0	lower lower	UC17	UC17	1.67	–1.93
22.5	lower lower	UC17	UC17	2.00	–1.79
22.0	lower lower	UC17	UC17	2.05	–1.85
21.5	lower lower	UC17	UC17	1.85	–2.00
21.0	lower lower	UC17	UC17	1.98	–1.90
20.5	lower lower	UC17	UC17	1.98	–1.79
20.0	lower lower	UC17	UC17	1.81	–1.93
19.5	lower lower	UC17	UC17	1.75	–1.81
19.0	lower lower	UC17	UC17	1.75	–1.74
18.5	lower lower	UC17	UC17	1.70	–2.11
18.0	lower lower	UC17	UC17	1.77	–2.11
17.5	lower lower	UC17	UC17	1.85	–2.17
17.0	lower lower	UC17	UC17	1.84	–1.82
16.5	lower lower	UC17	UC17	1.81	–1.87
16.0	lower lower	Base UC17	Base UC17	1.81	–1.77
15.5	lower lower	UC16d^{BP}	UC16iii	1.84	–1.79
15.0	lower lower	UC16d^{BP}	UC16iii	2.00	–1.67
14.5	lower lower	UC16d^{BP}	UC16iii	1.93	–1.67
14.0	lower lower	UC16d^{BP}	UC16iii	1.82	–1.70
13.5	lower lower	UC16d^{BP}	UC16iii	1.86	–1.78
13.0	lower lower	UC16d^{BP}	UC16iii	1.90	–1.66
12.5	lower lower	UC16d^{BP}	UC16iii	1.85	–1.84
12.0	lower lower	UC16d^{BP}	UC16iii	1.85	–1.90
11.5	lower lower	UC16d^{BP}	UC16iii	1.80	–2.02
11.0	lower lower	UC16d^{BP}	UC16iii	1.65	–2.07
10.5	lower lower	UC16d^{BP}	UC16iii	1.77	–1.90
10.0	lower lower	UC16d^{BP}	UC16iii	1.81	–2.02
9.5	lower lower	UC16d^{BP}	UC16iii	1.71	–2.09
9.0	lower lower	UC16d^{BP}	UC16iii	1.58	–1.98
8.5	lower lower	UC16d^{BP}	UC16iii	1.75	–1.83
8.0	lower lower	UC16d^{BP}	UC16iii	1.86	–1.89
7.5	lower lower	UC16d^{BP}	UC16iii	1.78	–1.86
7.0	lower lower	UC16d^{BP}	UC16iii	2.03	–1.39
6.5	lower lower	UC16d^{BP}	UC16iii	1.90	–1.73
6.0	lower lower	UC16d^{BP}	UC16iii	1.82	–1.68
5.5	lower lower	UC16d^{BP}	UC16iii	1.73	–1.67
5.0	lower lower	UC16d^{BP}	UC16iii	1.68	–1.75
4.5	lower lower	UC16d^{BP}	UC16iii	1.97	–1.50
4.0	lower lower	UC16d^{BP}	Base UC16iii	1.71	–2.02
3.5	lower lower	UC16d^{BP}	UC16ii	1.76	–1.71
3.0	lower lower	UC16d^{BP}	UC16ii	1.62	–1.94
2.5	lower lower	UC16d^{BP}	UC16ii	1.79	–1.81
2.0	lower lower	UC16d^{BP}	UC16ii	1.86	–1.90
1.5	lower lower	UC16d^{BP}	UC16ii	1.68	–1.66
1.0	lower lower	UC16d^{BP}	UC16ii	1.81	–1.72
0.5	lower lower	UC16d^{BP}	UC16ii	1.61	–1.63
0.0	lower lower	UC16d^{BP}	UC16ii	1.72	–1.64

three-point calibration of matrix matched and synthetic calibration solutions. Accuracy and reproducibility were controlled by multiple measurements of the reference materials JDo-1 (dolostone) and JLs-1 (limestone). Reproducibilities (2sd) of the analyses are better than 2.6% for Mg/Ca and better than 2.2% for Sr/Ca. Reproducibility of Mn/Ca is 2.8% for JDo-1 (~150 μmol/mol) and 8.0% for JLs-1 (~29 μmol/mol). Measured ratios agree with ratios calculated by Imai *et al.* (1996) within 2%, apart from Mg/Ca in JLs-1, which was measured to be 8% lower.

SEM screening of micromorphic brachiopods

A total of 20 pieces of brachiopod shells were coated in gold and optically checked using the FEI Quanta 250 SEM of the Natural History Museum of Denmark, University of Copenhagen, in order to identify potential textural alteration. Photographs were taken of general and peculiar features representative of each sample (Fig. 7). The preservation state of the secondary shell layers was of particular interest. In addition, it was checked whether the primary layers were completely removed by leaching. The shell fragments were therefore extracted after the leaching process. Due to lack of material, SEM investigations were not possible for certain specimens (Table 4).

Results

Nannofossil bio-events, biozonations and preservation

Most of the investigated samples exhibit moderate preservation with little etching and some diagenetic overgrowth. However, samples from the uppermost part of the succession (from 30.0 m up-section) exhibit poor to very poor preservation. Nannofossil counting was performed on 12 key coccolith species (Fig. 5; Table

Table 4. Micromorphic brachiopod (*Terebratulina faujasii*) stable isotope, trace element and SEM data

Samples	Additional specimen prepared	SEM inspection	SEM-determined alteration	Height (m)	δ^{13}C (‰ V-PDB)	δ^{18}O (‰ V-PDB)	Mg/Ca (mmol/mol)	Sr/Ca (mmol/mol)	Mn/Ca (µmol/mol)
A2 (1)		×		37.1	1.78	–0.60	10.6	1.21	124
A2 (2)				37.1	2.08	–0.47	10.8	1.25	114
A4 (1)				33.5	1.88	–0.99	10.0	1.15	138
A4 (2)	×	×		33.5	2.00	–0.70	10.6	1.26	92
A5 (1)		×		31.5	2.14	–0.57	9.8	1.35	76
A5 (2)	×	×	×	31.5	1.98	–1.33	9.9	1.03	147
A6 (1)		×		29.5	2.05	–1.08	9.6	1.29	90
A6 (2)	×	×		29.5	1.99	–1.09	9.9	1.20	111
A7 (1)		×	×	28.3	1.85	–2.04	9.3	0.96	148
A7 (2)	×	×		28.3	1.95	–1.26	10.0	1.23	106
A9 (1)		×	×	25.5	1.88	–1.48	9.6	0.95	185
A9 (2)	×	×	×	25.5	1.74	–1.36	9.9	0.94	207
A11 (1)		×	×	22.7	1.90	–1.11	10.0	0.89	162
A11 (2)	×	×		22.7	1.84	–1.20	10.0	1.12	129
A14 (1)				18.7	1.91	–0.58	10.4	1.37	77
A14 (2)	×	×	×	18.7	1.79	–1.56	10.0	1.03	147
A16 (1)				15.9	1.88	–0.90	9.8	1.08	114
A18 (1)		×		13.5	1.93	–0.81	10.3	1.34	76
A18 (2)	×	×		13.5	2.10	–0.39	10.3	1.48	57
A22 (1)		×		9.5	2.08	–0.65	9.8	1.39	67
A22 (2)	×	×		9.5	1.98	–1.12	10.3	1.31	90
A25 (1)		×		6.7	2.08	–0.44	9.5	1.42	45
A25 (2)	×	×		6.7	1.89	–0.70	10.1	1.31	71
A28 (1)		×		3.5	2.11	–0.38	11.4	1.46	68
A28 (2)	×			3.5	1.86	–1.29	10.5	1.19	126

Note that sample A2 (1) and A2 (2) are from the same specimen, resulting in 25 data points. In terms of the SEM-based optical preservation assessment, six of the 20 brachiopods are considered to be altered.

2). The LO of five of these was used to subdivide the succession into four of the main Upper Cretaceous (UC) biozones applied to the Boreal Province (BP) by Burnett (1998) and to the North Sea by Fritsen (1999) (Figs 3, 6; Table 2). The LO of *Reinhardtites anthophorus*, defining the base of UC16iii of Fritsen (1999), is recorded in the lowermost part of the succession (4.0 m) within the *spinosa-subtilis* zone of Surlyk (1984) (Fig. 3; Table 2). The LO of *Broinsonia parca constricta* (16.0 m), defining the base of UC17, is also encountered within the *spinosa-subtilis* zone. The LO of *Tranolithus orionatus* (24.0 m) lies within the *subtilis-pulchellus* zone and defines the base of UC18. The LOs of *Reinhardtites levis* and *Zeugrhabdotus bicrescenticus* coincide with a minor hardground at 34.0 m (Figs 2, 3) and do not allow differentiation of UC19i and UC19ii, thus representing an unconformity corresponding to the missing UC19i. The LOs of *R. levis* and *Z. bicrescenticus* are thus considered to define the base of UC19ii, which is entirely encompassed by the *pulchellus-pulchellus* zone. In addition, their LOs coincide with the LO of *Prediscosphaera mgayae*. The Hvidskud succession thus encompasses the Boreal nannofossil zones UC16ii – UC19ii (Figs 3, 6).

Bulk rock stable isotope results

A total of 82 bulk rock samples were analysed. The resulting $\delta^{13}C$ curve (Fig. 3) is characterised by an overall positive trend superimposed by several positive and negative fluctuations of higher order between 1.6 and 2.1‰. The lowermost part of the succession exhibits a positive excursion from 1.7 to 2.0‰ which is interrupted by a negative shift down to 1.6‰ at 9.0 m. The overlying interval is characterised by a progressive 0.5‰ increase, interrupted by two short-term negative excursions. The remaining part of the succession is characterised by an overall negative excursion from 2.0 to 1.8‰, interrupted by a significant short positive excursion.

The bulk rock oxygen isotope trend (Fig. 3) is characterised by an overall 0.2‰ decrease, with superimposed higher order positive and negative oscillations between –2.2 to –1.4‰. A five-point moving average was applied to the $\delta^{18}O$ data in order to highlight possible fluctuations and inflection points in the succession (Fig. 3).

A cross-plot of carbon and oxygen isotopes (Fig. 8) allows testing of diagenetic imprints which may result in a positive correlation (Jenkyns *et al.* 1995; Mitchell *et al.* 1997). The absence of a significant correlation in the bulk rock data suggests a relatively low impact of diagenesis.

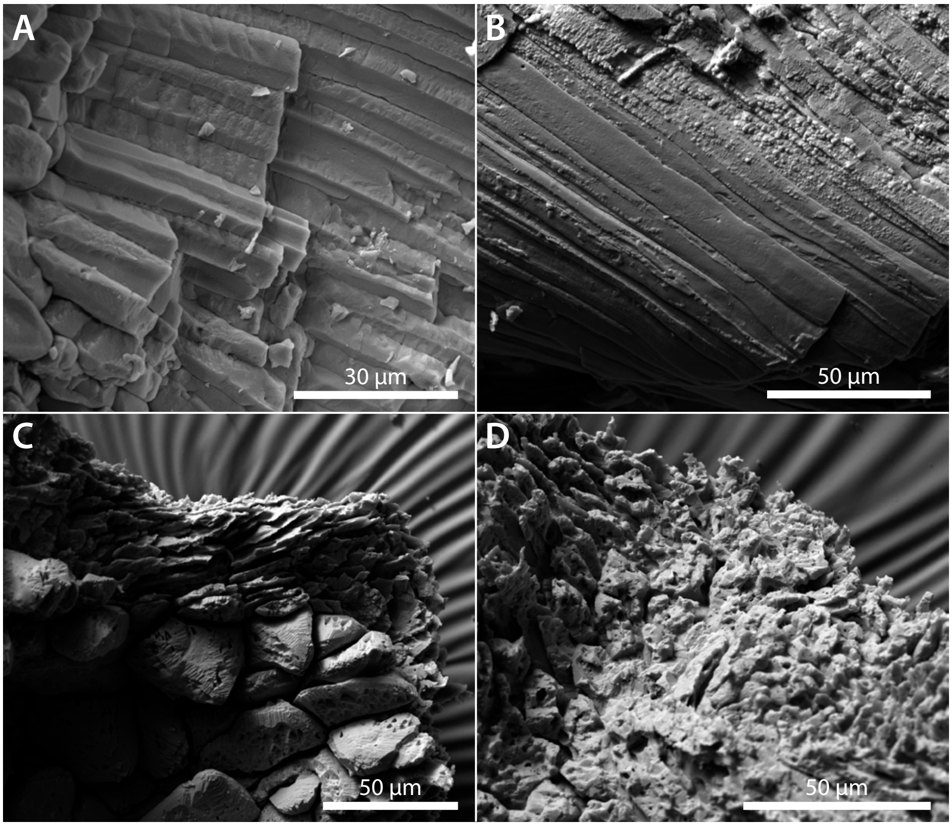

Fig. 7. Representative SEM pictures of four of the 24 leached brachiopod valves, showing (A–B) well-preserved secondary shell layers and (C–D) altered shell material. Regarding the SEM-based preservation assessment only, the shells are generally well-preserved and leaching has successfully removed the main part of the primary layer with only minor exceptions. **A**: A18 (2), 13.5 m. **B**: A25 (1), 6.7 m. **C**: A9 (1), 25.5 m. **D**: A9 (2), 25.5 m.

Screenings, trace element and stable isotope results for brachiopods

Binocular and SEM screenings show that the ultrastructures such as smooth surfaces and anvil-shaped crystals of the fibrous and lamellar structures of the secondary layers of most of the brachiopods are well-preserved (Fig. 7). Features resulting from the leaching process are ignored in this consideration. Six specimens show signs of diagenetic dissolution resulting in irregular surfaces. These specimens are considered to be altered (Fig. 7; Table 4). From the SEM images it can also be concluded that the leaching of the brachiopods has successfully removed the primary shell layers and adhered chalk.

The stable isotope values from the brachiopods are on average heavier than those of the bulk samples (Figs 3, 8). The brachiopod $\delta^{13}C$ trend shows a slight decline of ~0.2‰ (2.0 to 1.8‰) between 3.5 and 18.7 m, and a subsequent ~0.2‰ incline with a short-lived positive excursion (2.1‰) at 31.5 m. The brachiopod $\delta^{18}O$ trend shows a similar trend in the lower and upper part of the succession, and an overall negative excursion between 3.5 and 28.3 m with a change of –1.6‰ and the lightest value down to –2.0‰.

A cross-plot of the carbon and oxygen isotope values reveals a weak positive correlation (Fig. 8), which might indicate diagenetic alteration of the brachiopod shells (cf. Jenkyns *et al.* 1995; Mitchell *et al.* 1997).

Mg/Ca ratios range from 9.3 to 11.4 mmol/mol with an average of 10.1 mmol/mol. Sr/Ca ratios range from 0.89 to 1.48 mmol/mol and are strongly negatively correlated with Mn/Ca ratios that range from 45 to 207 μmol/mol ($r^2 = 0.88$) (Fig. 9). Negative correlations of Mn/Ca with $r^2 > 0.5$ are also observed for $\delta^{13}C$ and $\delta^{18}O$ (Fig. 9).

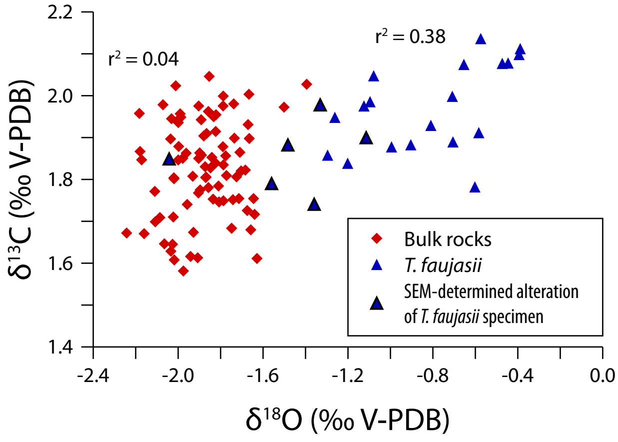

Fig. 8. Cross-plot of carbon and oxygen isotope ratios in bulk samples, showing no significant correlation, and in the micromorphic brachiopod *Terebratulina faujasii*, showing a weak positive correlation. Note the relatively light stable isotope values of the brachiopod specimens considered to be altered from the SEM-based preservation assessment.

Discussion

Diagenetic impact on brachiopod isotopic data

The strong negative correlations of Sr/Ca with Mn/Ca and $\delta^{18}O$ with Mn/Ca point to an important diagenetic imprint on the brachiopods (cf. Brand & Veizer 1981). Significantly, the six specimens that are considered to be altered by means of the SEM-based preservation assessment, are also the specimens with highest Mn/

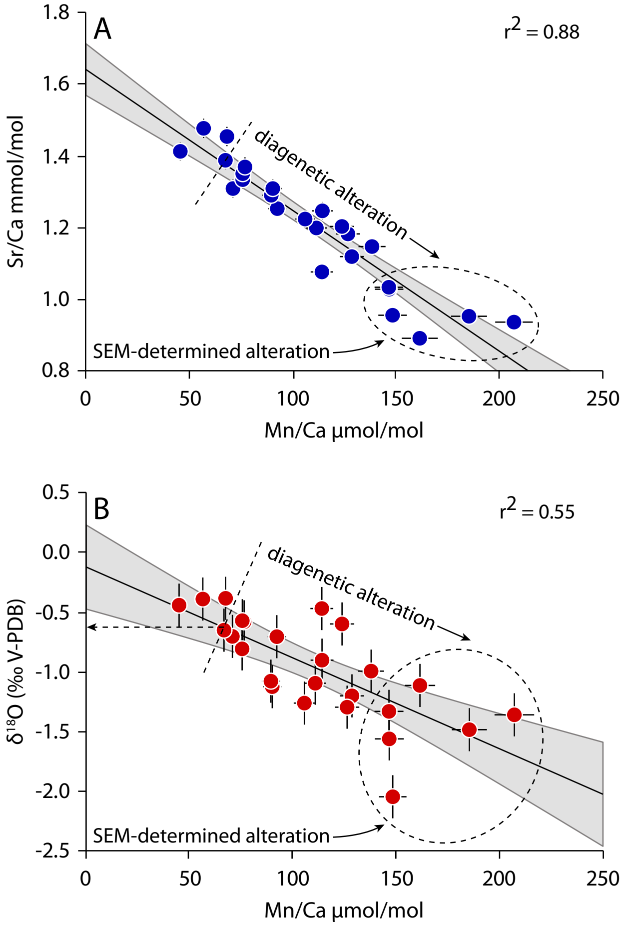

Fig. 9. Cross-plots of geochemical data for the micromorphic brachiopod *Terebratulina faujasii*. **A**: Co-variation of Sr/Ca ratios with Mn/Ca ratios. **B**: Co-variation of $\delta^{18}O$ values with Mn/Ca ratios. Brachiopod values corresponding to the upper-left of the correlation lines indicate the least altered specimens and probably reflect primary bottom water $\delta^{18}O$ values. By discarding the samples that are considered to be altered, it is evident that any $\delta^{18}O$ value lower than –0.6‰ cannot be interpreted with confidence as primary (B). Additionally, in each of the cross-plots, the specimens considered to be altered by means of SEM inspection are more or less clustered in the lower right corner with the highest Mn/Ca ratios (A–B), lowest Sr/Ca ratios (A), and some of the lightest $\delta^{18}O$ values (B), clearly signifying their degree of diagenetic alteration.

Ca ratios, the lowest Sr/Ca ratios (Fig. 9) and some of the lightest stable isotope values (Figs 3, 8; Table 4). Therefore, long-term trends in brachiopod δ^{18}O cannot be interpreted here. However, it can be inferred that values corresponding to the upper-left of the correlation lines point to the least altered values and probably reflect near to primary bottom water δ^{18}O values (Fig. 9).

Correlation of brachiopod and nannofossil zonations with carbon isotope stratigraphy

Carbon isotope records have proved to be a powerful tool for stratigraphic correlation (Gale *et al.* 1993; Tsikos *et al.* 2004; Voigt *et al*. 2010, 2012; Batenburg *et al.* 2012; Thibault *et al.* 2012a, b). Calibrating δ^{13}C curves with detailed biostratigraphic information additionally improves the stratigraphic reliability and helps to correlate biostratigraphic schemes between different palaeobiogeographic realms (Thibault *et al.* 2012a, b). The bulk δ^{13}C excursions of the Hvidskud succession, together with the nannofossil biostratigraphy, can be used for this purpose. A similar succession of nannofossil bio-events has been found in the upper Campanian – Maastrichtian Stevns-1 core, Stevns Klint, eastern Denmark (Fig. 1), from which a standard δ^{13}C curve was established for the Boreal Realm (Thibault *et al.* 2012a; Surlyk *et al*. 2013). The Stevns-1 core was drilled only 30 km from Møns Klint and displays an almost identical sequence of nannofossil bio-events from the LO of *R. anthophorus* when compared with Hvidskud (Fig. 10; Thibault *et al*. 2012a). The only exception is that the LO of *Z. bicrescenticus* occurs stratigraphically slightly higher in Stevns-1 than the coincident LOs of *R. levis* and *P. mgayae*. This is in contrast to the Hvidskud succession where the LOs of these three species are coincident (Fig. 10). The three bio-horizons occur at the hardground at 34.0 m, suggesting that the UC19i subzone is missing at Hvidskud (Figs 3, 10).

The δ^{13}C records of Hvidskud and Stevns-1 are correlated and calibrated by the nannofossil bio-events, allowing the establishment of a precise δ^{13}C stratigraphy for the Hvidskud succession (Fig. 10). The Stevns-1 core was sampled at a much higher resolution than the Hvidskud succession, and ambiguities in the correlation of the δ^{13}C profiles may thus exist. However, the correlation is strongly supported by a precise correlation of nannofossil bio-horizons between the two sites. The LO of *R. anthophorus* in both successions allows correlation of the lowermost part of the Hvidskud succession with Stevns-1. The lowermost 0.3‰ increase in the Hvidskud succession corresponds to the short-lived 0.2‰ positive excursion of the M1+ δ^{13}C event in Stevns-1 (Thibault *et al.* 2012a), and occurs within UC16d^{BP} of Burnett (1998) and the *spinosa-subtilis* zone of Surlyk (1984). The onset of event M1– is marked by an abrupt negative excursion in both successions and the top of this event coincides with the LO of *T. orionatus* (base of UC18). The M1– δ^{13}C event thus corresponds to the upper part of *spinosa-subtilis* and the lowermost part of *subtilis-pulchellus* brachiopod zones of Surlyk (1984). The LO of *B. parca constricta* is recorded within M1– in both successions (Thibault *et al.* 2012a) (Fig. 10). The overlying part of the Hvidskud succession can only be correlated with confidence on the basis of nannofossil bio-events. The LOs of *P. mgayae*, *R. levis* and *Z. bicrescenticus* appear concomitantly in the level of the hardground-related unconformity and thus confirm omission in this level. Their last occurrences, however, coincide with a significant negative δ^{13}C excursion in both successions, which can be used as a tie-point to subdivide the M2+ event in the uppermost part of the Hvidskud succession. The M2+ δ^{13}C event extends from the LO of *T. orionatus* and is comprised by UC18 and UC19 and the *subtilis-pulchellus* and *pulchellus-pulchellus* brachiopod zones (Fig. 10). As in the lowermost part of the succession, the relatively low sampling resolution, compared to that of Stevns-1, prohibits further correlation between the top of the Hvidskud succession and Stevns-1. The Hvidskud succession thus encompasses δ^{13}C events M1+ to M2+ of Thibault *et al.* (2012a).

The Maastrichtian Stage has recently been astronomically calibrated, and a precise geochronological age model has been proposed (e.g. Husson *et al.* 2011, 2012; Batenburg *et al.* 2012; Thibault *et al.* 2012b). In particular, an integrated framework of magnetostratigraphy, micro- and nannofossil biostratigraphy, cyclostratigraphy and δ^{13}C stratigraphy was established for the upper Campanian – Maastrichtian succession of Ocean Drilling Program (ODP) Site 762C, Leg 122, drilled in the western part of the central Exmouth Plateau off north-western Australia, eastern Indian Ocean (Galbrun 1992; Husson *et al.* 2011, 2012; Thibault *et al.* 2012b). This site was characterised by nearly continuous pelagic to hemipelagic sedimentation, allowing counting of cycles based on colour changes in the core and thereby the development of a cyclostratigraphic framework. The duration of each magnetochron encountered in the core was inferred from cycle counting, using an age of 66 Ma for the K–Pg boundary (Husson *et al.* 2011, 2012). ODP Site 762C thus constitutes a solid basis for large-scale correlations of the upper Campanian – Maastrichtian interval.

Sedimentation at the Indian Ocean ODP site took place within a mid-latitude, transitional calcareous plankton province of the southern hemisphere. Thibault *et al.* (2012b) noticed that many Maastrich-

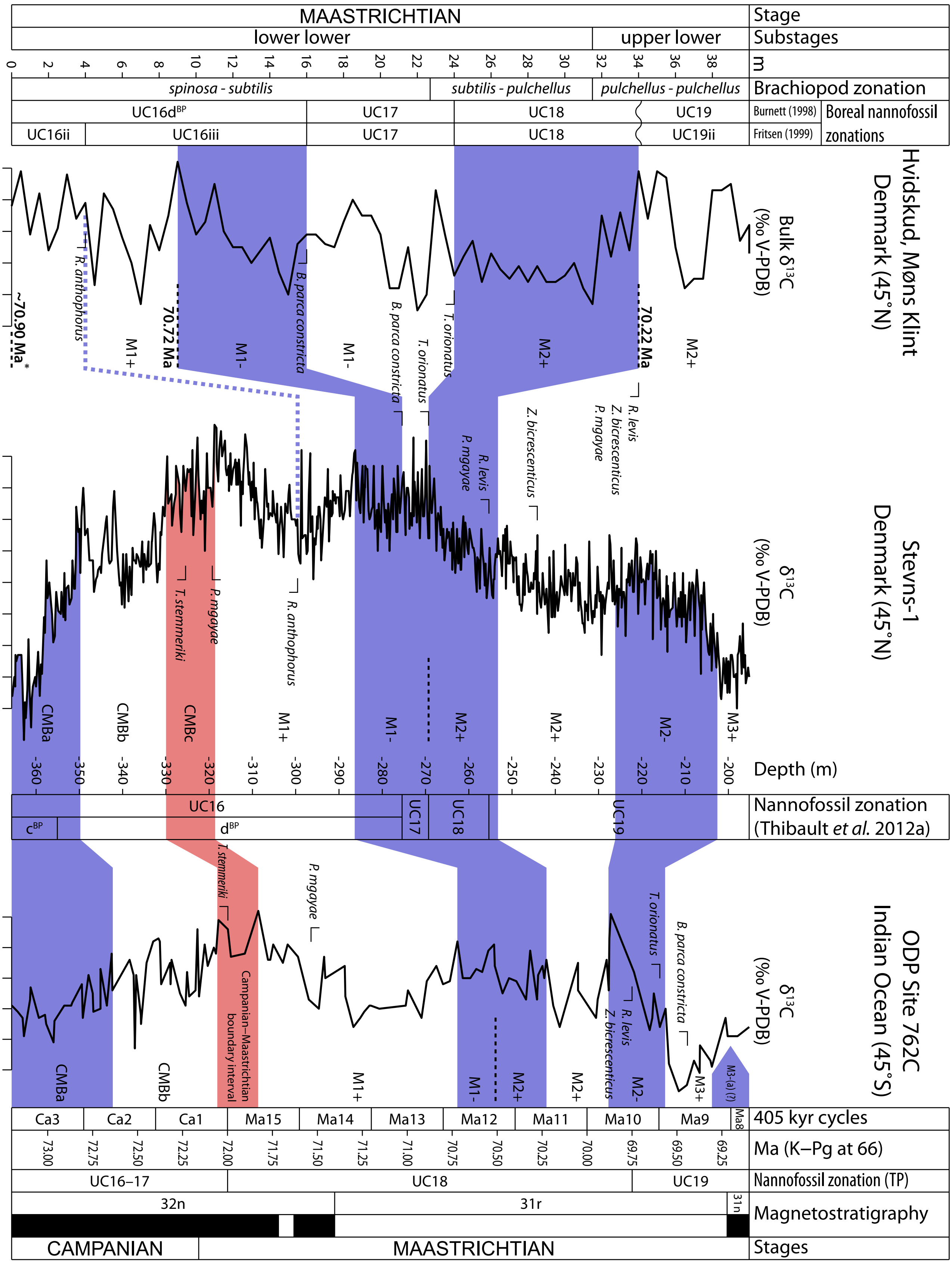
MAASTRICHTIAN
Stage
lower lower
upper lower
Substages
m
Brachiopod zonation
spinosa - subtilis
subtilis - pulchellus
pulchellus - pulchellus
Burnett (1998)
Fritsen (1999)
Boreal nannofossil zonations
UC16d^{BP}
UC16ii
UC16iii
UC17
UC18
UC19
UC19ii
Hvidskud, Møns Klint Denmark (45°N)
Bulk δ^{13}C (‰ V-PDB)
~70.90 Ma*
70.72 Ma
70.22 Ma
R. anthophorus
B. parca constricta
T. orionatus
R. levis
Z. bicrescenticus
P. mgayae
M1+
M1-
M2+
Stevns-1 Denmark (45°N)
δ^{13}C (‰ V-PDB)
T. stemmeriki
P. mgayae
R. anthophorus
CMBa
CMBb
CMBc
M2-
M3+
Depth (m)
Nannofossil zonation (Thibault et al. 2012a)
UC16
c^{BP}
d^{BP}
ODP Site 762C Indian Ocean (45°S)
δ^{13}C (‰ V-PDB)
Campanian–Maastrichtian boundary interval
M3-(a) (?)
405 kyr cycles
Ca3
Ca2
Ca1
Ma15
Ma14
Ma13
Ma12
Ma11
Ma10
Ma9
Ma8
Ma (K–Pg at 66)
Nannofossil zonation (TP)
UC16–17
Magnetostratigraphy
32n
31r
31n
Stages
CAMPANIAN

tian calcareous nannofossil bio-events were time-transgressive between this southern province and the Tethyan and Boreal realms. The $\delta^{13}C$ record for ODP 762C is, however, remarkably similar to that of Stevns-1 (Fig. 10; Thibault *et al*. 2012b). Stevns-1 can therefore be used as a reference curve for correlation of the Hvidskud succession with ODP 762C. This allows further chronostratigraphic constraints for the age model of the Hvidskud succession.

A precise correlation of the M1+ $\delta^{13}C$ event between Hvidskud and ODP 762C is not possible, as the correlation between Hvidskud and Stevns-1 in this interval is solely based on the LO of *R. anthophorus* (Fig. 10). The same problem applies in the upper part of the M2+ event above the LOs of *R. levis*, *Z. bicrescenticus* and *P. mgayae*. The M1– and M2+ events up until the LOs of *R. levis*, *Z. bicrescenticus* and *P. mgayae* can, however, be confidently correlated between the successions, allowing construction of an age model for this interval. Calibration to the ODP 762C profile reliably suggests a geochronological duration of this 25 m thick interval of 70.72 Ma – 70.22 Ma, encompassing the 405 kyr eccentricity cycles $Ma_{405}12$ – $Ma_{405}11$ within magnetochron C31r and nannofossil zone UC18 of the Transitional Province (cf. Husson *et al.* 2011; Thibault *et al.* 2012b). This corresponds to an inferred sedimentation rate of 5.0 cm kyr^{-1} (Fig. 10). Assuming that the sedimentation rate was largely uniform throughout, it can be used to calculate an estimated age for the base of the Hvidskud succession on the basis of its thickness. An age for the top of the succession cannot be determined due to the hiatus represented by the hardground unconformity at 34.0 m. The Hvidskud succession extends from ~70.90 Ma to at least 70.22 Ma, thus covering a time interval of at least 680 kyr (Fig. 10).

Climatic implications

The Maastrichtian was characterised by an overall long-term global cooling, superimposed by pronounced climate and temperature fluctuations (Li & Keller 1998a, b, 1999; Barrera & Savin 1999; Thibault & Gardin 2006, 2007). In the early Maastrichtian, the temperature of intermediate water masses decreased globally by 5–6°C, while sea-surface temperatures in mid and high latitudes decreased by 4–5°C. This cooling event was followed by a mid-Maastrichtian warming of 2–3°C in low and mid-latitudes with warmer but fluctuating temperatures continuing from the late part of chron C31r until the base of C30n. The late Maastrichtian was characterised by another global cooling event, followed by the end-Maastrichtian Deccan greenhouse warming (Li & Keller 1998a, 1999; Barrera & Savin 1999; Thibault & Gardin 2006, 2007, 2010).

The age model suggests that the Hvidskud succession correlates with the early Maastrichtian cooling event (cf. Barrera & Savin 1999; Thibault & Gardin 2006). Cool sea-surface temperatures are supported by a relatively common abundance of the calcareous nannofossil cool-water indicators *Ahmuellerella octoradiata* and *Kamptnerius magnificus* throughout the entire Hvidskud succession. This finding was also noted in the calcareous nannofossil assemblage of the Stevns-1 and Skælskør-1 drill cores (eastern Denmark) in the same stratigraphic interval (unpublished data of N. Thibault).

A slight trend towards warmer temperatures in the uppermost part of the succession may be indicated by an overall small decrease in bulk $\delta^{18}O$ values, suggesting that the top of the succession may correspond to the onset of the mid-Maastrichtian warming event. This inference, however, is tentative.

Brachiopods have proved to be a valuable resource in the reconstruction of past seawater temperatures, partly because their low-Mg calcite shells are relatively resistant to diagenetic alteration and because of the possibility of identifying altered samples (e.g. Veizer *et al.* 1999; Korte *et al.* 2005a, b, 2008). In the Hvidskud succession, the strong co-variation of Sr/Ca with Mn/Ca is indicative of a diagenetic trend (Brand & Veizer 1981). It is noticeable that the lightest $\delta^{18}O$ values in brachiopods are close to bulk $\delta^{18}O$ values (Figs 3, 8). Considering that the calcareous nannofossil assemblage points to some degree of diagenesis, as suggested from the microscope-based preservation assessment (Table 2), it is possible that a relatively warm or hyposaline diagenetic fluid impacted both brachiopod and bulk carbonates in the succession. For this reason, it is not reasonable to interpret bulk $\delta^{18}O$ data in further detail.

After discarding brachiopod $\delta^{18}O$ values aligned on

◀ Fig. 10. Correlation of $\delta^{13}C$ profiles between the Hvidskud succession, Stevns-1 drill core and ODP Site 762C, allowing correlation of brachiopod- and nannofossil zonations with $\delta^{13}C$ stratigraphy for Hvidskud. Correlation between Hvidskud and Stevns-1 is almost entirely based on the tie of the nannofossil bio-events due to the geographical proximity of the localities. The Hvidskud succession comprises carbon isotope events M1+ to M2+. Calibration to the ODP 762C $\delta^{13}C$ profile together with an inferred sedimentation rate of 5.0 cm kyr^{-1} suggests a geochronological age for the base of Hvidskud of ~70.9 Ma. It is not possible to calculate an age for the top of the succession. Note the diachronism of calcareous nannofossil bio-horizons and biozones between Hvidskud and Stevns-1 (Boreal Realm) and ODP Site 762C (intermediate latitudes of the southern hemisphere). *The calculation of the age of the base of Hvidskud (~70.9 Ma) is based entirely on the assumption that the inferred sedimentation rate was uniform throughout the lower part of the succession and can thus be used for age estimations.

the diagenetic correlation trend (Fig. 9), it appears that the few heaviest brachiopod values of –0.4 to –0.6‰ would represent the least altered signal for bottom water conditions (Figs 3, 9). A good preservation of the shell material in these specimens is also supported by low Mn/Ca ratios of ~50 μmol/mol and by the SEM screening which reveals that the shells are among the best preserved with well-preserved calcitic layered structures (Fig. 7). This near-pristine range of values (Fig. 3) may thus be used to estimate the minimum palaeotemperature of bottom waters of the Chalk Sea in the Danish Basin. Using the equation of Anderson and Arthur (1983) and a seawater δ^{18}O of –1‰ for a Late Cretaceous ice-free world, these heaviest brachiopod δ^{18}O values translate to a range of 13.6 to 14.3°C for bottom waters of the Chalk Sea during the early Maastrichtian cooling, at a palaeolatitude of *c*. 45°N. These palaeotemperature estimates may however be biased by the postulated presence of a small Antarctic ice cap at that time (Barrera & Savin 1999; Gallagher *et al*. 2008; Bowman *et al*. 2013).

Conclusions

A new nannofossil and δ^{13}C stratigraphy is established for the Hvidskud succession and correlated with the brachiopod zonation of Surlyk (1984). A chronostratigraphic and geochronological age model is proposed for the succession on the basis of correlation with the cored boreholes Stevns-1 and ODP Site 762C. Seawater temperatures are additionally inferred from combined bulk rock and brachiopod stable isotope data together with the distribution of calcareous nannofossils, brachiopod trace elements and SEM data.

The Hvidskud succession encompasses the Boreal nannofossil zones UC16ii to UC19ii within the lower Maastrichtian. These nannofossil zones are now tied to the brachiopod zonation.

Carbon isotope stratigraphy of the Hvidskud succession and correlation with the Stevns-1 core allow recognition of δ^{13}C events M1+ to M2+. The correlation of Hvidskud with Stevns-1 and the tie of this interval to the astronomically calibrated ODP Site 762C constrains an age of ~70.9 Ma for the base of the succession. The succession extends across the 405 kyr eccentricity cycles $\mathrm{Ma}_{405}13 – \mathrm{Ma}_{405}11$ in magnetochron C31r and across the Boreal lower lower and upper lower Maastrichtian boundary. The entire succession covers a time interval of at least 680 kyr, with an average sedimentation rate of 5.0 cm kyr^{-1}.

The chalk of Hvidskud was deposited during the early Maastrichtian cooling period and bulk oxygen isotope values remain relatively stable in the studied interval. A slight trend towards lighter values towards the top of the succession may represent the onset of the mid-Maastrichtian warming. Most brachiopod δ^{18}O values point to an impact of diagenesis. Near-pristine shell values can be narrowed to a range of –0.4 to –0.6‰. Considering a Late Cretaceous ice-free world, these values translate into a range of temperatures of 13.6 to 14.3°C for bottom waters of the Danish Chalk Sea (45°N) during the early Maastrichtian cooling episode. These estimates may however require correction if the presence of continental ice in Antarctica during the Maastrichtian is confirmed in the future.

Acknowledgements

The study was funded by the Carlsberg Foundation. Bo Petersen kindly provided technical support. We thank journal reviewers Emma Sheldon and Erik Thomsen as well as editor Jan Audun Rasmussen for constructive comments and corrections.

References

Anderskouv, K. & Surlyk, F. 2011: Upper Cretaceous chalk facies and depositional history recorded in the Mona-1 core, Mona Ridge, Danish North Sea. Geological Survey of Denmark and Greenland Bulletin 25, 60 pp.

Anderson, T.F. & Arthur, M.A. 1983: Stable isotopes of oxygen and carbon and their application to sedimentological and palaeoenvironmental problems. In: Arthur, M.A. *et al.* (eds): Stable Isotopes in Sedimentary Geochemistry. Society of Economic Palaeontologists and Mineralogists Short Course 10, 111–151.

Barrera, E. & Savin, S.M. 1999: Evolution of late Campanian–Maastrichtian marine climates and oceans. Geological Society of America Special Papers 332, 245–282.

Batenburg, S.J. *et al.* 2012: Cyclostratigraphy and astronomical tuning of the Late Maastrichtian at Zumaia (Basque country, Northern Spain). Earth and Planetary Science Letters 359–360, 264–278.

Birkelund, T. 1957: Upper Cretaceous Belemnites from Denmark. Det Kongelige Danske Videnskabernes Selskab, Biologiske Skrifter 9, 69 pp.

Bowman, V.C., Francis, J.E. & Riding, J.B. 2013: Late Cretaceous winter sea ice in Antarctica? Geology 41, 1227–1230.

Brand, U. & Veizer, J. 1981: Chemical diagenesis of a multicomponent carbonate system; 2, Stable isotopes. Journal of Sedimentary Research 51, 987–997.

Burnett, J. 1998: Upper Cretaceous. In: Bown, P.R. (ed.): Calcareous Nannofossil Biostratigraphy. Chapman and Hall/Kluwer Academic Publishers, London, 132–199.

Carpenter, S.J. & Lohmann, K.C. 1995: $\delta^{18}O$ and $\delta^{13}C$ values of modern brachiopod shells. Geochimica et Cosmochimica Acta 59, 3749–3764.

Esmerode, E.V., Lykke-Andersen, H. & Surlyk, F. 2008: Interaction between bottom currents and slope failure in the Late Cretaceous of the southern Danish Central Graben, North Sea. Journal of the Geological Society, London 165, 55–72.

Fritsen, A. 1999: A Joint Chalk Stratigraphic Framework. In: Joint Chalk Research Program Topic V. Volume 1. Norwegian Petroleum Directorate, 206 pp.

Galbrun, B. 1992: Magnetostratigraphy of Upper Cretaceous and lower Tertiary sediments, Sites 761 and 762, Exmouth Plateau, northwest Australia. Proceedings of the Ocean Drilling Program, Scientific Results 122, 699–716.

Gale, A.S., Jenkyns, H.C., Kennedy, W.J. & Corfield, R.M. 1993: Chemostratigraphy versus biostratigraphy: data from around the Cenomanian–Turonian boundary. Journal of the Geological Society, London 150, 29–32.

Gallagher, S.J., Wagstaff, B.E., Baird, J.G., Wallace, M.W. & Li, C.L. 2008: Southern high latitude climate variability in the Late Cretaceous greenhouse world. Global and Planetary Change 60, 351–364.

Griesshaber, E., Schmahl, W.W., Neuser, R., Pettke, T., Blüm, M., Mutterlose, J. & Brand, U. 2007: Crystallographic texture and microstructure of terebratulide brachiopod shell calcite: an optimized materials design with hierarchical architecture. American Mineralogist 92, 722–734.

Haq, B.V., Hardenbol, J. & Vail, P.R. 1988: Mesozoic and Cenozoic chronostratigraphy and cycles of sea-level change. In: Wilgus, C.K. *et al.* (eds): Sea-level Changes; an Integrated Approach. Society of Economic Paleontologists and Mineralogists (SEPM) Special Publication 42, 71–108.

Husson, D., Galbrun, B., Laskar, J., Hinnov, L., Thibault, N., Gardin, S. & Locklair, R.E. 2011: Astronomical calibration of the Maastrichtian (late Cretaceous). Earth and Planetary Science Letters 305, 328–340.

Husson, D., Galbrun, B., Thibault, N., Gardin, S., Huret, E. & Coccioni, R. 2012: Astronomical duration of polarity Chron C31r (Lower Maastrichtian): cyclostratigraphy of ODP Site 762 (Indian Ocean) and the Contessa Highway section (Gubbio, Italy). Geological Magazine 149, 345–351.

Håkansson, E. & Surlyk, F. 1997: Denmark. In: Moores, E.M. & Fairbridge, R.W. (eds): Encyclopedia of European and Asian Regional Geology. Chapman & Hall, 183–192.

Imai, N., Terashima, S., Itoh, S. & Ando, A. 1996: 1996 compilation of analytical data on nine GSJ geochemical reference samples, "Sedimentary rock series". Geostandards Newsletter 20, 165–216.

Jenkyns, H.C., Mutterlose, J. & Sliter, W.V. 1995: Upper Cretaceous carbon- and oxygen-isotope stratigraphy of deep-water sediments from the North-Central Pacific (Site 869, Flank of Pikinni-Wodejebato, Marshall Islands). Proceedings of the Ocean Drilling Program, Scientific Results 143, 105–108.

Johansen, M.B. & Surlyk, F. 1990: Brachiopods and the stratigraphy of the Upper Campanian and Lower Maastrichtian chalk of Norfolk, England. Palaeontology 33, 823–873.

Koch, C. & Young, J.R. 2007: A simple weighing and dilution technique for determining absolute abundances of coccoliths from sediment samples. Journal of Nannoplankton Research 29, 67–69.

Kominz, M.A., Browning, J.V., Miller, K.G., Sugarman, P.J., Mizintsevat, S. & Scotese, C.R. 2008: Late Cretaceous to Miocene sea-level estimates from the New Jersey and Delaware coastal plain coreholes: an error analysis. Basin Research 20, 211–226.

Korte, C., Jasper, T., Kozur, H.W. & Veizer, J. 2005a: $\delta^{18}O$ and $\delta^{13}C$ of Permian brachiopods: a record of seawater evolution and continental glaciations. Palaeogeography, Palaeoclimatology, Palaeoecology 224, 333–351.

Korte, C., Kozur, H.W. & Veizer, J. 2005b: $\delta^{13}C$ and $\delta^{18}O$ values of Triassic brachiopods and carbonate rocks as proxies for coeval seawater and palaeotemperature. Palaeogeography, Palaeoclimatology, Palaeoecology 226, 287–306.

Korte, C., Jones, P.J., Brand, U., Mertmann, D. & Veizer, J. 2008: Oxygen isotope values from high-latitudes: Clues for Permian sea-surface temperature gradients and Late Palaeozoic deglaciation. Palaeogeography, Palaeoclimatology, Palaeoecology 269, 1–16.

Li, L. & Keller, G. 1998a: Maastrichtian climate, productivity and faunal turnovers in planktic foraminifera in South Atlantic DSDP sites 525A and 21. Marine Micropaleontology 33, 55–86.

Li, L. & Keller, G. 1998b: Abrupt deep-sea warming at the end of the Cretaceous. Geology 26, 995–998.

Li, L. & Keller, G. 1999: Variability in Late Cretaceous climate and deep waters: evidence from stable isotopes. Marine Geology 161, 171–190.

Liboriussen, J., Ashton, P. & Tygesen, T. 1987: The tectonic evolution of the Fennoscandian Border Zone. Tectonophysics 137, 21–29.

Mitchell, S.F., Ball, J.D., Crowley, S.F., Marshall, J.D., Paul, C.R.C., Veltkamp, C.J. & Samir, A. 1997: Isotope data from Cretaceous chalks and foraminifera: environmental or diagenetic signals? Geology 25, 691–694.

Mogensen, T.E. & Korstgård, J.A. 2003: Triassic and Jurassic transtension along part of the Sorgenfrei–Tornquist Zone in the Danish Kattegat. In: Ineson, J.R. & Surlyk, F. (eds): The Jurassic of Denmark and Greenland. Geological Survey of Denmark and Greenland Bulletin 1, 439–458.

Parkinson, D., Curry, G.B., Cusack, M. & Fallick, A. 2005: Shell structure, patterns and trends of oxygen and carbon stable isotopes in modern brachiopod shells. Chemical Geology 219, 193–235.

Rasmussen, S.L. & Surlyk, F. 2012: Facies and ichnology of an Upper Cretaceous chalk contourite drift complex, eastern Denmark, and the validity of contourite facies models. Journal of the Geological Society, London 169, 435–447.

Roth, P.H. 1983: Jurassic and Lower Cretaceous calcareous nannofossils in the western North Atlantic (Site 543): biostratigraphy, preservation and some observation on biogeography and paleoceanography. Initial Reports of the Deep Sea Drilling Project 76, 587–621.

Schulz, M.-G. 1979: Morphometrisch-variationsstatistische Untersuchungen zur Phylogenie der Belemniten-Gattung *Belemnella* im Untermaastricht NW-Europas. Geologisches Jahrbuch A 47, 3–157.

Steinich, G. 1965: Die artikulaten Brachiopoden der Rügener Schreibkreide (Unter-Maastricht). Paläontologische Abhandlungen A 2, 1–220.

Stemmerik, L., Surlyk, F., Klitten, K., Rasmussen, S.L. & Schovsbo, N. 2006: Shallow core drilling of the Upper Cretaceous Chalk at Stevns Klint, Denmark. Geological Survey of Denmark and Greenland Bulletin 10, 13–16.

Stenestad, E. 1972: Træk af det danske bassins udvikling i Øvre Kridt. Dansk Geologisk Forenings Årsskrift for 1971, 63–69.

Surlyk, F. 1969: En undersøgelse over de articulate brachiopoder i det danske skrivekridt (ø. campanien og maastrichtien) med en oversigt over skrivekridtets sedimentologi og skrivekridthavets flora og fauna. Unpublished prize dissertation. University of Copenhagen, 319 pp.

Surlyk, F. 1970: Die Stratigraphie des Maastricht von Dänemark und Norddeutschland aufgrund von Brachiopoden. Newsletters on Stratigraphy 1, 7–16.

Surlyk, F. 1979: Maastrichtian brachiopods from Denmark. In: Birkelund, T. & Bromley, R.G. (eds): Cretaceous – Tertiary Boundary Events, Symposium. The Maastrichtian and Danian of Denmark, University of Copenhagen, 45–50.

Surlyk, F. 1982: Brachiopods from the Campanian–Maastrichtian boundary sequence, Kronsmoor (NW Germany). Geologisches Jahrbuch A 61, 259–277.

Surlyk, F. 1984: The Maastrichtian Stage in NW Europe, and its brachiopod zonation. Bulletin of the Geological Society of Denmark 33, 217–223.

Surlyk, F. & Birkelund, T. 1977: An integrated stratigraphical study of fossil assemblages from the Maastrichtian White Chalk of northwestern Europe. In: Kauffman, E.G. & Hazel, J.E. (eds): Concepts and Methods of Biostratigraphy. Dowden, Hutchinson & Ross, Stroudsburg, 257–281.

Surlyk, F. & Lykke-Andersen, H. 2007: Contourite drifts, moats and channels in the Upper Cretaceous chalk of the Danish Basin. Sedimentology 54, 405–422.

Surlyk, F., Rasmussen, S.L., Boussaha, M., Schiøler, P., Schovsbo, N.H., Sheldon, E., Stemmerik, L. & Thibault, N. 2013: Upper Campanian–Maastrichtian holostratigraphy of the eastern Danish Basin. Cretaceous Research 46, 232–256.

Thibault, N. & Gardin, S. 2006: Maastrichtian calcareous nannofossil biostratigraphy and paleoecology in the Equatorial Atlantic (Demerara Rise, ODP Leg 207 Hole 1258A). Revue de micropaléontologie 49, 199–214.

Thibault, N. & Gardin, S. 2007: The late Maastrichtian nannofossil record of climate change in the South Atlantic DSDP Hole 525A. Marine Micropaleontology 65, 163–184.

Thibault, N. & Gardin, S. 2010: The calcareous nannofossil response to the end-Cretaceous warm event in the Tropical Pacific. Palaeogeography, Palaeoclimatology, Palaeoecology 291, 239–252.

Thibault, N., Harlou, R., Schovsbo, N., Schiøler, P., Minoletti, F., Galbrun, B., Lauridsen, B.W., Sheldon, E., Stemmerik, L. & Surlyk, F. 2012a: Upper Campanian–Maastrichtian nannofossil biostratigraphy and high-resolution carbon-isotope stratigraphy of the Danish Basin: Towards a standard $\delta^{13}C$ curve for the Boreal Realm. Cretaceous Research 33, 72–90.

Thibault, N., Husson, D., Harlou, R., Gardin, S., Galbrun, B., Huret, E. & Minoletti, F. 2012b: Astronomical calibration of upper Campanian–Maastrichtian carbon isotope events and calcareous plankton biostratigraphy in the Indian Ocean (ODP Hole 762C): Implication for the age of the Campanian–Maastrichtian boundary. Palaeogeography, Palaeoclimatology, Palaeoecology 337–338, 52–71.

Tsikos, H. *et al.* 2004: Carbon-isotope stratigraphy recorded by the Cenomanian–Turonian Oceanic Anoxic Event: correlation and implications based on three key localities. Journal of the Geological Society, London 161, 711–719.

Ullmann, C.V., Campell, H.J., Frei, R., Hesselbo, S.P., Pogge von Strandmann, P.A.E. & Korte, C. 2013: Partial diagenetic overprint of Late Jurassic belemnites from New Zealand: Implications for the preservation potential of δ^7Li values in calcite fossils. Geochimica et Cosmochimica Acta 120, 80–96.

Veizer, J. *et al.* 1999: $^{87}Sr/^{86}Sr$, $\delta^{13}C$ and $\delta^{18}O$ evolution of Phanerozoic seawater. Chemical Geology 161, 59–88.

Vejbæk, O.V. & Andersen, C. 2002: Post mid-Cretaceous inversion tectonics in the Danish Central Graben – regionally synchronous tectonic events? Bulletin of the Geological Society of Denmark 47, 139–144.

Voigt, S., Friedrich, O., Norris, R.D. & Schönfeld, J. 2010: Campanian – Maastrichtian carbon isotope stratigraphy: shelf – ocean correlation between the European shelf sea and the tropical Pacific Ocean. Newsletters on Stratigraphy 44, 57–72.

Voigt, S., Gale, A., Jung, C. & Jenkyns, H. 2012: Global correlation of Upper Campanian – Maastrichtian successions using carbon isotope stratigraphy: development of a new Maastrichtian timescale. Newsletters on Stratigraphy 45, 25–53.

Instructions to authors

The Bulletin publishes articles normally not exceeding 30 printed pages, notes not longer than 4 pages, and short contributions of maximum 1 printed page. Longer articles and monographs are also published, but in this case it is advisable to consult the chief editor before submitting long manuscripts. Short contributions may be comments on previously published articles, presentation of current scientific activities, short scientific notes, or book reviews.

Manuscripts with complete sets of illustrations, tables, captions, etc., should be submitted electronically to the chief editor (lml@geus.dk). The **main text** with references and figure captions should be either in Word or pdf format, **figures** should be in either pdf, jpeg, or tiff format, and **tables** should be in Word text format, i.e. written in lines with tab spacing between table columns, or in Excel format. "Word tables" are discouraged because they are not re-formatted easily. Consult the editor before submitting other formats.

Manuscripts will be reviewed by two referees; suggestions of referees are welcome. The final decision on whether or not a manuscript will be accepted for publication rests with the chief editor, acting on the advice of the scientific editors. Articles will be published in the order in which they are accepted and produced for publication.

Manuscript

Language – Manuscripts should be in English. Authors who are not proficient in English should ask an English-speaking colleague for assistance before submission of the manuscript.

Title – Titles should be short and concise, with emphasis on words useful for indexing and information retrieval. An abbreviated title to be used as running title must also be submitted.

Abstract – An abstract in English must accompany all papers. It should be short (no longer than 250 words), factual, and stress new information and conclusions rather than describing the contents of the manuscript. Conclude the abstract with a list of key words.

Main text – Use 1.5 or double spacing throughout, and leave wide margins. Italics should be used only in generic and species names and in some Latin abbreviations (e.g. *c, et al., ibid., op. cit*).

Spelling – Geological units named after localities in Greenland, formal lithostratigraphical units and intrusions named after localities in Greenland remain unchanged even if the eponymous locality names have since been changed in accordance with modern Greenlandic orthography.

References to figures, tables and papers – References to figures and tables in the text should have the form: Fig. 1, Figs 1–3, Table 3 or as (Smith 1969, fig. 3) when the reference is to a figure in a cited paper.

References to papers are given in the form Smith (1969) or (Smith 1969). Combined citations by different authors are separated by a semicolon; two or more papers by same author(s) are separated by commas. Citations are mentioned chronologically and then alphabetically. Use '*et al.*' for three or more authors, e.g. Smith *et al.* (1985).

Reference list

Use the following style:

Smith, A.A. 1989: Geology of the Bulbjerg Formation. Bulletin of the Geological Society of Denmark 38, 119–144. [Note that name of journal is given in full].

Smith, A.A., Jensen, B.B. & MacStuff, C.C. 1987: Sandstones of Denmark, 2nd edition, 533 pp. New York: Springer Verlag. [For more than 10 authors, use first author followed by *et al.*].

Smith, A.A., Jensen, B.B. & MacStuff, C.C. 1992: Characterization of Archean volcanic rocks. In: Hansen, D.D. *et al.* (eds): Geology of Greenland. Geological Survey of Denmark and Greenland Bulletin 40, 1397–1438. [More than three editors – therefore *et al.* form is used].

Sorting – Danish letters æ, ø and å (aa) are treated as ae, o and a (aa), respectively.

References are sorted by:

1: Alphabetically by the first author's surname
2: Papers by one author: two or more papers are arranged chronologically
3: Papers by two authors: alphabetically after second author's name. Two or more papers by the same two authors: chronologically.
4: Papers by three or more authors: chronologically. Papers from the same year are arranged alphabetically after second, third, etc. author's name.

Authors themselves are responsible for the accuracy and completeness of their references. The reference list must include all, and only, the references cited in the paper (including figures, tables etc).

Illustrations

May be prepared in either black and white or colour. There is no colour charge. Horizontal illustrations are much to be preferred. Size of smallest letters in illustrations should not be less than 5.5 pt. Remember scale.

All figures (including photographs) should be submitted in electronic form ready for direct reproduction, i.e. having the dimensions of the final figure with a standard resolution of 300 dpi for photographs. Preferred formats are pdf, tiff and jpg.

Size – The width of figures must be 82 mm, 125 mm or 171 mm. Maximum height is 223 mm.

Captions – Captions to figures and plates must be delivered on separate pages, preferably at the end of the manuscript.

Supplementary data files

Supplementary files are accepted. Such files may provide e.g. analytical data tables, detailed data documentation, illustrations with special effects, or videos.

Proofs

Authors receive page proofs of the article after technical production. The cost of any alterations against the final manuscript will be charged to the author.

Content, vol. 62

ISSN 2245-7070